

Department of Pure and Applied Chemistry

**AN EXPERIMENTAL AND COMPUTATIONAL INVESTIGATION OF
TRANSITION METAL-FREE REACTIONS**

by

MARK ALLISON

A thesis submitted to the Department of Pure and Applied Chemistry, University of Strathclyde, in part fulfillment of the regulations for the degree of Doctor of Philosophy in Chemistry.

2018

Declaration of Ownership

This thesis is the result of the author's original research. It has been composed by the author and has not been previously submitted for examination which has led to the award of a degree.

The copyright of this thesis belongs to the author under the terms of the United Kingdom Copyright Acts as qualified by University of Strathclyde Regulation 3.50. Due acknowledgement must always be made of the use of any material contained in, or derived from, this thesis.

Signed:

Date:

“We're all just traveling through our lives, we will reach our destination, so just hang on for the ride.”

-Jaret Reddick

Acknowledgements

First and foremost, I wish to offer my sincerest thanks to Professor John Murphy and Professor Tell Tuttle for granting me the opportunity to complete my postgraduate studies under their supervision. I am most thankful for their support and advice throughout the years and for always staying positive about research.

I'd like to also thank members of technical staff at the university, in particular Craig Irving (NMR), Patricia Keating (Mass Spectrometry) who do an excellent job not only in maintaining the equipment but are excellent sources of knowledge in their respective fields.

The Murphy and Tuttle groups have been there to provide great support in the lab and all the post-docs, current and former PhD students and the undergraduates who have all played their part in helping to solve problems but have also been great fun outside of the lab. There has been plenty of laughter and good nights in the pub and thanks to everyone in the group I have certainly become a more outgoing confident person.

My family have been supportive of me throughout all my studies both undergraduate and postgraduate. They've always had faith in me and I've tried my best to continually do them proud, even if they do not understand much of what I do.

My partner Rachael may only have come into my life halfway through but has been a hugely important influence on finishing and keeping me going when I've found it tough. She has always been a positive influence and a big supporter.

Everyone at the rugby has also been a help throughout my PhD, whether it had been taking an interest, offering encouragement or just providing a great distraction from the work to focus on games; for those few h on a Saturday nothing else mattered.

And last but not least, my wee dog Millie who is always there and happy to see me and whose face could make me smile even at the toughest times.

Publication List

1. Electron-Transfer and Hydride-Transfer Pathways in the Stoltz–Grubbs Reducing System (KO^tBu/Et₃SiH)

Andrew J. Smith, Allan Young, Simon Rohrbach, Erin F. O'Connor, **Mark Allison**, Hong-Shuang Wang, Dr. Darren L. Poole, Dr. Tell Tuttle, Prof. Dr. John A. Murphy

Angew Chem Int Ed, 2017, **56**, 13747–13751

2. Initiation of Transition Metal-Free Cross Coupling Reactions by Thermally Generated Diradicals and Radicals*

Mark Allison, Raymond Chung, Tell Tuttle, John A. Murphy

Angew Chemie, Manuscript in Preparation

3. Dual Roles for Potassium Hydride in Haloarene Reduction: CS_NAr and SET Reduction *via* Organic Electron Donors Formed in Benzene*

Joshua P. Barham, Samuel E. Dalton, **Mark Allison**, Giuseppe Nocera, Allan Young, Matthew P. John, Thomas McGuire, Sebastien Campos, Tell Tuttle, John A. Murphy

JACS, Manuscript in Preparation

4. Intramolecular Communication between π -systems in the Cleavage of C–O and C–C σ -bonds by Organic Super Electron Donors

Jonathan Chua Zijian, **Mark Allison**, Jason Masuda, Tell Tuttle, John A. Murphy

Manuscript in Preparation

5. Ring-Opening and Cyclisation of *N*-Arylindoles Using the Stoltz-Grubbs Reducing System (Et₃SiH/KO^tBu)

Andrew J. Smith, Jude N. Arokianathar, **Mark Allison**, Darren L. Poole, Tell

Tuttle, John A. Murphy

Angew Chemie, Manuscript in Preparation

* Publication related to work in thesis

Abbreviations list

AIBN – azobisisobutyronitrile

AMVN – azomethylvaleronitrile

BHAS – Base-promoted homolytic aromatic substitution

CGF – Contracted gaussian functions

CPCM – conductor-like polarisable continuum model

DET – Double electron transfer

DFT – Density Functional Theory

DMAP – 4-dimethylaminopyridine

DMEDA – N,N'-dimethylethylenediamine

DMF – dimethylformamide

DMSO – dimethyl sulfoxide

EPR – electron paramagnetic resonance

GCMS – Gas chromatography mass spectroscopy

GEA – gradient expansion approximation

GGA – generalized gradient approximation

GTO – gaussian type orbitals

HAS – homolytic aromatic substitution

HAT – hydrogen atom transfer

HDDA – hexadehydro-Diels-Alder

HF – Hartree-Fock

HMPA - hexamethylphosphoramide

HOMO – Highest occupied molecular orbital

ICP-MS – inductively coupled plasma mass spectrometry

KHMDS – potassium hexamethyldisilane

KO^tBu – potassium *tert*-butoxide

LDA – Local density approximation

LUMO – Lowest unoccupied molecular orbital

MO – molecular orbital

NHC – *N*-heterocyclic carbene

ppb – parts per billion

SCE – saturated calomel electrode

SED – super electron donor

SET – single electron transfer

STO – slater type orbitals

TBAB – tetra-*n*-butylammonium bromide

TBAF – tetra-*n*-butylammonium fluoride

TBS – *tert*-butyldimethylsilyl

TDAE – tetrakis(dimethylamino)ethylene

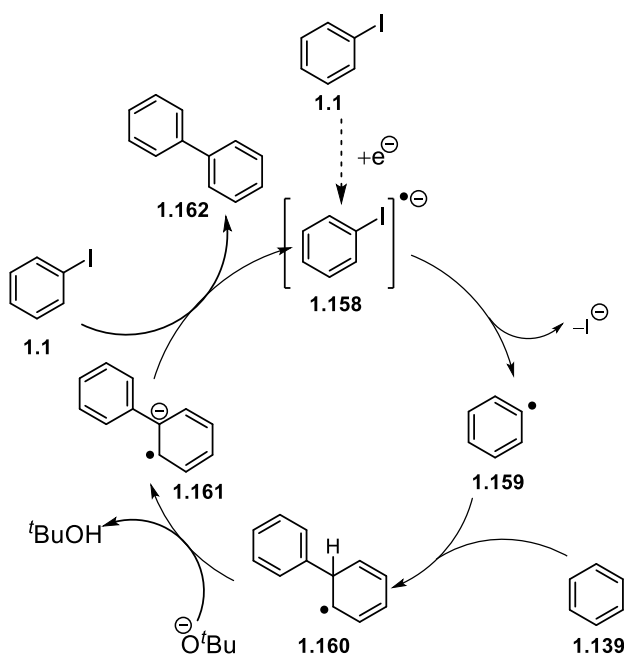
TMS – trimethylsilyl

TTF – tetrathiafulvalene

UV – ultraviolet

Abstract

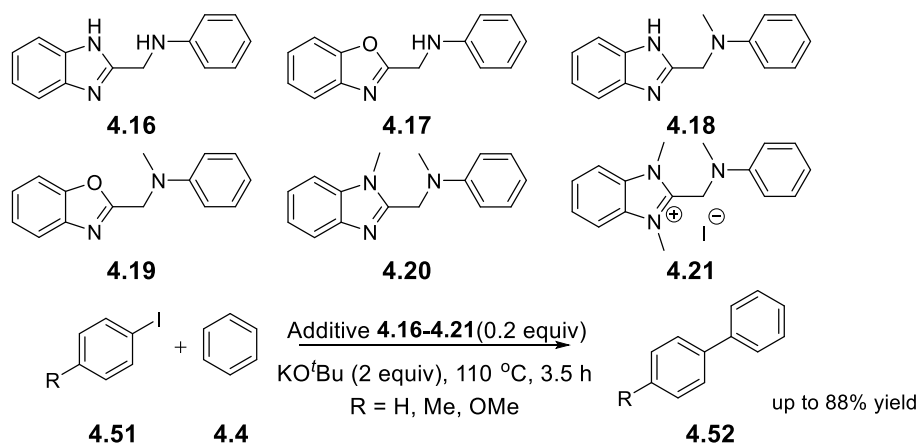
Over recent decades transition metal-catalysed cross-coupling has been developed significantly, opening up new areas of reactivity in both an academic and industrial environment. However, over recent years transition metal-free coupling reactions of haloarenes to arenes, proceeding by the Base-promoted Homolytic Aromatic Substitution (BHAS) mechanism have been widely reported in the literature. These reactions work well when initiated by organic electron donors that are formed in situ from organic additives of various types. The work in this thesis builds on previous work carried out within the Murphy group and other groups working in this field.



Scheme 1 – BHAS mechanism proposed by Studer and Curran as responsible for transition metal-free cross coupling reactions.

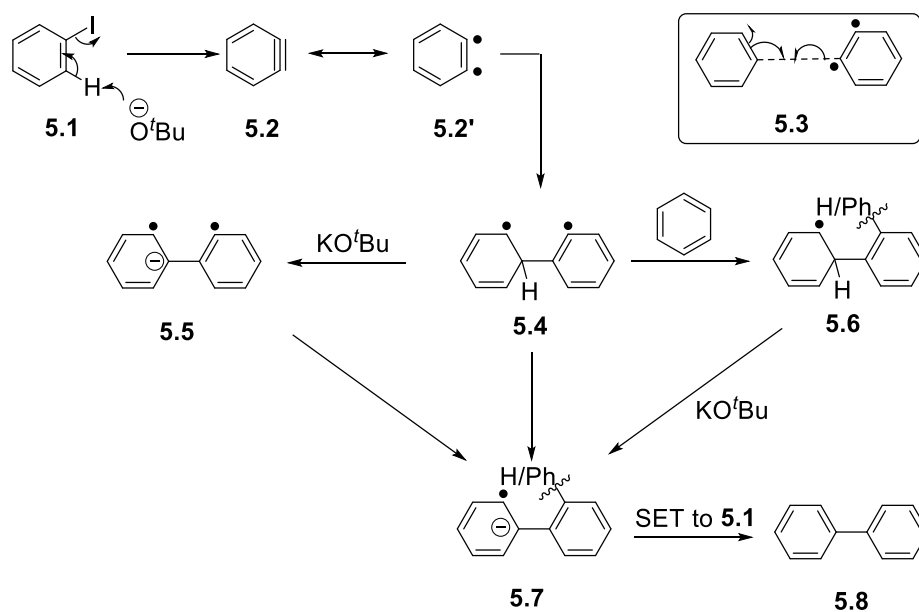
The work in this thesis looks at transition metal-free reactions in two forms; firstly looking at new additives that could form electron donors to initiate the BHAS mechanism and secondly, looking at where coupling reactions are occurring when there is no electron donor present. The final aspect of this thesis looks at exploring observations seen in experiments with haloarenes and potassium hydride.

The first set of work was looking at a series of additives that were designed to form electron-rich alkenes, a common feature of electron donors, under basic conditions. These were studied both computationally and experimentally and this work showed these can work together effectively in studying electron donors.



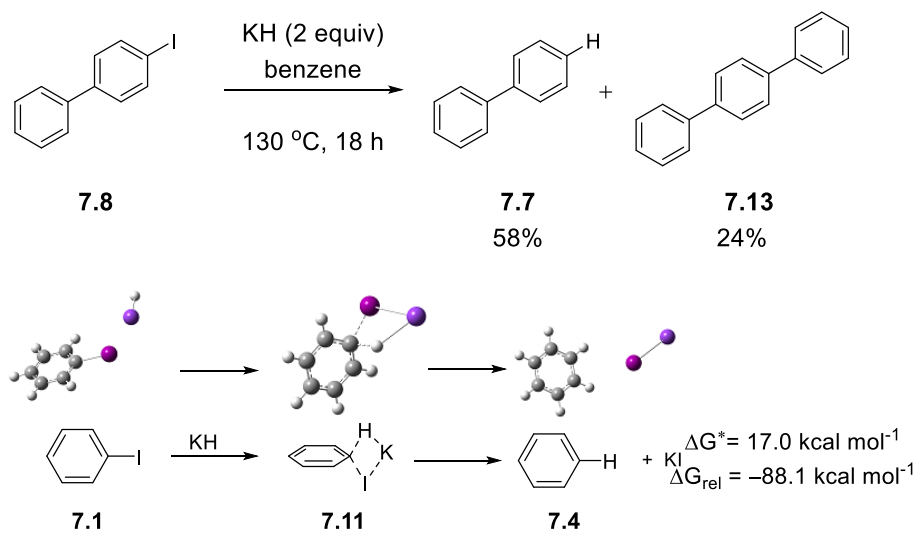
Scheme 2 – Additives used in Chapter 4 produced high yields of coupled products

While these reactions proceed in good yield when there is an electron donor present in the reaction, when there is no electron donor a measurable amount of cross coupling still occurs. A plausible mechanism, shown in scheme 3, has been proposed for the initiation of the BHAS pathway. This thesis shows that biradicals, generated in Bergman cyclisations and hexadehydro-Diels-Alder reactions, can indeed act as a source of initiation for this pathway. This thesis now shows that additives that afford arenediyls, provide independent initiation of the coupling reactions for this substrate in the absence of electron donors, supporting a similar capability for benzyne generated by base-dependent means.



Scheme 3 – Proposed benzyne initiation of the BHAS cycle

In reactions performed by other members of the Murphy group involving haloarenes and KH, some interesting reaction products were observed. In this thesis these have been rationalised using computational studies.



Scheme 4 – This thesis proposes formation of **7.7** proceeds via the four-membered transition state calculated

Contents

Declaration of Ownership	I
Acknowledgements	III
Publication List	IV
Abbreviations list.....	VI
Abstract.....	IX
Contents.....	XII
1. Literature Review.....	1
1.1 Palladium Cross Coupling	1
1.2 Sonogashira Coupling Reactions	3
1.3 Early Attempts at Transition Metal-Free Cross Coupling.....	4
1.4 Cross Coupling <i>via</i> Benzyne	5
1.5 Hexa-dehydro-Diels-Alder (HDDA) reaction	8
1.6 Benzyne-Mediated Cross Coupling Reactions	9
1.7 Organic Electron Donors	12
1.8 New Attempts at Transition Metal-Free Cross Coupling	21
1.9 Transition Metal-Free Heck-type Reactions	25
1.10 Initiation of Transition Metal-Free Cross Coupling Reactions	28
2. Introduction.....	52
2.1 Project Aims and Motivation	52
2.2 Layout of the Thesis	53
3. Computational Theory¹¹⁷.....	54
3.1 Quantum Mechanics	54
3.2 Density Functional Theory	54
3.2.1 Electron Density	54

3.2.2	Pair Density	55
3.2.3	Hohenberg-Kohn Theory	56
3.2.4	Kohn-Sham Approach	58
3.3	Functionals and Basis Sets	60
3.3.1	Functionals	60
3.3.2	Hybrid Functionals	62
3.3.3	Basis Sets	63
3.4	Solvation Models	65
3.5	Marcus Theory	66
4.	A New Range of Electron Donors for Transition Metal Free Synthesis	70
4.1	Introduction	70
4.2	Generation of potential electron donor	71
4.4	Marcus theory calculations	76
4.5	Experimental Results	79
4.5.1	Substrate synthesis	79
4.5.2	Coupling reactions with unhindered iodoarenes	80
4.5.3	2-Iodo- <i>m</i> -xylene reactions	82
4.5.4	Is the full molecule required?	85
4.5.5	Is KO ^t Bu essential for the reaction to proceed?	86
4.6	Conclusions	87
4.7	Future Work	90
5.	Benzyne Initiation of Base-Promoted Homolytic Aromatic Substitution	91
5.1	Introduction	91
5.2	Results and Discussion	94
5.2.1	<i>o</i> -Benzyne	94
5.2.2	Alternative Methods of Forming <i>o</i> -Benzyne	96
5.2.3	<i>p</i> -Benzyne as an Additive	97
5.2.4	Control Reactions	102
5.2.5	Alkyl Radical Addition	104
5.3	Conclusions	106

5.4 Future Work	107
6. Computational Analysis of Biradical Initiation of BHAS cycle.....	108
6.1 Introduction	108
6.2 Computational Methods	109
6.3 <i>Ortho</i> -Benzyne Attack on Benzene	109
6.4 Conclusions	115
6.5 Future Work	117
7. Computational Analysis of Potassium Hydride reactions with haloarenes	118
7.1 Introduction	118
7.2 Investigation of Pierre Mechanism	119
7.3 Bromine Atom Abstraction by Alkyl Radicals.....	124
7.4 Hydrogen Atom Abstraction by Aryl Radicals	127
7.5 Reactions of Dihalodurenes Mediated by KH	128
7.6 Conclusions	130
7.7 Future Work	131
8. Overall Conclusions.....	132
9. Experimental	137
9.1 General experimental information	137
9.2 Experimental Procedures for Chapter 4	139
9.3 NMR spectra for compounds synthesised in Chapter 4	163
9.4 Experimental procedures for Chapter 5	173
9.5 Example Internal Standard Calculation.....	209
9.5.1 Reactions with 2-iodo- <i>m</i> -xylene	209
9.6 NMR structures for compounds synthesised in Chapter 5.....	211
10. References.....	231

1. Literature Review

As chemists, we are ever looking for synthetic methods that are cheaper, greener and safer alternatives to well established and versatile palladium cross-coupling reactions. There is now a new branch of cross-coupling reactions that proceed in the absence of palladium or any other transition metals.

To set the research in this thesis in context, this introduction will examine historical transition metal cross coupling reactions, then moving on to transition metal-free cross coupling reactions, from their origins to recent developments and current mechanistic insights. In addition to the cross coupling reactions, this review will also look at a number of other transformations that are later exploited in the thesis, such as those related to benzyne and hexa-dehydro Diels Alder (HDDA) reactions. Electron donors are an important class of reagents in both transition metal-free cross coupling reactions, and also, in previous work with the Murphy group; throughout the review both of these aspects, transition metal-free cross coupling and alternative reductions, will be discussed.

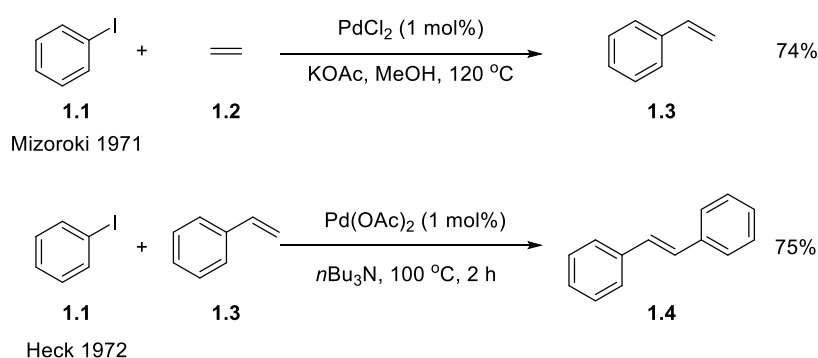
1.1 Palladium Cross Coupling

A historical challenge for synthetic chemists has been to develop new methods of forming C-C bonds. Over recent decades, there have been large advances in palladium-catalysed cross coupling chemistry and, more recently, in dual catalysis with other precious metals.

Palladium cross coupling has been extensively developed and widely used in both industry and academia.¹ The power of these catalysts cannot be overestimated and must not be underestimated. This was recognized in 2010 when Heck, Negishi and Suzuki were awarded the Nobel prize in chemistry for their work in "palladium-catalyzed cross couplings in organic synthesis".² Use of palladium catalysts is not without issue. For example, these catalysts are often very expensive. The counter-argument to this is that they are catalysts, and their regeneration allows for re-use and this cuts the cost; nonetheless, cheaper alternatives that are equally as good in performance are desirable.

Another issue, particularly in the pharmaceutical industry, is the extensive purification that is required for the products. As transition metals are often toxic, these must be removed from products before they can be used as medicines. In addition to this, it is also possible that trace amounts of transition metals can be responsible for false positives in researching new drugs. Removing the need for any of these to be used initially would therefore be helpful for the pharmaceutical industry.

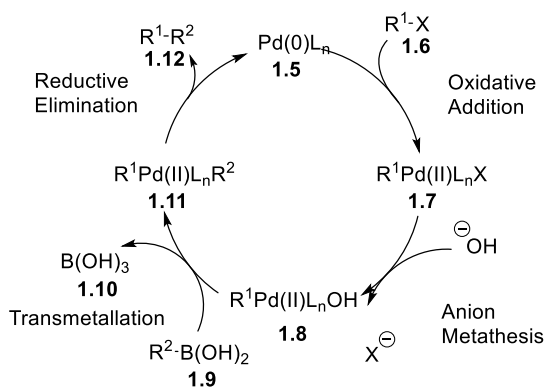
Palladium cross coupling has grown ever since Heck^{3, 4} and Mizoroki⁵ first reported their coupling of aryl or vinyl halides to alkenes back in the early 1970s (Scheme 1.1).



Scheme 1.1 – Heck-Mizoroki coupling of iodobenzene to alkenes^{4, 5}

The idea of coupling an aryl or vinyl halide or triflate to a coupling partner is a feature of many different palladium-catalysed reactions; there are a number of different well studied coupling partners for these reactions including organoborons (Suzuki),⁶ organotin (Stille),⁷ organomagnesiums (Kumada),⁸ organozincs (Negishi),⁹ organosilicons (Hiyama)¹⁰ and organocoppers from deprotonated alkynes (Sonogashira).¹¹

The most widely studied of these cross coupling reactions is the Suzuki reaction. The general catalytic cycle is shown in Scheme 2.^{12, 13} An aryl halide or triflate, **1.6** oxidatively adds to palladium (0) species, **1.5** to get a palladium (II) complex, **1.7**. From here, a hydroxide anion displaces the halide or triflate to give the new complex **1.8**. There is then a transmetalation step with the boronic acid to produce complex **1.11** which, upon reductive elimination, produces the coupled product **1.12** and regenerates the palladium (0) species, **1.5** starting the cycle again.



Scheme 1.2 – Suzuki catalytic cycle^{12, 13}

In addition to boronic acids, a wide range of other boron species have been developed such as boronic esters,¹⁴ pinacol boranes **1.14**¹⁵ and alkyl boranes **1.15**.¹⁶ Some of these are shown in Figure 1.1. The Suzuki reaction is still being developed by many groups and is still widely used in industry.¹⁷

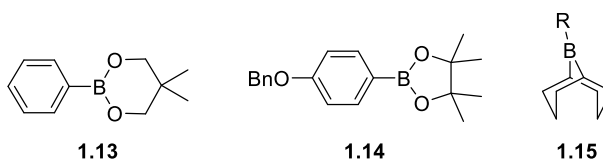
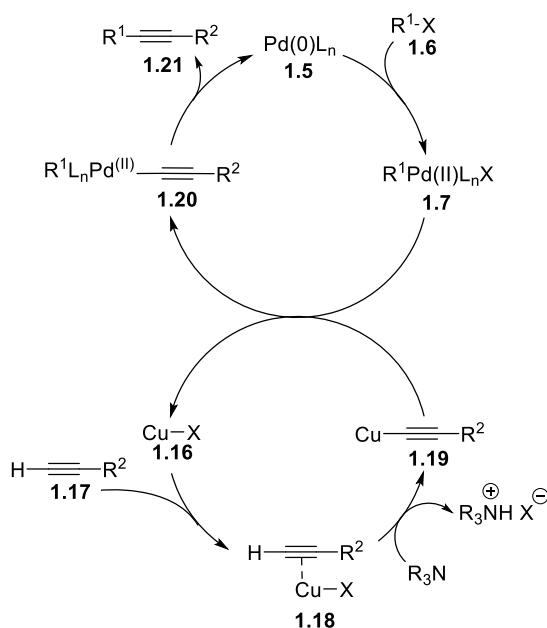


Figure 1.1 – Examples of boron species used in Suzuki cross coupling reactions¹⁴⁻¹⁶

1.2 Sonogashira Coupling Reactions

The Sonogashira reaction is the cross coupling of terminal alkynes with aryl/vinyl halides, often using a copper species as a co-catalyst to generate a Cu-acetylide *in situ*. This reaction has been important for synthesising enynes and enediynes which are important precursors for natural products,¹⁸ pharmaceuticals¹⁹ and molecular organic materials,²⁰ as the reaction is very tolerant to a wide range of functional groups and can therefore be used flexibly in a synthesis. The catalytic cycle is shown in Scheme 1.3.

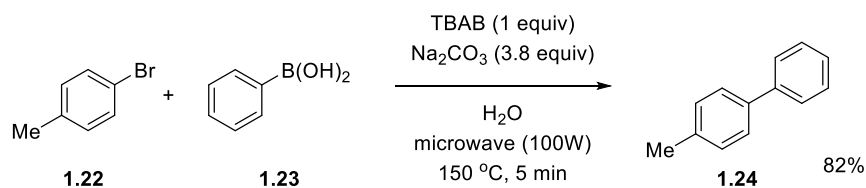


Scheme 1.3 – Sonogashira co-catalytic cycle²¹

Similarly to the Suzuki cycle, (Scheme 1.2) the first step is an oxidative addition to the palladium to form complex **1.7**. While this is going on, the terminal alkyne **1.17** complexes with the copper co-catalyst to form **1.18**. It is believed that this lowers the pK_a of the terminal proton, allowing for relatively weak bases such as triethylamine to do the deprotonation and generating the Cu-acetylide, **1.19**. This Cu-acetylide then undergoes transmetalation with the palladium complex **1.7** to generate the new palladium complex **1.20** whilst regenerating the copper catalyst, **1.16**. From here, the palladium complex undergoes a reductive elimination, generating the newly coupled alkyne **1.21** and restarting the cycle again.

1.3 Early Attempts at Transition Metal-Free Cross Coupling

In 2003 Leadbeater and Marco published a paper that was the first report of a transition metal-free cross coupling. They set out to investigate Suzuki couplings with very low palladium loadings (0.4 mol%) to couple boronic acids with aryl iodides, bromides and chlorides.²² They then found that using tetrabutylammonium bromide (TBAB) as an additive, they could then avoid the palladium completely.²³



Scheme 1.4 – Leadbeater’s transition metal-free Suzuki coupling²³

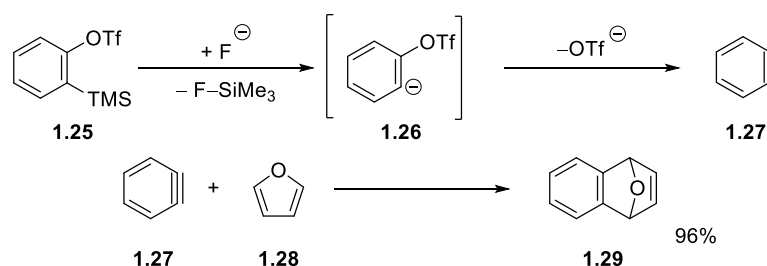
The next step was to analyse the reaction mixture to try and ensure that these reactions were in fact transition metal-free. To do this they used new glassware apparatus, reagents (from a range of suppliers) and they also analysed the crude product mixture for palladium content. The analysis showed that there was no palladium down to the detection limit of the apparatus (less than 0.1 ppm).²⁴ Other elements such as copper and ruthenium were also tested for, as these had been previously shown to promote coupling reactions.²⁵ However, again none of the metals tested for was present in a concentration above 1 ppm.

Despite all the analysis and steps taken to show that these were transition metal-free Suzuki couplings, in 2005 Leadbeater published a new paper reassessing the transition metal-free methodology. In contrast to their earlier publication, they now proposed that palladium contaminants down to 50 ppb found in the sodium carbonate were responsible for the reactivity observed.²⁶ They demonstrated in this later paper coupling of aryl bromides to boronic acids using 100-2500 ppb palladium catalyst loading. While low level palladium coupling reactions are a useful synthetic tool, ensuring that this low level isn’t present is an extra challenge in the search for truly transition metal-free reactions.

1.4 Cross Coupling *via* Benzyne

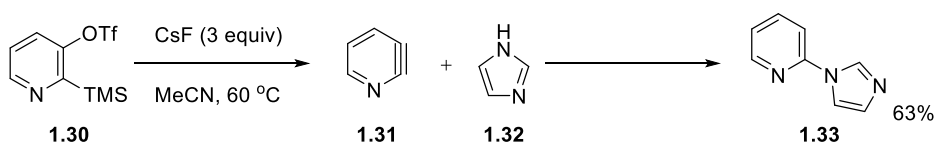
The existence of benzyne as a reactive intermediate in organic transformations has been known since its discovery in the 1940’s where Wittig announced that the product from his reaction of phenyllithium with fluorobenzene was biphenyl, following work up with water.²⁷ It took until 1961 for physical evidence of the short-lived intermediate to be presented.²⁸ There are numerous ways of generating benzyne known in the literature.²⁹⁻³³ One of the most common is Kobayashi’s 1,2-elimination of *o*-trimethylsilylphenyl

triflate. This exploits the strength of the Si-F bond and the triflate anion as a good leaving group. A fluoride anion attacks **1.25** to generate intermediate **1.26**. Triflate ion is then eliminated to generate benzyne, **1.27**. This can then undergo a Diels-Alder reaction with furan, **1.28**, to produce 1,4-dihydronaphthalene-1,4-endo-oxide, **1.29**, (Scheme 1.5)



Scheme 1.5 – Kobayashi's 1,2-elimination of *o*-trimethylsilylphenyl triflate³⁰

The original paper has been cited >500 times showing the significance of this method of forming benzyne. Garg *et al.* recently developed this idea further by moving away from benzyne and towards 2,3-pyridyne, **1.31**, as a heterocyclic aryne. These can be trapped with a variety of nucleophiles. This is a potentially useful building block for functionalized heterocycles.³⁴



Scheme 1.6 – Garg trapping of 2,3-pyridyne to imidazole, **1.32**³⁴

In addition to extending the scope of aryne reactions, Garg *et al.* have also investigated the regioselectivity observed in aryne reactions. This is fundamentally down to the “aryne distortion” effect. They studied a range of 3-substituted benzyne molecules **1.34** computationally and what they found was that the bigger the difference between angle ‘A’ and angle ‘B’ the more regioselective nucleophilic attack would be (Table 1.1).³⁵ They then took this even further to apply the computational methods used for studying the benzyne as a predictive tool for the selectivity of reactions of differently substituted benzyne and indolynes; however there is no experimental evidence yet to back up these predictions.³⁶

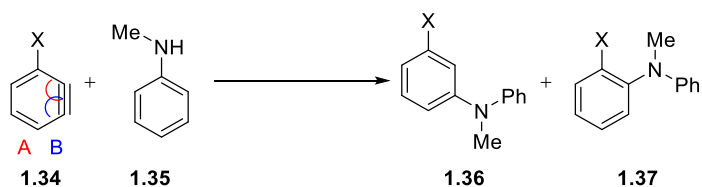
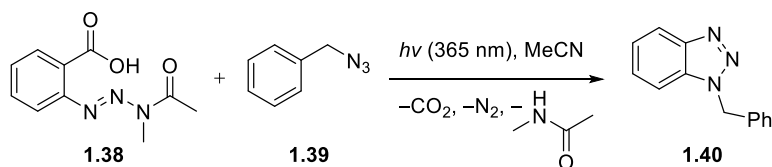


Table 1.1 – Aryne distortion effect on regioselectivity³⁵

X	A	B	Δ (angle difference between A & B)	Experimental ratio of products 1.36:1.37
OMe	120°	135°	15°	100:0
F	118°	135°	17°	100:0
Cl	121°	132°	11°	20:1
Br	122°	132°	10°	13:1
I	124°	130°	6°	9:1

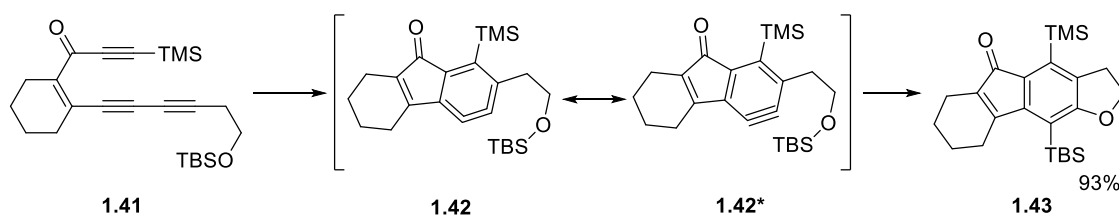
In addition to Kobayashi's method of generating benzyne, there are a number of alternatives. One of these was proposed by Schnarr and co workers who envisioned a fast photochemical generation of benzyne. To do this, they synthesized compound **1.38** and, upon generation of benzyne under UV light, this was trapped with an azide partner (Scheme 1.7).²⁹



Scheme 1.7 – Schnarr photochemical generation of benzyne²⁹

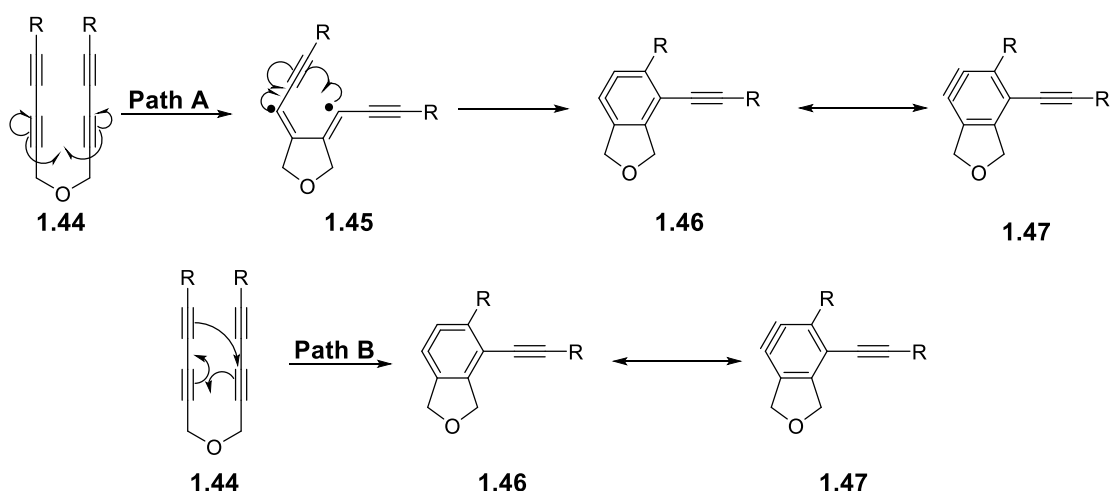
1.5 Hexa-dehydro-Diels-Alder (HDDA) reaction

Hoye *et al.* have recently extensively studied the hexa-dehydro-Diels-Alder (HDDA) reaction (Scheme 1.8).³² In the example shown, **1.41** cyclises to produce intermediate **1.42**. This is then intramolecularly trapped to afford the product **1.43**. What was notable about this method of generating benzyne is that the rearrangement proceeds purely thermally without the need for external reagents or UV light, unlike Kobayashi and Schnarr's methods.



Scheme 1.8 – HDDA rearrangement of **1.41**³²

After the initial discovery in 2012, the Hoye group did a lot of work deciphering the mechanism of the cyclisation for a general substrate **1.44**. There were two possibilities (Scheme 1.9): path A, which is a two-step radical pathway, and path B which is a more conventional concerted Diels-Alder pathway.



Scheme 1.9 – Two possible pathways for HDDA rearrangement

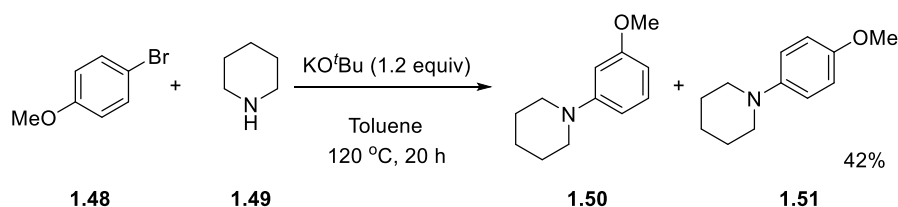
In 2015 they reported a computational study on the two proposed pathways and they found that the highest barrier in path A was 25.5 kcal mol⁻¹, whereas path B had a barrier

of 31.5 kcal mol⁻¹. Both pathways led to the same product. The conclusion from this work was that path A was the more probable route based on calculations.³⁷ In 2016, a follow-up paper was published looking at substituent effects on the cyclisation and found that it was more conclusive that path A was the mechanism of the cyclisation. They also noted that the biradical intermediate **1.45** was extremely short-lived as there are no radical by-products observed experimentally, and this was supported by their computational study.³⁸

The Hoye group have used the HDDA rearrangement in a number of different ways, such as for making polycyclic aromatic compounds,³⁹ and for biaryl synthesis⁴⁰ and in the trapping of polyfunctional natural products.⁴¹ They have now furthered the reactivity by performing a photochemical HDDA reaction. This has allowed the cyclisation to be performed at significantly lower temperatures, down to -70 °C.⁴² These reports show the utility of the HDDA rearrangement and that it is an effective new method of generating benzyne. Other groups have exploited the reaction in natural product synthesis,^{43, 44} the making of organic coatings^{45, 46} and also in polymerizations.^{47, 48}

1.6 Benzyne-Mediated Cross Coupling Reactions

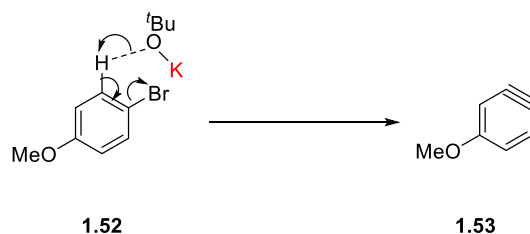
Benzyne has also found applications in cross coupling reactions. An early example was when Djakovitch *et al.* were investigating heterogeneous palladium catalysts and observed that differing ratios of *meta*- and *para*- products were forming in the reaction of 4-bromoanisole, **1.48** with piperidine **1.49**. Benzyne being the reason for this was proposed after a reaction without the palladium catalyst afforded the same *meta* and *para* isomers.⁴⁹



Scheme 1.10 – Djakovitch benzyne coupling of 4-bromoanisole, **1.48** with piperidine,

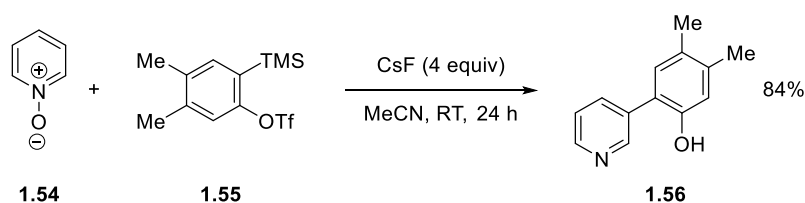
1.49⁴⁹

In this case benzyne was generated from deprotonation *ortho* to the bromine and subsequent elimination of the bromide (Scheme 1.11). The aryne produced is then nucleophilically attacked by the piperidine to produce the observed products. To generate the benzyne in this way, a base of the strength of KO^tBu is required.



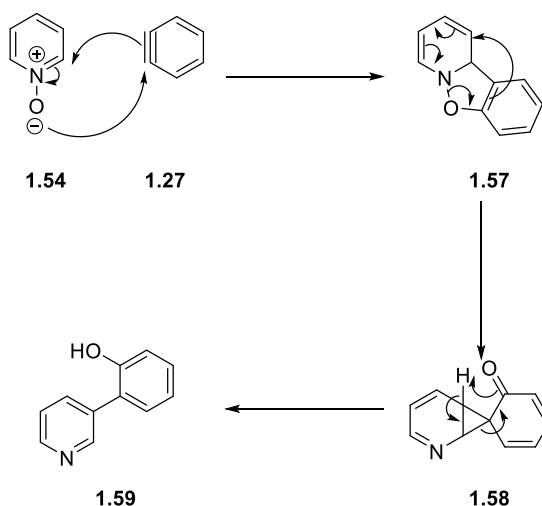
Scheme 1.11 – Generation of Benzyne

From as early as 2003, research groups have been utilizing benzyne intermediates to perform C-O and C-N arylations.⁵⁰⁻⁵² Larock and Liu discovered that they could perform C-C couplings using silylaryl triflates as benzyne precursors and pyridine-*N*-oxides as coupling partners.⁵³



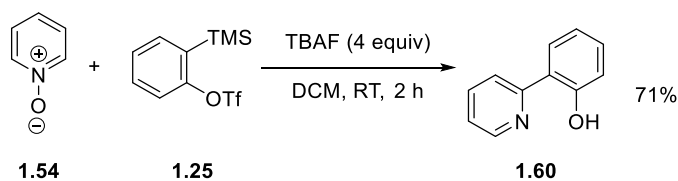
Scheme 1.12 – Synthesis of substituted pyridine *via* benzyne⁵³

It might have been expected that the coupling would have been in 2- position of the pyridine; however, their proposed mechanism (Scheme 1.13) justifies their observation of regioselectivity being in the 3-position.



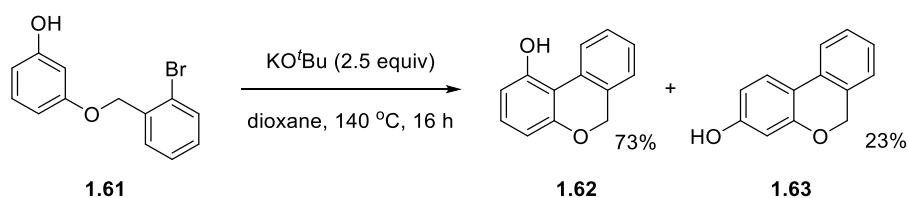
Scheme 1.13– Proposed mechanism⁵³ of benzyne coupling to pyridine-*N*-oxide.

In 2012 Liu published a modification, where the selectivity changed from the 3- to the 2- position. This was achieved by switching the fluoride source to tetrabutylammonium fluoride (TBAF) and the solvent from acetonitrile to dichloromethane.⁵⁴



Scheme 1.14 – Alternative regioselectivity for benzyne coupling to pyridine-*N*-oxide⁵⁴

Daugulis was able to use Djakovitch's observations of benzyne being produced from deprotonation *ortho* to a halide to achieve the intramolecular coupling of aryl halides with phenols in an excess of KO^tBu and the polar solvent, dioxane (Scheme 1.15).⁵⁵

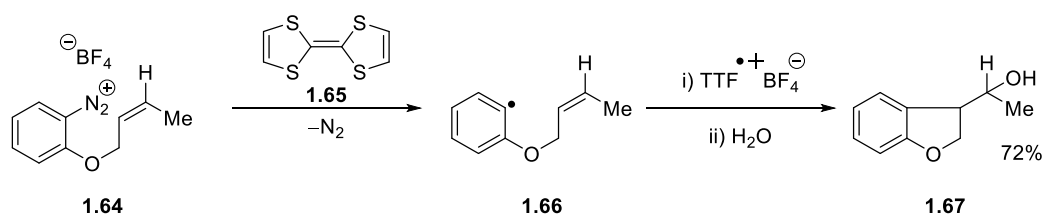


Scheme 1.15 – Intramolecular arylation of phenols using aryl halides

Despite trying other bases, it was found that KO^tBu was by far the best; other butoxides such as sodium and lithium, produced some product, although in lower yields. However, weaker bases such as K₂CO₃, did not produce any of the products.

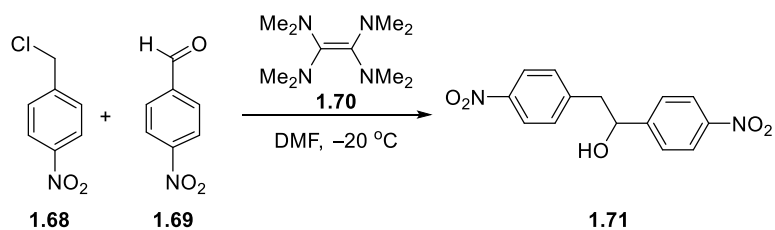
1.7 Organic Electron Donors

Highly reactive organic reducing agents known as “super electron donors” (SED) have been discovered and developed based on often relatively simple molecular design. A SED is defined as an organic molecule capable of reducing iodobenzenes.⁵⁶ Early work in this area arose from industry where tetrakis(diethylamino)ethene (TDAE) a weaker donor was discovered.⁵⁷ Some 20 years later a sulfur analogue, tetrathiafulvalene (TTF), **1.65** was prepared by Wudl *et al.*⁵⁸ In the 1990s, Lewis *et al.* explored TTF’s reactivity with arenediazonium salts. What was proposed was that TTF would reduce the diazonium salt, **1.64** to the aryl radical, **1.66**. This radical could then add onto the alkene in a 5-*exo-trig* cyclisation to afford the cyclized product **1.67** upon work up.⁵⁹



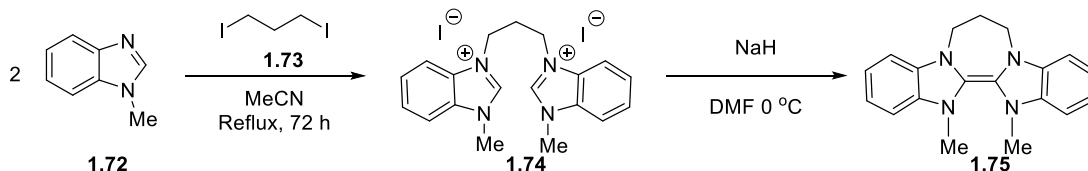
Scheme 1.16 – TTF reduction of arenediazonium salt, **1.64**⁵⁹

This was an early example of an organic electron donor being used in organic synthetic reactions. The Murphy group wanted to develop this further and expand electron donors; for this they had to learn two lessons. The first was that the gain of aromaticity is an important driving force that often determines the strength of organic donors. The second was that nitrogen is more helpful than sulfur in producing successful electron donors.⁶⁰ Meanwhile, Médebielle and co-workers decided to look back at the reactivity of TDAE, **1.70**. Using TDAE they were able to reduce acyl chlorides⁶¹ and electron-poor benzyl chlorides.^{62, 63} TDAE was able to reduce *p*-nitrobenzyl chloride, **1.68** down to an anion which was then able to nucleophilically attack an aldehyde, **1.69** producing the product **1.71** (Scheme 1.17).⁶²



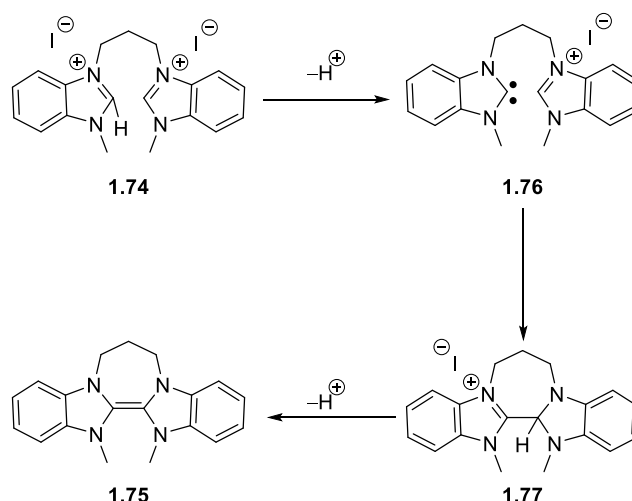
Scheme 1.17 – Médebielle *et al.* used TDAE to reduce *p*-nitrobenzyl chlorides⁶²

TDAE was not capable of reducing iodobenzenes, however, so this led to the design of SEDs. In 2005 by Murphy *et al.*⁶⁴ reported the use a benzimidazole-derived organic super electron donor, **1.75**, capable of reducing aryl iodides. This synthesis of the precursor salt **1.74** was straightforward from readily available starting materials shown in Scheme 1.18.



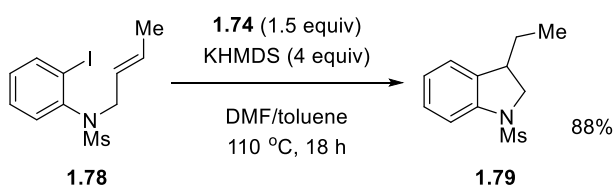
Scheme 1.18 – Synthesis of benzimidazole derived SED, **1.75**⁶⁴

To form the donor from salt, **1.74** it firstly needs to be deprotonated to form a carbene **1.76** which then attacks the other benzimidazolium moiety to form **1.77**. There is then a second deprotonation which leads to the active neutral donor species **1.75**. What makes this SED particularly effective is the 4 strong π -electron donating nitrogen atoms surrounding an alkene and also upon oxidation, aromaticity is gained in the five-membered rings.



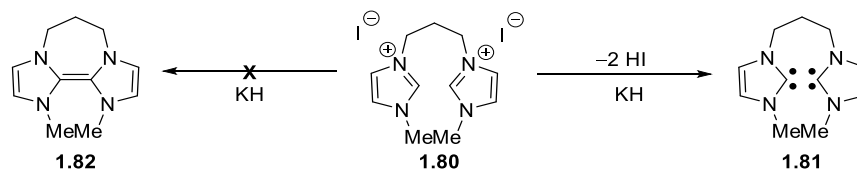
Scheme 1.19 – Mechanism of active donor formation

This donor was used to reduce a number of different aryl iodides, producing cyclised products in good yield. In this reaction, the active donor is generated *in situ* using KHMDS as the base. When the same reactions were attempted with aryl bromides, the reactions proceeded much more sluggishly and, with aryl chlorides, there was little-to-no reactivity observed.



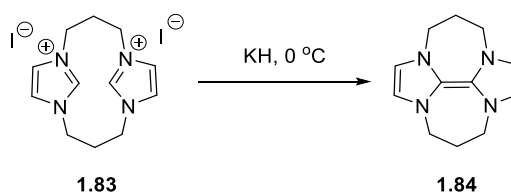
Scheme 1.20 – Cyclisation of **1.78** using SED **1.75**

This was the first example of a neutral organic electron donor in its ground state being capable of reducing an iodoarene. However, as it was known that gaining aromaticity increases the strength of an electron donor, the Murphy group next looked at forming an imidazole-derived donor; on oxidation this would afford a greater aromatic stabilisation. To prepare a similar salt, **1.80** to the benzimidazole-derived, **1.74**, would prove ineffective as a source of **1.82** as Chen *et al.* had previously shown that a dicarbene, **1.81** formed from deprotonation of **1.80** rather than the desired electron-rich alkene, **1.82**.⁶⁵



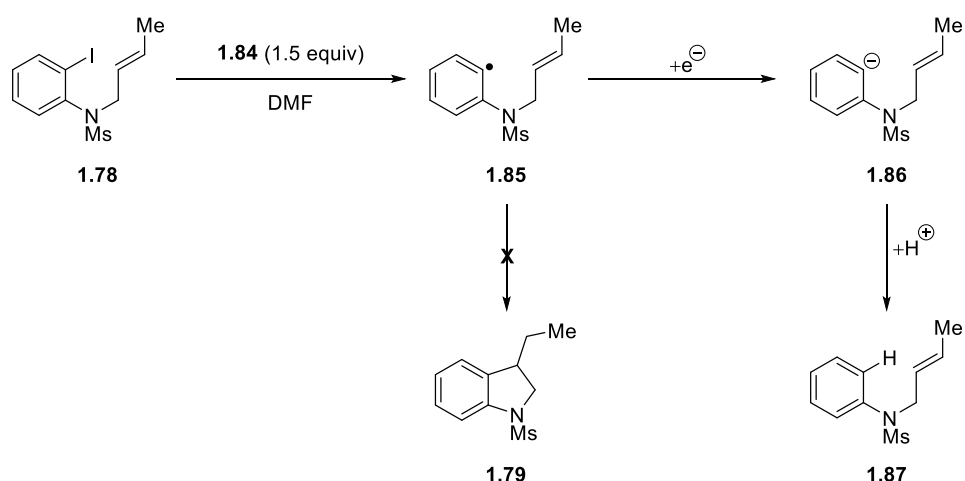
Scheme 1.21 – Dicarbene formation from **1.80**⁶⁵

To overcome this, following Chen's example it was decided to try the doubly-bridged imidazole salt **1.83**. This was capable of forming the electron-rich alkene, **1.84**, in the same way as the benzimidazole derived donor (i.e. deprotonation with NaH).



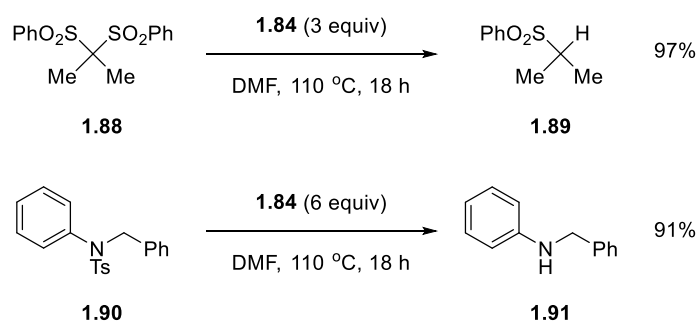
Scheme 1.22 – Formation of donor **1.84** from salt **1.83**

When this donor was used in the same type of reaction as that studied with the benzimidazole derived donor, **1.75**, the major product was the deiodinated arene, **1.87**, rather than the cyclized product **1.79**. This suggested that a second electron was rapidly donated from the donor to **1.85** as if an aryl radical, **1.85** had even a modest lifetime, this would rapidly cyclize to ultimately afford **1.79**.⁵⁶



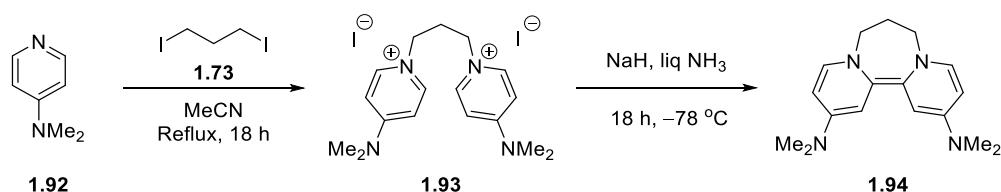
Scheme 1.23 – Generation of aryl anion using donor **1.84**

In addition to being able to reduce aryl iodides, this imidazole-derived donor was also capable of performing the reductive cleavage of sulfones and arenesulfonamides. Classical methods for this reduction often used alkali metals, SmI_2 with HMPA or LiAlH_4 ; this method using an organic SED used less harsh conditions without the need for aggressive metal-containing reducing agents.⁶⁶ This method was very effective in the reduction of sulfones and certain arenesulfonamides with yields >90%.



Scheme 1.24 – Reduction of sulfones and sulfonamides using SED **1.84**⁶⁶

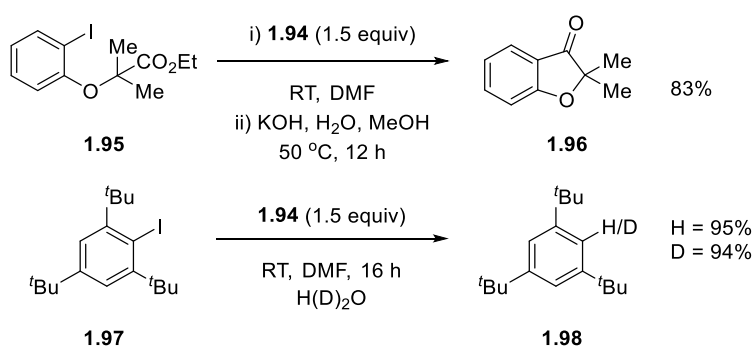
While this donor was effective and strong, the synthesis was an issue in that in the reaction in which it was prepared, the salt **1.83** had to be separated from a macrocyclic analogue. As a result, a more convenient but equally effective electron donor was sought. The solution to this was the 4-DMAP derived donor, **1.94**. This was easily synthesized from precursor salt, **1.93**, itself easily prepared from DMAP, **1.92** and 1,3-diiodopropane, **1.73** with minimal purification required.^{67, 68}



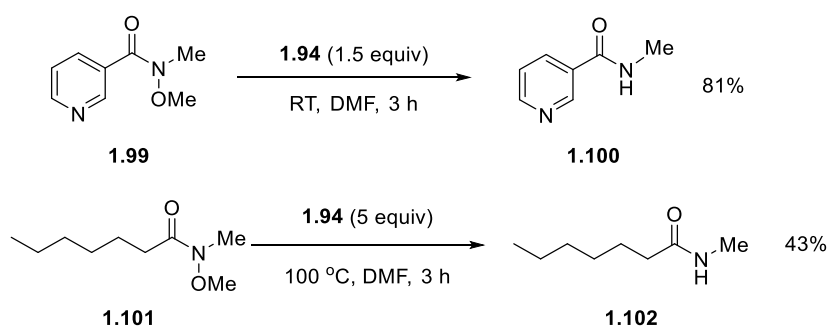
Scheme 1.25 – Synthesis of 4-DMAP derived donor **1.94**^{67, 68}

Again, like the previously reported examples, this SED was also capable of reducing aryl iodides (Scheme 1.26). An example is shown where substrate **1.95** cyclises to **1.96**. To undergo this transformation, **1.95** receives 2 electrons; these could both come from one molecule of DMAP donor **1.94** or one each from two molecules of DMAP donor **1.94**. Here DMAP donor **1.94** reduces **1.95** to an aryl anion which attacks the ester in a 5-*exo*-

trig cyclisation, losing ethoxide anion and producing product **1.96**. Another double-electron transfer (DET) example, is where substrate **1.97** gets reduced to an aryl anion and this picks up either a proton or deuteron depending on the source, producing **1.98**. At room temperature, DMAP donor **1.94** was capable of reducing aryl iodides; by increasing the temperature to 100 °C, 9-bromoanthracene and 9-chloroanthracene were both reduced to anthracene showing the strength of donor **1.94**.⁶⁹ Donor **1.94** was further tested with Weinreb amides, e.g. **1.99**, and was able to perform the reductive cleavage of N-O bonds. This was achieved in good yield with a wide range of substrates, although some more challenging substrates, e.g. **1.101** required higher temperatures and more equivalents of the donor to force the reaction to completion.⁷⁰

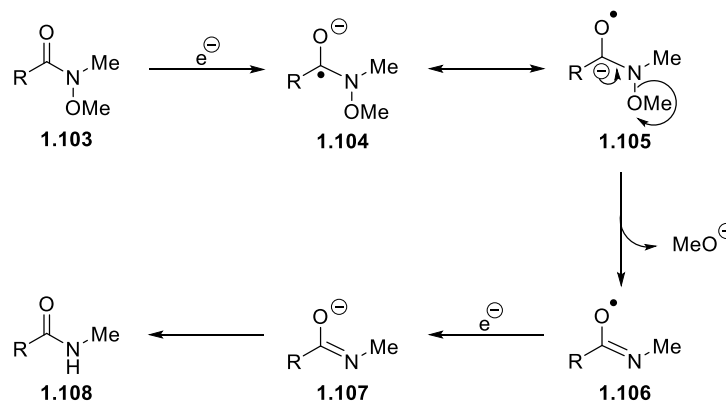


Scheme 1.26 – Reduction of aryl iodides by **1.94** by SET and DET pathways⁶⁹



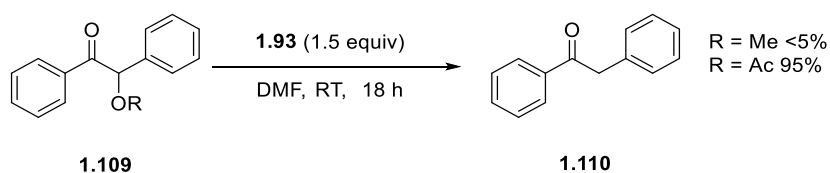
Scheme 1.27 – Reductive cleavage of Weinreb amides by **1.94**⁷⁰

To achieve this reduction, **1.94** donates an electron into the LUMO of the Weinreb amide, **1.103**, this forms the radical anion **1.104**, a resonance form of which is **1.105**. This can fragment as shown to form the new radical **1.106**. Following a second electron transfer and pick of a proton on work up, the product **1.108** is formed.



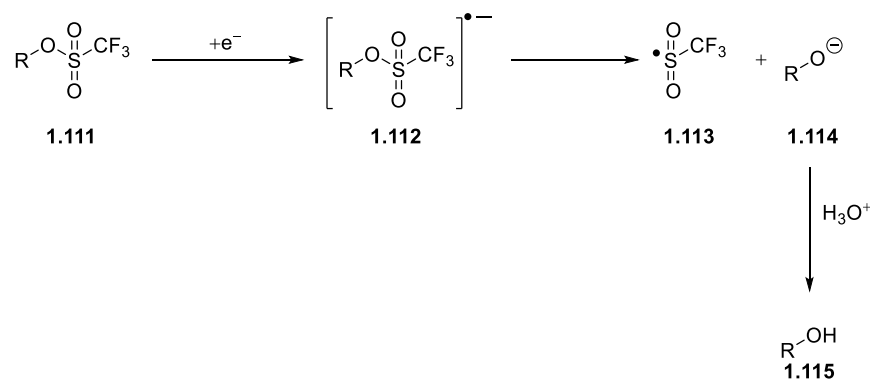
Scheme 1.28 – Mechanism of reductive cleavage of Weinreb amides⁷⁰

In addition to the reductive cleavage of N-O bonds, the 4-DMAP derived donor **1.94**, has also been shown to reductively cleave C-O σ -bonds in acyloin derivatives and S-O bonds in aliphatic and aryl triflates. Cutulic *et al.* firstly showed the C-O bond cleavage could occur in excellent yield at room temperature; however, this depended on the stabilisation of the anionic leaving group in **1.109**. When the leaving group was methoxide, very little reduced product was recovered (<5%). However, when the methoxy group was replaced with more electron-withdrawing groups, such as pivalate or acetate, then excellent yields of benzyl ketones **1.110** were achieved (93-98%). The mechanism proposed for this cleavage is analogous to that of the Weinreb amide N-O cleavage.⁷¹



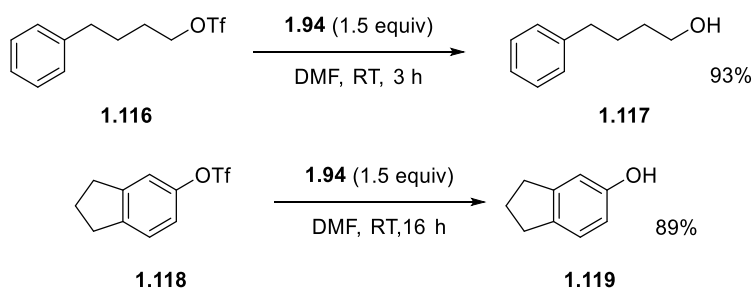
Scheme 1.29 – Reductive cleavage of C-O σ -bonds in acyloin derivatives⁷¹

Jolly *et al.* later went on to show that when donor **1.94** was reacted with aliphatic and aryl triflates, the corresponding alcohols were produced. The proposed mechanism of this cleavage is again very similar to the Weinreb amide N-O bond cleavage. In this case the triflate, **1.111** receives an electron from the donor to generate a radical anion, **1.112**. **1.112** then undergoes an easy fragmentation to afford a radical, **1.113** and anion, **1.114** pair. Upon work up **1.114** can pick up a proton to form the alcohol **1.115**.⁷²



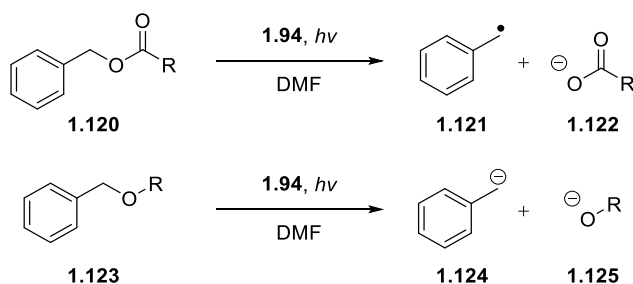
Scheme 1.30 – Mechanism of reductive cleavage of S-O bonds⁷²

As shown in Scheme 1.31, this was a useful method of reducing triflates to alcohols with mild reaction conditions.



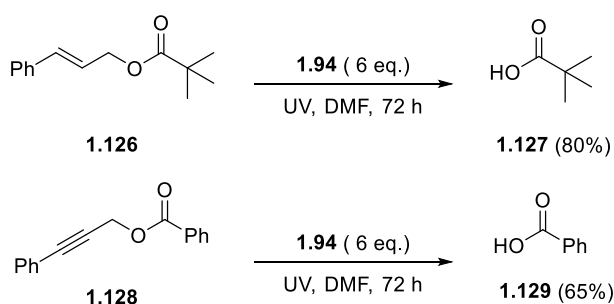
Scheme 1.31 – Reduction of triflates by donor **1.94**

This theme of reductive cleavage was even further exploited when Doni *et al.* looked into the cleavage of benzylic esters and ethers. What made this work interesting was that fragmentation occurred after SET for esters but after double electron transfer for ethers. Another significant observation of this work was that irradiating the DMAP derived donor, **1.94**, with ultra violet light at 365 nm enhanced the reducing capability of the donor and allowed the reduction of substrates that they would not necessarily be expected to be capable of reducing.⁷³



Scheme 1.32 – Differing mechanisms of reductive cleavage for benzylic esters and ethers⁷³

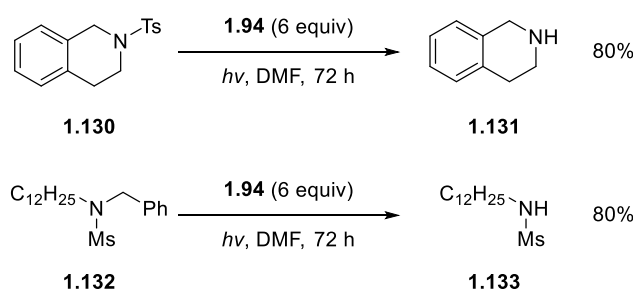
Chua *et al.* later extended the cleavage of esters to extended π -systems. In this case the electron often gets injected into one side of the molecule and then works round the π -system to achieve the desired cleavage. The π -system could be extended using either vinyl or alkyl links. Again, photoactivating the DMAP donor allowed it to be of sufficient strength to reduce these substrates.



Scheme 1.33 – Reductive cleavage of esters in extended π -systems⁷⁴

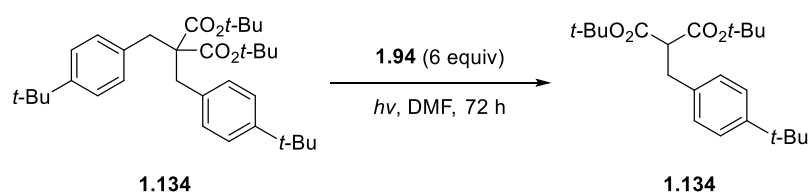
These transformations again show the strength of the DMAP donor **1.94**. As previously mentioned, photoactivation of **1.94** increases the strength and this is further shown in the cleavage of S-N and C-N bonds by photoactivated **1.94**.⁷⁵ Scheme 1.24 had shown that, in the ground state, donor **1.84** could reduce arenesulfonamides. This was possible as the nitrogen leaving group was stabilized by resonance. However, this was not possible with dialkyl arenesulfonamides as there the prospective nitrogen leaving group would have no resonance stabilisation and this made the reduction impossible. By photoactivating donor **1.94** this was able to reductively cleave dialkyl arenesulfonamide, **1.130**, to the parent amine, **1.131**. An alternative example is the reductive C-N bond

cleavage of **1.132** to **1.133**; this was an example where the nitrogen involved in the cleavage was not in a ring.



Scheme 1.34 – Photoactivated reductive cleavage of challenging S-N and C-N bonds⁷⁵

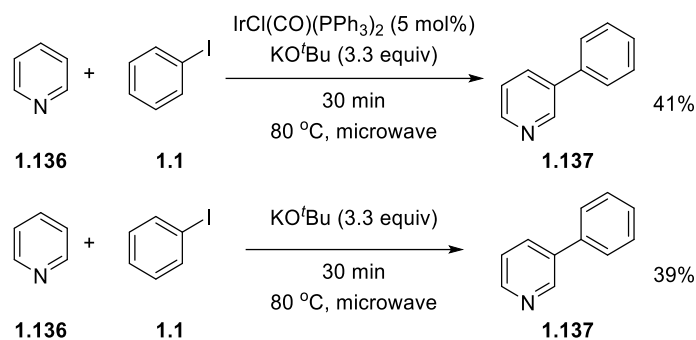
Recently Doni *et al.* further exploited this idea to selectively reduce arenes over malonates and cyanoacetates. This was surprising, as esters are easier to reduce (~ -3.0 V vs SCE) than arenes (~ -3.6 V vs SCE). This was the first example of preferential benzylic C bond cleavage over reaction at the esters.⁷⁶



Scheme 1.35 – Selective cleavage of sp^3 benzylic carbon bond over cleavage at the ester⁷⁶

1.8 New Attempts at Transition Metal-Free Cross Coupling

Itami *et al.* were the first to publish a transition metal-free biaryl coupling whilst proposing an SET mechanism. The research group were investigating various iridium catalysts in the reaction between aryl iodides and electron-deficient heterocycles under microwave conditions. However, whilst carrying out a “blank” reaction with iodobenzene, **1.1**, and pyridine, **1.135**, without any iridium catalyst present, they found that the reaction yield of their desired product was similar to the yield found when using their best iridium catalyst, (Scheme 1.36).



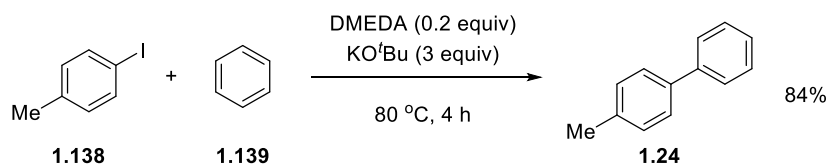
Scheme 1.36 – Itami’s transition metal-free biaryl synthesis⁷⁷

Having found this unexpected result, they then looked at other aryl halides coupling to **1.136** under similar reaction conditions. It was found that iodobenzene was the most efficient, followed by bromobenzene whilst chloro- and fluorobenzene produced no significant yield of product.

As with the earlier Leadbeater work, Itami’s work also appeared to be transition metal-free. To prove that this was indeed the case, Itami *et al.* extensively purified the reagents and thoroughly cleaned the glassware. ICP-MS analysis of the potassium *tert*-butoxide showed no transition metals above the detection limits of the equipment (60 ppb for Pd). Although this was encouraging, Leadbeater showed that even lower concentrations of palladium could be responsible for the reactivity.

Itami *et al.* found that the reaction conditions developed were applicable to pyridazine, pyrimidine and quinoxaline, all of which coupled with iodobenzene in moderate yields. The reactions of 3- and 4-iodoanisole with pyrazine did not give the regioisomers associated with a benzyne-mediated process. This suggested there was an alternative pathway driving these reactions. As the reaction was completely shut down in the presence of radical scavengers, it was proposed that these reactions were proceeding via a radical-based mechanism.

Following on from Itami’s work, other research groups began to publish their own transition metal-free biaryl coupling reactions using different conditions. The first of these was by Kwong and Lei *et al.*,⁷⁸ who successfully used a combination of potassium *tert*-butoxide and different reagents to promote the coupling of 4-iodotoluene, **1.138** and benzene, **1.139**, Scheme 1.37.

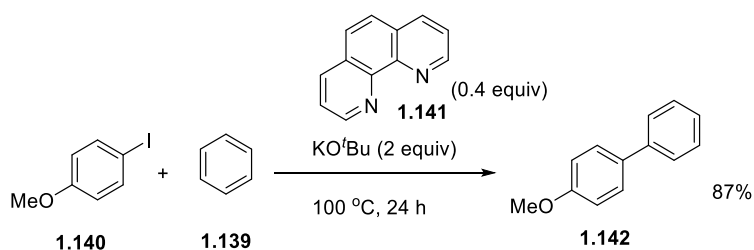


Scheme 1.37 – Transition metal-free coupling under Lei conditions⁷⁸

Whilst a number of different organic additives, often diamines and alcohols with free –NH or –OH, were observed to promote this reaction as additives, it was found that potassium *tert*-butoxide was the only base that was effective in the transformation. On the basis that a mixture of regioisomers was not formed, Lei ruled out the possibility of a benzyne-based mechanism. Similarly to Itami’s work, radical scavengers shut down the reaction. To this point, there had been no mechanism proposed. Previously, however Wotiz *et al.* had reported the formation of pyrazine radical anion species from the reaction of vicinal diamines such as DMEDA with a strong base;⁷⁹ it was thought that a similar condensation to a radical anion could potentially be the source of radical initiations in these coupling reactions. An alternative source of initiation from DMEDA could be a series of deprotonations to form an electron-rich alkene that could act as an electron donor in these transformations.

At around the same time, two independent groups (Shi *et al.*⁸⁰ and Hayashi *et al.*⁸¹) were publishing work on the same transformation as reported by *Lei et al.* Their work however centred on the use of 1,10-phenanthroline, **1.141**, and derivatives of this, to promote biaryl coupling reactions. Both groups however proposed differing mechanisms.

Shi *et al.* had set out to probe cobalt-catalysed biaryl synthesis. Despite obtaining a good yield with their “catalyst”, like Itami before, in the absence of their catalyst, the yield was comparable. Their initial work focused on the coupling between 4-iodoanisole, **1.140** and benzene, **1.139**, in the presence of potassium *tert*-butoxide and phenanthroline, Scheme 1.38.



Scheme 1.38 – Biaryl synthesis promoted by phenanthroline by Shi *et al.*⁸⁰

Shi proposed that a combination of π,π -stacking and ion- π interactions could give rise to a complex shown in Figure 1.2. This complex was proposed to be responsible for initiating the radical process by electron transfer to an aryl halide, but this was simply a proposal. There was no experimental or computational evidence provided for this.

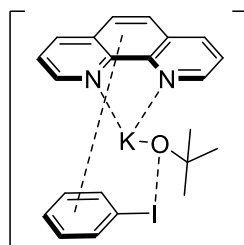
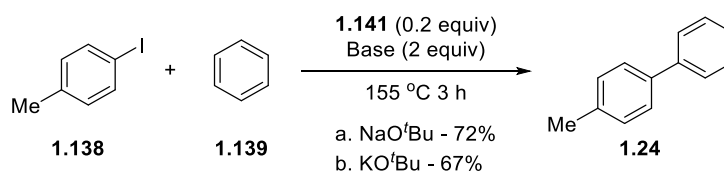


Figure 1.2 – Complex proposed by Shi that initiates a radical process⁸⁰

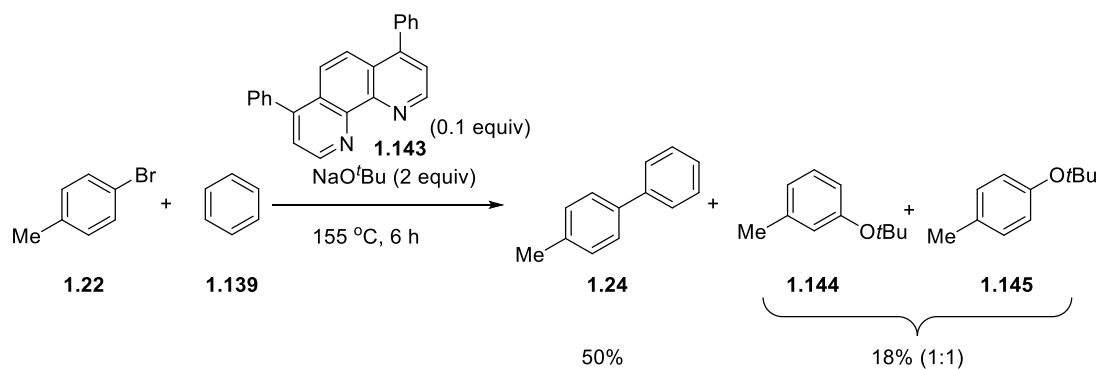
A shortcoming of Shi's work was that there was no investigation of base effects. However, Hayashi *et al.* did investigate this factor in more detail using very similar reagents. They took the reaction between 4-iodotoluene, **1.138**, and benzene, **1.139**, as their model reaction and attempted the biaryl synthesis, producing **1.24**, using **1.141** in combination with a number of different bases, (Scheme 1.39).



Scheme 1.39 – Investigation of alkoxide base in the biaryl synthesis⁸²

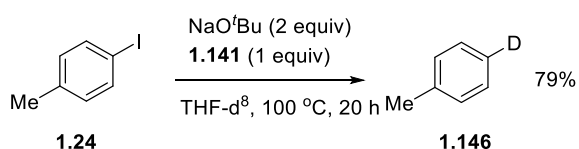
Contrary to Lei's result,⁷⁸ they found that sodium *tert*-butoxide offered a comparable yield to that seen with potassium *tert*-butoxide.

An interesting observation in Hayashi's work was that elevated temperatures did produce 3- and 4-(*tert*-butoxy)toluenes, **1.144/1.145**, (Scheme 1.40) characteristic of an aryne-mediated reaction, along with the expected coupled product. This suggests that, at these higher temperatures, benzyne formation occurs from deprotonation *ortho* to the bromide.



Scheme 1.40 – Evidence of the presence of benzyne in Hayashi coupling reactions⁸¹

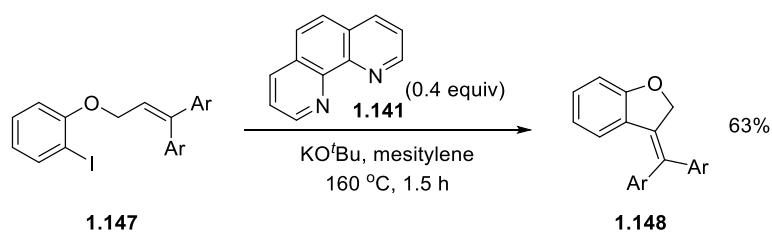
To support the idea that an aryl radical was being formed from the dissociation of an aryl halide radical anion, 4-iodotoluene, **1.138** was treated with phenanthroline, **1.141** and sodium *tert*-butoxide in deuterated THF. 4-Deuteriotoluene, **1.146** was obtained in good yield (79%), showing that aryl radicals were being formed by the dissociation of iodide from the aryl ring (Scheme 1.41).



Scheme 1.41 – Abstraction of deuterium from THF-d⁸

1.9 Transition Metal-Free Heck-type Reactions

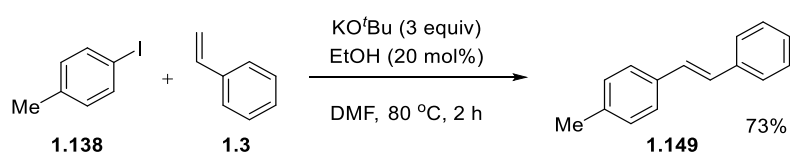
A number of groups looked at Heck-type reactions using this transition metal-free methodology. Bui *et al.* looked at an intramolecular reaction with **1.147** receiving an electron and undergoing a 5-*exo-trig* cyclisation to form **1.148**.⁸³



Scheme 1.42 – Heck-type cyclisation of **1.147** in presence of **1.141**/KO^tBu⁸³

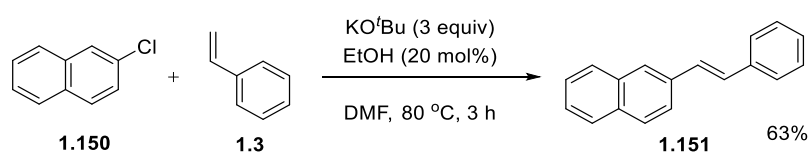
They proposed that the electron was transferred to the aryl iodide from the complex suggested by Shi *et al.*⁸⁰ Through this reaction, they were able to prepare a range of benzofurans, although with not much variation in the functional groups.

Hayashi *et al.* were also able to perform Heck-type reactions mediated by KO^tBu. Where their method differed from Bui was that theirs was intermolecular from an aryl halide to a styrene derivative.⁸⁴ These reactions used ethanol as an additive and DMF as the solvent with KO^tBu as the base; compared with other reactions, they feature relatively low temperatures and short reaction times of 80 °C and 2 h respectively.



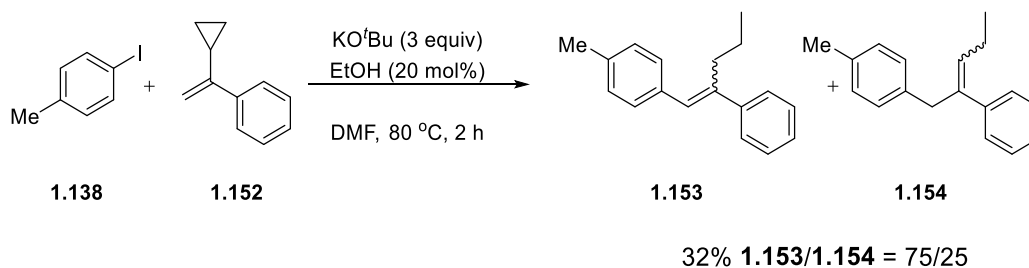
Scheme 1.43 – Hayashi *et al.* Heck-type coupling reaction⁸⁴

They propose that the electron is transferred from *tert*-butoxide anion directly to form the aryl radical that attacks styrene. This proposal is up for debate as there was a number of alternative electron donors that could have been in the solution. A significant reaction that was performed was a coupling of 2-chloronaphthalene with styrene. Aryl chlorides are often more difficult to reduce than aryl iodides but, under these conditions, Hayashi *et al.* were able to produce the coupled product in 63% yield.



Scheme 1.44 – Hayashi's coupling of 2-chloronaphthalene with styrene⁸⁴

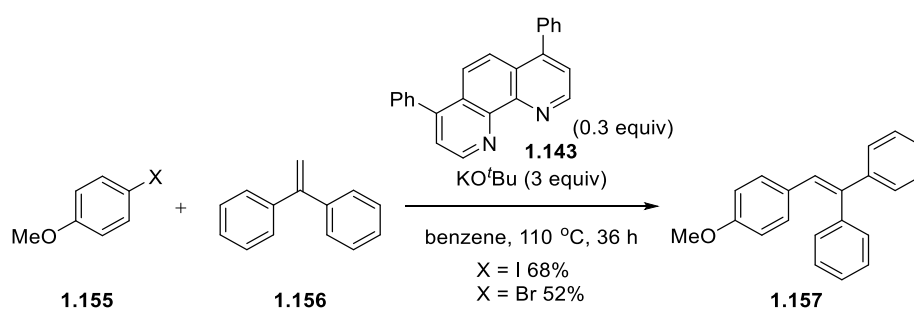
An interesting feature of this work was evidence for radicals by use of radical clock, **1.152**. In this case they performed the reaction with 4-iodotoluene, **1.138**, KO^tBu, EtOH and DMF as before. As they gained two products (**1.153** and **1.154**) both of which had the cyclopropane ring opened, this was evidence for the mechanism involving radicals; what it didn't give evidence for the source of the electron.



Scheme 1.45 – Evidence for radicals in Hayashi's transition metal-free Heck reactions⁸⁴

Shi *et al.* also published an arylation of alkenes through an “organocatalytic radical process”.⁸⁵ In their version, they take iodo/bromo arenes and couple these to 1,1-diphenylethylene, **1.156**, in the presence of bathophenanthroline, **1.143**, KO^tBu and benzene. They developed a relatively wide substrate scope on the aryl iodide but had only one example of an alkene without two phenyl groups attached.

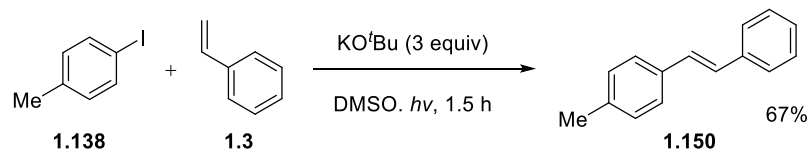
They proposed that the electron is transferred to the aryl halide from a complex formed between **1.143** and KO^tBu, as had been proposed a number of times.



Scheme 1.46 – Shi's coupling of aryl halides with 1,1-diphenylethylene **1.156**⁸⁵

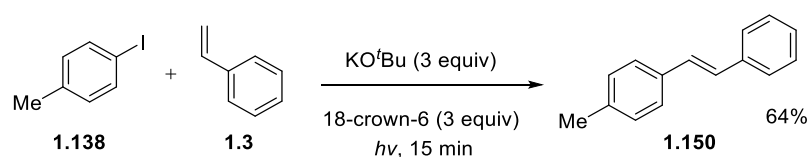
A final group who looked at transition metal-free Heck-type reactions was the Rossi group.⁸⁶ Previous to this work, the reactions had required high temperatures and a solvent, but Rossi claimed to have a different approach that was solvent-free and

operated at room temperature. The initial study looked at photoirradiation of 4-iodotoluene, **1.138**, styrene **1.3**, KO^tBu and DMSO at room temperature and gave a yield of 67% with 86% conversion of the starting aryl iodide.



Scheme 1.47 – Rossi’s Heck-type coupling reaction with DMSO under photo condition⁸⁶

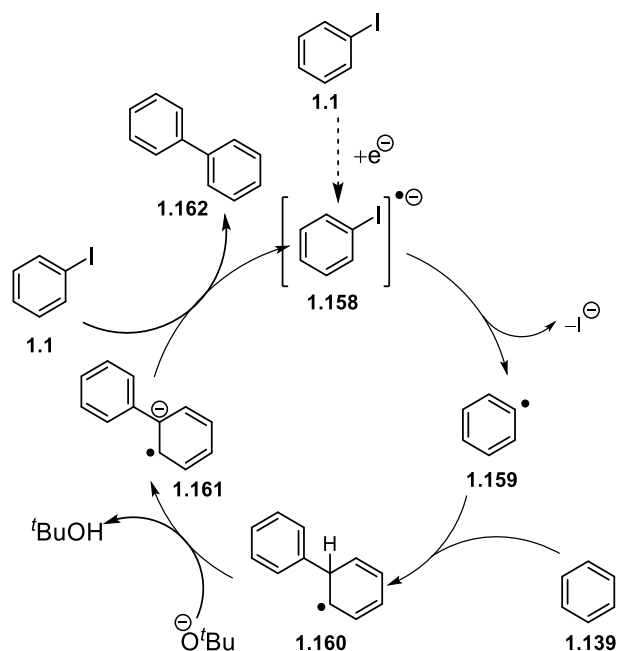
Initially when the reaction was attempted without DMSO, no yield of product was recovered. This was suspected to be due to the insolubility of KO^tBu in the reaction medium. To overcome this, 18-crown-6 ether was added to the reaction mixture to coordinate to the potassium cation. After this addition, the yield of the solvent-free reaction increased to 64%. Their proposal was that the free butoxide anion could act as the electron donor, as it is known that in photostimulated reactions KO^tBu can start the chain process.^{87, 88} This reaction worked with iodine, bromine and chlorine as the halide. It is also known that KO^tBu is capable of deprotonating DMSO to form an anion capable of reducing iodoarenes however as only DMSO and DMF (this can also form electron donor with KO^tBu) were the only solvents used, there was no evidence that it wasn’t one of these species that initiated these reactions.



Scheme 1.48 – Solvent-free Heck-type reaction⁸⁶

1.10 Initiation of Transition Metal-Free Cross Coupling Reactions

In 2010, an essay from Studer and Curran proposed that a base-promoted homolytic aromatic substitution (BHAS) mechanism, (Scheme 1.49),⁸⁹ is involved in these transition metal-free transformations.



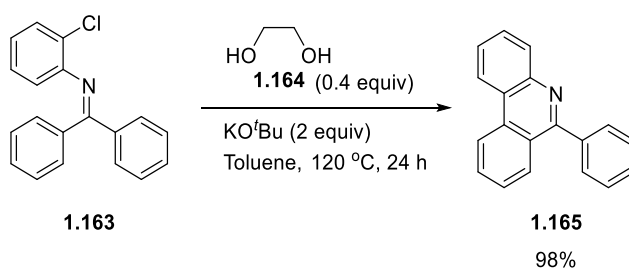
Scheme 1.49 – Widely accepted BHAS mechanism proposed by Studer and Curran⁸⁹

The key feature of the mechanism is the generation of the radical anion, **1.161**, that is known to be a powerful reducing agent. The pathway shows that after an aryl iodide receives an electron, there is a loss of iodide generating an aryl radical, **1.159**. This radical reacts with benzene to give rise to a cyclohexadienyl radical, **1.160**. This radical is deprotonated by *tert*-butoxide to form the radical anion, **1.161**, and this transfers an electron to another aryl iodide molecule, propagating the cycle and the resulting radical anion rearomatises to produce the coupled product, **1.162**.

A shortfall of Studer and Curran's proposed mechanism is that it does not detail where the electron responsible for the initiation of the cycle comes from. The source of this electron was still under debate.

More recently, Studer and Curran have published another paper; this time they changed their terminology and proposed that the electron is a catalyst. They propose this ideology in not only BHAS reactions but also Heck, substitution and cross-dehydrogenative coupling radical reactions. They don't suggest any changes to the mechanisms of these reactions or where the electron comes from but merely suggest that the electron is the catalyst.⁹⁰

While a lot of research was being carried out into understanding how 1,10-phenanthroline, **1.141** was promoting biaryl synthesis, a number of other research groups were demonstrating that other simple molecules could promote these reactions. Kwong *et al.* demonstrated that ethylene glycol, **1.164**, was capable of promoting the intramolecular arylation of aryl chlorides e.g. **1.163**, to form the coupled product **1.165**, (Scheme 1.50).

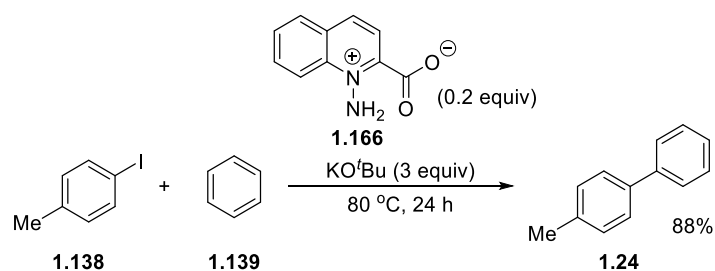


Scheme 1.50 – Intramolecular arylation of aryl chlorides⁹¹

Kwong's research showed that a number of diols promoted the transformation. However, when 1,2-diamines were employed in the reactions, they did not yield as much product. Another significant observation of Kwong's work was that aryl chlorides were successful in these transformations. Until this point, success with aryl chlorides had been limited and highly challenging.

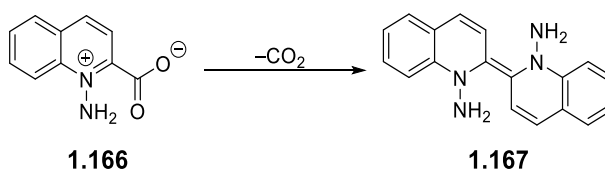
A number of publications had shown that amino acids and related structures are similarly capable of promoting biaryl coupling. Jiang *et al.* sought to develop a series of analogous reagents that could also achieve such reactions. Their work was based on the idea that the metal ion from butoxide complexes MO^tBu to the heteroatoms in the simple molecule, thus creating the species capable of initiating the reaction. As the phenanthroline complex of a metal ion example is a 5-membered cyclic complex, they proposed that forming a 6-membered cyclic complex would provide enhanced reactivity.⁹²

To test their hypothesis, **1.166** was used as a promoter and the coupling of 4-iodotoluene, **1.138** and benzene, **1.139** with potassium *tert*-butoxide as the base, was chosen as a model reaction, (Scheme 1.51). This work showed that the molecules they designed were capable of promoting the reaction.



Scheme 1.51 – Biaryl coupling under Jiang's conditions⁹²

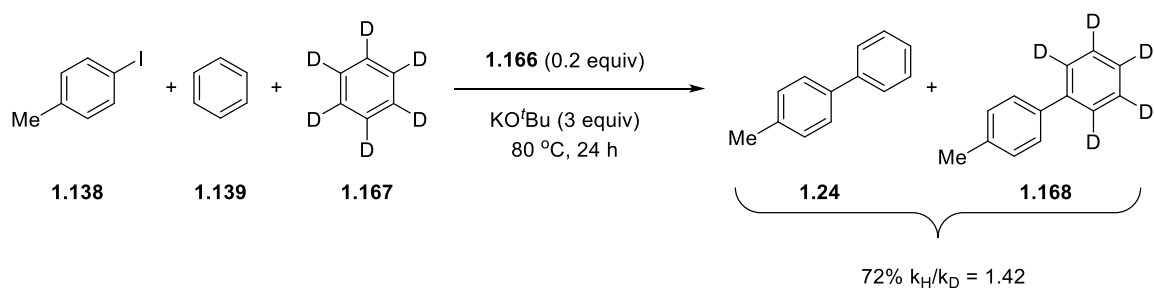
An alternative to a 6-membered cyclic complex being the initiation could be a dimerisation of 2 molecules of **1.166** through the loss of CO₂ to form **1.167**, which resembles a standard SED reagent.⁹³



Scheme 1.52 – An alternative species that could initiate Jiang's coupling reactions

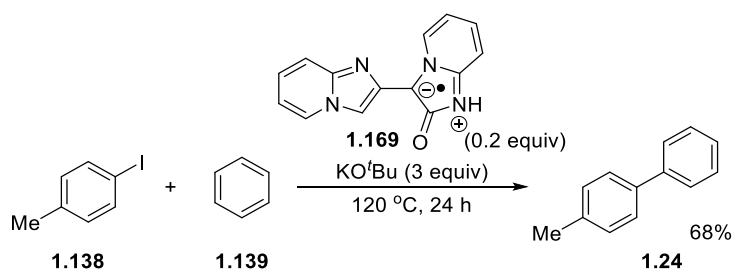
To rule out the possibility of a benzyne-mediated reaction, the reaction was run in the absence of their promoters. These reactions gave none of the desired product. Benzyne-mediated reactions generally require a higher temperature to initiate, or at least this was the reason given for the lack of reaction.

When alternative bases (sodium *tert*-butoxide, potassium carbonate and potassium hydroxide) were tested under the same reaction conditions, none was capable of forming the desired product.⁹⁴ As part of their study a kinetic isotope experiment was carried out, (Scheme 1.53). They found the k_H/k_D was 1.42. Their observation of a low k_H/k_D implies that the rate determining step in these reactions is not the loss of hydrogen/deuterium. If the ratio had been significantly higher, then the loss of hydrogen or deuterium would have been the rate determining step.



Scheme 1.53 – Kinetic isotope experiment showing that loss of H/D is not the rate determining step⁹²

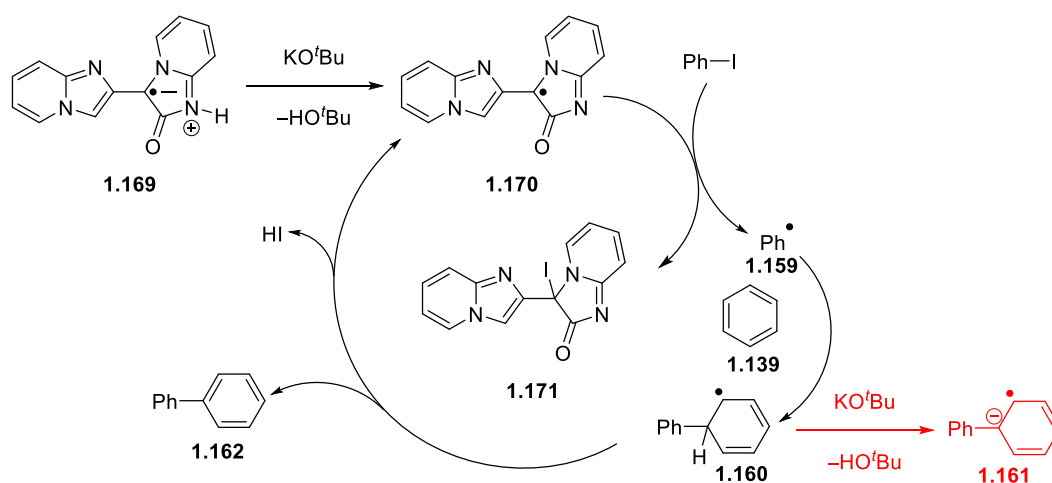
Li *et al.* investigated stabilised organic radicals as a source of initiation.⁹⁵ Their choice was the stable zwitterionic radical Hbipo, **1.169**, this was employed in the same way as other additives such as phenanthroline, **1.141**, in substoichiometric amounts and excess KO^tBu in benzene. This structure for radical **1.169** however is not possible as either deprotonation or hydrogen abstraction of an sp^3 carbon adjacent to the carbonyl group in any precursor would produce either an anion or a radical respectively, but not the radical anion shown.



Scheme 1.54 – Coupling of 4-iodotoluene with benzene in the presence of stabilised zwitterionic radical **1.169** by Li *et al.*

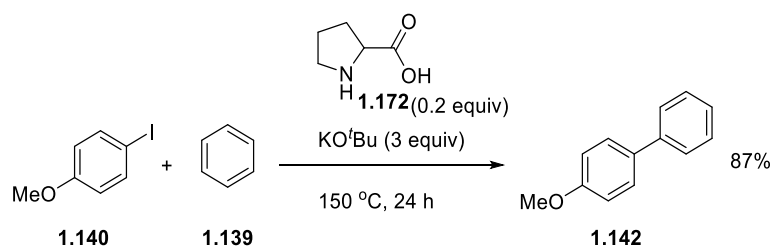
Although the radical cannot exist, they propose that the reaction proceeds through a homolytic aromatic substitution (HAS) pathway. They propose that Hbipo, **1.169** is deprotonated by KO^tBu to form radical **1.170** (charges do not balance in this transformation) this radical then abstracts iodide from the aryl iodide generating a phenyl radical, **1.159**. This phenyl radical then attacks a molecule of benzene to generate cyclohexadienyl radical **1.160**, they propose that this radical causes homolysis of the C-I bond formed from the abstraction carried out by **1.170**, (this looks like a most unlikely atom transfer as a highly reactive phenyl radical, **1.159**, is generated from a highly

stabilised captodative radical **1.170**) regenerating the radical and propagating the cycle. There is nothing to suggest that cyclohexadienyl radical **1.160** couldn't be deprotonated by KO^tBu to form radical anion **1.161** and it could be this entity that propagates the cycle in a BHAS cycle. The initiation of the BHAS cycle could be from an electron donor formed *in situ* in the reaction mixture. (Scheme 1.55 has issues; firstly, the charges do not balance in the deprotonation and secondly the abstraction of iodine from iodobenzene is unlikely to occur. This scheme is shown as published however, it is unlikely to be accurate)



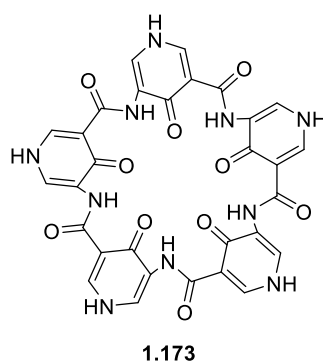
Scheme 1.55 – Proposed HAS mechanism by Li *et al.*⁹⁵

In 2012 Tanimori *et al.* looked specifically at proline, **1.172**, and other amino acids as biaryl-coupling promoters. Previous investigations into the reactivity of proline never went above 100 °C. However, in this work, the temperature was increased to 150 °C and subsequently the yield of product **1.142** improved significantly, from 47% to 87%, for the coupling of 4-iodoanisole and benzene, (Scheme 1.56). Increasing the temperature does however increase the contribution of the benzyne-mediated pathway (discussed fully in Scheme 1.70) and this should be noted when looking at the increased yield.

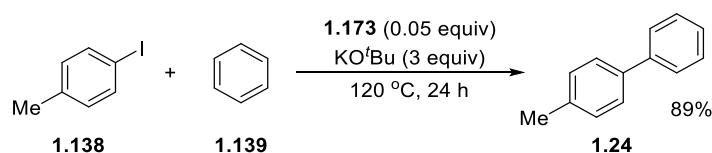


Scheme 1.56 – Biaryl coupling under Tanimori's conditions⁹⁶

Zeng *et al.* proposed a macrocyclic aromatic pyridone pentamer as a highly efficient additive for direct arylations of unactivated arenes.⁹⁷ They proposed that the macrocycle, **1.173**, would act in the same way as 18-crown-6 ether did in Rossi's photoactivated Heck-type reaction by liberating the butoxide anion allowing it to be the electron donor that initiated the reaction. Using **1.173** as the additive they were able to couple aryl iodides to benzene in high yield, while radical inhibitors stopped the reaction. They didn't do any investigation into their proposal for electron transfer. It is possible that the pentamer is deprotonated by KO^tBu and becomes electron-rich, this could be an electron donor that initiates the reaction rather than free butoxide anion, as an electron transfer from KO^tBu has been shown to be unfavourable.

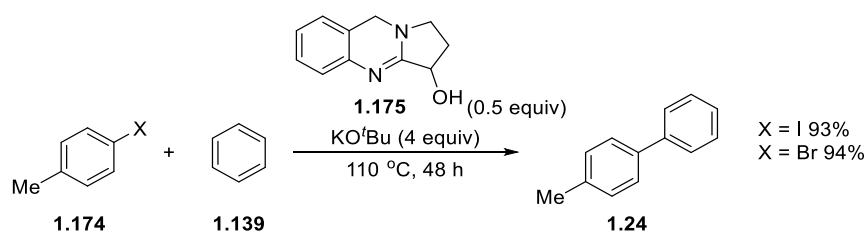


Scheme 1.57 – Macrocyclic aromatic pyridone pentamer⁹⁷



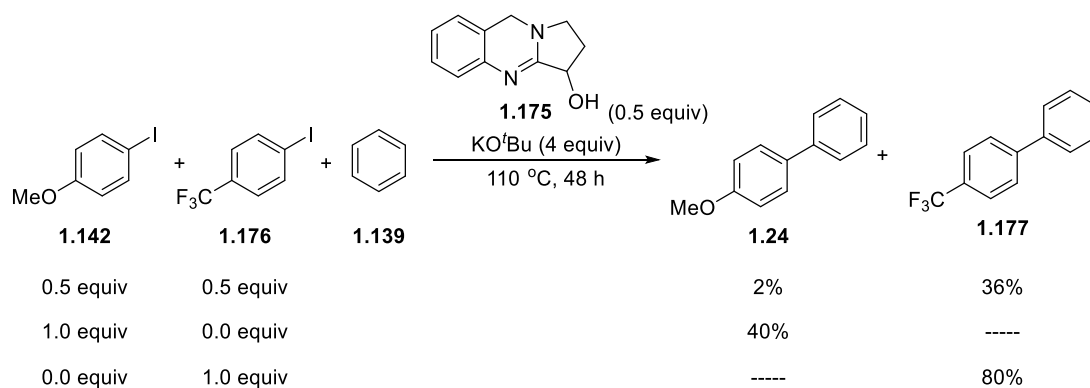
Scheme 1.58 – Zeng's reactions with aryl iodides and benzene in presence of **1.173** and KO^tBu

Kumar *et al.* investigated vasicine, **1.175**, as an additive for their coupling reactions. By using vasicine in substoichiometric amounts, with an excess of KO^tBu in benzene, with iodoarenes they were able to achieve yields of coupled product of up to 94%. When they switched to bromoarenes the reactions still proceeded equally as effectively in just as high a yield. The reaction time they used was longer than other groups at 48 h.⁹⁸ It is likely that **1.175** undergoes a double deprotonation to form an electron-rich alkene between the nitrogen and oxygen. It would be this species that would initiate the reaction.



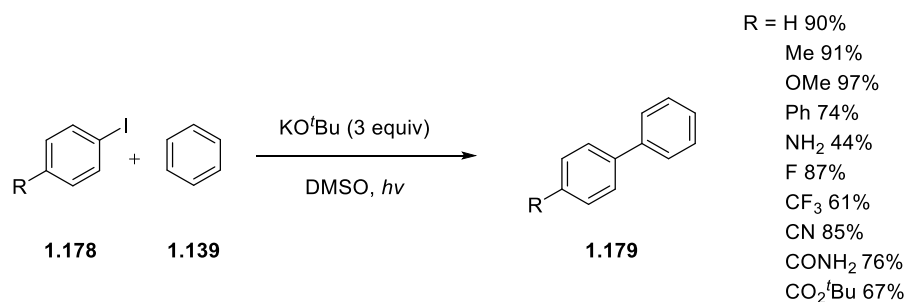
Scheme 1.59 – Kumar’s coupling of haloarenes with benzene using vasicine, **1.175**, as the additive⁹⁸

In a competition reaction, they performed the reaction for only 2 h and the yield was only 2% lower. In this competition, experiment they also found selectivity for an electron-deficient iodide over an electron-rich aryl iodide, (Scheme 1.60).⁹⁸



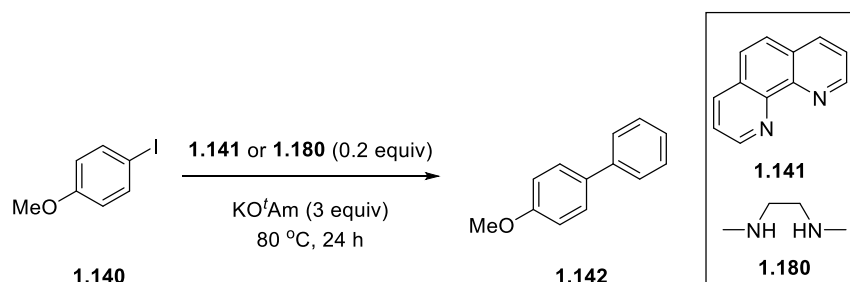
Scheme 1.60 – Competition reactions performed by Kumar *et al.*⁹⁸

Rossi *et al.* have also looked at transition metal-free coupling reactions. Similar to their Heck-type reaction, these reactions were performed at room temperature. They were able to develop a wide substrate scope.



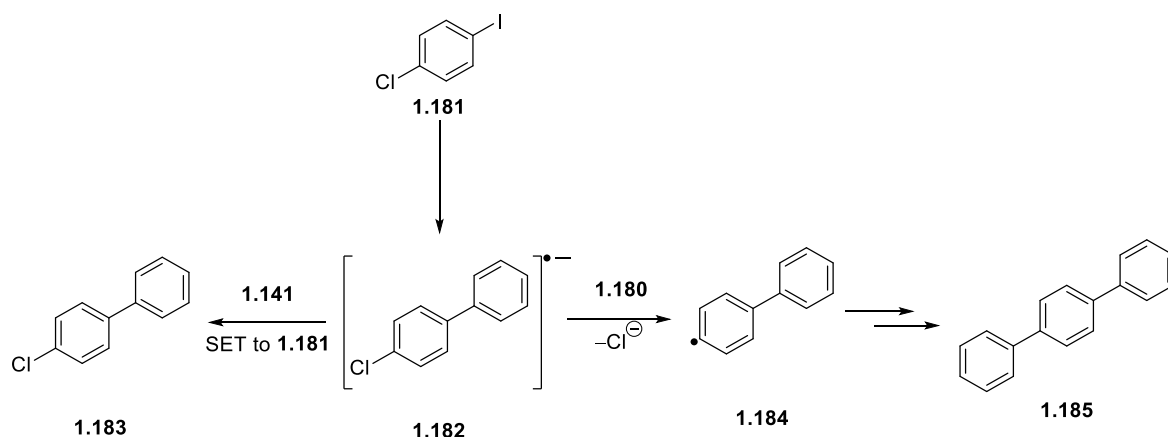
Scheme 1.61 – Rossi's photo cross coupling reactions⁹⁹

In 2015 Xu published a paper claiming “ligand-controlled chemoselectivity” in their transition metal-free cross coupling reactions that were promoted by potassium *tert*-amylate.¹⁰⁰ Their ligands of choice were DMEDA, **1.180** and phenanthroline, **1.141**. These were both known to promote the coupling of aryl halides to unactivated benzene in the presence of KO^tBu and it was also known that these reactions were chemoselective.



Scheme 1.62 – Xu's KO^tAm-mediated cross coupling¹⁰⁰

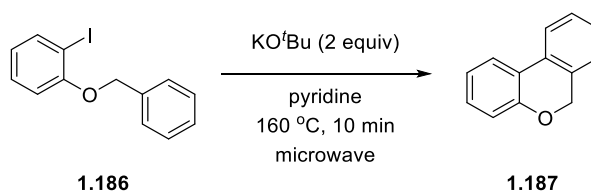
They claim that in a dihaloarene such as, **1.181**, different ligands give different products and this is therefore chemoselective. When phenanthroline was used as the additive, a single coupled product, **1.183** was formed and when DMEDA was the additive, the twice coupled product terphenyl, **1.185**, was formed.



Scheme 1.63 – Difference in chemoselectivity from the different additives¹⁰⁰

Their rationale for this was that when radical anion, **1.182** was formed in the presence of phenanthroline, **1.141**, the electron was transferred via this to another molecule of dihaloarene, whereas with DMEDA the electron in radical anion **1.182** remained in the molecule eventually losing chloride anion and then coupling to another molecule of benzene. Their proposal therefore is that the reaction depends on the nature and strength of the complex formed.

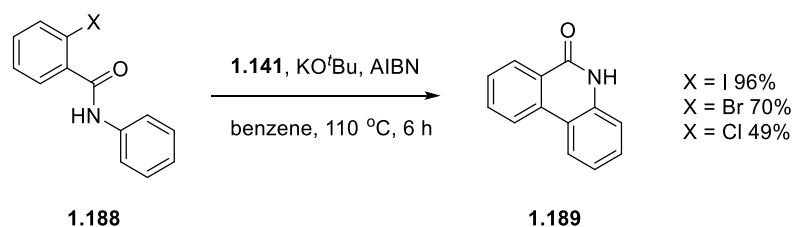
In 2011 Charette *et al.* published a paper detailing intramolecular coupling reactions. These were performed using potassium *tert*-butoxide in pyridine, and there was no diamine or diol species in the reaction. However, to their surprise, they managed to gain good yields of the coupled product **1.187**, (Scheme 1.64).



Scheme 1.64 – Biaryl coupling observed by Charette *et al.*¹⁰¹

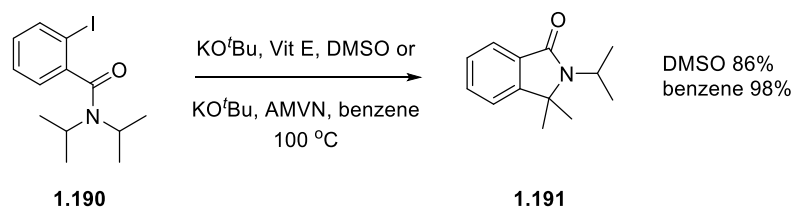
Although this reaction proceeds at high temperature, a benzyne-mediated pathway was ruled out as no products of trapping by butoxide anions were isolated or detected and, as with other similar reactions, this reaction was shut down by the addition of radical scavengers. As a result, a SET mechanism was proposed. However, there was no obvious electron donor species present in the reaction.

Kumar *et al.* also looked at intramolecular cyclisations by preparing biaryl lactams. They used the same phenanthroline/ KO^tBu mixture as seen previously by other groups; however, they also required AIBN to be present for the reaction to proceed. Their reactions were successful with iodine, bromine and chlorine in the *ortho* position.¹⁰²



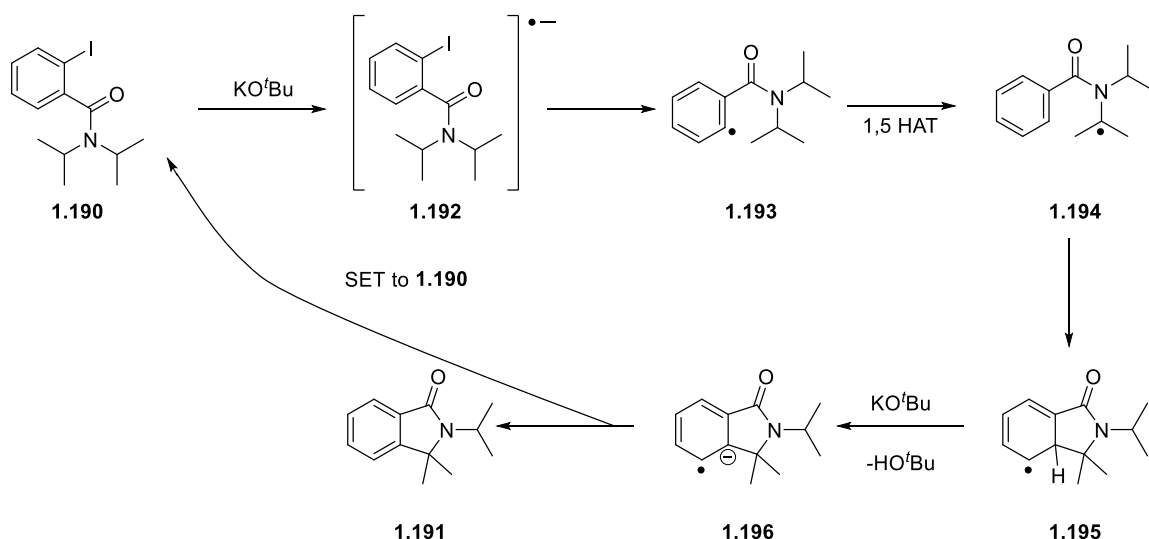
Scheme 1.65 – Phenanthroline promoted formation of biaryl lactams¹⁰²

A couple of years later, Kumar *et al.* further developed their cyclisations to include unreactive tertiary sp^3 C-H bonds. The conditions used were slightly different to those used previously; in DMSO they needed vitamin E as an additive and in benzene they used the radical initiator azomethylvaleronitrile (AMVN), with both cases being in the presence of KO^tBu .¹⁰³



Scheme 1.66 – Cyclisation of **1.190** to form **1.191**¹⁰³

The mechanism proposed in these reactions is slightly different to the BHAS coupling mechanism as it involves a 1,5 HAT. What is not clear from the proposed mechanism is where the electron transfer that initiates the cycle comes from. The propagation electron transfer will come from radical anion, **1.196**. In the paper, it's suggested that electron transfer comes from KO^tBu .¹⁰³ Whether or not the KO^tBu was donating an electron to **1.190** is unclear, but Kumar *et al.* found that KO^tBu was essential to the success of their reactions both in DMSO and benzene.



Scheme 1.67 – Proposed mechanism for sp^3 coupling by Kumar *et al.*¹⁰³

The absence of any obvious electron donors in Charette's work (Scheme 1.65) prompted an investigation by Murphy *et al.* into the initiation of these reactions. It had been suggested in the related work of Shi that a complex between a "ligand" and KO^tBu (Figure 1.3) is the species that donates an electron to an aryl iodide and, in turn, initiates the BHAS cycle. However when the energy profile of this complex donating an electron to aryl iodide were modelled using Marcus theory, it was found to be very endergonic ($+63.9 \text{ kcal mol}^{-1}$) and therefore unfavorable. When carrying out reactions of KO^tBu with phenanthroline a dark green precipitate was isolated. This was found to be converted into a dimer of phenanthroline, **1.197** on work-up.

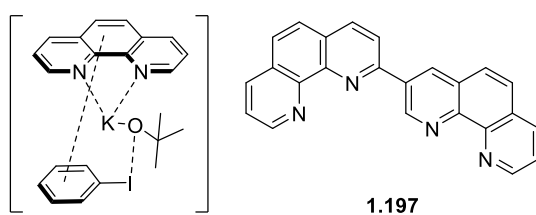
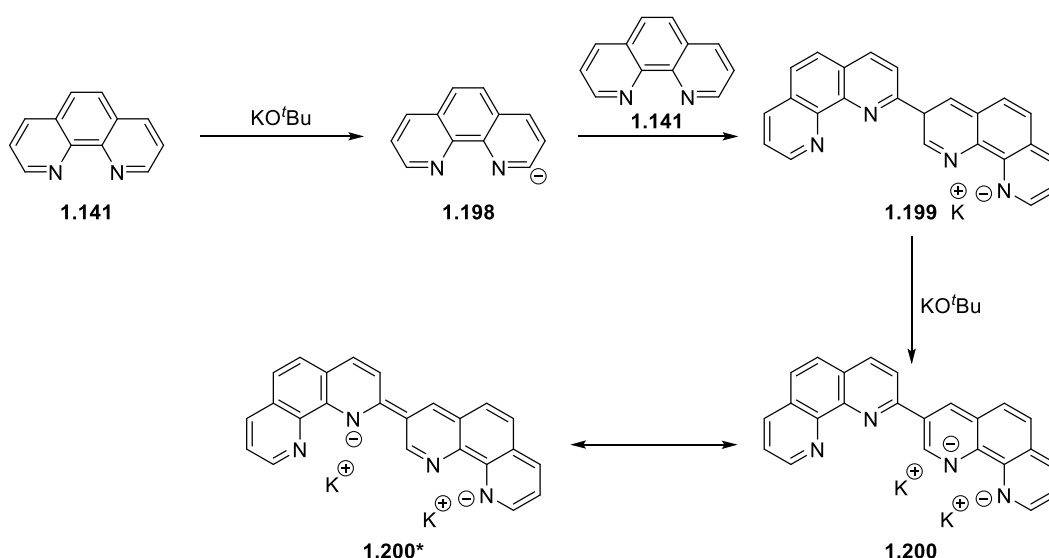


Figure 1.3 –Left: phenanthroline/ KO^tBu complex proposed by Shi *et al.* Right: phenanthroline dimer isolated by Murphy *et al.*¹⁰⁴

This precipitate was found to be very air-sensitive but when quenched with iodine, a very good electron acceptor, product **1.197** was isolated. This raised the question that if this is being formed in the reactions following work-up, what species could be donating the electron to the aryl halide? The dimer was formed by deprotonation and attack on

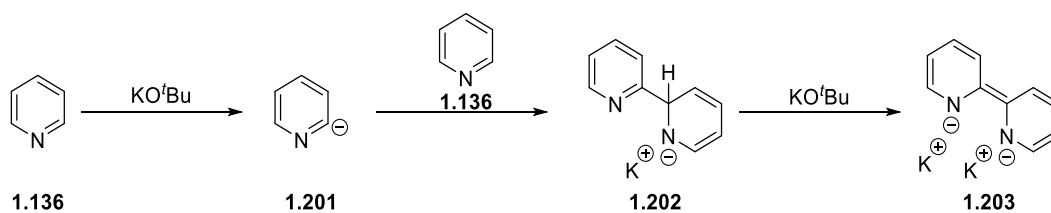
a second phenanthroline molecule to give **1.199**, a subsequent deprotonation gives **1.200** this species was proposed to be the electron donor in these reactions. The formation of this species was calculated to be exergonic ($-30 \text{ kcal mol}^{-1}$) and the electron transfer energy of this species to an aryl iodide was calculated to be favourable. This suggests that this is the more likely electron donor in these reactions compared to the phenanthroline/ KO^tBu complex.

This still left the question about why the reactions with pyridine as the solvent working as an electron donor. One option would be the deprotonation *ortho* to the iodide generating benzyne and this could attack the arene and start the subsequent reaction (this option will be discussed in more detail later). The alternative is that a similar dimerization with pyridine occurs.



Scheme 1.68 – Formation of dimer **1.200** through deprotonations with KO^tBu

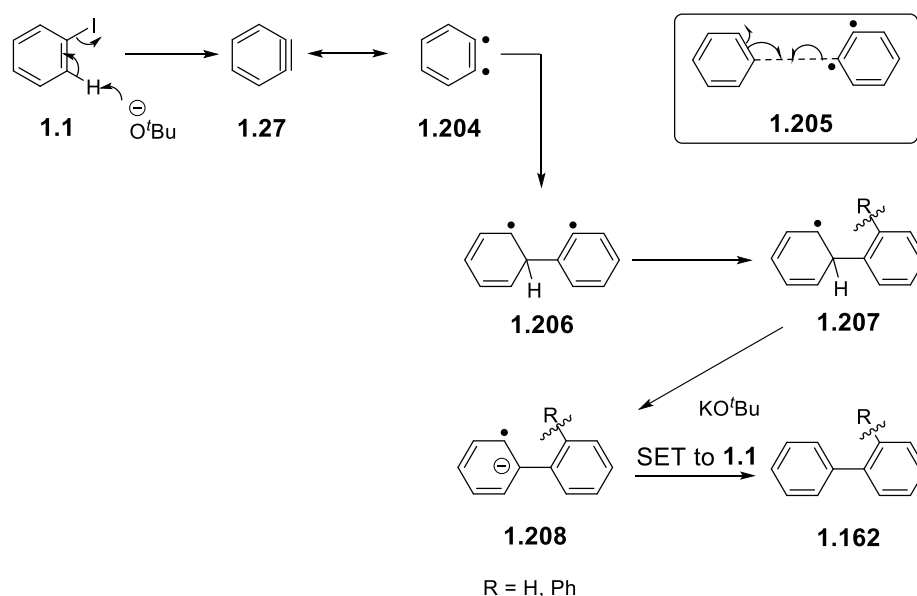
Similar to that shown for phenanthroline in Scheme 1.68, the deprotonation of pyridine was found to be more difficult than that of phenanthroline as the complexation between KO^tBu and pyridine is not as strong as KO^tBu and phenanthroline. Using similar blank reactions to those with phenanthroline, 2,2'-bipyridine was isolated as the major isomer. To get to this molecule from pyridine it would be expected that pyridine, **1.136** would be deprotonated and attack a second pyridine molecule to form **1.202**. Upon a second deprotonation, the electron-rich alkene **1.203** can be formed and, again, quenching with iodine allowed isolation of the dimer.



Scheme 1.69 – Formation of pyridine dimer **1.203**

These observations provide a rationale for why transformations performed by Itami and Charette, where no obvious electron donor is present, still produce the expected product in good yield.

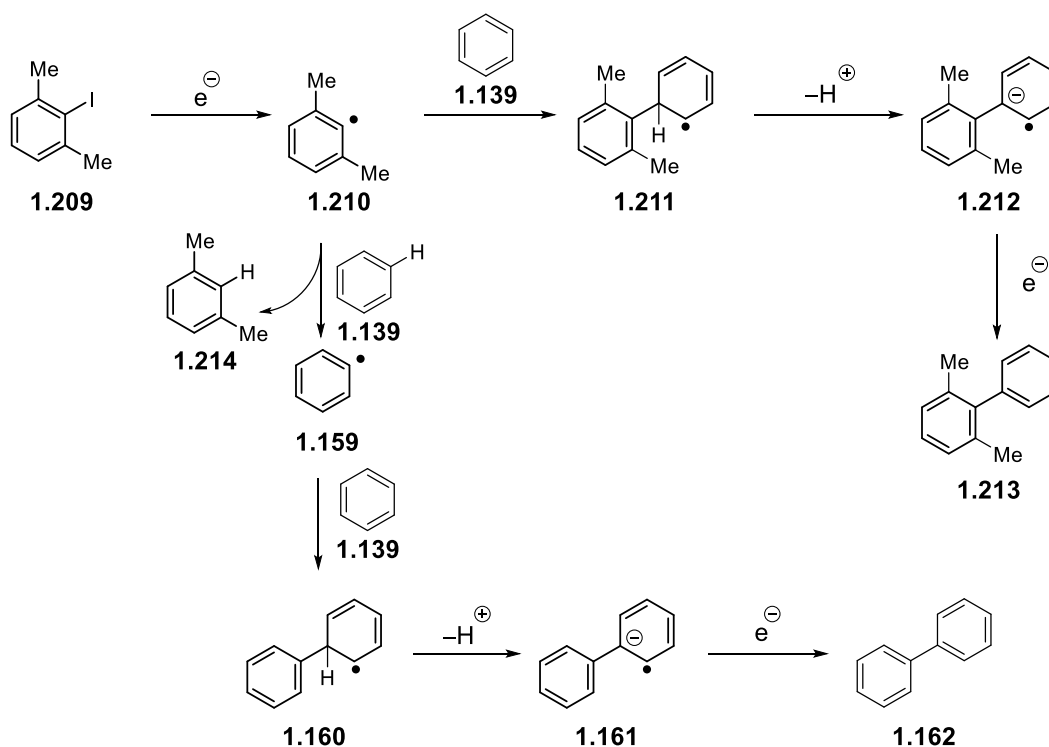
What still isn't clear from the observation of dimers is what happens when there is only benzene, KO^tBu and aryl iodide present. Murphy *et al.* proposed that this was due to benzyne, **1.27** acting as a biradical, **1.204** attacking a molecule of benzene. The resulting biradical can abstract a hydrogen atom or form a C-C bond with another molecule of benzene before being deprotonated to generate a radical anion, **1.208** equivalent to that observed in the BHAS cycle. It is proposed that this radical anion then donates an electron to an aryl iodide, starting the cycle in the normal fashion.



Scheme 1.70 – Benzyne initiation of the BHAS cycle¹⁰⁴

To test whether this was the primary source of initiation, or whether electron transfer from the additives was the major source, 2-iodo-*m*-xylene, **1.209** was used as the aryl

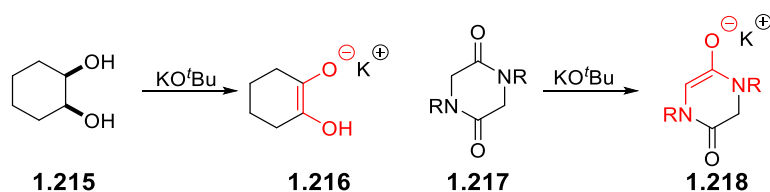
halide. As both positions *ortho* are blocked to deprotonation, the benzyne source of initiation shown in Scheme 1.70 is not possible. Where reactivity is observed in these reactions, the source of initiation needs to be from an external additive. A characteristic of reactions with 2-iodo-*m*-xylene, **1.209**, is that the coupled products observed are perhaps not as would be expected. Instead of 2,6-dimethylbiphenyl, **1.213**, being the only product, what is observed is a mixture of **1.213** and biphenyl, **1.162** in a 1:3.8 repeatable ratio. This is due to the fact that radical **1.210**, formed after electron transfer, finds it easier to abstract a hydrogen atom from benzene than attack the benzene ring. The rest of the mechanism follows the same as the BHAS mechanism whether it is radical **1.210** or **1.159** that attacks a molecule of benzene, leading respectively to **1.213** and **1.162**.



Scheme 1.71 – Reaction pathways of **1.209** with benzene

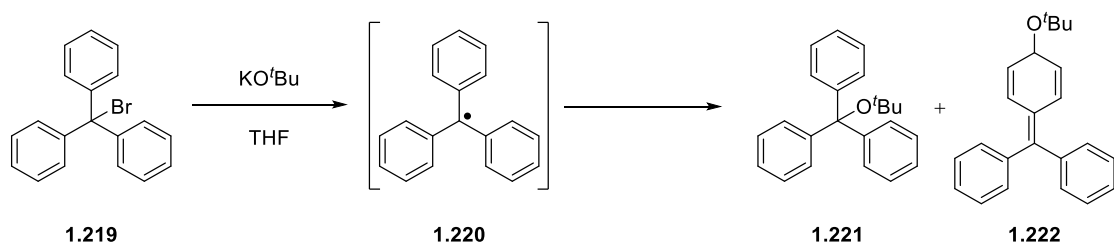
While electron transfer from organic additives is a common source of initiation for transition metal-free coupling reactions, there is still a large diversity of additives that required investigation. In 2014 Murphy *et al.* attempted to identify the roles of amino acids, alcohols and 1,2-diamines in these coupling reactions.¹⁰⁵ What was found was that often simple organic molecules can be transformed into electron donors through a

series of deprotonations. Enolates such as **1.216** and **1.218**, formed from diol **1.215** and diketopiperazine **1.217**, are examples.



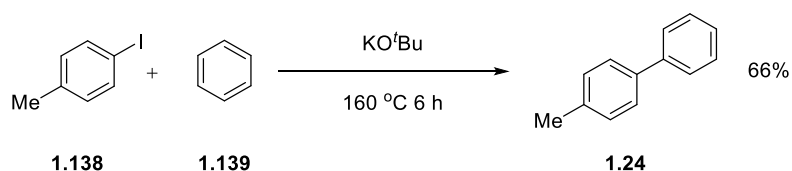
Scheme 1.72 – Formation of electron-rich enolates¹⁰⁵

Other groups have suggested that the initiation, when there is no electron donor present in fact comes directly from KO^tBu . Ashby *et al.*¹⁰⁶ proposed that alkoxides could act as electron donors as they observed EPR-active species when reacted with triphenylmethyl bromide, **1.219**, in THF. The radical they identified was triphenylmethyl radical, **1.220**. It was proposed that this was formed from single electron transfer from KO^tBu to **1.219**, and subsequent loss of bromide anion led to the triphenyl methyl radical, **1.220**. In these reactions they found that (*tert*-butoxymethanetriyl)benzene, **1.221**, was the major product with [(4-*tert*-butoxy)cyclohexa-2,5-dien-1-ylidene]methylene]dibenzene, **1.222** as the minor product.



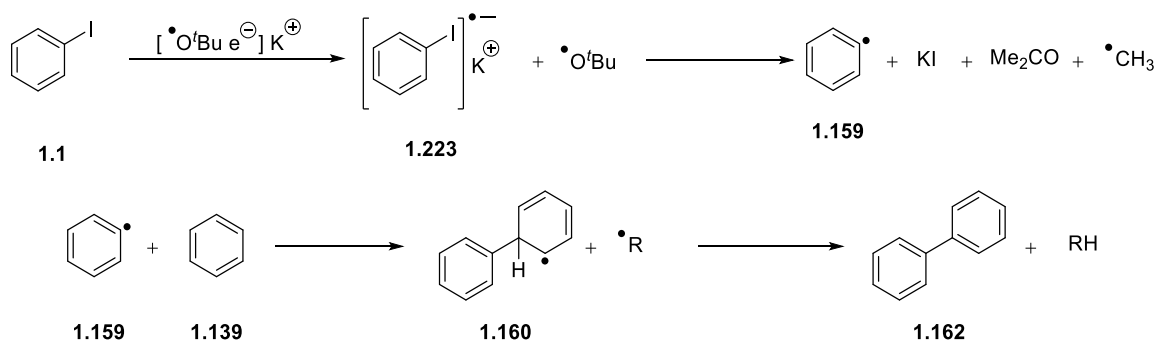
Scheme 1.73 – Ashby's report of EPR active species **1.220** from reaction with **1.219** and KO^tBu ¹⁰⁶

Wilden *et al.* have also suggested that potassium *tert*-butoxide itself could be the electron donor, (Scheme 1.74). They noticed that, in the absence of electron donors, coupling reactions between aryl iodides and benzene can still proceed with only KO^tBu and heat. Other groups have also noticed this. However, their yield was significantly higher than previous reports (66%). All substrates that were tested had *ortho* protons, so there is still the possibility of benzyne formation (Scheme 1.74).



Scheme 1.74 – Wilden coupling of **1.138** in the absence of electron donors

It was suggested that, after donation from butoxide to the aryl iodide, the resulting butoxyl radical intermediate collapsed to acetone and a methyl radical. Meanwhile the aryl iodide, having received the electron, would lose the iodide and form an aryl radical which can then attack benzene to form the resulting radical **1.160**, the methyl radical would then abstract a hydrogen from this, producing biphenyl and methane.



Scheme 1.75 – Proposed radical process to biaryl formation by Wilden *et al.*¹⁰⁷

In a similar way to Wilden *et al.*, Jutand *et al.* have also published a proposal that from an interaction between KO^tBu and phenanthroline, **1.141** leads to a phenanthroline radical anion, **1.224**, and it is this radical anion that initiates the BHAS cycle.

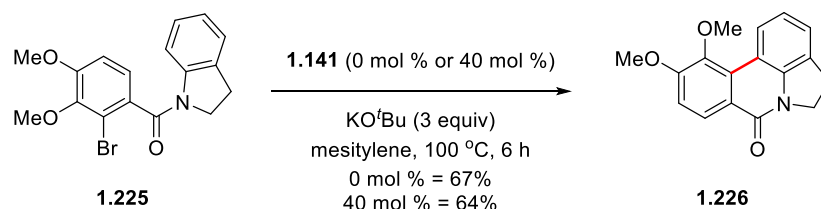


Scheme 1.76 – Jutand *et al.* proposed formation of phenanthroline radical anion, **1.224** that initiates BHAS cycle¹⁰⁸

Their evidence was based on an EPR study; they noticed when KO^tBu was mixed with phenanthroline, **1.141** in an appropriate solvent, that splitting patterns were observed

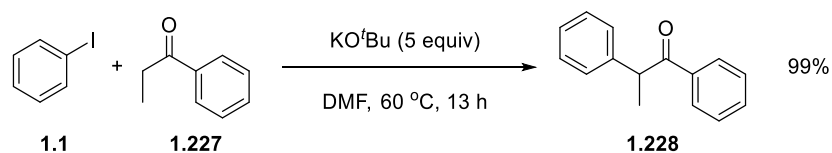
indicating the presence of a radical species. Their conclusion from this study is that phenanthroline, **1.141**, has been acting as an electron relay to transfer an electron between KO^tBu and aryl halides.¹⁰⁸ However, there is a large difference in the oxidation and reduction potentials of KO^tBu and phenanthroline making it unlikely for KO^tBu to reduce phenanthroline. Therefore it is likely that the observed radical had a different origin.

The lack of necessity for organic additives has been a source of debate in proposing the source of initiation in BHAS reactions; however, KO^tBu often appears to be an essential reactant in these reactions. Bisai *et al.* published two papers applying the phenanthroline/ KO^tBu system to intramolecular cyclisations during total synthesis of *Amaryllidaceae* alkaloids *e.g.* oxoassoanine, **1.226**,^{109, 110} While they performed reactions with organic additives (often phenanthroline, **1.141**) they found that these reactions also proceeded in the absence of the additives and only KO^tBu was essential for the reaction to proceed. They suggest that when there is no additive present, the initiation comes from SET from KO^tBu to the aryl halide, **1.225**.



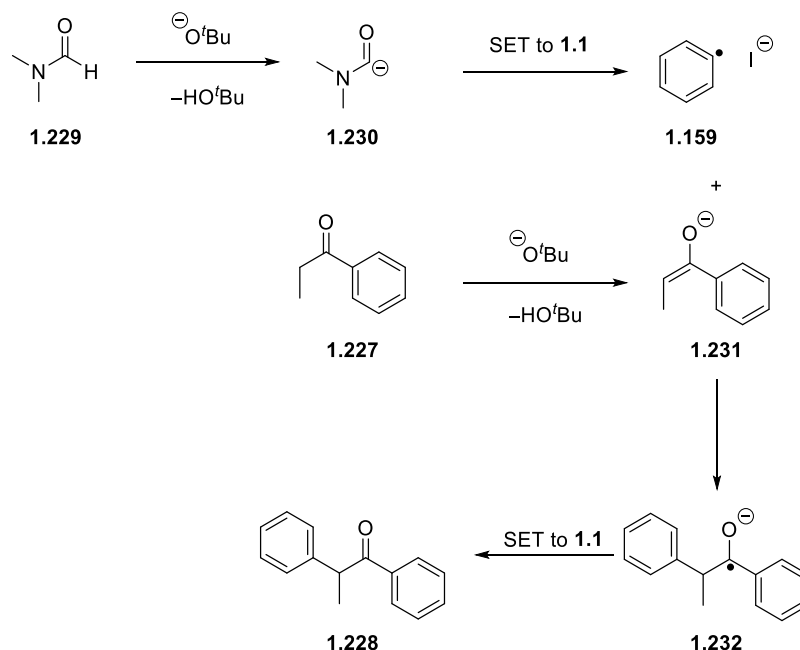
Scheme 1.77 – Bisai *et al.* intramolecular cyclisation of **1.225** to form **1.226**^{109, 110}

In 2015 Taillefer *et al.* reported a transition metal-free arylation of enolisable aryl ketones. In their reactions they did not have any organic additives present. What they used was a mixture of KO^tBu and DMF as this was essential to observing reactivity. When the base was changed to either LiO^tBu or NaO^tBu , the yield decreased to below 5%. Similarly, when the solvent was changed, there was a similar effect.



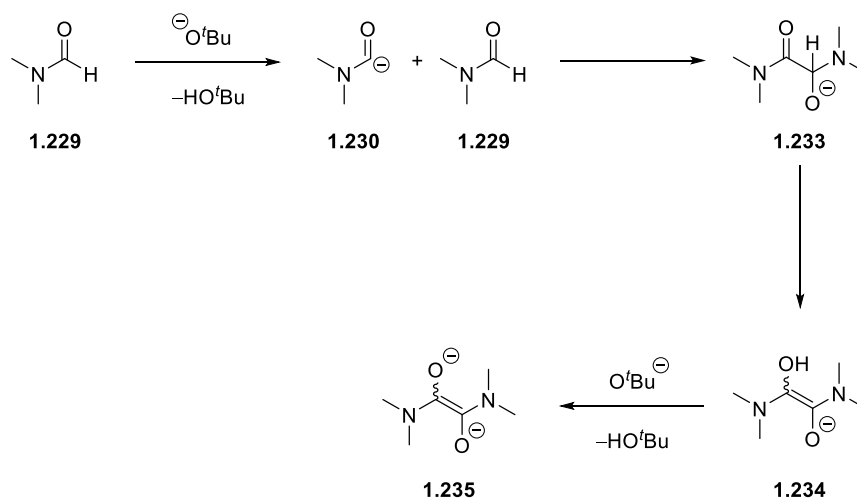
Scheme 1.78 – Taillefer's arylation of enolisable aryl ketones¹¹¹

They proposed that DMF was deprotonated and the resulting anion donated an electron to iodobenzene **1.1** to initiate the cycle. The resulting radical, **1.159**, then attacks enolate, **1.231** formed *in situ* to form a radical anion **1.232** and this radical anion donates an electron to another molecule of iodobenzene, **1.1** propagating the cycle and forming the desired product.



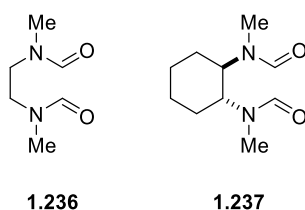
Scheme 1.79 – Proposed cycle of transition metal-free arylation of enolizable aryl ketones by Taillefer *et al.*¹¹¹

The Murphy group also looked into these types of reactions to investigate the role of DMF, and came up with their alternative proposal.¹¹² Having performed a reaction coupling 2-iodo-*m*-xylene, **1.209** with benzene, **1.139** they recovered a small amount of the biphenyl **1.162** and 2,6-dimethylbiphenyl **1.213** mixture (2.6%), (Scheme 1.82). They were in agreement that DMF was the source of the electron donor, however a different method of how this formed was proposed. Rather than a single molecule of DMF being deprotonated and donating an electron to the aryl iodide it is proposed that the deprotonated DMF, **1.230** (Scheme 1.80) attacks a second neutral DMF, **1.229** to form anion, **1.233** and after proton transfer this forms enolate **1.234**, which is a species that had more characteristics of an electron donor, based on previous studies.¹⁰⁵ If enolate **1.234**, was to undergo a second deprotonation then the resulting structure, **1.235**, would be an even stronger electron donor.



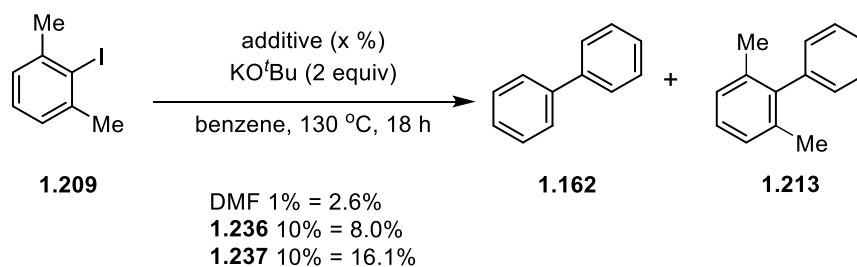
Scheme 1.80 – Alternative proposal for electron donor formation from DMF by
Murphy *et al.*¹¹²

To determine whether or not it was a dimer that was the electron donor, two additives were prepared to try and mimic this reactivity. The first was a linear diformamide, **1.236** and the second a more conformationally restricted diformamide, **1.237**.



Scheme 1.81 – Diformamide additives prepared by Murphy *et al.*¹¹²

When these were also used in coupling reactions with 2-iodo-*m*-xylene and benzene, it was found that the yield of coupled products **1.162** and **1.213** significantly increased from 1% DMF alone to the linear diformamide and then even larger increase with the conformationally restricted diformamide. (see Scheme 1.82)

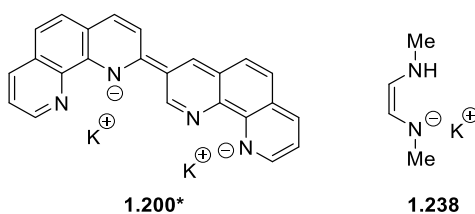


Scheme 1.82 – 2-Iodo-*m*-xylene coupling with benzene to produce mixture of **1.162** and **1.213** using diformamide additives¹¹²

Interestingly when the temperature of this reaction was lowered to 110 °C, time decreased to 4 h and amount of additive lowered to 0.5%, the yield of coupled product increased for additives **1.236** (19.6%) and **1.237** (31.6%) while 1% DMF gave a yield of 0.4% under these conditions. This work did not disprove the work carried out by Taillefer *et al.*, but did offer an alternative proposal.

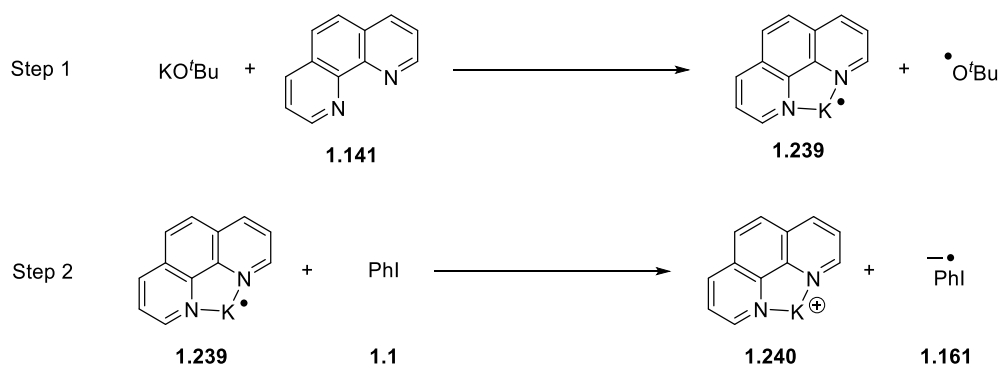
Another person who has explored the initiation step of the BHAS cycle is Patil.¹¹³ This was a computational study of the electron transfer to iodobenzene **1.1** from different species;

1. KO^tBu alone
2. The KO^tBu/phenanthroline complex proposed by Shi *et al.*⁸⁰
3. The electron relay system proposed by Jutand and Lei¹⁰⁸
4. The phenanthroline dimer, **1.200*** and deprotonated DMEDA **1.238** directly to iodobenzene as proposed by Murphy *et al.*^{104, 105}



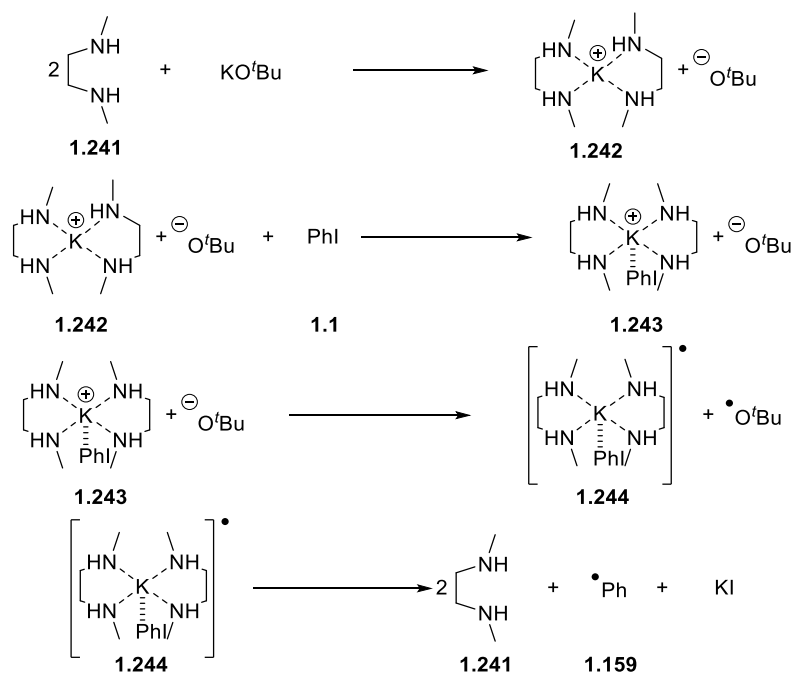
Scheme 1.83 – Proposed electron donors studied by Patil¹¹³

Reaction with KO^tBu alone was found to be very endergonic at 114.5 kcal mol⁻¹, suggesting that direct electron transfer from this to iodobenzene is unlikely to be achievable; moving on, the reaction of the complex proposed by Shi *et al.* was found to be very endergonic as well at 109.6 kcal mol⁻¹, while an alternative complex with DMEDA was found to be just as unfavourable at 113.9 kcal mol⁻¹. The third case, looking at the electron relay (Scheme 1.85) was more interesting.



Scheme 1.84 – Generation of phenanthroline potassium complex and subsequent electron transfer to iodobenzene

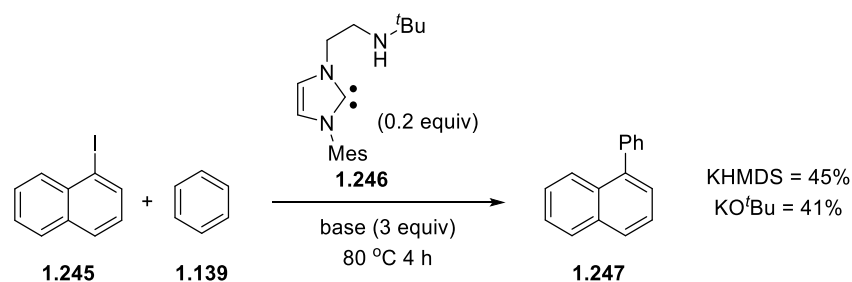
The first step with DMEDA, producing the butoxyl radical, was endergonic 42.0 kcal mol⁻¹, and the second step of electron transfer to iodobenzene showed $\Delta G_{\text{rel}} = 61.2$ kcal mol⁻¹ therefore making the overall energy of this process to be 103.2 kcal mol⁻¹ again unfavourable. The calculations were also performed for DMEDA case and again the energy was also unfavourable (104.9 kcal mol⁻¹). Using the donors proposed in the Murphy group the electron transfer to iodobenzene was still endergonic, 54.8 kcal mol⁻¹ for the phenanthroline dimer, **1.200*** and 79.7 kcal mol⁻¹ for the deprotonated DMEDA, **1.238** however the dissociation of the iodide in these cases to produce the phenyl radical and iodide anion was exergonic at -38.1 kcal mol⁻¹. This meant that the overall reaction profiles, i.e. ΔG_{rel} for these donors to the reactive aryl radical and iodide ion was 16.7 kcal mol⁻¹ and 41.6 kcal mol⁻¹ for the **1.200*** and **1.238** respectively, making these potentially achievable particularly in the phenanthroline dimer case. However even in these cases there are potentially high barriers to overcome so Patil looked at alternative explanations for the success of these reactions. His proposal was that two molecules of the additive complex to the potassium ion, **1.239** and this promotes the electron relay.



Scheme 1.85 – Electron relay proposed by Patil¹¹¹

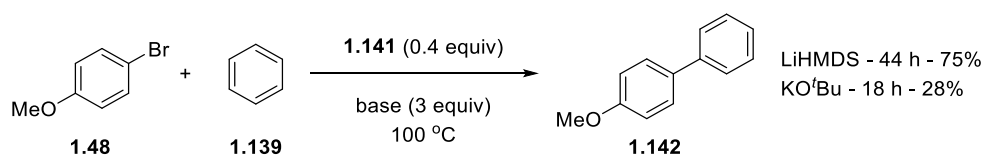
Overall the energy ΔG_{rel} for this transformation was 38.7 kcal mol⁻¹ for both DMEDA and also phenanthroline (not shown). This is lower than direct electron relay through phenanthroline proposed by Jutand and Lei however it is still not overall extremely favorable. The conclusion from this paper was that the initiation of the BHAS cycle was not a one step process and was most likely proceeding through the electron relay (Scheme 1.85). The calculations in the paper discount the complex proposed by Shi *et al.* as well as discounting direct electron transfer from any electron donor or KO^tBu to an acceptor. An issue of this paper is that it dealt fully in relative energies; the barriers would be higher than the energies reported and this could have an effect on the conclusions that could be drawn.

While the precise method of initiation is still under debate in the majority of papers, KO^tBu appears to be essential to the success of the reaction. However there are exceptions to this and recently Chen *et al.* were able to couple 1-naphthyl iodide, **1.245** with benzene, **1.139** in the presence of their NHC additive, **1.247** and KHMDS instead of KO^tBu finding a higher yield in this case (45% KHMDS to 41% KO^tBu).¹¹⁴ There is the possibility that similar to the Murphy group's benzimidazole-derived donors¹¹⁵ that the NHC is dimerising to form an electron donor that is initiating these reactions.



Scheme 1.85 – Chen *et al.*'s coupling reaction using KHMDS as alternative base to KO^tBu¹¹⁴

Similarly, Kappe *et al.* attempted to perform the reactions with phenanthroline, **1.141** as the additive and LiHMDS as the base and found that the reaction also proceeded, albeit in a longer length of time. These showed that KO^tBu was not always essential to these reactions.¹¹⁶



Scheme 1.86 – Kappe *et al.*: study of base on the BHAS coupling reaction¹¹²

This review has covered the background and scope of current transition metal-free reactions. While there has been a lot of study and interest in performing and understanding the mechanism of the transition metal-free coupling reactions, there is still work ongoing in the Murphy group and beyond. Some of this work bears on my research, and will be discussed throughout the thesis.

2. Introduction

2.1 Project Aims and Motivation

Upon starting my research in the Murphy and Tuttle groups, the research interests were in the development and understanding of transition metal-free cross coupling reactions. Having recently published several papers exploring the mechanism of these coupling reactions,^{104, 105} the Murphy group believe that the initiation source for these transformations is an electron transferred to a haloarene from an electron donor. This work aimed to build on the existing knowledge of electron donors and attempts to fill in the blanks, specifically why some reactions work with no electron donor present.

The initial study in Chapter 4, looks at developing a new family of additives that would be capable of performing transition metal-free cross coupling reactions. This was a dual study employing both synthetic organic chemistry and density functional theory (DFT) and a secondary aim of this work was to further show how these methods can aid each other to potentially predict what would be a good electron donor and what would not.

Chapters 5 and 6 look at why reactions, where no electron donors are added, often work. Again, this was explored both in the lab and computationally. It had been proposed that the background reaction was initiated by benzyne, formed from haloarenes acting as a biradical; however, the only evidence for this was that when the formation of benzyne from the haloarene substrate was prevented, the coupling was inhibited. The aim of this new work was to add in an external source of benzyne to reactions, where benzyne formation from the substrate is blocked, to determine if this is a source of initiation.

Recent work performed by other members in the Murphy group involving transition metal-free reactions using potassium hydride raised some interesting questions. It was decided that using DFT analysis to explore these reactions could be helpful in explaining how these reactions were proceeding, and this is the aim of the research reported in Chapter 7.

2.2 Layout of the Thesis

As there is a number of different computational studies in this thesis, Chapter 3 describes the background to the computational theory, and also a deeper explanation of some of the methods that will be used throughout the thesis, to give support and meaning to the results.

The bulk of the results are described in chapters 4 to 7. Chapter 4 looks at the development of new potential electron donors, based around benzimidazole and benzoxazole substructures. Chapter 5 is an experimental look at the benzyne initiation of transition metal-free coupling reactions; in this chapter the hexadehydro Diels-Alder reaction and Bergman cyclisation were utilized in initiating these reactions. Chapter 6 follows on from the previous chapter with a computational study of the biradical initiation of these reactions. Finally, chapter 7 explores various transformations observed in reactions with potassium hydride and haloarenes.

After the results and discussion in chapter 8 there are conclusions about the thesis as a whole and suggestions of potential future work. In chapter 9 there are full experimental details and characterisation of compounds made during the research.

3. Computational Theory¹¹⁷

3.1 Quantum Mechanics

Quantum mechanics is a sub-section of computational chemistry that is applied to systems at the atomic level to exploit the wave-particle duality of atoms. The fundamental equation of quantum mechanics is shown in Equation 3.1.

$$\vartheta\psi = e\psi$$

Eq. 3.1

This equation returns any physical property, e , of a system which is dependent on the operator, ϑ , when applied to the wavefunction, ψ . The aim of quantum mechanics is to calculate the exact wavefunction of a system, as from the wavefunction all physical properties can be extracted. An example of this being used is in the Schrödinger equation shown in Equation 3.2.

$$\hat{H}\psi = E\psi$$

Eq. 3.2

The Schrödinger equation applies the Hamiltonian operator, \hat{H} , to the wavefunction order to extract the energy, E , of a system. A common approach in extracting the energy is to solve the N -electron wavefunction utilising the Hartree-Fock (HF) approximation. However the approach that has been used for this work is to determine the electron density of the system.¹¹⁸ Physical properties are dependent on the electron density so these can be calculated using the method known as density functional theory (DFT).

3.2 Density Functional Theory¹¹⁷

3.2.1 Electron Density

Electron density is a measure of the probability of an electron being in a given area of space i.e., the higher electron density the greater probability of an electron being there.

Electron density is defined as multiple integrals over the spin coordinates of all the electrons in the system and over all the spatial orbitals except for one.

$$\rho(\vec{r}) = N \int \dots \int |\psi(\vec{x}_1, \vec{x}_2, \dots, \vec{x}_N)|^2 ds_1 d\vec{x}_2 \dots d\vec{x}_N$$

Eq. 3.3

This determines the likelihood of finding an electron out of the N -present electrons within a volume of $d\vec{r}$ with a chosen spin whilst the remaining $N-1$ electrons have chosen positions and spin represented by the wave function. The multiple integral shows the probability of one specific electron being within the volume of $d\vec{r}$. Since electrons are indistinguishable the probability of finding any electron is the single electron multiplied by the number of electrons N .

Electron density is both measurable and observable. Due to the attractive force from the nucleus, maximum values for electron density exist. This is down to the singularity of $-Z_A/r_{iA}$ which becomes non-continuous as $r_{iA} \rightarrow 0$ resulting in a cusp that is directly related to Z_A . The dependence on the nuclear charge can be shown by:

$$\lim_{r_{1A} \rightarrow 0} \left[\frac{\delta}{\delta r} + 2Z_A \right] \bar{\rho}(\vec{r}) = 0$$

Eq. 3.4

Where $\bar{\rho}(\vec{r})$ the spherical average of the electron density. The exponential decay for large electron-nuclei distances can be calculated by:

$$\bar{\rho}(\vec{r}) \propto \exp[-2\sqrt{2I}|\vec{r}|]$$

Eq. 3.5

With I being the first ionization energy of the system.

3.2.2 Pair Density

Electron density can be expanded to not only find one electron with a particular spin in a given volume but to find two electrons with opposing spins, with two given volumes. The remaining-2 electrons in this case being assigned arbitrary spin and position. This is known as pair density and is defined as:

$$\rho_2(\vec{x}_1, \vec{x}_2) = N(N-1) \int \dots \int |\psi(\vec{x}_1, \vec{x}_2, \dots, \vec{x}_N)|^2 d\vec{x}_3 \dots d\vec{x}_N$$

Eq. 3.6

Similar to electron density the pair density is also a positive number and is symmetrical about coordinates in space.

3.2.3 Hohenberg-Kohn Theory

Hohenberg-Kohn theory shows how electron density can be used to determine all the physical properties of a particular system, by determination of the Hamiltonian.¹¹⁸ Since $\rho(\vec{r})$ contains the same information contained in the Hamiltonian these can be shown to relate directly and as a result so do the ground state energies.

$$\rho(\vec{r}) \Rightarrow \{N, Z_A, R_A\} \Rightarrow \hat{H} \Rightarrow \Psi_0 \Rightarrow E_0$$

Eq. 3.7

The ground state energy, E_0 , and its energy components, are all functionals of the ground state electron density.

$$E_0[\rho_0] = E_{Ne}[\rho_0] + T[\rho_0] + E_{ee}[\rho_0]$$

Eq. 3.8

The E_{Ne} component is system dependent and can therefore be described using the electron density equation shown below;

$$E_0[\rho_0] = \int \rho_0(\vec{r})V_{Ne}d\vec{r} + T[\rho_0] + E_{ee}[\rho_0]$$

Eq. 3.9

The final two terms in the equation are independent of system variable and so can be replaced by the Hohenberg-Kohn functional, F_{HK} .

$$E_0[\rho_0] = \int \rho_0(\vec{r})V_{Ne}d\vec{r} + F_{HK}[\rho_0]$$

Eq. 3.10

From this equation it can be suggested that the ground state energy can be determined from only the F_{HK} . This functional contains the functional for both the kinetic energy and the interelectronic repulsion.

$$F_{HK}[\rho] = T[\rho] + E_{ee}[\rho] = \langle \Psi_0 | \hat{T} + \hat{V}_{ee} | \Psi_0 \rangle$$

Eq. 3.11

As the functionals $T[\rho]$ and $E_{ee}[\rho]$ are not known the ground state cannot be determined only from the F_{HK} functional. The only extractable information from the F_{HK} functional is $E_{ee}[\rho]$ functional.

$$E_{ee}[\rho] = \frac{1}{2} \iint \frac{\rho(\vec{r}_1)\rho(\vec{r}_2)}{r_{12}} d\vec{r}_1 d\vec{r}_2 + E_{ncl}[\rho] = J[\rho] + E_{ncl}[\rho]$$

Eq. 3.12

The $E_{ee}[\rho]$ functional consists of the coulomb term $J[\rho]$ and the non-classical electron-electron interaction term, $E_{ncl}[\rho]$. The major challenge for DFT is finding expressions for the unknown functionals $T[\rho]$ and $E_{ncl}[\rho]$.

The second principle of Hohenberg-Kohn theory involves using the variation principle to determine the ground state density.

$$E_0 \leq E[\tilde{\rho}] = F_{HK}[\tilde{\rho}] + E_{Ne}[\tilde{\rho}]$$

Eq. 3.13

This shows that when the functional $F_{HK}[\tilde{\rho}]$, is applied to a reasonable trial density the energy calculated will be either greater than or equal to the ground state energy. The only time it will be equal to the ground state energy will be when the trial density is equal to the exact density. Therefore, the Hohenberg-Kohn theory shows that electron density can be used as a replacement for the wavefunction when solving the Schrödinger equation.

3.2.4 Kohn-Sham Approach

The Kohn-Sham approach builds upon the principles of Hohenberg-Kohn theory and has provided a practical method of implementing electron density for DFT methods.¹¹⁹ The significant flaw in orbital-free models is the poor representation of kinetic energy terms; the idea in the Kohn-Sham model is to split the kinetic energy functional into two terms. One of these is calculated exactly and the other is a small correction term. Comparing this to the Hartree-Fock approximation where the kinetic energy was determined by using the Slater determinants as the form of the wavefunction. This meant that the description of the system was that it is composed of N non-interacting particles moving within the effective potential V_{HF} . In the Kohn-Sham approach a system of non-interacting electrons is used as a reference orbital-based system, and so the corresponding Hamiltonian, H_s , neglects and electron-electron interactions.

$$\hat{H}_s = -\frac{1}{2} \sum_i^N \nabla_i^2 + \sum_i^N V_s(\vec{r}_i)$$

Eq.3.14

The $V_s(\vec{r}_i)$ is an effective local potential. The ground state wavefunction is a Slater determinant, Θ_s , which is made up of Kohn-Sham spin orbital, ϕ , where the \hat{f}^{KS} is the one electron Kohn-Sham operator

$$\hat{f}^{KS} \phi_i = \varepsilon_i \phi_i, \quad i = 1, 2, \dots, N.$$

Eq.3.15

$$\hat{f}^{KS} = -\frac{1}{2} \nabla_i^2 + V_s(\vec{r})$$

Eq. 3.16

The Hamiltonian for the non-interacting particles system is a sum of the one-electron operators, \hat{f}^{KS} of the single electrons. The artificial non-interacting system is connected to the actual system by choosing the effective potential V_s so that densities of both the systems are equal.

$$\rho_s(\vec{r}) = \sum_i^N \sum_s |\varphi_i(\vec{r}, s)|^2 = \rho_0(\vec{r})$$

Eq. 3.17

Kohn and Sham aimed to determine the kinetic energy of the system by using a fictitious system of non-interacting electrons that has an effective potential, V_s , to match the resulting density with that of the actual system. To determine the V_s , the energy of the system was investigated to identify the known and unknown parameters.

The kinetic energy of the non-interacting system is determined from the orbitals using

$$T_s = -\frac{1}{2} \sum_i^N \langle \varphi_i | \nabla^2 | \varphi_i \rangle$$

Eq. 3.18

Because the kinetic energy is different for the non-interacting system and the actual system, it is adapted to

$$F[\rho(\vec{r})] = T_s[\rho(\vec{r})] + J[\rho(\vec{r})] + E_{xc}[\rho(\vec{r})]$$

Eq. 3.19

$$E_{xc}[\rho(\vec{r})] \equiv (T(\rho) - T_s[\rho]) + (E_{ee}[\rho] - J[\rho]) = T_c[\rho] + E_{ncl}[\rho]$$

Eq. 3.20

T is the kinetic energy for the actual system and T_s is the kinetic energy for the non-interacting electrons. Therefore the residual kinetic energy not accounted for by the T_s is defined as T_c . The E_{ncl} is the non-classical electronic contributions (electron-electron interactions) to the potential energy. The result of this is that the unknown parameters are effectively summed up and combined into the E_{xc} term, which is defined as the exchange correlation energy. This allows the kinetic energy to be determined more efficiently. Therefore the interacting real system energy can be expressed as;

$$E[\rho(\vec{r})] = T_s[\rho] + J[\rho] + E_{xc}[\rho] + E_{Ne}[\rho]$$

Eq. 3.21

3.3 Functionals and Basis Sets

3.3.1 Functionals

In the local density approximation (LDA) a hypothetical uniform electron gas is assumed to move in a positive background charge. The electron density is a constant value and remains finite even as the volume or the number of electrons approach infinity. The uniform electron gas is used because the exchange and correlation energies are known for this hypothetical system. Within LDA, the E_{xc} can be written as:

$$E_{xc}^{LDA}[\rho] = \int \rho(\vec{r}) \varepsilon_{xc}(\rho(\vec{r})) d\vec{r}$$

Eq. 3.21

$\varepsilon_{xc}(\rho(\vec{r}))$ indicates the exchange correlation energy per particle of a uniform electron gas at a particular density. The probability of finding an electron in this gas is also included. $\varepsilon_{xc}(\rho(\vec{r}))$ can be further defined by splitting the exchange and correlation contributions:

$$\varepsilon_{xc}(\rho(\vec{r})) = \varepsilon_x(\rho(\vec{r})) + \varepsilon_c(\rho(\vec{r}))$$

Eq. 3.22

The LDA can be further extended to an unrestricted case dependent on two spin densities, $\rho_\alpha(\vec{r})$ and $\rho_\beta(\vec{r})$, where $\rho_\alpha(\vec{r}) + \rho_\beta(\vec{r}) = \rho(\vec{r})$. This allows for better results in the cases of odd numbers of electrons, for example radicals, by having the two spin densities. This leads to the local spin density approximation.

$$E_{xc}^{LSD}[\rho_\alpha, \rho_\beta] = \int \rho(\vec{r}) \varepsilon_{xc}(\rho_\alpha(\vec{r}), \rho_\beta(\vec{r})) d\vec{r}$$

Eq. 3.23

$\rho_\alpha(\vec{r}) \neq \rho_\beta(\vec{r})$ is known as the spin-polarised case and the degree of spin polarization can be measured through the spin polarization parameter ξ :

$$\xi = \frac{\rho_\alpha(\vec{r}) - \rho_\beta(\vec{r})}{\rho(\vec{r})}$$

Eq. 3.24

Where $\xi = 0$ indicates there are equal numbers of each spin state, while $\xi = 1$ indicates that only one type of spin is present in the system.

LDA is a good starting point in determining the exchange correlation energy but does not effectively deal with many realistic systems within chemistry. As the electron density is not uniform throughout a molecular system, as the LDA suggests. A method of improving this approximation is to account for the electron density gradient $\nabla\rho(\vec{r})$, which is usually heterogeneous. The LDA is the first term in a Taylor series. The gradient expansion approximation (GEA) can be shown as:

$$E_{xc}^{GEA}[\rho_\alpha, \rho_\beta] = \int \rho \varepsilon_{xc}(\rho_\alpha(\vec{r}), \rho_\beta(\vec{r})) d\vec{r} + \sum_{\sigma, \sigma'} \int C_{xc}^{\sigma, \sigma'} \rho_\alpha, \rho_\beta \frac{\nabla\rho_\sigma \nabla\rho_{\sigma'}}{\rho_\sigma^{2/3} \rho_{\sigma'}^{2/3}} d\vec{r} + \dots$$

Eq. 3.25

The GEA can be used in a system where the electron density is not completely uniform but has small changes in it. It would be expected however, to provide improved accuracy on LDA, although this is not necessarily the case.

A functional that utilizes the gradient of charge density belongs to the set of functionals known as generalized gradient approximations (GGA). These are defined as:

$$E_{xc}^{GGA}[\rho_\alpha, \rho_\beta] = \int f(\rho_\alpha, \rho_\beta, \nabla\rho_\sigma \nabla\rho_{\sigma'}) d\vec{r}$$

Eq. 3.26

As with the LDA it is possible to split E_{xc}^{GGA} into its exchange and correlation energies. The exchange energy can be defined as the LDA equivalent and the correlation energy as shown.

$$E_{xc}^{GGA} = E_x^{GGA} + E_c^{GGA}$$

Eq. 3.27

$$E_x^{GGA} = E_x^{LDA}$$

Eq. 3.28

$$E_c^{GGA} = - \sum_{\sigma} \int F(s_{\sigma}) \rho_{\sigma}^{\frac{3}{4}}(\vec{r}) d\vec{r}$$

Eq. 3.29

$$E_{xc}^{GGA} = E_x^{LDA} - \sum_{\sigma} \int F(s_{\sigma}) \rho_{\sigma}^{\frac{3}{4}}(\vec{r}) d\vec{r}$$

Eq. 3.30

3.3.2 Hybrid Functionals

Hybrid functionals use the ability to determine the value of the exchange energy from pure density functionals and exact HF exchange whilst relying on approximations for the correlation energy. Different hybrid functionals contain different weightings of several functionals. The M06 set of functionals are frequently used; these contain hybrid and GGA type functionals. This broad range of functionals provide good results for main group thermochemistry, transition metal chemistry as well as noncovalent interactions. The M06 functionals contain a variety of parameters for the combinations of the components that make up the functional so that computational jobs can be tailored to the system that is being investigated. For example M06-L is a localized functional with 0% Hartree-Fock exchange and is good for transition metals, M06-HF is the opposite of this where the full Hartree-Fock exchange energy is present and is designed for long range charge transfer in DFT. M06-2X is the functional used throughout this report. It is

somewhere in between the M06-L and M06-HF functional (containing 54% of HF exact exchange) and as such is able to cover a wider range of properties.¹²⁰ Throughout this thesis the M06-2X functional is used.

3.3.3 Basis Sets

A basis set is a set of functions that describe the molecular orbitals (MO) used to estimate the wavefunction to solve Schrödinger's equation. Commonly used types of basis set are Gaussian Type Orbitals (GTO). GTO can be written in terms of Cartesian coordinates as shown:

$$\eta^{GTO} = Nx^l y^m z^n \exp(-\alpha r^2)$$

Eq. 3.31

Where N is the normalization factor, α is the orbital exponent that determines the size of the resulting function and the sum of l , m and n determines the orbital shape, i.e., $l + m + n = 1$ is a p-orbital.

An alternative type of basis set is the Slater Type Orbitals (STO) and can be shown through:

$$\eta^{STO} = Nr^{n-1} \exp(-\zeta r) Y_{lm}(\theta, \phi)$$

Eq. 3.32

STO offer the exact eigenfunctions of a hydrogen atom. Where STO differ from GTO is that STOs do not have any radial nodes. Despite STOs being more accurate in describing orbitals due to the high computational cost contracted GTO basis sets are often used instead.¹²¹ These consist of several primitive gaussian functions that are linearly combined to give one contracted gaussian function (CGF). The CGF is an approximation of a STO but comes at a lower computational cost.

There are several different types of basis sets which have different levels of accuracy. Minimal basis sets are the simplest form and often run quickest however they are the

least accurate; conversely double or triple-zeta basis sets have an increased number of functions and therefore are more accurate but come at a higher computational cost.

To gain a high level of accuracy often high-level basis sets need to be used however not all the electrons in an atom take part in the chemistry of reactions, so often only the valence electrons require the higher level basis sets. Therefore, similar accuracy can be achieved treating the valence electrons with double/triple-zeta basis sets and the core electrons with a minimal basis set. Where the valence and core electrons are split it is called a split-valence basis set for example 6-311G Gaussian basis set. 6-311G is a triple-zeta split-valence basis set that describes Gaussian-type orbitals. The 6 in the basis set means that 6 GTOs are linearly added to form the CGF. It is this CGF that is applied to the core electrons in each atom of the molecule. The -311 part means that three basis functions are used to describe the valence electrons. Of this the 3 is a CGF whilst the 1s are single GTOs.

Polarisation functions (d,p) can be added to the basis sets. These functions are of higher angular momentum than would be required for the atom, giving the orbitals more flexibility to find the lowest energy conformation. The d adds polarization to the non-hydrogen atoms and the p adds polarization to the hydrogen atoms. Similarly diffuse functions can also be added to extend the CGFs further from the nucleus. These are particularly useful for anions and larger elements that have electrons further from the nucleus. These are noted with '+' for non-hydrogen atoms only and '++' for all atoms in a molecule including the hydrogens.

Often basic basis sets such as 6-31G and 6-311G do not accommodate heavy elements. These should therefore be modelled with additional functions. As there are a large number of inert core electrons rather than model these with a minimal basis set this is replaced with an effective core potential or pseudo potential.

There are no definitive rules for what makes the best basis set for a particular system, instead basis sets can be adapted to different chemical systems to find an appropriate functional/basis set combination. Once these are selected then a computational software package such as Gaussian can model the system and determine the required properties. While these can be tailored to a particular system it is important when

comparing different systems the same functional/basis set has been used as these frequently give different results.

3.4 Solvation Models

As chemical reactions are rarely carried out in a gaseous environment and solvent-solute interactions often alter a system it is important that a solvation model is included in the calculations that are being studied. Solvation models are often built around polarisable dielectrics. The conductor-like polarisable continuum model (CPCM) is one such model and is used throughout this report. The solvent molecules are considered to form a cavity centered by the molecules of interest, and a surface representing the cavity walls is defined by small sections. The conductor-like reaction field is due to a polarized charge on the cavity surface. For systems where the solvent has a finite dielectric constant the charges can be calculated by:

$$\mathbf{S}\mathbf{q} = -f(\epsilon)\mathbf{V}$$

Eq. 3.34

Where \mathbf{V} and \mathbf{q} are vectors that total the electrostatic potential due to the solute molecules and the solvent charges respectively. \mathbf{S} is made up of a matrix with 2 components S_{ii} and S_{ij} :

$$S_{ii} = 1.0694 \sqrt{\frac{4\pi}{a_i}}$$

Eq. 3.35

$$S_{ij} = \frac{1}{|r_i - r_j|}$$

Eq. 3.36

The value of $f(\epsilon)$ is generally determined by:

$$f(\varepsilon) = \frac{\varepsilon - 1}{\varepsilon + X}$$

Eq. 3.37

Where X is often taken as zero or a half.

Equation is usually solved iteratively and after n iterations yields:

$$q_i^{(n)} = -\frac{1}{S_{ii}} \left[f(\varepsilon)V_i + \sum_{i \neq j} \frac{q_j^{(n-1)}}{|r_i - r_j|} \right]$$

Eq. 3.38

The charge at i is dependent on the potential of the solute and on the potential of all of the other charges at the previous iteration.

3.5 Marcus Theory

In 1992 Rudolph A. Marcus was awarded the Nobel Prize in chemistry for his contributions to the theory of electron transfer reactions in chemical systems. He developed the theory that later became famous as Marcus theory.¹²²⁻¹²⁵

Electron transfer, in its simplest case involves two molecules – one donates an electron to the other, which accepts it – as a result both molecules will undergo a considerable change in structure. If these molecules are in solution, the solvent would also need to undergo change as it would move from solvating two molecules with their initial number of electrons to two new molecules with a different number of electrons. This requires a change in solvation to reorganize around the newly formed molecules. These changes are required for electron transfer to occur, and to carry out these changes in structure will require energy to overcome the reaction barrier. Therefore, the amount of energy required to overcome the barrier determines the rate of electron transfer.

It is in working out this barrier that Marcus theory comes in to play. The theory assumes that the two molecules undergoing electron exchange are loosely bound to each other.

The required energy for structural changes is named the “reorganization energy” and is termed ‘ λ ’. The reorganization energy can be expressed as:

$$\lambda = \lambda_i(a) + \lambda_i(r)$$

Eq. 3.39

Where:

$$\lambda_i(a) = E_{da}(r_a) + E_{da}(r_r)$$

Eq. 3.40

$$\lambda_i(r) = E_{dr}(r_r) + E_{dr}(r_a)$$

Eq. 3.41

r_a and r_r specify the coordinates of the structures before electron transfer and the structures after electron transfer, whilst E_{da} and E_{dr} identify the energy of the anion or radical at the desired coordinates. $\lambda_i(a)$ gives the inner sphere reorganization energy of the anion and $\lambda_i(r)$ gives the inner inner sphere reorganization energy of the radical.

In Figure 3.1 two curves are shown, the blue represents the energy of the starting structures while the orange represents the products after electron transfer. The minima illustrate the equilibrium energy of the molecules in each case. The point at which the curves intersect each other is the point where electron transfer occurs, i.e. the activation energy. The reorganization energy is the difference between the minima of the left curve and a point vertically above on the upper part of the other curve.

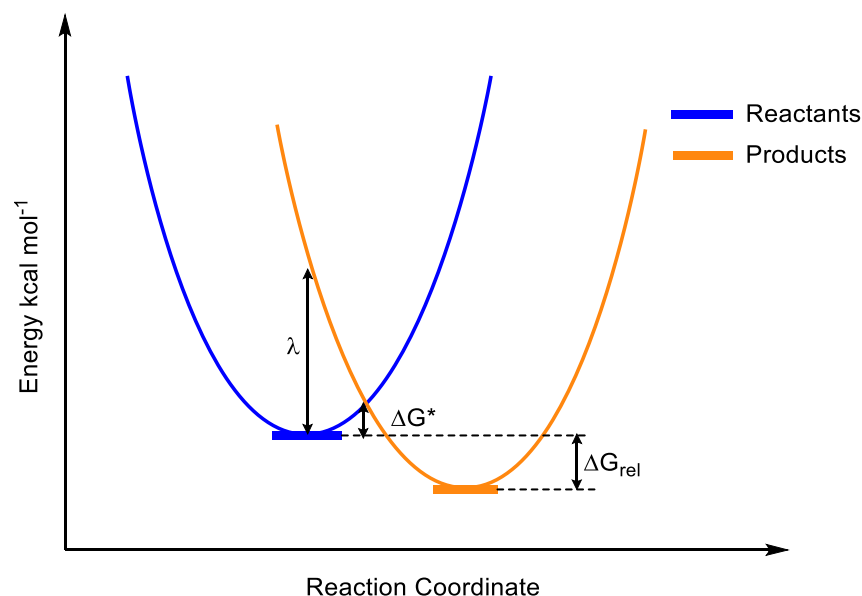


Figure 3.1 – Representation of Marcus theory. Blue line is before electron transfer, orange line is after electron transfer

As seen in Figure 3.1 the activation energy to undergo electron transfer is only part of the overall reorganisation energy. Marcus incorporated this into his theory by incorporating the factor ‘¼’ into his general equation for the rate of electron transfer.

The relative free energy of products relative to starting structures is calculated from the energy of optimized structures, both donor and acceptor before and after electron transfer:

$$\lambda = (E_{dr}(r_r) + E_{ar}(r_r)) - (E_{da}(r_a) + E_{an}(r_n))$$

Eq. 3.42

An expression to calculate the energy barrier can then be derived from the difference in the coordinates of the turning point of each parabola and is:

$$\Delta G^* = \frac{\lambda}{4} \left(\frac{1 + \Delta G_{rel}}{\lambda} \right)^2$$

Eq. 3.43

To calculate this, however, the values of ΔG_{rel} and λ must already be known. The method used to obtain all the required information is known as the Nelsen four-point method

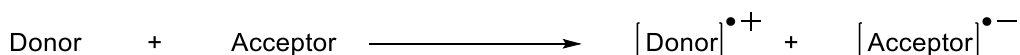
and requires a series of optimization and single point energy calculations to be performed. The electron donor and electron acceptor are both optimized before electron transfer as singlets. They are then reoptimized after either the loss or gain of an electron as radical anion or cations as appropriate. The difference between the energy of before and after electron transfer gives ΔG_{rel} .

The reorganisation energy (λ) is determined computationally by splitting the reorganisational energy into its internal and external components, and because studies showed that the external reorganisation effect is minimal, only the internal reorganisation energy is used (Equation 3.44). The reorganisational energy (λ) is calculated computationally by optimising the geometries of both the acceptor and donor species, before and after the electron transfer.

$$\lambda = \frac{\lambda_i(D) + \lambda_i(A)}{2}$$

Eq. 3.44

When the optimised geometry is obtained for the electron donor species, before SET, then a single point energy (SPE) calculation is performed using a different charge and multiplicity of the system to reciprocate that of the electron donor species after SET. This is repeated for all the optimised geometries (both of the electron acceptor and donor).



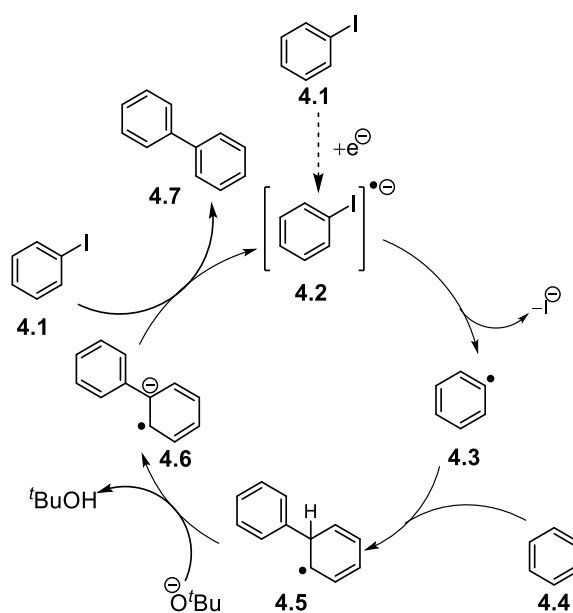
Scheme 3.1 – Electron transfer from donor to acceptor

An alternative to Nelsen's four-point method has recently been reported.¹²⁶ This method optimises the donor and acceptor molecules as a complex before and after SET. The calculations are performed as a singlet and triplet to model this, and SPE calculations are performed with the alternative multiplicities to model this fully.

4. A New Range of Electron Donors for Transition Metal Free Synthesis

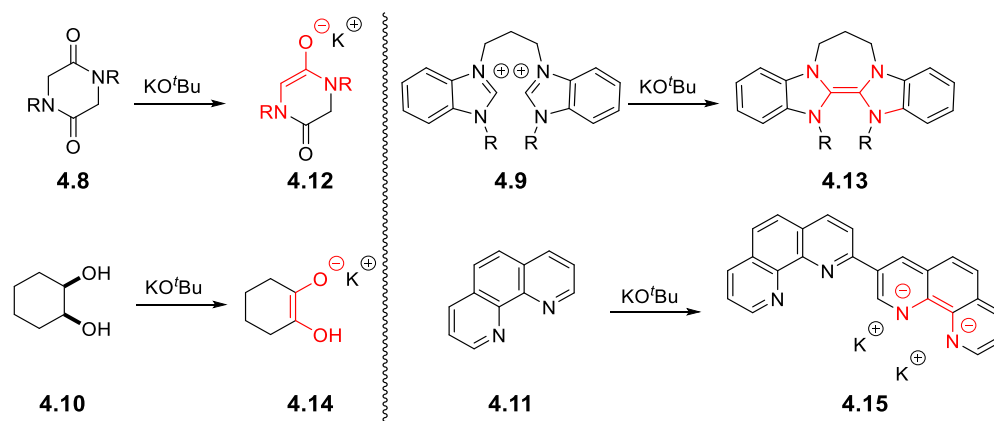
4.1 Introduction

Over the past decade, there has been an explosion of interest in transition metal-free cross coupling.^{56, 77, 80, 82, 104, 127} While still in its infancy, not using transition metals in reactions has significant potential advantages, such as lower costs and less toxicity. It is often proposed that these reactions proceed *via* a base-promoted aromatic substitution pathway (BHAS) (Scheme 4.1). This was firstly proposed by Studer and Curran back in 2011.⁸⁹ This cycle requires an initiation of some sort. Murphy proposed that this source of initiation was through electron transfer to an aryl iodide, **4.1**, to generate the aryl radical, **4.3** starting the cycle.¹⁰⁴



Scheme 4.1 – BHAS cycle proposed by Studer and Curran⁸⁹

This electron transfer often occurs from an organic electron donor. These are often generated *in situ* following deprotonation by a strong base such as KO^tBu. A selection of common additives and their respective proposed electron donors are shown in Scheme 4.2. Common features of organic electron donors are an electron-rich double-bond, often surrounded by heteroatoms.



Scheme 4.2 – *In situ* formation of electron donors

This was the grounding for this work where the aim was to design molecules that could form electron-rich double-bonds *in situ* through deprotonation with potassium *tert*-butoxide (KO^tBu). The particular set of molecules that were chosen to be studied are shown in Figure 4.1. These were all prepared to be studied experimentally and also modelled computationally to analyse how likely these were going to be able to form what would be expected to be the active electron donor and more specifically to determine whether or not they would be capable of transferring an electron to an aryl iodide.

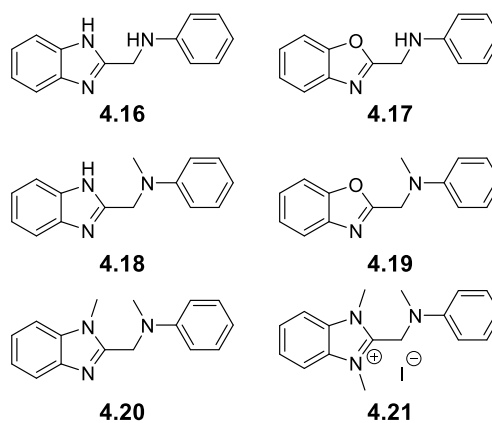
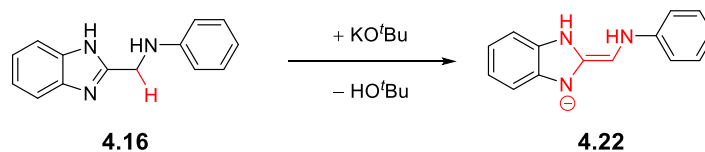


Figure 4.1 – Additives designed to generate electron donors *in situ* on treatment with base

4.2 Generation of potential electron donor

To generate a species that resembles the electron donors shown above, these additives require to be deprotonated at the sp^3 -carbon in the centre of the molecule. This would

generate an electron-rich double-bond as shown in Scheme 4.3 where **4.16** is deprotonated to generate the electron-rich core in **4.22**.



Scheme 4.3 – Deprotonation of central sp^3 -carbon generates an electron-rich alkene surrounded by three heteroatoms

The heteroatoms would also likely be deprotonated where this is a possibility and, as such, having negatively charged heteroatoms surrounding the double-bond would mean that this is even more electron-rich and therefore a potentially stronger electron donor. This would mean that, in terms of donation ability, **4.24** > **4.23** > **4.22**. However, what is not known is how much of each species could be present in a reaction mixture.

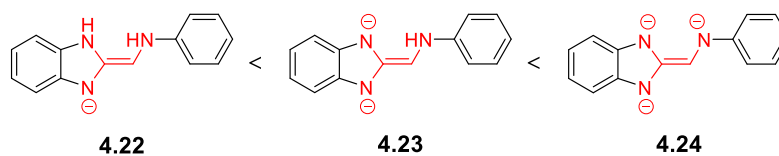


Figure 4.2 – Proposed donor strength depending on deprotonation state

The computational study for deprotonation of the additives was undertaken on Gaussian 09¹²⁸ using the functional M06-2X¹²⁰ with basis set 6-311++G(d,p).^{129, 130} All calculations were carried out using the C-PCM implicit solvent model^{131, 132} with the dielectric constant for benzene ($\epsilon = 2.2706$). *tert*-Butoxide anion was used as the base, as recently this has been shown to give results that are close to that of KO^tBu tetramer in previous calculations, and is more computationally efficient to use. It is known that KO^tBu exists as a tetramer in the solid state,¹³³ but when studied alongside a dimer, KO^tBu and $^-O^tBu$ it was found that $^-O^tBu$ gave comparable results to the tetramer whilst improving the computational efficiency of the calculations.¹³⁴ When deprotonation of the proton on the benzimidazole nitrogen was attempted, this was found to be barrierless and extremely favourable with $\Delta G_{rel} = -41.6$ and -39.0 kcal mol⁻¹ for **4.16** and **4.18** to **4.25** and **4.26** respectively (Table 4.1). This was attributed to resonance stabilisation of the resulting anion with the rest of the benzimidazole moiety and

suggests that where this is present, it will be the most likely position to be deprotonated first.

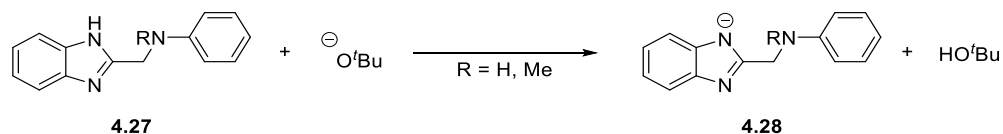


Table 4.1 – Deprotonation of benzimidazole proton energy

Start	Product	ΔG_{rel} (kcal mol ⁻¹)
 4.16	 4.25	-41.6
 4.18	 4.26	-39.0

The aniline position was studied as well, as this was another position that was potentially easier to deprotonate than the carbon. Table 4.2 shows that transformations were again favourable and, although transition state geometries were found their energies were negligible. It is again reasonable to conclude that the proton on the aniline nitrogen will easily be deprotonated. Going from triamine **4.16** to the monodeprotonated triamine **4.29** was calculated, to show that it is possible to deprotonate this from the neutral species and **4.25** to **4.30** shows that the energy changes when there is already negative charge present in the molecule. This is still exergonic, however, and combining the energies going from **4.16** to **4.30** is -33.4 kcal mol⁻¹ and neither step has an energy barrier.

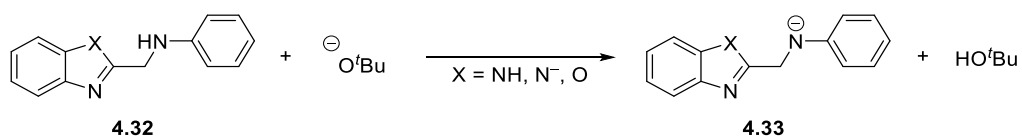


Table 4.2 – Deprotonation of aniline nitrogen energy

Start	Product	ΔG_{rel} (kcal mol ⁻¹)
 4.16	 4.29	-31.7
 4.25	 4.30	-1.7
 4.17	 4.31	-22.6

This led to looking at the central carbon deprotonations. This is the most important deprotonation as, without this being possible, then the electron-rich alkene cannot be formed. While it may seem surprising and unlikely to build a large negative charge through a series of deprotonations on a substrate, there are recent examples of dianions being identified as the active in electron donors in initiation of BHAS reactions.¹³⁵ The deprotonation of the central carbon was calculated for all the additives designed in all possible deprotonation states, as shown in Table 4.3.

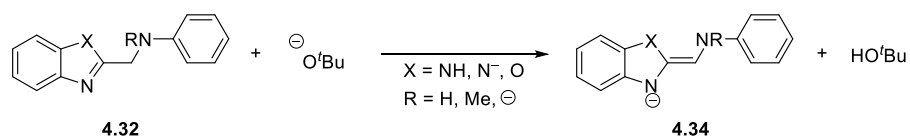
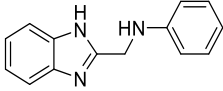
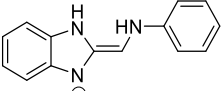
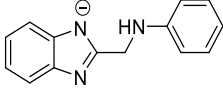
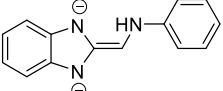
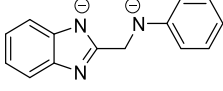
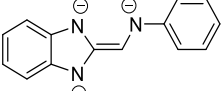
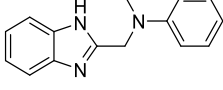
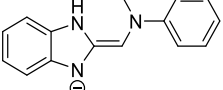
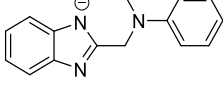
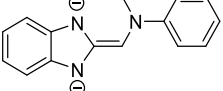
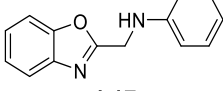
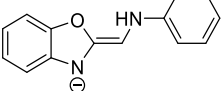
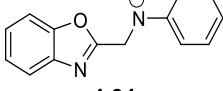
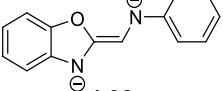
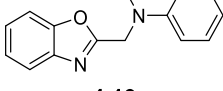
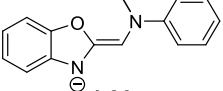
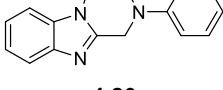
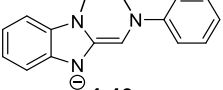
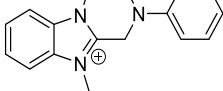
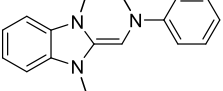


Table 4.3 – Deprotonation of the central carbon

Start	Product	ΔG^\ddagger (kcal mol ⁻¹)	ΔG_{rel} (kcal mol ⁻¹)
 4.16	 4.22	15.5	8.9
 4.25	 4.23	32.1	24.6
 4.30	 4.24	36.1	34.5
 4.18	 4.35	8.8	1.1
 4.26	 4.36	16.4	-0.8
 4.17	 4.37	9.8	4.1
 4.31	 4.38	20.6	3.3
 4.19	 4.39	4.4	-2.5
 4.20	 4.40	3.3	-5.5
 4.21	 4.41	0.0	-14.0

What this table showed was that it is possible to generate what is predicted to be the active donor form of the additives. The deprotonation of the central carbon of additive **4.16** is endergonic regardless of the number of deprotonations before. The formation of the mono and dianionic electron-rich alkene is certainly possible. The trianionic species is unlikely to exist in any significant concentration. However, if formed it would potentially be a very efficient electron donor. Additives **4.17** and **4.18** could both form donors that are mono and dianionic. Additives **4.19**, **4.20** and **4.21** could all form the electron-rich alkenes favourably.

4.4 Marcus theory calculations

The next step was to look at the electron transfer from these electron-rich alkene species to aryl iodides. This was done by applying Marcus theory to these systems. The Nelsen four-point method¹³⁶ was used for all systems. The possible electron-rich alkenes **4.22-4.24**, **4.35-4.41**, shown in Table 4.3, were optimised as anions (or as a neutral species in the case of **4.41**) to model their structure before electron transfer. These were then optimised as radical cations for after electron transfer, these coupled with the corresponding calculations for iodobenzene gave ΔG_{rel} . To find ΔG^\ddagger a series of SPE calculations were performed with all species previously optimised in their opposite spin states i.e neutral donor would have a SPE calculation as a radical cation and a radical cation would have a SPE calculation as a neutral species. This allowed the reorganization energy to be calculated and subsequently ΔG^\ddagger (For a more detailed description of the calculations see Chapter 3). When the aryl iodides were optimised as radical anions, the iodide dissociated spontaneously from the aryl radical and this can be seen by the location of spin density shown in Figure 4.3.

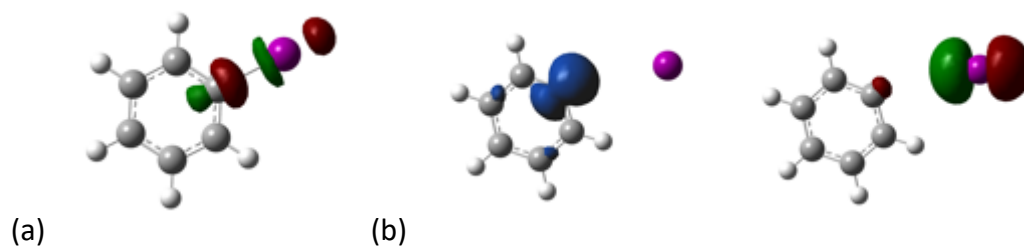


Figure 4.3 – (a) LUMO of neutral iodobenzene (b) The left image shows the presence of an aryl radical shown by the spin density and the right image shows the iodide anion is the HOMO

These results allowed proposals to be made about which species could perform electron transfer and which species are unlikely to perform this (Table 4). It would appear that the neutral species **4.41** would not be an efficient electron donor as it is very disfavoured. The monoanions (**4.22**, **4.35**, **4.37**, **4.39** and **4.40**) all have achievable barriers however, their reactions are all endergonic. This suggests that these could be electron donors but they are unlikely to be efficient. Dianions (**4.23**, **4.36** and **4.38**) like the monoanions have achievable barriers but the reactions of the dianions are all exergonic. This means that should the dianions form they are likely to be much more efficient electron donors than the monoanions. The trianion **4.24** is the least likely species to form based on the previous calculations. However, if it was to form, then it would be a very strong electron donor as it has a very low energy barrier and is very exergonic.

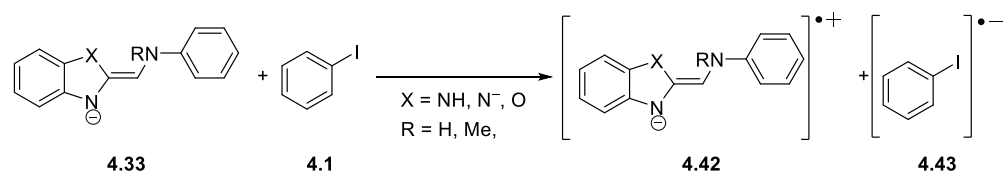
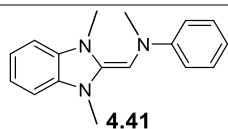


Table 4 – Electron Transfer energies to iodobenzene, **4.1**

Electron-rich Alkene	ΔG^\ddagger (kcal mol ⁻¹)	ΔG_{rel} (kcal mol ⁻¹)
 4.22	25.9	15.0
 4.23	25.8	-42.4
 4.24	2.3	-88.7
 4.35	25.7	15.3
 4.36	2.5	-39.3
 4.37	23.0	12.4
 4.38	2.6	-40.0
 4.39	26.9	17.1
 4.40	24.0	12.8



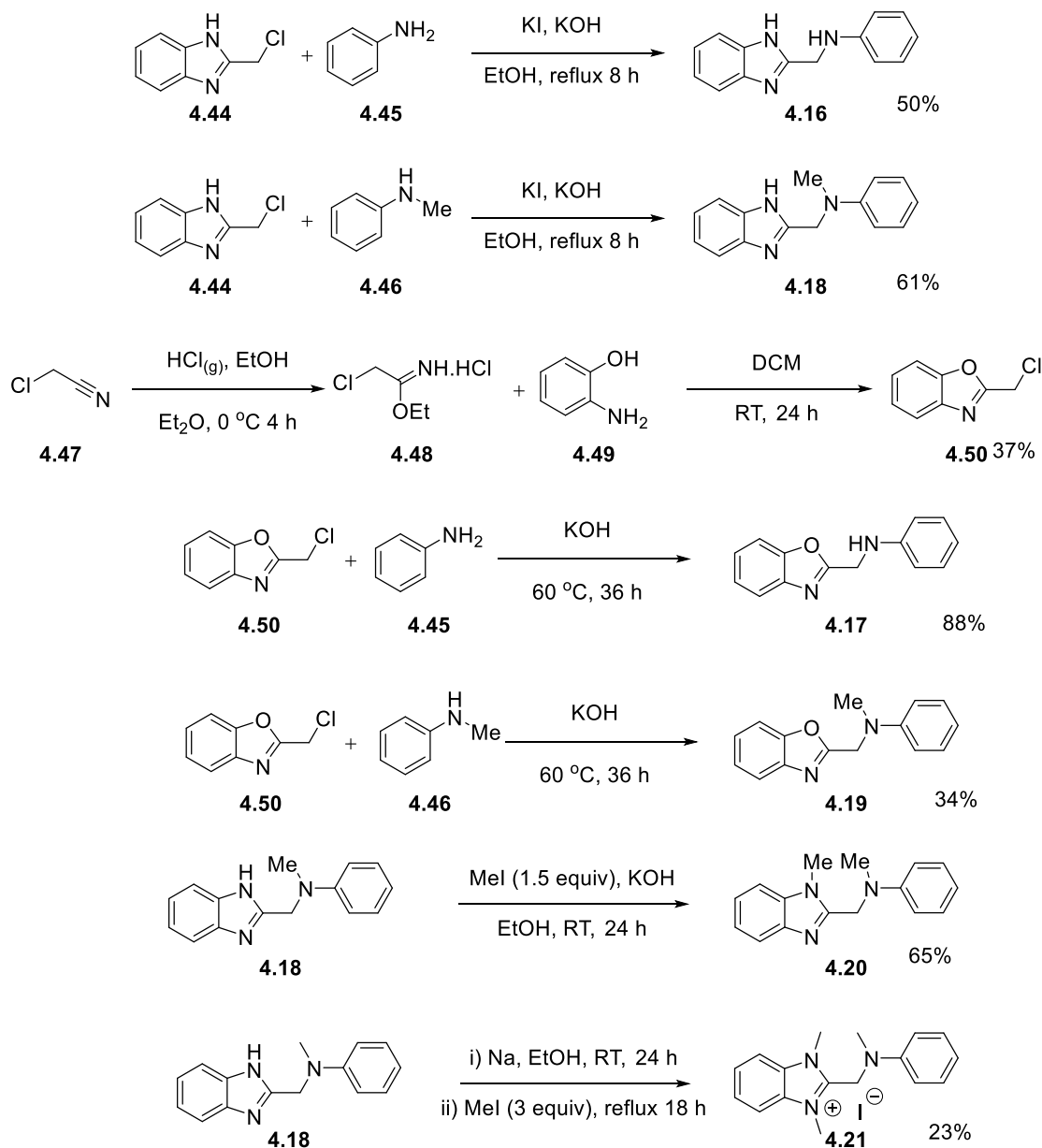
68.3(3)

68.3(0)

4.5 Experimental Results

4.5.1 Substrate synthesis

The proposed additives **4.16-4.21** were all prepared as shown in Scheme 4.4. The syntheses all start from relatively straightforward organic molecules and generally require a small number of steps to prepare.



Scheme 4.4 – Preparation of additives **4.16-4.21**

4.5.2 Coupling reactions with unhindered iodoarenes

The next step was to use these additives in coupling reactions between aryl iodides and benzene. These reactions followed a standard set of conditions outlined in the recent paper by Murphy *et al.*¹⁰⁴ These reactions were always performed in sealed pressure tubes under an inert atmosphere. The initial study looked at 3 unhindered iodoarenes – iodobenzene, 4-iodotoluene and 4-iodoanisole, to couple to benzene under these conditions and the results are shown below in Table 4.5.

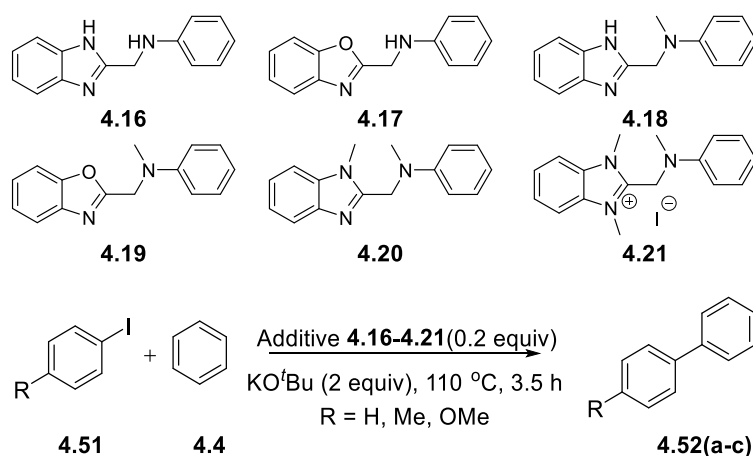


Table 4.5 – Standard reaction conditions for coupling reactions with prepared additives

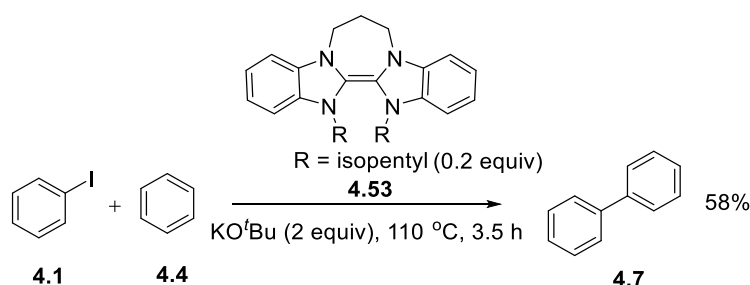
4.16-4.21

Additive	Biphenyl	4-methylbiphenyl	4-methoxybiphenyl
	(R=H 4.52a)	(R=Me 4.52b)	(R=OMe 4.52c)
	Yield	Yield	Yield
Blank	7%	5%	<1%
4.16	88%	71%	79%
4.17	74%	69%	67%
4.18	47%	22%	38%
4.19	42%	4%	14%
4.20	19%	12%	38%

4.21	14%	5%	6%
-------------	-----	----	----

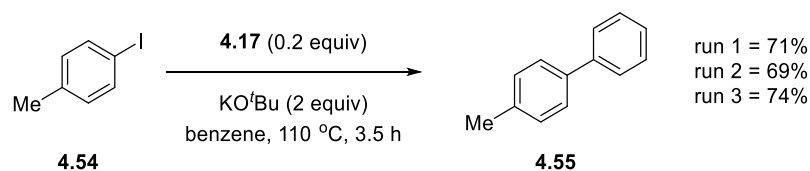
In the blank reactions, the yield was very low; it has been reported at higher temperatures that higher yields of coupled product have been observed.^{105, 107} This is attributed to a background initiation by benzyne (discussed fully in Chapters 5 and 6). At the lower temperature of 110 °C, this background source of initiation occurs in lower amounts than in higher temperature reactions. This suggests that the coupled product observed above these low background levels in these reactions will be as a direct result of electron transfer from an electron donor, formed by the additive being deprotonated by KO^tBu.

From the results when additives are present, **4.16** and **4.17** give the highest yields and it would be expected that these are the best additives for promoting these reactions. Additive **4.18** also gave yields significantly higher than the blank reaction; however, this was lower than the **4.16** and **4.17**. This was somewhat surprising as **4.17** and **4.18** were computationally both predicted to form dianions and there it was thought they would have had similar reactivity. Additives **4.19** and **4.20** were also predicted to have similar reactivity and in general this is the case, although the reaction of **4.19** with iodobenzene, **4.1**, gives a surprisingly high yield of coupled product, especially compared to the reaction with 4-iodotoluene which gave a lower yield than the blank reaction. As predicted, additive **4.20** gave very limited reactivity. To get an idea how these additives compare to a known successful SED, a side-experiment was performed using benzimidazole-derived donor **4.53** under the same conditions (Scheme 4.5). This reaction gave a yield of 58%. This suggests that additives **4.16** and **4.17** are performing better than the benzimidazole donor.



Scheme 4.5 – Reaction of iodobenzene and benzene in the presence of **4.53**

As **4.17** was a successful additive, it was decided to observe the repeatability of reactions with this style of additive. The chosen substrate in this case was 4-iodotoluene **4.54**, and what was observed was that over three simultaneous reactions the yields of 4-methylbiphenyl **4.55** were within 5%. These results suggest that reactions using these additives are repeatable and reproducible within a small experimental error.

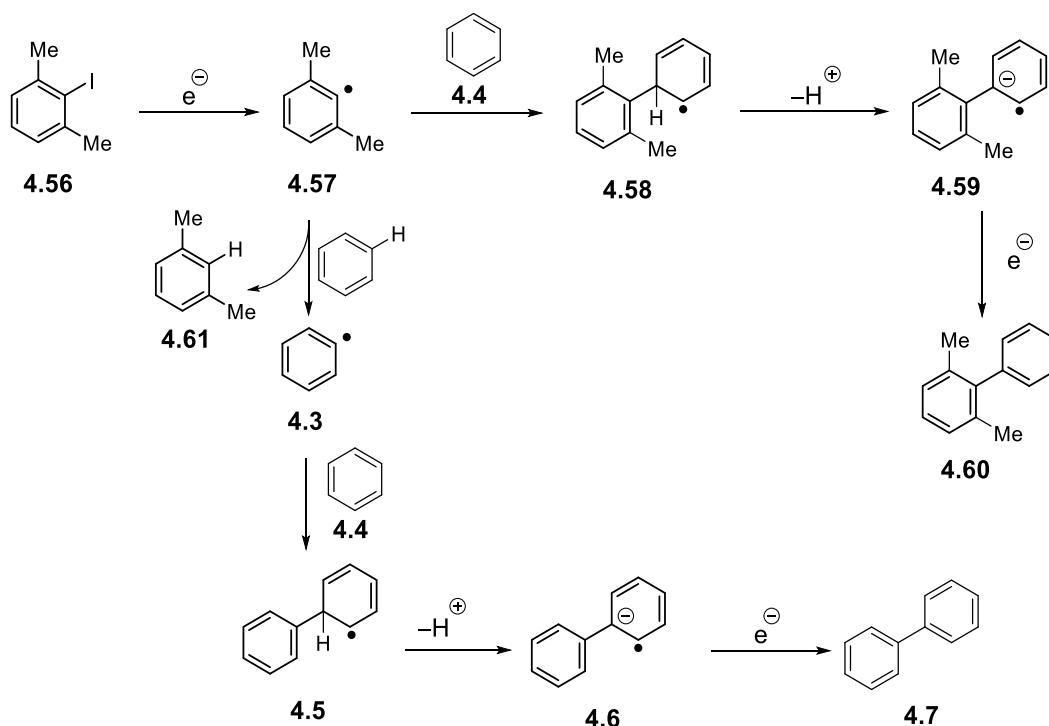


Scheme 4.6 – Repeatability study of coupling reaction between **4.54** and benzene in presence of additive **4.17**

4.5.3 2-Iodo-*m*-xylene reactions

As there is the possibility of benzyne formation and subsequent initiation in substrates with protons *ortho* to the iodide, the next step was to perform reactions with these additives, where the *ortho* positions are blocked with methyl groups, preventing benzyne formation. The substrate used for this was 2-iodo-*m*-xylene, **4.56**.

A characteristic of coupling reactions between 2-iodo-*m*-xylene, **4.56** and benzene, **4.4** is that the coupled products observed are perhaps not as would be expected. Instead of solely 2,6-dimethylbiphenyl, **4.60** being the product, what is observed is a mixture of **4.60** and biphenyl, **4.7** in a 1:3.8 repeatable ratio. This is due to the radical **4.57** formed after electron transfer finding it easier to abstract a hydrogen atom from benzene than to attack the benzene ring with formation of a C-C sigma bond. The rest of the mechanism follows the same as the BHAS pathway whether it is radical **4.57** or **4.3** that forms the new C-C sigma bond following attack of the benzene ring.



Scheme 4.7 – 2-Iodo-*m*-xylene alternative benzene attack options

As the radical generated (**4.57**) from single electron transfer to 2-iodo-*m*-xylene, **4.56** is hindered, this reacts more slowly and, to overcome this, higher temperatures are required to get the reaction to proceed. Even with these increased temperatures, the yields are significantly lower than for the unblocked aryl iodides. Another drawback of reactions with 2-iodo-*m*-xylene is that the mixture of products produced, **4.7** and **4.60** is inseparable (*m*-xylene is also formed in these reactions but is not observed); therefore, the yields are reported as mixtures and don't represent isolated single compounds. The advantage of using this substrate, however, is that reactivity observed is most likely coming from the electron donor, (either preformed or generated *in situ*). Thus, despite the lower yields and inseparable mixtures produced, these are important reactions in determining the success of the additives being used in these reactions.

As before, all the additives were now used in reactions, along with a blank reaction with no additive present. For these reactions, the temperature was increased from 110 °C to 130 °C and time from 3.5 h to 18 h. The results are shown in Table 4.6.

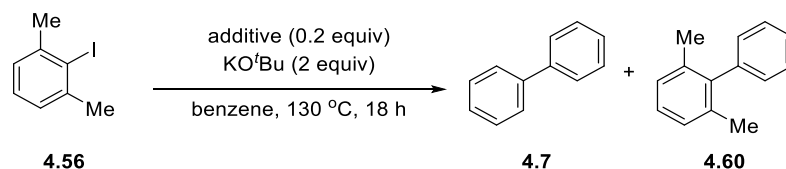


Table 4.6. Combined reaction yields of **4.7** and **4.60** from coupling of **4.56** and benzene

Additive	Yield 4.7 + 4.60
Blank	<1 mg
4.16	40.0 mg
4.17	34.1 mg
4.18	19.6 mg
4.19	15.6 mg
4.20	<1 mg
4.21	2.4 mg

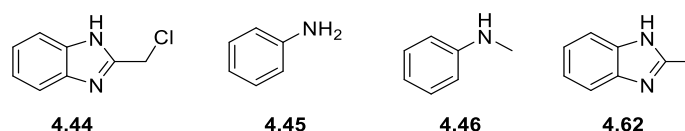
Based on 116 mg (0.5 mmol) 2-iodo-*m*-xylene, **4.56** being used in these reactions. Theoretical highest yield is 80 mg based on 4:1 **4.7**:**4.60**.

In work published in 2014, the Murphy group defined effective donors as those that yield more than 25 mg of product in these reactions.¹⁰⁵ Donors that give less than 0.5 mg of product are ineffective. Based on this reasoning, it can be said that **4.16** and **4.17** are effective donors. **4.18** and **4.19** are weakly effective. **4.20** is shown to be totally ineffective. However **4.21** does yield a very small amount of biphenyl, which was unexpected based on the computational predictions. This could be background reactivity; however, if it is due to electron transfer then at best it can be considered very weakly effective.

These results broadly agree with the unhindered aryl iodides where again **4.16** and **4.17** performed better than the other four additives, **4.18** and **4.19** perform to some extent and are similar in performance to one another. **4.20** and **4.21** produce little of the coupled product in either reaction. This suggests that, if an electron donor is being formed in these cases, then it is not strong enough to efficiently donate an electron to aryl iodides to initiate the BHAS cycle. What this also tells us is that di- and tri-anions make the most effective electron donors and the monoanions and neutral species are less effective in promoting these coupling reactions.

4.5.4 Is the full molecule required?

As it is not clear what form of the additive is responsible for the reactivity observed, reactions with different substructures of the additives were used as additives in their own right. If reactivity was observed with these substructures, then perhaps it is not the electron-rich alkene that is responsible for reactivity observed or is there an alternative electron donor being formed in these additives that is responsible for the reactivity.



Scheme 4.8 – Additives used to determine whether the full molecule is required

2-Chloromethylbenzimidazole **4.44**, aniline **4.45** and *N*-methylaniline **4.46** were commercial samples that were used as additives in coupling reactions between iodobenzene and benzene. 2-Methylbenzimidazole **4.62** was prepared to also be used as a fragment of the full additive. The aim of these reactions was to identify if electron donors were being formed in the fragments and this would have allowed more readily available organic materials to be used as additives.

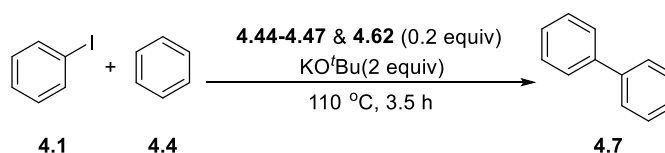
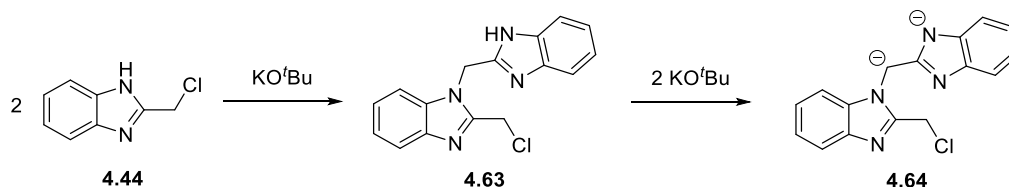


Table 4.7 – Reaction yields for coupling reactions with additives **4.44-4.47** and **4.62**

Partial Additive	Yield 4.7
4.44	50%
4.45	<1%
4.46	<1%
4.62	1%

With the exception of **4.44** none of the partial additives produced biphenyl **4.7** in significant yield. This was surprising as recently Jiao *et al.* published work showing *N*-methylaniline **4.46** was an efficient promoter of these coupling reactions,¹³⁷ this was a

contradiction of this works findings. Scheme 4.9 shows a possible mechanism for **4.44** to form a dianion **4.64** that could potentially act as an electron donor and could explain the observed reactivity.

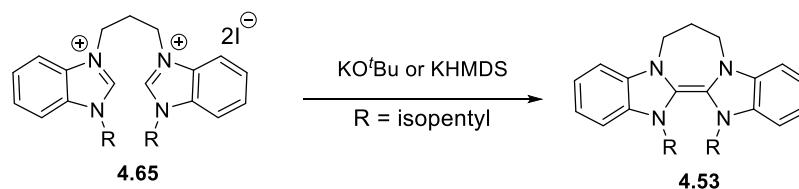


Scheme 4.9 – Possible formation of electron source in reaction with 2-chloromethylbenzimidazole **4.44** and KO^tBu

The reason is unclear for the reactivity observed with **4.44** as the additive; however, the overall yield is still lower than the most effective donors, **4.16** and **4.17**, suggesting that the full additive is required for an efficient reaction to proceed. It is certainly true that the aniline portion of the additive is ineffective in promoting the BHAS cycle and it in fact suppresses the background reactivity and affords only trace amounts of coupled product

4.5.5 Is KO^tBu essential for the reaction to proceed?

It has been proposed by a number of groups that KO^tBu is in fact the electron donor in these biaryl coupling reactions. If this was the case, then the additives used (both currently and previously) would not be able to carry out the transformation without KO^tBu regardless of the effectiveness of the donor. To investigate this, a number of coupling reactions were carried out with a benzimidazole-derived donor **4.53** that has been previously shown to work in biaryl couplings.



Scheme 4.10 – Formation of benzimidazole-derived electron donor **4.53** for parent salt

4.65

The initial base chosen to try and carry out the transformation was potassium bis(trimethylsilyl)amide (KHMDs). This is a strong non-nucleophilic base (pKa 25) that has been previously shown to generate the benzimidazole donor **4.53**, *in situ* from the parent salt, **4.65** and it would be expected to be capable of deprotonating radical **4.5** to generate radical anion **4.6** that would propagate the cycle, while this is unlikely to donate an electron to an aryl iodide. The two reactions were carried out under the same set of conditions as the coupling reactions for Table 4.5.

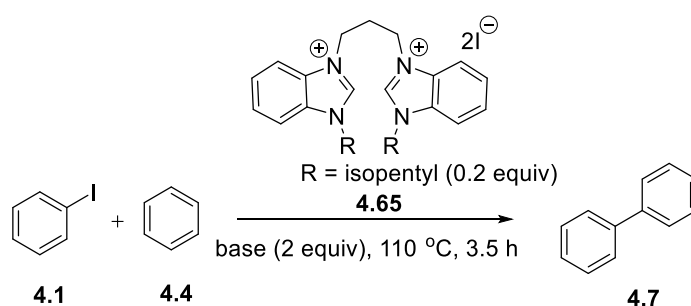


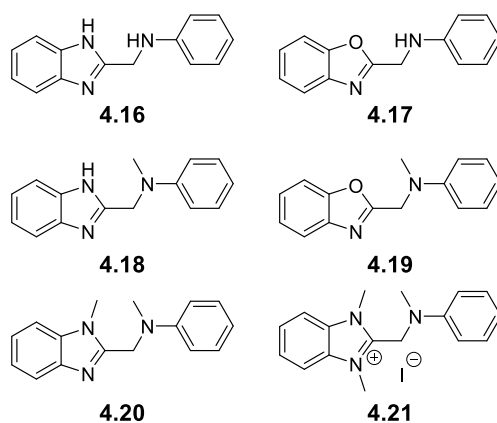
Table 4.8 – Comparison of bases in BHAS coupling reactions

Base	Yield 4.7
KO ^t Bu	58%
KHMDS	43%

These initial results suggest that KO^tBu is not essential to allow the reaction to proceed; however it does afford a higher yield than the alternative KHMDs.

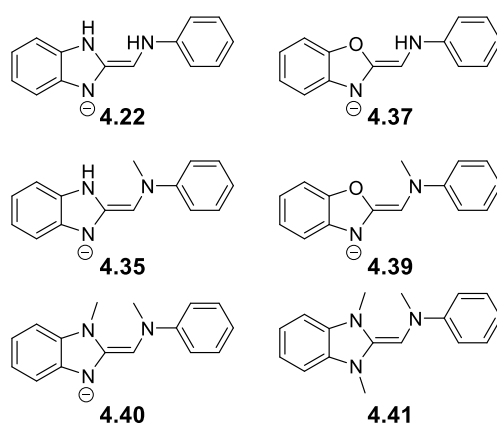
4.6 Conclusions

The initial computational study looked at the six proposed additives and the probability of an electron-rich alkene being formed and then the probability of this donating an electron to an aryl iodide.



Scheme 4.10 – Additives studied for their potential electron donor formation and ability

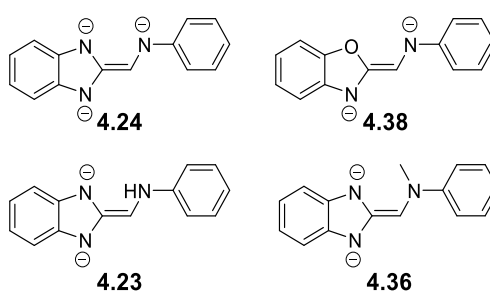
Looking at the deprotonations, it was found that **4.19**, **4.20** and **4.21** were all capable of easily undergoing a single deprotonation to generate the electron-rich alkenes. **4.17** and **4.18** would be able to form both singly and doubly deprotonated structures without a large energy penalty and it would be proposed that the doubly deprotonated structures would be better electron donors. Triamine **4.16** would be capable of forming singly and doubly deprotonated structures without large energy penalties: However, the third deprotonation was found to be quite endergonic. While it was still possible to be formed it would be more likely that a doubly deprotonated structure would be formed.



Scheme 4.11 – Electron-rich alkenes predicted to be ineffective electron donors

Despite being the most likely electron-rich alkenes to form, **4.23**, **4.26** and **4.27** are theoretically the least likely to be efficient electron donors. Neutral triamine **4.27** was calculated to be particularly unfavourable. Additives **4.17** and **4.18** were shown to be capable of forming both the mono and dianionic electron-rich alkenes. The monoanionic

electron-rich alkenes were endergonic for transferring an electron to iodobenzene, however not so disfavoured in energy to be impossible. The electron transfer from the dianionic electron-rich alkenes to iodobenzene was found to be exergonic and these were predicted to be good electron donors. Additive **4.16** is capable of forming three different levels of electron-rich alkene, the monoanionic electron-rich alkene **4.22** and dianionic electron-rich alkene **4.23** are both relatively favourable to form and, if they do, are capable of donating an electron to iodobenzene, with the formation of the dianionic species being particularly exergonic. Should the trianionic electron-rich alkene, **4.24** form, then this would be very likely to donate an electron to iodobenzene.



Scheme 4.12 – Electron-rich alkenes predicted to be effective electron donors

From the computational study, it was predicted that **4.16** would be the best additive for use in transition metal-free coupling reactions, closely followed by **4.17** and **4.18**. Despite all being favourable to form electron-rich alkenes, **4.19**, **4.20** and **4.21** were predicted to be inefficient additives for the reactions.

In experiments what was found was that **4.16** and **4.17** were the best additives for achieving successful coupling of iodoarenes to benzene. Additive **4.18** was also relatively successful but not to the same extent as **4.16** and **4.17**. The other additives that were predicted to be unsuccessful were unsuccessful.

There was broad agreement between the computational and experimental results. This suggests that this method is a useful tool for predicting the effectiveness of electron donors. However, there is not 100% success rate, and this is a reason why physical experiments are still important.

4.7 Future Work

For this research future work would be to investigate the successful additives in different bond formations to investigate what other transformations they can perform. A drawback of the additives is that, to form effective donors, they require a strong base and this limits the reactions they can perform.

A useful investigation would be to perform cyclic voltammetry on these additives in basic solution to get a true understanding of the donor strength being formed. This would also give clues to whether the trianion **4.25** was being formed as this would have a significantly higher reductive potential than dianions predicted to form from donors **4.17** and **4.18**.

Modifying the aniline side of the additives to try other amines for, example *n*-butylamine, would be an interesting investigation to try and find stronger electron donors. With the computational knowledge newly designed additives could relatively quickly be proposed or dismissed, cutting the number of synthetic reactions required to be performed.

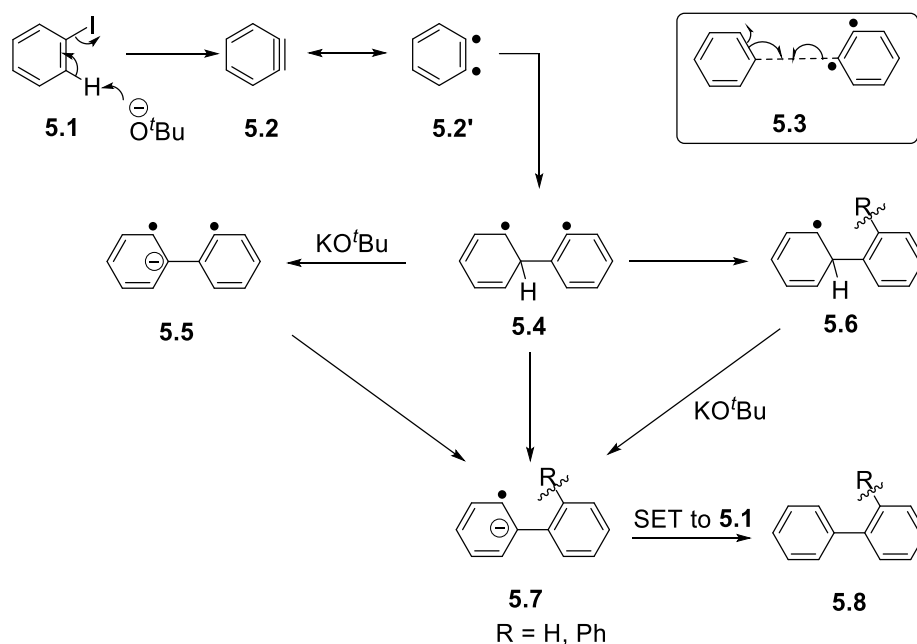
In addition to modifying the aniline side a second aniline group (or derivative) could be added leaving only one proton to for KO^tBu to attack to form the electron rich alkene.

Adding electron donating groups to the benzimidazole would make the electron rich alkene even more electron rich and this could be a method of increasing the strength of these donors.

5. Benzyne Initiation of Base-Promoted Homolytic Aromatic Substitution

5.1 Introduction

It has been observed in past papers and also the previous chapter that the presence of an electron donor is not always essential to initiate BHAS reactions.^{56, 77, 80, 82, 104, 127} While there are a number of proposals for how these reactions are initiated, this background source of initiation is still a source of debate. Some reports have suggested that the source of initiation comes directly from the KO^tBu .¹⁰⁷ However, this has been shown to be energetically disfavored. An alternative proposal by Murphy *et al.*¹⁰⁴ suggested that the source of the initiation was due to benzyne **5.2**, (Scheme 5.1) being formed and acting as a biradical, **5.2'**.^{104, 138, 139}



Scheme 5.1 – Proposed mechanism for biradical initiation of BHAS cycle¹⁰⁴

This biradical can add to a molecule of benzene, to form distal biradical **5.4**. The aryl radical within this species is likely to be much more reactive than the cyclohexadienyl radical, and this is expected either to abstract a hydrogen or to add to another benzene

ring; the result of either step is represented as **5.6**. This species undergoes deprotonation by KOtBu to afford **5.7**, and this would transfer an electron to the aryl iodide **5.1**, initiating the BHAS cycle. (An alternative sequence of steps is possible, in principle, where deprotonation of biradical **5.4** occurs to form **5.5**. Reaction of the aryl radical leads to **5.7** en route to **5.8** (Scheme 5.1).¹²⁶

Benzyne formation through this method features only in the initiation step of the coupling process, and so a small number of benzyne molecules suffices to initiate the cycle. To date, the only evidence implicating benzyne as a source of initiation has arisen through using a substrate such as 2-iodo-*m*-xylene, **5.9**. With that substrate, it is not possible to deprotonate adjacent to the iodide, and therefore benzyne cannot be produced; in such cases, and in the absence of any electron donor, the reaction is blocked and only trace yields of coupled products have ever been observed (significantly less than 1% -see below for a possible explanation of these traces of product). Hence this substrate is very helpful in unravelling the mechanism of these reactions.

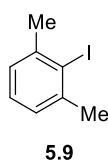
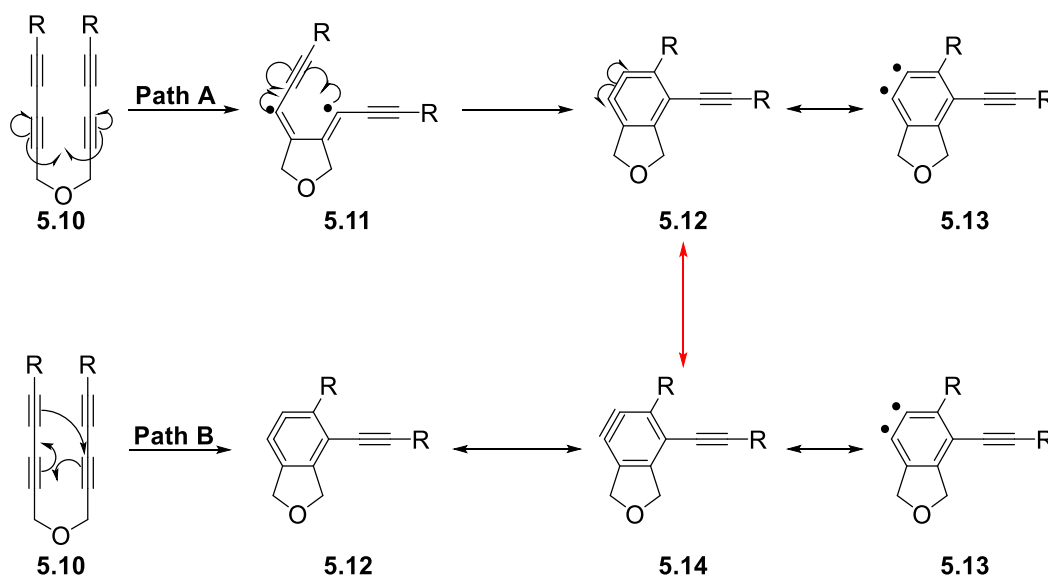


Figure 5.1 – 2-iodo-*m*-xylene

Going forward, our aim was to see if this blockage could be bypassed by using different additives to generate radicals thermally under the conditions of the coupling reaction. We selected both benzene-1,2-diyls (benzyne)²⁷ and benzene-1,4-diyls to be prepared respectively by the hexahydro-Diels-Alder (HDDA) reaction³² and the Bergman cyclisation.¹⁴⁰ If successful in initiating the coupling of **5.9** to benzene, this would support our interpretation of the role of benzyne in the initiation of the coupling process. In addition, we have tested thermal radical initiators for the coupling process and demonstrate that these are also able to promote the coupling reactions.

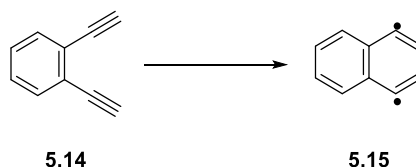
The hexadehydro Diels-Alder (HDDA) rearrangement³² has been studied extensively by the Hoye group and they have determined that the cyclisation occurs *via* a two-step

biradical process. This is illustrated for substrate **5.10** in Scheme 5.2, **path A**, where the biradical intermediate **5.11** is implicated, rather than the alternative closed shell concerted cyclisation to **5.12** (Scheme 5.2, **path B**).^{37, 38} This thermal method of generating *o*-benzyne was chosen here because of its simplicity, as it generates benzyne without added reagents.



Scheme 5.2 – Two proposed pathways for HDDA rearrangements; the upper biradical **path A** is now accepted³⁷

Whereas *o*-benzyne can be viewed as a 1,2-biradical, arene-1,4-biradicals are produced in the Bergman cyclisation. Starting from an enediyne, **5.14**, the molecule thermally cyclises to generate a 1,4-biradical species or “*p*-benzyne”, **5.15** (Scheme 5.3).¹⁴⁰ Recently, the Bergman cyclisation has been utilised in natural product synthesis, particularly in the synthesis of anti-tumor agents.¹⁴¹⁻¹⁴⁵

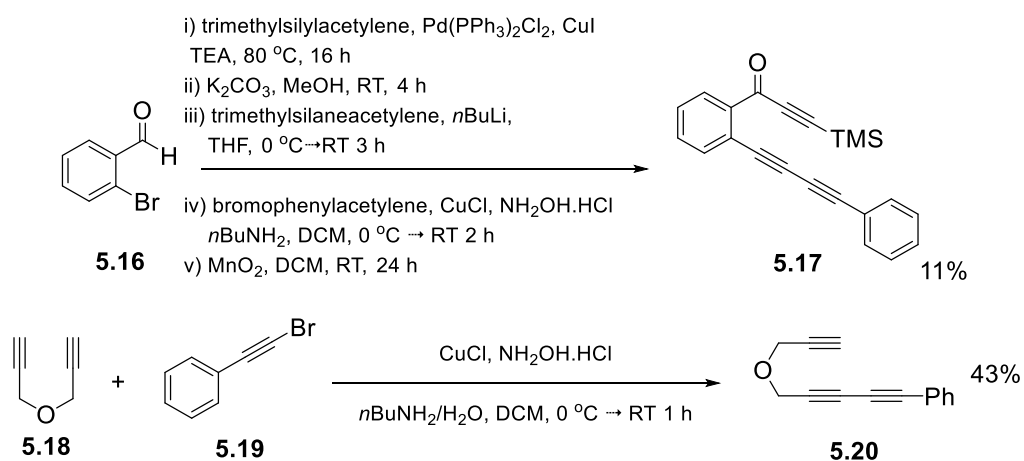


Scheme 5.3 – Bergman cyclizations of enediynes generate 1,4-biradicals

5.2 Results and Discussion

5.2.1 *o*-Benzyne

To demonstrate *o*-benzyne as a source of initiation of the BHAS cycle, substrates **5.17** and **5.20** were prepared by literature methods (Scheme 5.4).^{32, 146} These are designed to undergo HDDA rearrangements.



Scheme 5.4 – Preparations of substrates designed to undergo HDDA transformations

This was explored firstly with the substrate 2-iodo-*m*-xylene, **5.9** (Table 5.1) to establish whether the additives were effective in promoting the coupling to benzene. As mentioned above, this substrate is not capable of producing benzyne on treatment with base and, as a result, observation of coupling in the presence of an additive would provide evidence that the additive is responsible for the initiation. Successful coupling reactions with substrate **5.9** routinely do not afford high yields, but BHAS reactions lead to a diagnostic ratio (approx 4:1 of biphenyls **5.8** : **5.21**). We firstly assessed a blank reaction, i.e. with no additive, and observed small traces of coupled products. It is proposed that this background reactivity could be due to adventitious traces of palladium (or copper) contaminants in the KO^tBu reagent or on the glassware or

potential 4-iodo-*m*-xylene impurities in the 2-iodo-*m*-xylene.¹⁰⁴ The 4-iodo-*m*-xylene would be capable of forming benzyne. (To test this, reactions using palladium and copper catalysts as additives were performed and are discussed later).

Both **5.17** and **5.20** were successful in producing significant yields of coupled product compared to the blank reaction without any additive. What is also important is that the ratio in both cases is indicative of that observed in BHAS reactions when a super electron donor is used as the additive. The ability of these additives to initiate the BHAS cycle was then tested using an unhindered iodoarene, 4-iodotoluene, **5.22**.

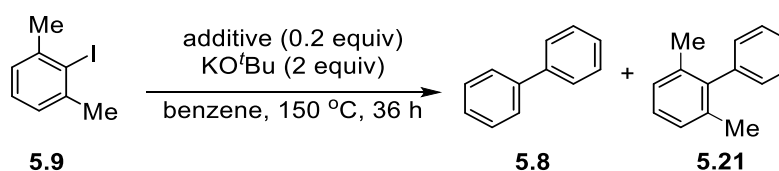


Table 5.1. 2-Iodo-*m*-xylene coupling reaction results

Additive	Yield 5.8 ^[a]	Yield 5.21 ^[a]
-	1%	<1%
5.17	9%	3%
5.20	29%	7%

[a] – yield determined by NMR using 1,3,5-trimethoxybenzene as internal standard

As 4-iodotoluene, **5.22**, has *ortho* protons it is susceptible to background benzyne generation (as evidence for this, butoxide addition products can be seen in blank reactions). As a result of this, the blank reaction yields are a lot higher than those when using 2-iodo-*m*-xylene **5.9**. When additives **5.17** and **5.20** are used in these reactions they both produce coupled product in a noticeably higher yield than the corresponding blank reactions.

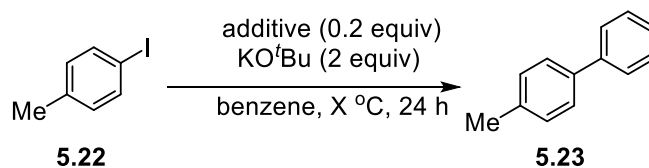
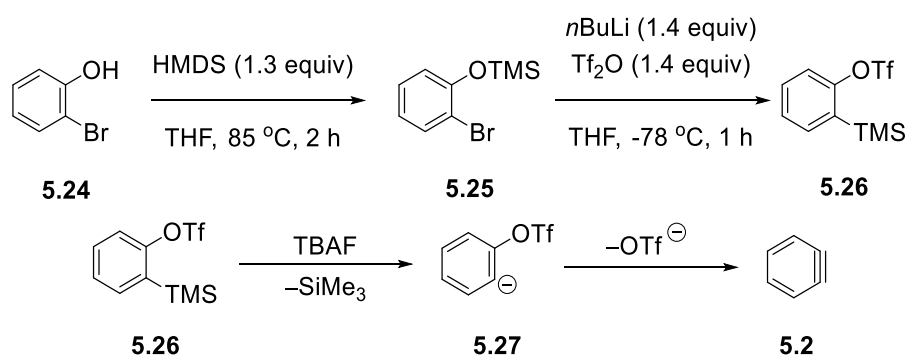


Table 5.2. Coupling reaction results using 4-iodotoluene, **5.22**

Additive	Temperature °C	Yield 5.23 ^[a]
-	130/150	20%/37%
5.17	130	42%
5.20	150	61%

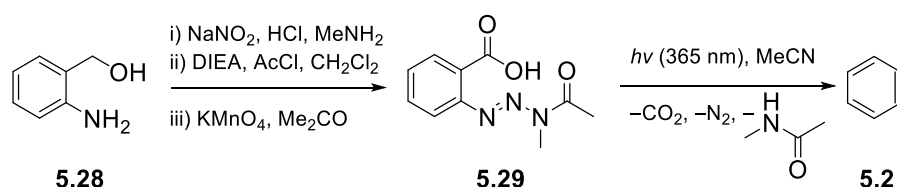
5.2.2 Alternative Methods of Forming *o*-Benzyne

Other methods of forming *o*-benzyne are known in the literature. Some of these precursors were also prepared to be used as additives in these BHAS reactions, and determination of their effectiveness were also attempted. Firstly Kobayashi's method of generating benzyne (Scheme 5.5) was investigated, **5.26** was synthesised according to literature procedure³⁰ and this was used in coupling reactions in the same way as **5.17** and **5.20**.



Scheme 5.5 – Kobayashi's method of forming benzyne³⁰

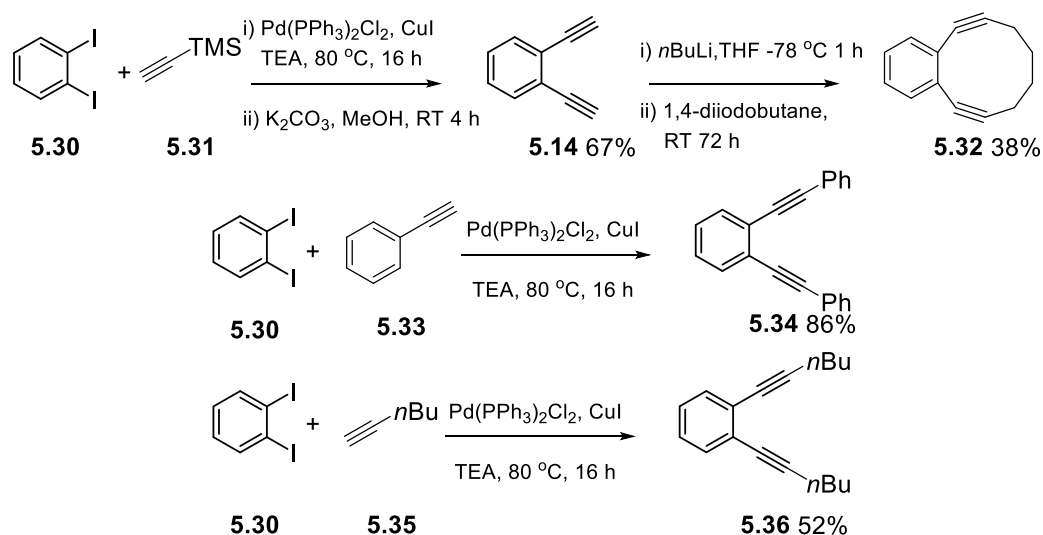
These reactions were unsuccessful however. It is thought that the tetrabutylammonium fluoride (TBAF) was potentially interfering with the BHAS cycle. Another alternative that was attempted was a substrate proposed by Schnarr *et al.*²⁹ that, under UV irradiation, breaks down to benzyne releasing CO₂ and N₂. This substrate was synthesised and again used in coupling reactions. This method also failed to improve the yield of coupled product above the yield of the blank reactions. This was potentially due to the lack of high temperature in UV reactions as the BHAS cycle often requires higher temperatures to proceed. Another potential issue is the lack of solubility of the Schnarr substrate in benzene.



Scheme 5.6 – Schnarr UV irradiation method of forming benzyne²⁹

5.2.3 *p*-Benzyne as an Additive

Substrates **5.14**, **5.32**, **5.34** and **5.36** were prepared.^{147, 148} The synthesis of these substrates is shown in Scheme 5.7. All of these substrates were used as external additives in standard coupling conditions to demonstrate their ability to initiate the BHAS cycle.^{104, 112}



Scheme 5.7 – Additives prepared to undergo Bergman cyclisations in coupling reactions.

These substrates were then used in the same coupling reactions as those used with the *o*-benzyne substrates. Again, firstly the additives were used in the coupling reactions of 2-iodo-*m*-xylene **5.9**, and benzene, Table 5.3.

Substrates **5.14**, **5.32**, **5.34** and **5.36** gave significant product yields above the blank reactions. This suggests that *p*-benzyne is also capable of initiating the BHAS cycle. A significant reaction was when **5.32** was used at 110 °C. There are few examples of coupling 2-iodo-*m*-xylene with benzene using the BHAS method at this temperature but substrate **5.32** was shown to be capable of promoting the reaction even at this lower temperature.

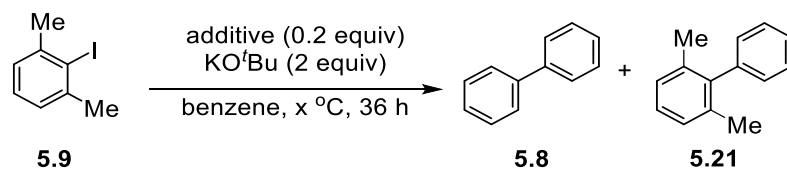


Table 5.3. 2-Iodo-*m*-xylene coupling reaction results using Bergman cyclisation additives

Additive	Temperature	Yield 5.8 ^[a]	Yield 5.21 ^[a]
-	150	1%	<1%
5.14	150	13%	4%
5.32	150	26%	6%
5.32	110	12%	2%
5.34	150	11%	3%
5.36	150	30%	8%

[a] – Yield determined by NMR using 1,3,5-methoxybenzene as internal standard

As with the HDDA substrates, the Bergman substrates were then used as additives in reactions with 4-iodotoluene **5.22**, and benzene.

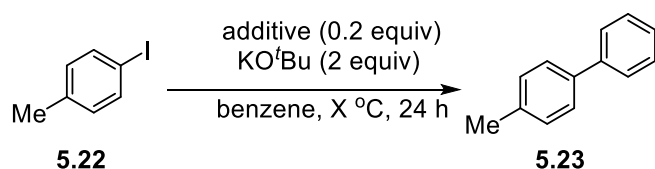


Table 5.4. 2-Iodo-*m*-xylene coupling reaction results with Bergman cyclisation additives

Additive	Temperature	Yield 43 ^[a]
-	110/130/150	5%/20%/37%
5.14	110/130/150	34%/41%/68%
5.32	110	33%
5.34	150	17%
5.36	150	66%

[a] – isolated yields

Compounds **5.14**, **5.32** and **5.36** were all successful in increasing the yield of these reactions above the blank reactions, Table 5.4. However additive **5.34** suppressed the yield; **5.34** was reported to not cyclise until higher temperatures than that used in the reaction.¹⁴⁹ This didn't explain why this additive did promote the reaction with 2-iodo-*m*-xylene however as these were equally performed at temperature lower than the reported cyclisation temperature. Additive **5.14** was able to promote the reaction down to 110 °C as was **5.32**. Additive **5.36** gave a high yield at 150 °C as it did with the 2-iodo-*m*-xylene **5.9**.

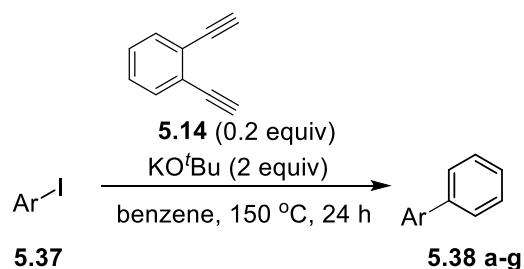


Table 5.5. Coupling reactions with different aryl iodides

Aryl iodide	Yield 5.38 ^[a]	Yield 5.38 ^[a] no additive present
4-iodotoluene 5.38a	68%	37%
4-iodoanisole 5.38b	85%	27%
3-iodotoluene 5.38c	65%	32%
Iodobenzene 5.38d	61%	43%
4-iodobiphenyl 5.38e	65%	54%
1-iodonaphthalene 5.38f	44%	19%
4-fluoroiodobenzene 5.38g	52%	8%

[a] – isolated yields

1,2-Diethynylbenzene, **5.14** was chosen as an additive to explore a range of aryl iodides to expand on 4-iodotoluene **5.22**. The reactions in table 5.5 were performed alongside the corresponding blank reaction, i.e. without **5.14**. What was observed was that for all the substrates explored the reactions with additive **5.14** produced more coupled product than those without the additive present. The yields of the blank reactions were

variable depending on the substrate, but repeatable for each substrate. It was surprising that there was such a variation on the blank reaction yields and there was no obvious reason for these differences. One suggestion for why this is the case could be the relative ease of benzyne generation or contamination with metals in the different substrates. However, this has not yet been explored.

5.2.4 Control Reactions

In order to determine whether the reactivity was the result of the biradical species being formed from the additives, a number of additives that were incapable of forming biradicals were used. Phenylacetylene, **5.33**, has only one triple bond, and so cannot undergo the Bergman cyclisation to form the *p*-benzyne diadical. Diphenylbutadiyne, **5.39**, was also deployed, this was formed as a by-product of the Cadiot-Chodkiewicz reaction. If traces of copper were being retained in a π -complexed form by alkyne additives from their syntheses, this would be a representative compound to probe if there was any effect from such species on the coupling of iodoarenes to benzene.

1,4-Bis(phenylethynyl)benzene, **5.40**, was formed using the same Sonogashira conditions as used in the other Bergman substrates. A lack of reactivity in reactions where this is the additive is evidence that any residual palladium or copper species in the additives is not responsible for the reactivity is observed. In addition to these, a reaction using a palladium catalyst as an additive was also performed to determine if palladium complexes can give rise to BHAS products. There are very few examples of palladium being used to couple aryl halides to benzene. It is not clear what type of palladium species is responsible for the observed reactivity - it could be Pd(I), Pd(II), or, more unlikely, Pd(IV) - more investigation would be required to determine the pathway that palladium is responsible for.¹⁵⁰⁻¹⁵⁵

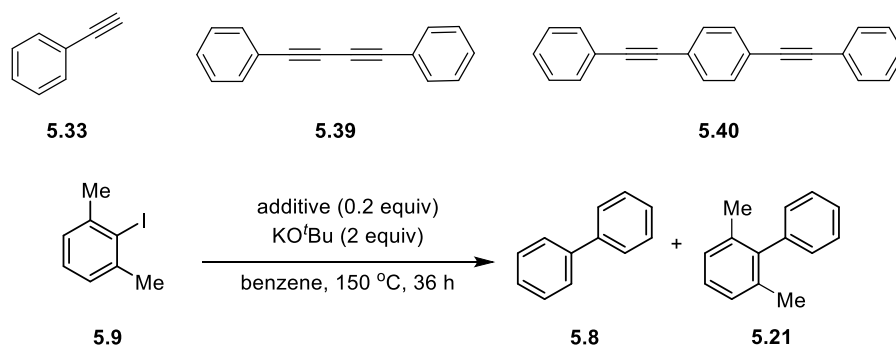


Table 5.6. Coupling reactions with 2-iodo-*m*-xylene with additives that can't form biradicals

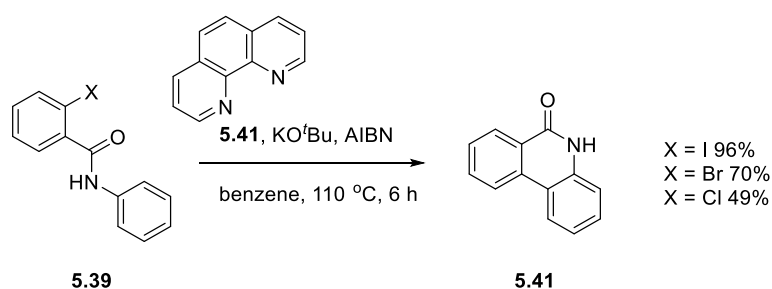
Additive	Yield 5.8 ^[a]	Yield 5.21 ^[a]
5.33	6%	1%
5.39	4%	1%
5.40	5%	1%
Pd(OAc) ₂ ^[b]	5%	11%
CuI ^[b]	1%	<1%

[a] – yield determined by NMR using 1,3,5-trimethoxybenzene as internal standard. [b] – 0.05 equivalents

With the exception of CuI all of these produced higher yields of coupled products than the blank reactions with 2-iodo-*m*-xylene **5.9**. This was surprising as it was expected that none of these should be able to promote the reaction. However, all these yields were much lower than those with the biradical additives present. From this it can be said that although, when in high enough quantities, these control additives can promote the reaction above the yield of the blank reaction, in the much smaller quantities that would be present in the additives these would not be the major source of initiation. Had these been the primary source of initiation in these amounts the yields would have been as high or higher than with the biradical additives.

5.2.5 Alkyl Radical Addition

After showing that arenediyls were capable of initiating the BHAS cycle, the next step was to look at alkyl radical initiators. As alkyl radicals are less reactive than aryl radicals it was unclear if an alkyl radical would be capable of attacking a benzene molecule. Recently Kumar *et al.* reported the synthesis of phenanthridinones utilizing KO^tBu with substoichiometric amounts of azoisobutyronitrile (AIBN).¹⁰²



Scheme 5.8 – Kumar’s synthesis of phenanthridinones

Using several radical initiators, it was shown that 4-iodotoluene, **5.22**, could be coupled to benzene producing 4-methylbiphenyl, **5.23**, (Table 5.7). Di-*tert*-butyl peroxide gave a very high yield (88%) at 150 °C, as butoxyl radicals could collapse to methyl radicals (either of these two radicals could also initiate the reaction) and acetone and if the acetone was deprotonated by KO^tBu, then the resulting enolate would be a good electron donor and it is possible that this would be initiating the BHAS cycle. The source of initiation in reactions where azo-initiators were used had to be the alkyl radicals either attacking benzene or abstracting a hydrogen atom from benzene. All these azo-initiators have a ten hour half-life at less than 100 °C, therefore over 24 h it would be expected that the majority of the initiator will have broken down to the radical. Of the azo-initiators, AIBN was the most successful followed by 1,1'-azobis(cyclohexanecarbonitrile) with 4,4'-azobis(4-cyanovaleric acid) being the least successful. However as it was the unblocked 4-iodotoluene that was used in these reactions, there could still be background benzyne formation occurring.

To overcome this we again used 2-iodo-*m*-xylene, **5.9** to block the benzyne and show that the initiation is due to radical initiator and not any background reactivity.

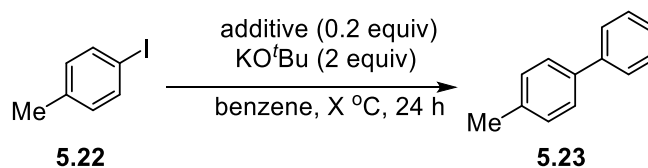


Table 5.7. Coupling reactions of 4-iodotoluene using radical initiators

Additive	Temperature (°C)	Yield 5.23 ^[a]
-	110/150	5%/37%
Ditert-butyl peroxide	150	88%
AIBN	110	40%
1,1'-Azobis(cyclohexanecarbonitrile)	110	31%
4,4'-Azobis(4-cyanovaleric acid)	110	22%

[a] Isolated Yields

While the yields (Table 5.8) in these reactions were modest at best, they are examples of alkyl radicals initiating the BHAS cycle when benzyne is unable to be produced. In this case the yields are all comparable, suggesting that it is in fact the butoxyl (or methyl) radical that is responsible for the initiation and not acetone. If it was acetone that was responsible based on the results in Table 5.7, the yield from using di-*tert*-butyl peroxide would be significantly higher than from the azo compounds used and as can be seen in Table 5.8, this is not the case. Compared to other successful additives, for example **5.17** and **5.32**, these yields were lower but, compared to control and blank reactions, the yields were significantly greater.

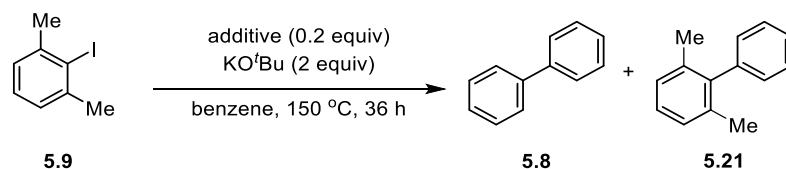


Table 5.8. Coupling reactions of 2-iodo-*m*-xylene with benzene using radical initiators as additives

Additive	Yield 5.8 ^[a]	Yield 5.21 ^[a]
-	1%	<1%
Di-<i>tert</i>-butyl peroxide	12%	3%
AIBN	11%	3%
1,1'-Azobis(cyclohexanecarbonitrile)	11%	4%

[a] Yields determined using 1,3,5-trimethoxybenzene as an internal NMR standard.

5.3 Conclusions

This work has shown that biradical species are capable of initiating the BHAS cycle. However, there is the need for higher temperatures or longer reaction times, compared to previously reported electron-donor promoted transition-metal free coupling reactions. The reactions that contain the biradical initiator always give significantly higher product yields than those without. It would be thought that the initiation in the reactions without the additive is also due to benzyne being generated through the proposed deprotonation ortho to the iodide. The extent of benzyne formation depends on the substituents on the aryl iodide and although it varies between different aryl iodides it is repeatable for specific aryl iodides. This work is also able to show that alkyl radical initiators are capable of initiating transition metal-free coupling reactions.

5.4 Future Work

The observations of different substrates giving different yields in the blank reactions is an area of this research that could be explored in more depth. This could be explored by isolation of butoxide addition to benzyne products as if it is the concentration of benzyne responsible for higher yields then there will be a higher yield of addition products.

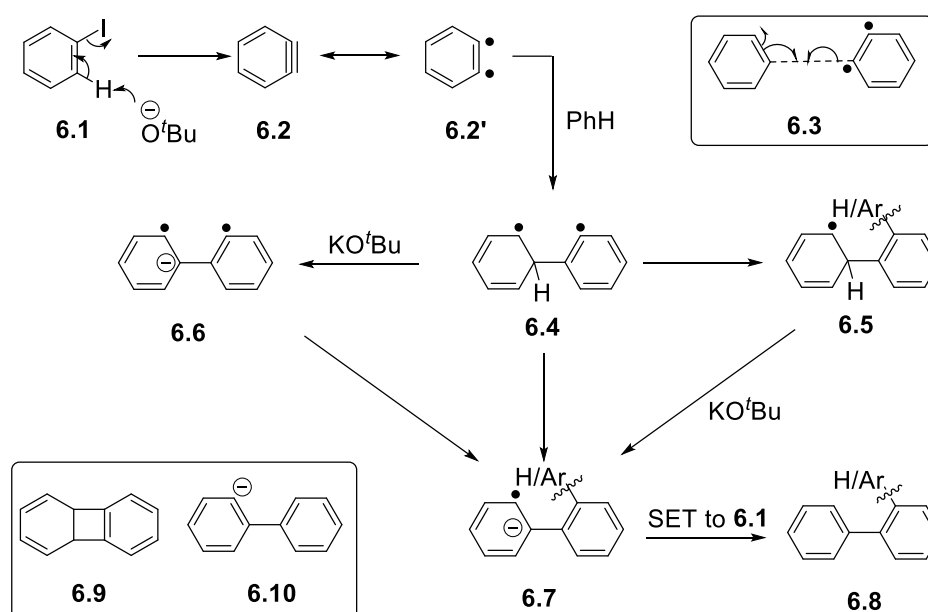
It would also be useful to explore a wider range of alkyl radical initiators and probe the mechanism to determine how these proceed. If radicals are adding to the arenes, then it would be interesting to isolate products of this type. Using a large haloarene would enable this.

The power of both biradical and alkyl radical initiation has not been fully explored and it would be useful to explore bromo- and chloroarenes to investigate if these can be coupled to benzene in this way.

6. Computational Analysis of Biradical Initiation of BHAS cycle

6.1 Introduction

As shown in the introduction and discussed in chapter 5, it is proposed that benzyne acting as a biradical, can attack benzene and, through subsequent steps, can form a radical anion that is capable of transferring an electron to a haloarene and therefore initiating the BHAS cycle. Having shown experimentally that adding external sources of benzyne (both *ortho* and *para*) can promote the BHAS cycle, this work investigated computationally the reasons why there was success in these reactions. Biradicals are not trivial to model computationally and there are not many examples in the literature where these have been successfully modelled.^{156, 157} While the proposed mechanism is shown in Scheme 6.1, there are alternative pathways that can occur.



Scheme 6.1 – Proposed mechanism for biradical initiation of BHAS cycle¹⁰⁴

For example, biradical **6.4** is capable of cyclising to form a 4-membered ring species, **6.9**. If the unpaired electrons of biradical anion **6.6** can pair to form biaryl anion **6.10** then this species is more likely to form **6.8** than initiate the BHAS cycle. As what is being

proposed is just an initiation, it is not required to be the most likely mechanism to occur; it instead is required to be a possible transformation and reasonable to be in competition with the alternative pathways. This chapter aims to show how feasible the proposed pathway is.

6.2 Computational Methods

Density Functional Theory (DFT) calculations were performed using Gaussian 09.¹²⁸ The functional of choice for this chapter was M06-2X^{158, 159} with 6-311++G(d,p) basis set on all atoms.^{130, 160, 161} All calculations were performed using the C-PCM implicit solvent model^{131, 132} with the dielectric constant for benzene ($\epsilon = 2.2706$). Unless explicitly stated, the reported energies are free energies.

6.3 *Ortho*-Benzyne Attack on Benzene

The reaction between benzyne **6.2** and benzene was calculated on both the singlet and triplet surfaces. By measuring the electronic energy, the relative stability of the closed shell singlet benzyne to the triplet biradical was calculated to be $\Delta E = 32.2 \text{ kcal mol}^{-1}$. This is consistent with the experimentally determined singlet-triplet splitting for *o*-benzyne of $\Delta E = 37.5 \text{ kcal mol}^{-1}$.¹⁶² However, reaction between benzene and the *o*-benzyne requires the biradical *o*-benzyne, which is stabilised in the open shell (or broken) singlet biradical state (characterized by a calculated S^2 value of 0.746) and is $12.7 \text{ kcal mol}^{-1}$ below the energy of the triplet biradical. The reaction occurs on the singlet biradical surface with an activation barrier of $7.2 \text{ kcal mol}^{-1}$, which is slightly lower in energy than the analogous reaction on the triplet surface $\Delta G^* = 8.4 \text{ kcal mol}^{-1}$, Figure 6.1).

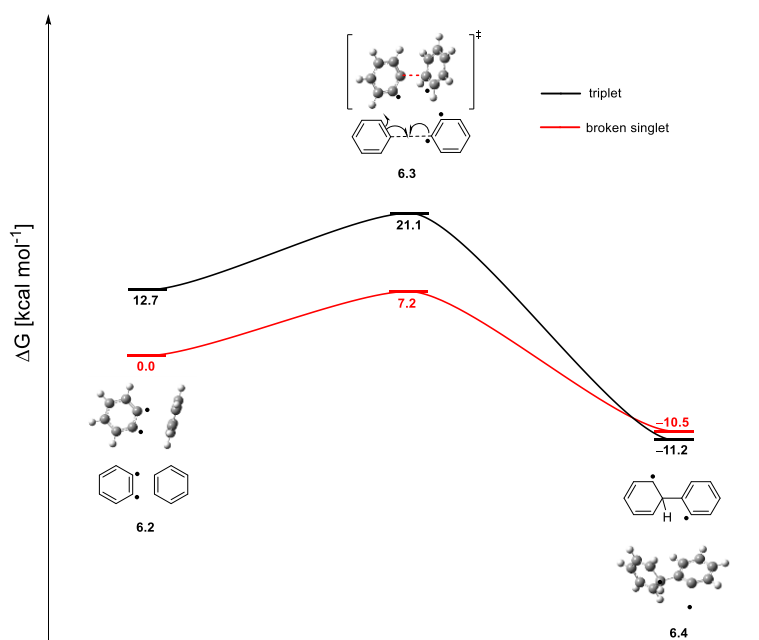


Figure 6.1 – Benzyne attack on benzene in triplet and broken singlet forms.

The resulting phenyl dicyclohexadienyl radical (**6.4**, Figure 6.2) adopts a twisted geometry with the radical centres in an approximate trans conformation ($\bullet\text{CCCC}\bullet$ dihedral angle = 110°). By looking at the spin density of this structure it can be seen that it has radical nature. Being spread over the two rings it is proposed that this is indeed a biradical species. This orientation limits the through space coupling of the radical centres and results in a slight preference for the triplet state over the broken singlet biradical state ($S^2 = 1.047$) by $0.7 \text{ kcal mol}^{-1}$.

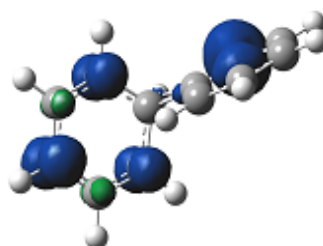


Figure 6.2 – Spin density of biradical **6.4**

Formation of the tricyclic product, 4a,8b-dihydrobiphenylene (**6.9**, Figure 6.4) therefore requires rotation around the central C–C bond (Figure 6.4), which occurs with a small barrier of $4.3 \text{ kcal mol}^{-1}$ in the triplet state ($4.7 \text{ kcal mol}^{-1}$ in the singlet state) to generate

the *cis* intermediate ($\bullet\text{CCCC}\bullet$ dihedral angle = 28°) where the singlet-triplet splitting is increased to $1.2 \text{ kcal mol}^{-1}$.

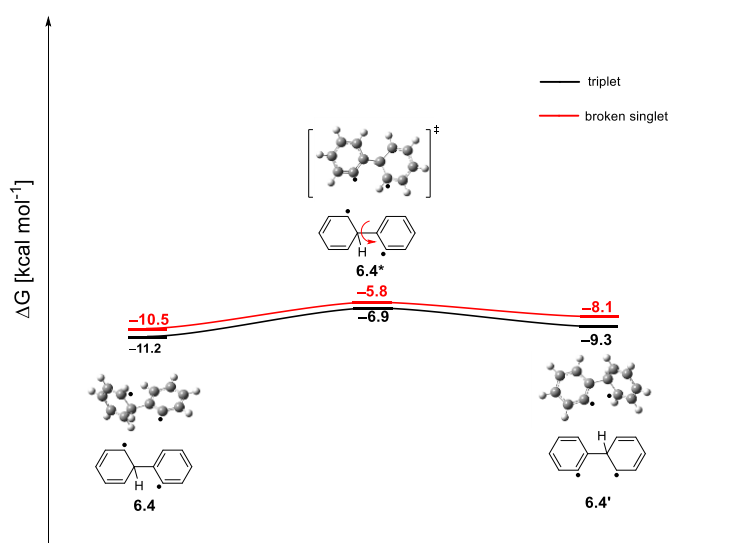


Figure 6.3 – Rotation of **6.4** to form the *cis* conformer, capable of cyclising

Despite the small energy gap between the conformations and triplet/singlet energies, in this conformation the singlet biradical is able to rapidly collapse to the tricyclic product (**6.9**, Figure 6.4) with a minimal barrier of $2.1 \text{ kcal mol}^{-1}$ in a strongly exergonic reaction ($\Delta G = -44.8 \text{ kcal mol}^{-1}$, relative to the *cis* intermediate, **6.4'**). The biradical electronic structure collapses in the formation of **6.9** on the singlet surface (transition state **6.11** has a calculated S^2 value of 0) such that the final product represents a closed shell singlet, which is $\Delta G = 47.4 \text{ kcal mol}^{-1}$ lower in energy than the original reactant state involving the closed shell singlet *o*-benzyne. In contrast, the triplet structure is unstable as the *cis* conformation and formation of **6.9** in the triplet excited state has an activation barrier of $\Delta G^* = 23.6 \text{ kcal mol}^{-1}$ in an endergonic reaction ($\Delta G = 6.4 \text{ kcal mol}^{-1}$).

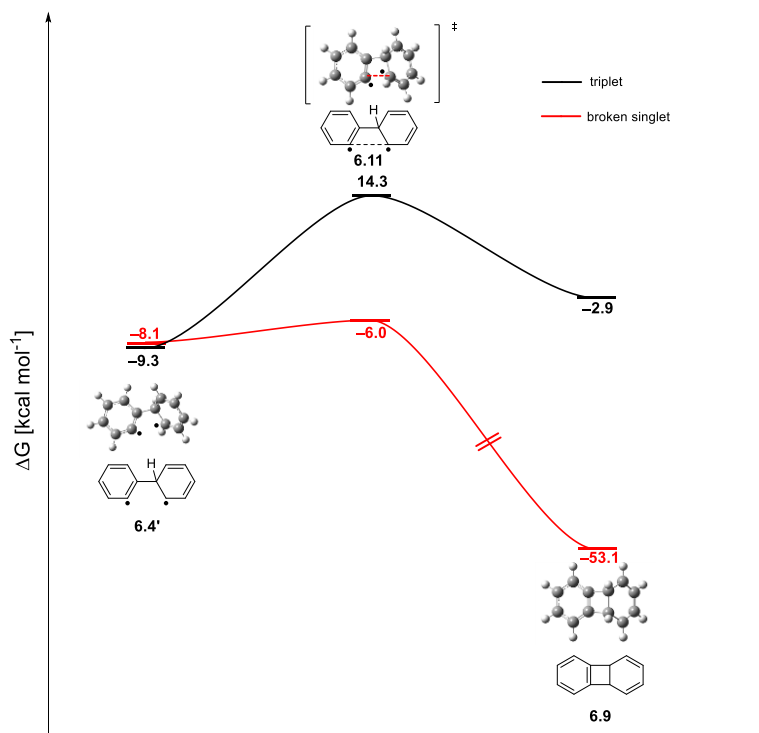


Figure 6.4 – Cyclisation of biradical **6.4** to form 4a,8b-dihydrobiphenylene **6.9**

Despite being a favourable transformation to form **6.9**, if it is formed exclusively then benzyne would not be a source of initiation for the BHAS cycle. However, from biradical **6.4** there are alternative pathways that could lead to a species that would be more likely to initiate the BHAS cycle.

It is possible that the biradical could either abstract a hydrogen from another molecule of benzene or alternatively attack another molecule of benzene by forming a C-C σ -bond. These calculations were performed exclusively using biradical singlets as this was seen to be more accurate in the previous calculations.

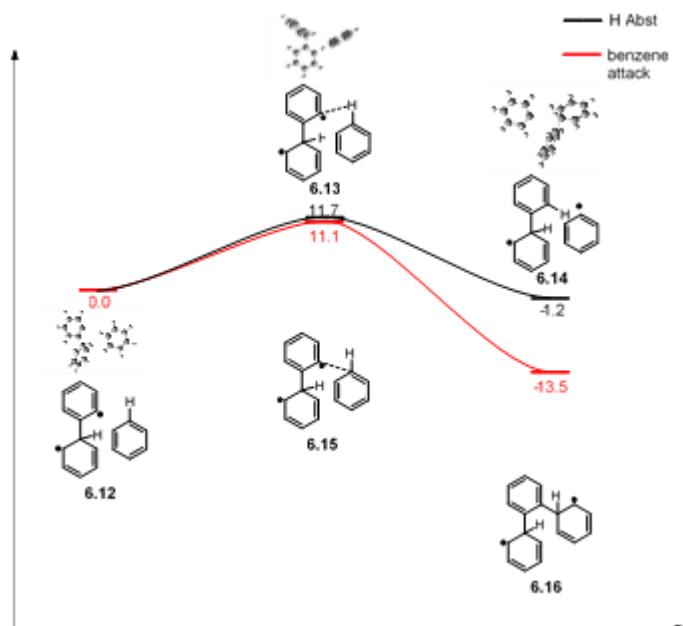


Figure 6.5 – Hydrogen abstraction vs benzene attack of intermediate **6.12**

While both the hydrogen abstraction ($11.7 \text{ kcal mol}^{-1}$) and C-C bond formation with benzyne ($11.1 \text{ kcal mol}^{-1}$) have similar barriers that are equally achievable, the C-C bond formation has a greater thermodynamic driving force as it is more exergonic overall at $-13.5 \text{ kcal mol}^{-1}$ compared to only $-4.2 \text{ kcal mol}^{-1}$ for the hydrogen atom abstraction. This could be due to the unstable free aryl radical that is being produced in the latter reaction relative to the more delocalised biradical when benzene is attacked to form a C-C σ -bond. Both of these are possible however, so the next step is to look at deprotonation to generate the radical anion **6.7** required to donate an electron another molecule of aryl iodide.

There was however, another possible pathway from the biradical **6.17** and that was that it could be deprotonated to form a biradical anion **6.6**. This was found to be quite favourable with an achievable barrier of $17.7 \text{ kcal mol}^{-1}$ and very favourable relative energy of $-52.3 \text{ kcal mol}^{-1}$. The product from this deprotonation was found to only be a local minimum as a biradical and when further optimised collapsed to a biphenyl anion, **6.10** with an overall relative energy of $-88.6 \text{ kcal mol}^{-1}$. Although the barrier is higher for this transformation relative to the hydrogen abstraction or attack on the π -system of benzene this is still a possible transformation and if some molecules go down this pathway they will not be capable of initiating the BHAS cycle.

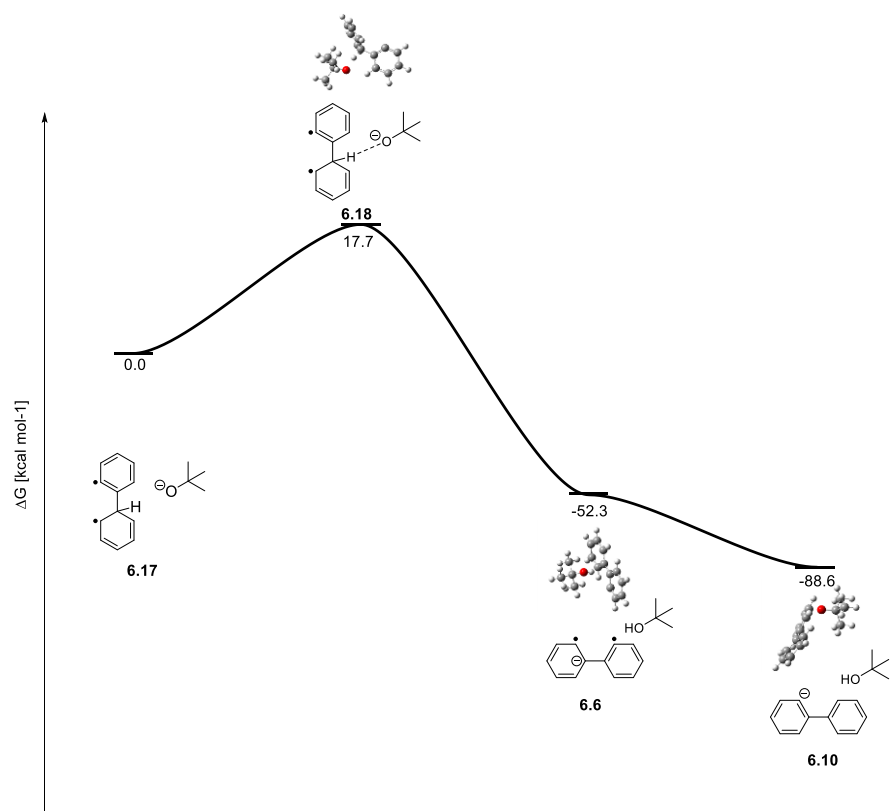


Figure 6.6 – Deprotonation of biradical **6.17** to form biradical anion **6.6** and subsequently biphenyl anion **6.10**

The calculation was performed with the product from the hydrogen abstraction as this had only one site for deprotonation, it would be expected that the energy profile of the product from benzene attack would be comparable. What was found was that the deprotonation to form the radical anion was almost barrierless at 1.5 kcal mol⁻¹ and was thermodynamically favourable with a relative energy of -32.7 kcal mol⁻¹.

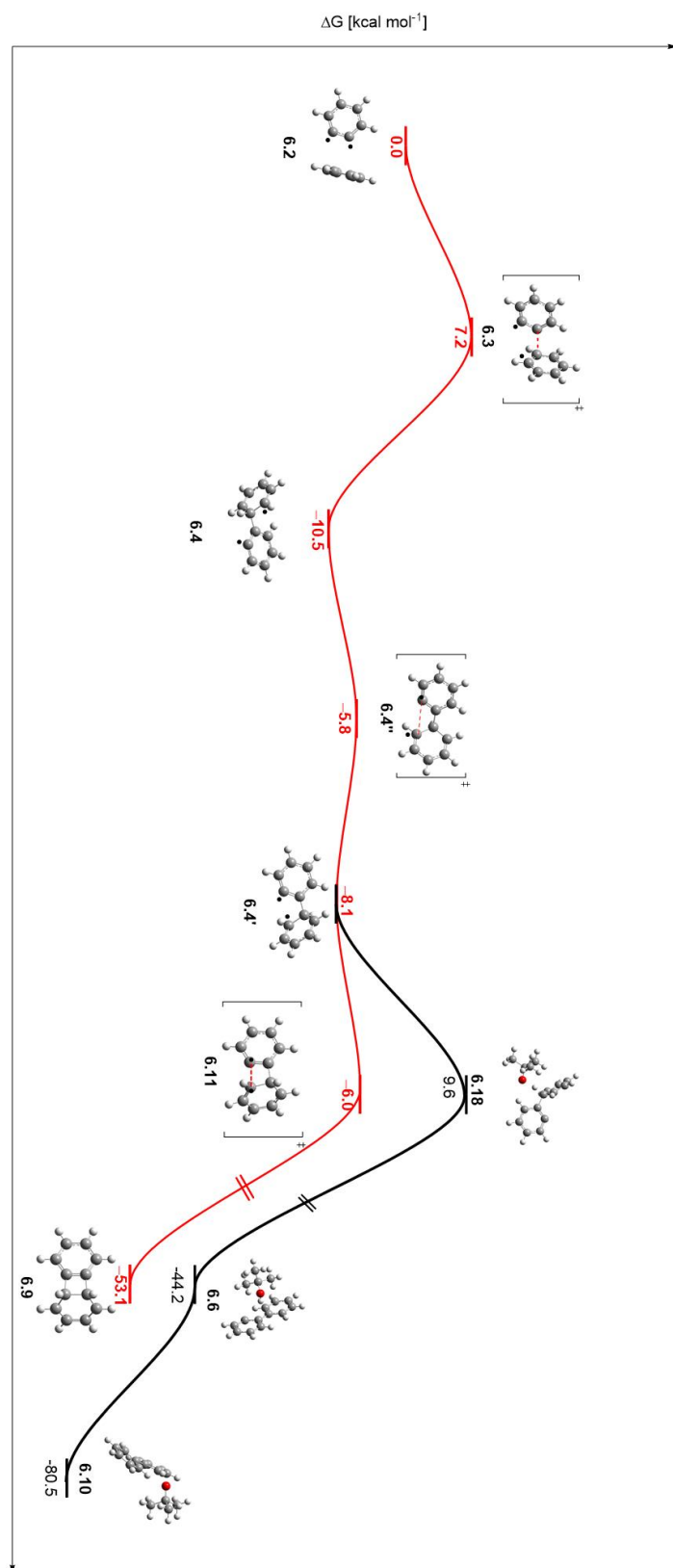


Figure 6.8 – overall energy transformation starting from benzyne

Running the calculations as broken singlets as opposed to triplet structures allowed for more realistic observations, while it brought challenges such as some structures collapsing to closed shell singlets.

Although not observed in experimental reactions, formation of 4a,8b-dihydrobiphenylene **6.9** appears to be a favourable side reaction. Despite this, overall from **6.2** to **6.7** it is an exergonic process of $-44.5 \text{ kcal mol}^{-1}$ and none of the barriers is too big to prevent the required transformations for initiation.

Reaction yields in blank reactions are always lower than those with an alternative source of initiation, such as an electron donor. It is possible that these competing pathways together with the addition of butoxide to benzyne (thereby preventing benzyne from behaving as a biradical) contribute to these lower yields.

6.5 Future Work

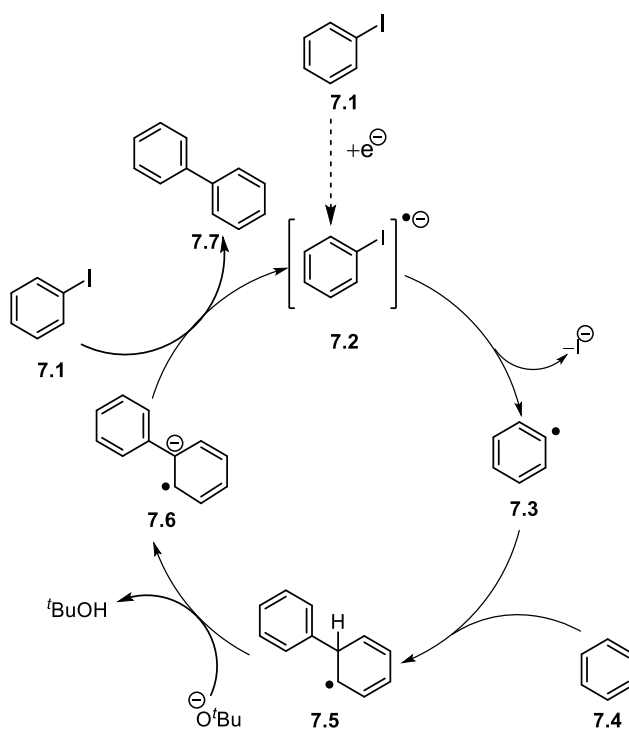
This work has only explored *o*-benzyne attacking benzene and the subsequent transformations. In the experimental work, *p*-benzyne in the form of Bergman cyclisations was used to initiate the BHAS cycle and it would be interesting to explore the *para* biradical pathway. In this case there is unlikely to be any four-membered ring formation, and so potentially this route has fewer alternative pathways. This additional work could fully explain the observations from the experimental benzyne chapter.

Another idea would be to model the *o*-benzyne and *p*-benzyne biradicals abstracting I, Br & Cl from aryl halides. This would be an alternative way of generating aryl radicals to initiate the BHAS cycle.

7. Computational Analysis of Potassium Hydride reactions with haloarenes

7.1 Introduction

The transition metal-free dehalogenative coupling reaction between haloarenes and arenes, mediated by a base (typically KO^tBu) and an organic additive is now well established in the chemical literature. This was shown in the introduction and added to in Chapter 4.^{77, 78, 80, 81, 104, 105} The BHAS mechanism has a well characterised propagation cycle of this radical chain reaction (Scheme 7.1).



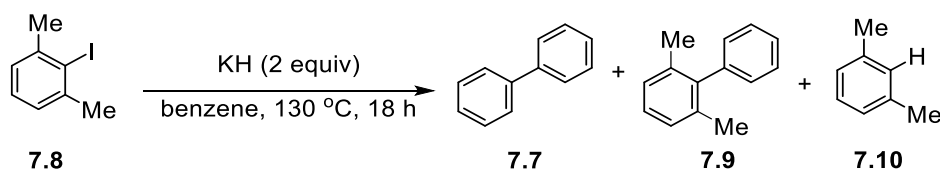
Scheme 7.1 – BHAS cycle proposed by Studer and Curran⁸⁹

The source of the initial electron as discussed throughout the thesis is still debated. The Murphy group's recent study critically examined the evidence presented for KO^tBu as a single electron donor to haloarenes in a number of different reports and found that in each case, organic additives initiate the BHAS reaction by forming organic electron donors *in situ*.¹¹² Whilst organic additives are not absolutely required for most

substrates in this transformation,^{107, 109, 163} they significantly enhance the yield of the coupled products, simultaneously allowing reactions to be conducted at lower temperatures and for a shorter duration. In the absence of suitable organic additives, BHAS reactions can be initiated by arynes (benzyne) (discussed fully in Chapters 5/6), formed by base-induced elimination of HX from substrate haloarenes ArX such as **7.1**. Throughout this chapter a number of molecules have been truncated for the computational calculations from the physical experiments to improve the computational efficiency.

7.2 Investigation of Pierre Mechanism

Josh Barham (JB) and Sam Dalton (SD) in the Murphy research group performed reactions where they attempted to couple 2-iodo-*m*-xylene, **7.8** to benzene in the presence of an organic additive and a base (either KO^tBu or KH) (Scheme 7.2). It was noticed that in a reaction without phenanthroline present and with KH as the base that 2-iodo-*m*-xylene was completely consumed. Small quantities of coupled products **7.7** and **7.9** were recovered. However, the major product of these reactions was the dehalogenated product **7.10**.

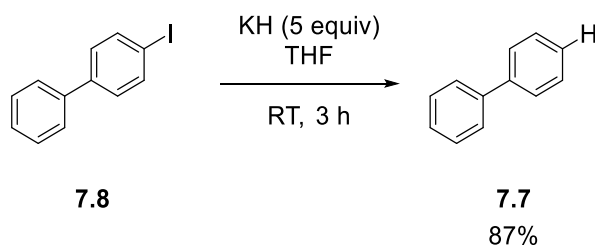


Scheme 7.2 – 2-iodo-*m*-xylene reactions with benzene in the presence of KH

It has been previously reported by Pierre¹⁶⁴ that iodobenzene treated with KH in THF at room temperature was efficiently dehalogenated and it was proposed that the same reaction was occurring in our reaction with 2-iodo-*m*-xylene. Pierre suggested that 1) due to the order of reactivity being ArI > ArBr >> ArCl and 2) since H₂ was not released in the reaction, that these dehalogenations were not proceeding *via* a formal S_NAr or benzyne mechanism.

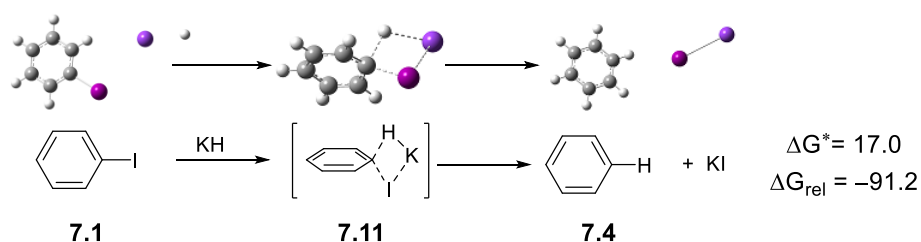
To probe the mechanism, JB subjected the less volatile 4-iodobiphenyl to Pierre conditions. In THF, biphenyl was successfully isolated in 87% yield; when the solvent was

changed to THF-d⁸ the yield dropped to 62% but crucially, no deuterium incorporation was observed. This suggested that the H atom is obtained from KH and not the solvent. Interestingly there was no reaction with NaH in THF, nor with KH in benzene as the solvent at room temperature.



Scheme 7.3 – Reactions of 4-iodobiphenyl in THF with KH

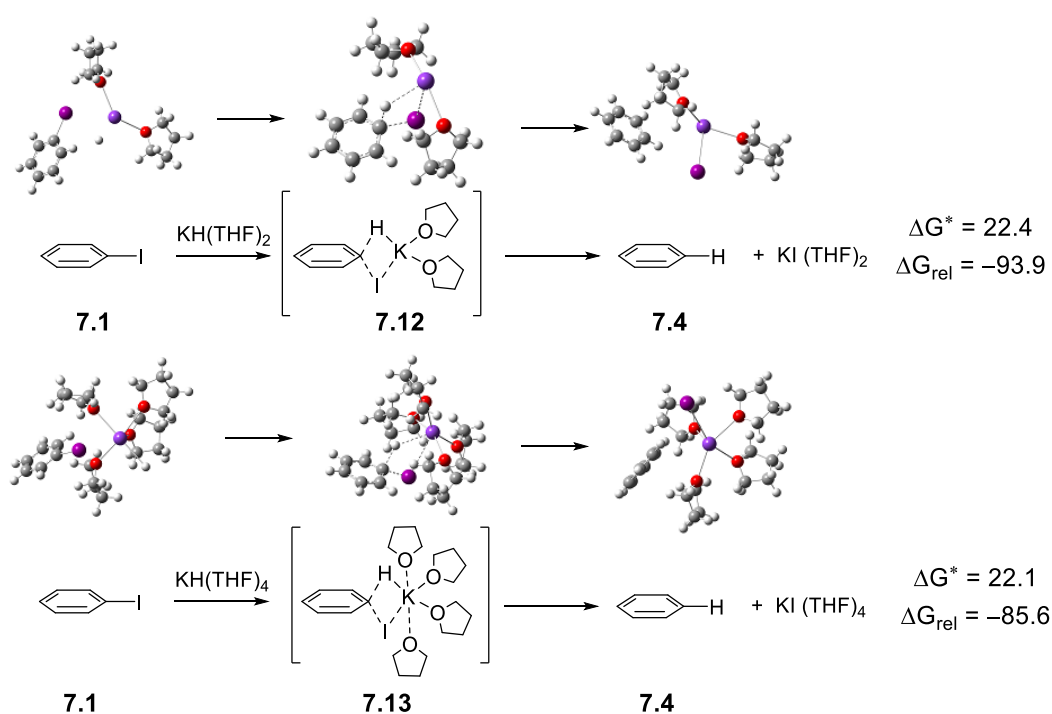
Pierre proposed that these reactions were proceeding *via* a concerted aromatic substitution featuring a 4-membered transition state.¹⁶⁴ Recently there have been a number of groups that have also proposed concerted nucleophilic aromatic substitutions.¹⁶⁵⁻¹⁶⁸ A recent paper from Chiba *et al.*¹⁶⁹ also proposed a concerted nucleophilic substitution and their computational study into the mechanism helped to guide this research. In this work, the mechanism was modelled computationally to look at the energy profile of this transformation. The initial model was performed using M062-X functional with 6-31+G* basis set for carbon and hydrogen atoms and MWB56 basis set for iodine atoms. The C-PCM implicit solvent model was used^{131, 132} with the dielectric constant for THF ($\epsilon = 7.4257$).



Scheme 7.4 – KH displacement of iodide in THF fully implicit solvent

This model featured a fully implicit solvent and suggested that the displacement of iodide with hydride was very favourable with a barrier of 17.0 kcal mol⁻¹. This is consistent with previous experimental observations. To try and model this more

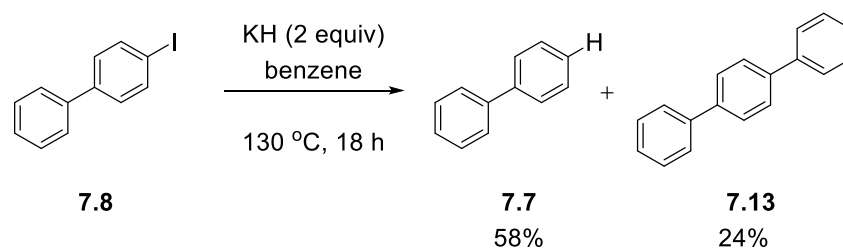
accurately, it was decided to try adding in two or four explicit THF molecules, as ligands, to the system to observe any changes in the energy profile. This was due to examples in Chiba's work where he adds in two explicit THF molecules, as ligands. They used NaH, so as potassium is larger it was thought that having four THF molecules may have more of an effect.



Scheme 7.5 – Displacement of iodide with KH with the addition of explicit THF molecules

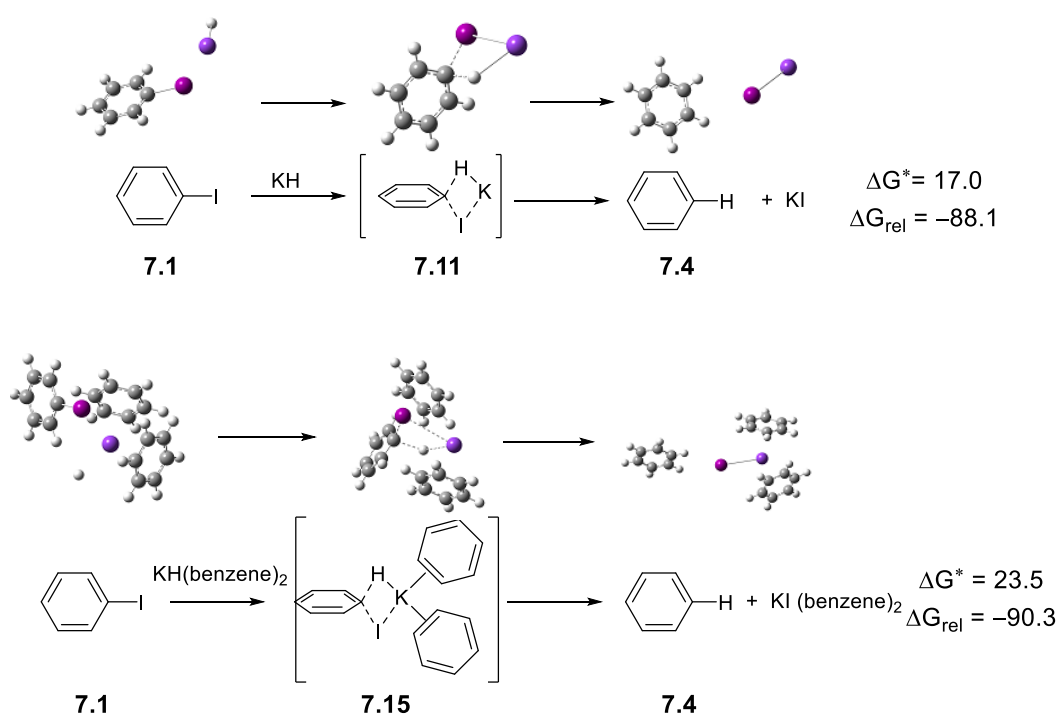
Adding in explicit THF increases the barrier energy by $\sim 5 \text{ kcal mol}^{-1}$; however, the relative energy does not experience as significant a change. Increasing from two to four THF molecules did not influence the energy profile and, as the computational cost increased it was decided to use only two explicit solvent molecules when moving forward.

The reactions performed by JB and SD were performed in benzene however, and required a higher temperature to proceed. The displacement of iodide by hydride was modelled in benzene ($\epsilon = 2.2706$) as the implicit solvent.



Scheme 7.6 – Reactions of 4-iodobiphenyl in benzene with KH

These were modelled (i) as a naked system, devoid of explicit solvent and (ii) with two explicit benzene molecules present in a similar fashion to the THF example.

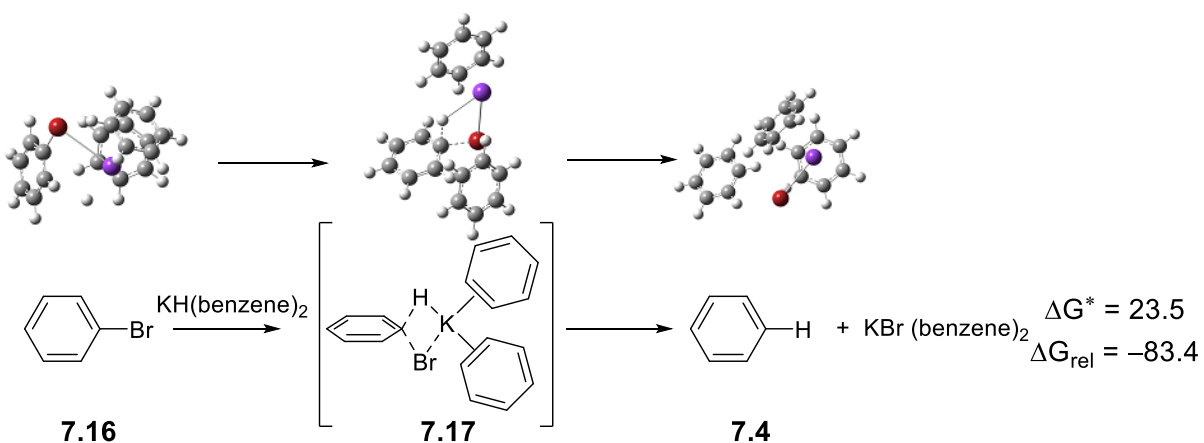


Scheme 7.7 – Displacement of iodide with KH in benzene calculations

What was again observed is an increase in barrier energy with the addition of two explicit benzene molecules, as ligands. The energy profile suggests that the displacement is again favourable in benzene with a low barrier of 23.5 kcal mol⁻¹, especially at the temperature being used in the reactions performed. Whilst Pierre observed 100% conversion in THF, and JB/SD observed 87% yield in THF, despite the small difference in barrier energy, the yield for reactions in benzene was only 58%. A reasonable explanation of this would be the lack of solubility of the KH in benzene which

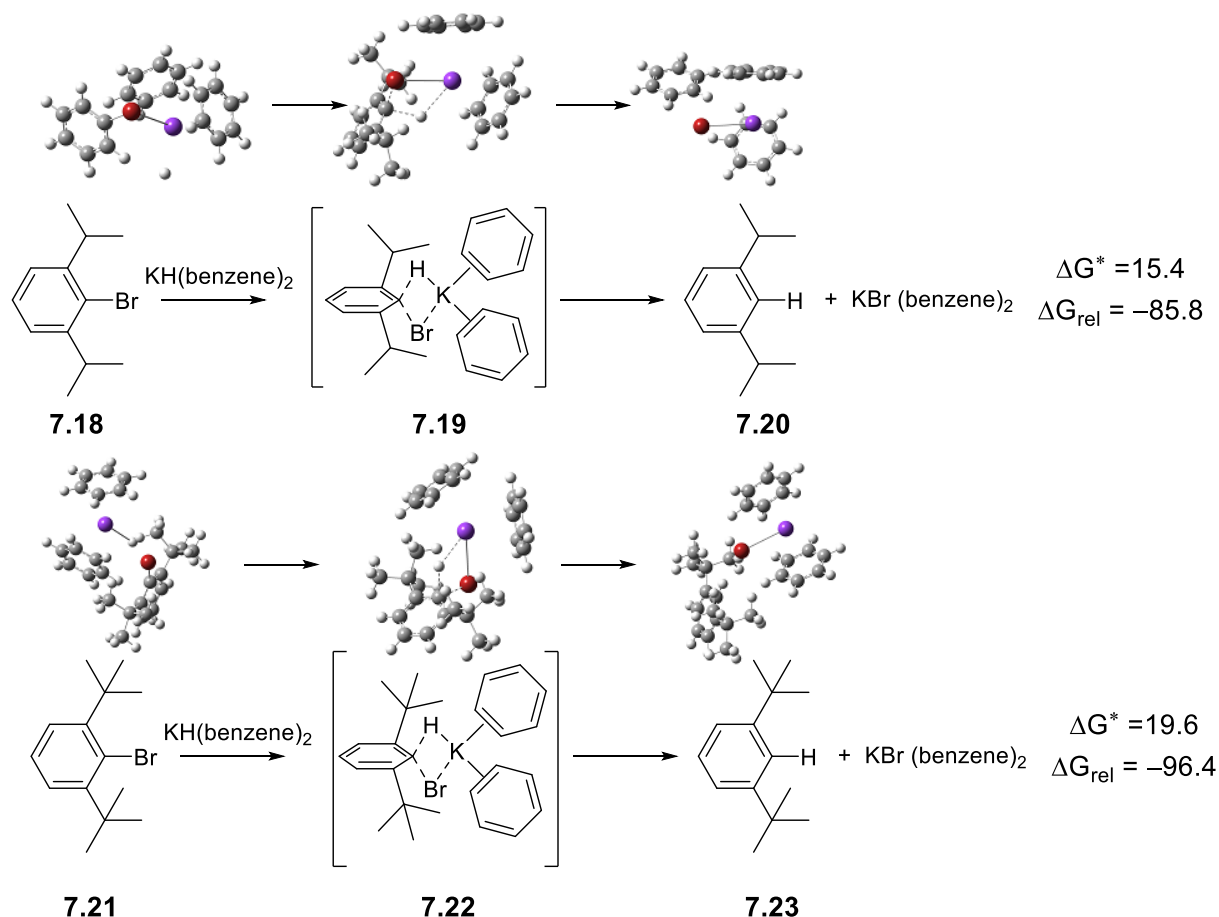
computational calculations do not take account of, but would affect the reactivity of the physical experiment.

The iodine of **7.1** was then replaced with bromine as in **7.16** and the displacement was again modelled in benzene with 6-31+G* as the basis set for all atoms.



Scheme 7.8 – KH displacement of bromine

This was another favourable transformation and there was no significant energy change going from iodine to bromine.



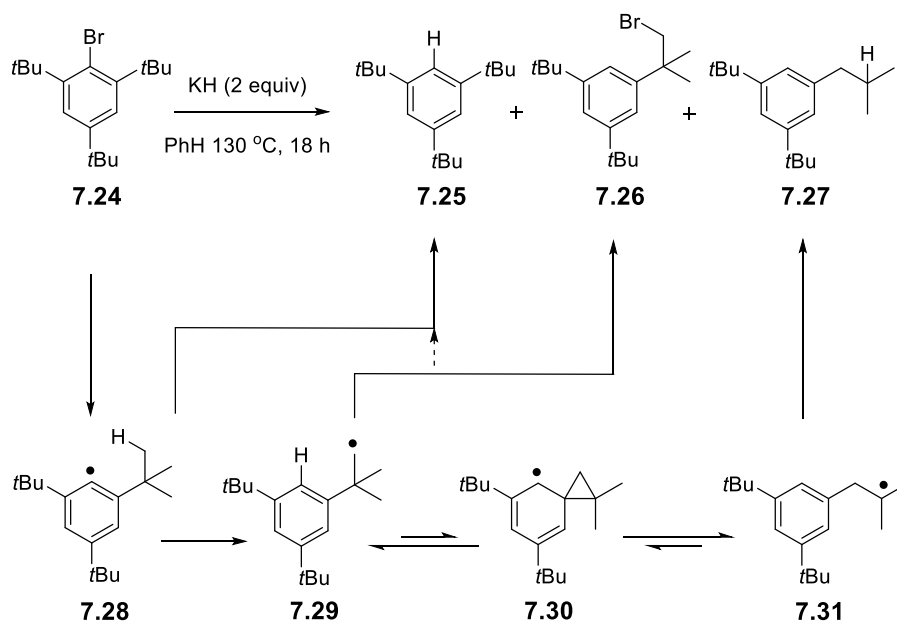
Scheme 7.9 – KH displacement of bromine with hindered structures **7.18** and **7.21**

A more significant calculation was when isopropyl and *tert*-butyl groups were added to the *ortho* positions. Isopropyl groups in the *ortho* positions lowered the energy barrier of this transformation to 15.4 kcal mol⁻¹. It is thought that this is due to the isopropyl groups being pushed out the plane by the bulky bromine and when the hydride attacks they are able to settle back into the plane. When these were changed to *tert*-butyl groups the energy barrier is still lower than when hydrogens are in the *ortho* positions but is increased compared to isopropyl groups. This is most likely due to increased steric bulk around the bromine making attack by the potassium hydride more difficult, but overall it is still a favourable transformation.

7.3 Bromine Atom Abstraction by Alkyl Radicals

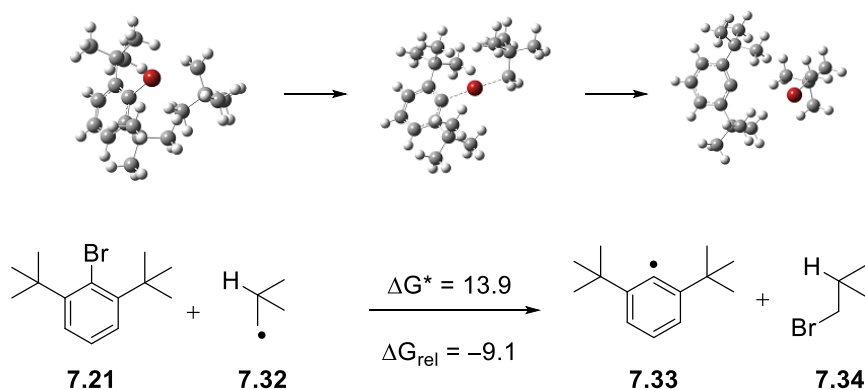
Following reactions performed by JB, it was noticed that when 2,4,6-tri-*tert*-butyl bromobenzene **7.24** was reacted with KH and benzene, a variety of products were

produced, notably (i) the dehalogenated product **7.25**, (ii) a product **7.26** formed from bromine abstraction from **7.29** by an alkyl radical, and (iii) a product formed from neophyl rearrangement of radical **7.29** to form **7.31**; this then abstracts a hydrogen to form **7.27**.



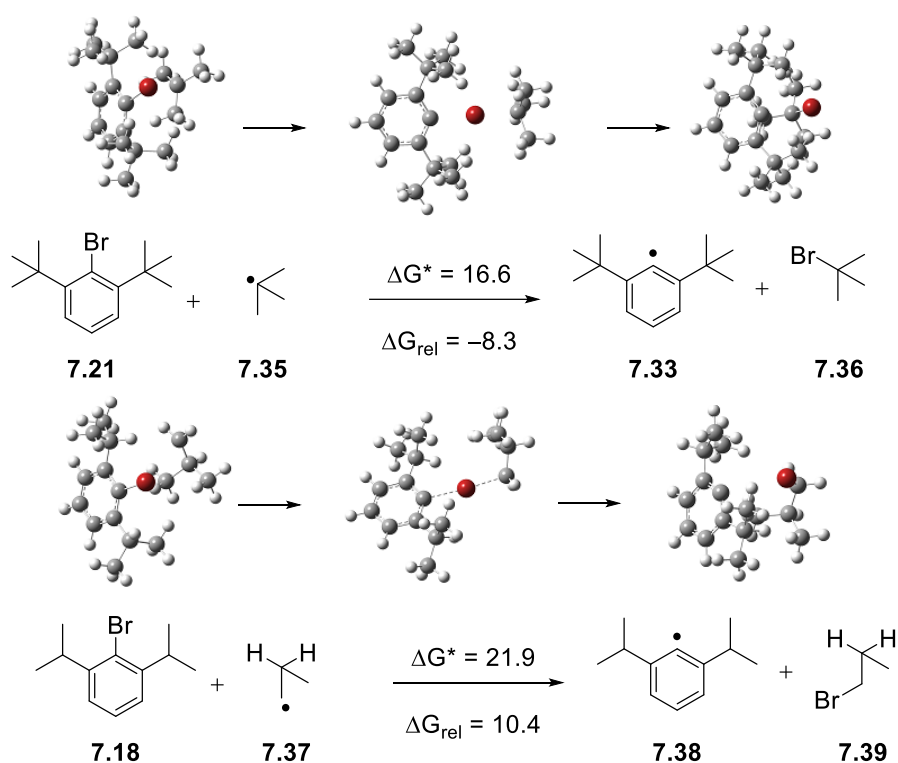
Scheme 7.10 – KH-mediated reactions of 2,4,6-tri-*tert*-butylbromobenzene, **7.24**

While it is proposed that these are all formed through a radical pathway. It was not clear where radicals would come from initially; however, it was unexpected that an alkyl radical, if present in the reaction, would abstract a bromine atom to produce product **7.26**. To model this, truncated versions of the molecules involved in the abstraction were modelled.



Scheme 7.12 – Bromine abstraction by alkyl radical **7.32**

From the calculated energy profile, the radical **7.32** can abstract a bromine from 2,6-ditertbutyl bromobenzene, **7.21**. The exergonic nature is surprising but is due to the bulky halogen putting strain on the bulky butyl groups and these relax when the bromine leaves and the radical is formed. To further investigate this *tert*-butyl radical **7.35** and propyl radical **7.37** were modelled abstracting bromine from **7.21** and **7.18**.

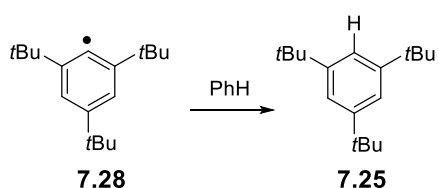


Scheme 7.13 – Alternative bromine abstractions

The primary radical has a lower energy barrier than the tertiary radical. This would be expected as the primary radical is less hindered than the tertiary radical. The isopropyl example is endergonic, and this is believed to be the case as there is less strain in the parent 2,6-diisopropyl bromobenzene structure, the C-Br bond is therefore relatively stronger than in the *tert*-butyl cases and as there is less relief from the strain there is less to gain after the abstraction, explaining why this is endergonic when the *tert*-butyl examples are exergonic.

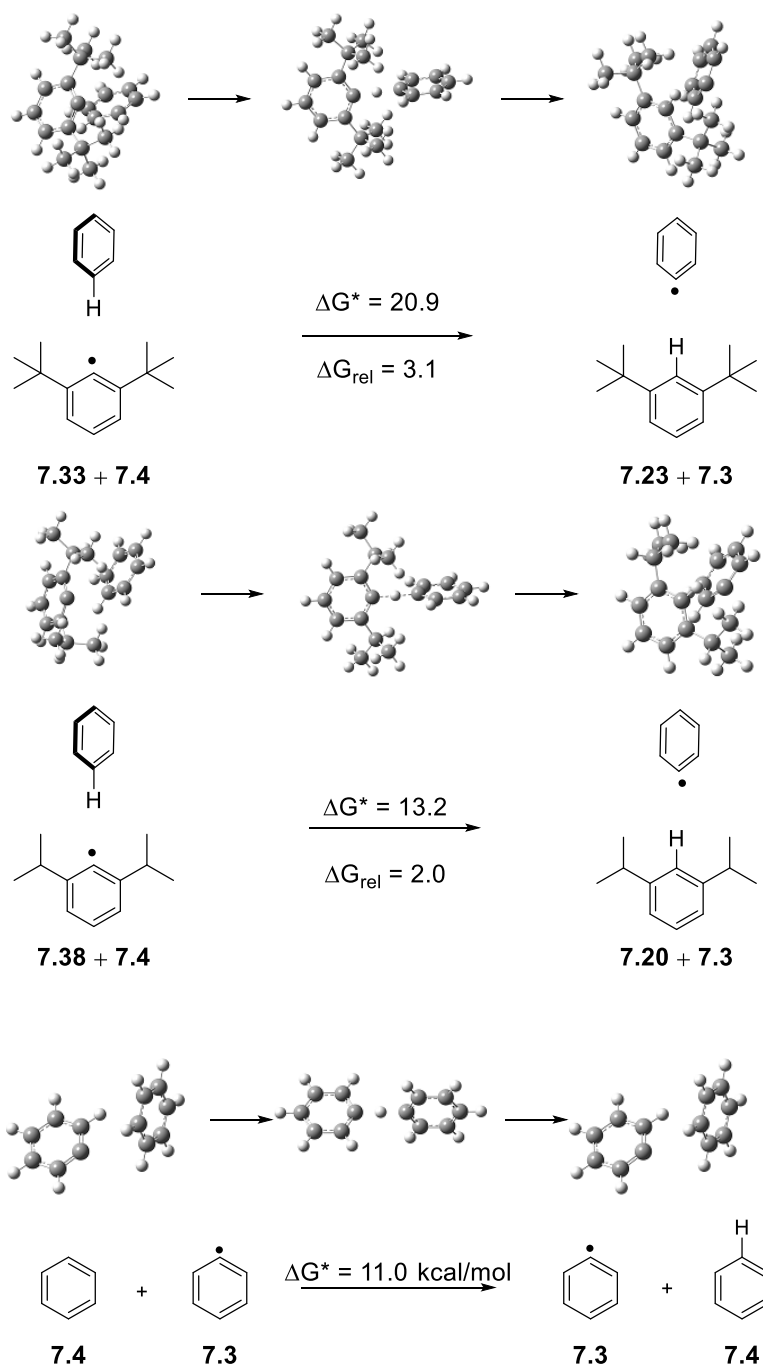
7.4 Hydrogen Atom Abstraction by Aryl Radicals

It was thought that **7.25** could be formed from the radical **7.28**, generated from Br abstraction, abstracting a hydrogen from a molecule of benzene. This along with the corresponding isopropyl example was modelled to examine the feasibility of this. In addition, for comparison an unhindered aryl radical was also modelled.



Scheme 7.13 – Formation of **7.25** from radical **7.28**

What was found that the *tert*-butyl example **7.33** to **7.23** had an achievable barrier of 20.9 kcal mol⁻¹ and was overall a relatively energy neutral process as both aryl radicals would be equally as stable. Moving to the propyl example, **7.38** to **7.20** the barrier decreased to 13.2 kcal mol⁻¹ due to the decrease in steric hindrance around the radical centre. This barrier dropped further to 11.0 kcal mol⁻¹ in the unhindered example, **7.4** to **7.3**.

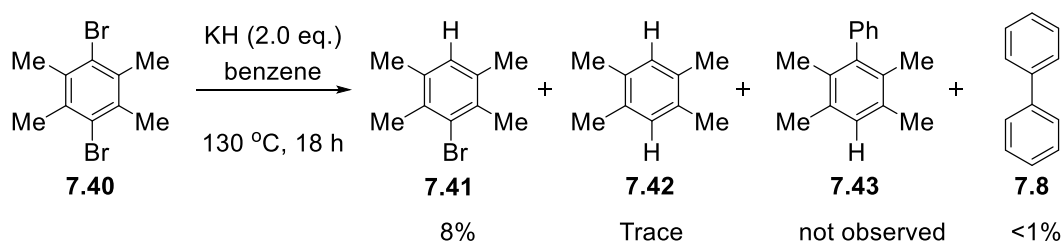


Scheme 7.14 – Hydrogen abstraction from benzene with radicals **7.33**, **7.38** and **7.3**

7.5 Reactions of Dihalodurenes Mediated by KH

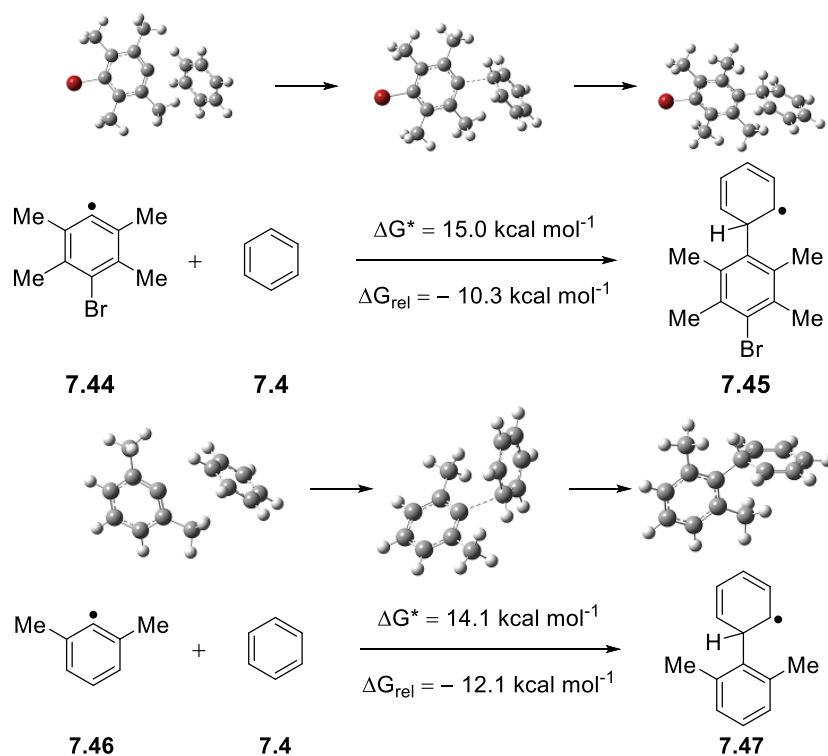
In reactions performed by Giuseppe Nocera he reacted **7.40** with KH in benzene. It was noticed that the dehalogenation reaction occurred but if this was going *via* the same process as described in the previous calculations then an aryl radical such as **7.44** would be formed. As has been seen in several reactions *m*-xylyl radicals, **7.46** couples with

benzene to form biaryl products,^{104, 105, 112} therefore it was surprising that no significant quantities of coupled product were observed.



Scheme 7.15 – Reactions with dihalodurene, **7.40** with KH in benzene

To try and explain these observations it was decided to model both radicals **7.44** and **7.46** attacking benzene to try and notice if there was a significant energy difference.



Scheme 7.16 – radicals **7.44** and **7.46** attacking benzene forming C-C σ -bonds

From the energies calculated there is no obvious reason why if radicals of the type **7.44** are formed that it cannot couple to form biphenyl species. The angles between the methyl groups and radical centre were also similar 120.9° for durene (**7.44**) 122.5° for *meta* xylene (**7.46**). The angle did become a little smaller and this accounts for the small

increase in barrier but not the lack of observed coupled products. The reason for this still remains unknown.

7.6 Conclusions

While potassium hydride has been well characterized as a strong base in classical studies, this work has shown that haloarenes have been able to undergo various transformations mediated by KH. These have started through a dehalogenation producing aryl radicals that are capable of undergoing various different pathways depending on the haloarene substrate and conditions employed. Experiments have brought to light a number of interesting products, the computational study undergone in this chapter has sought to rationalize these. A shortfall of the study is that there is still currently no explanation of how initial aryl radicals are formed.

By studying the Pierre dehalogenation a four-member transition state, similar to that proposed by Chiba *et al.*¹⁶⁹ is a likely mechanism for this transformation and is energetically favourable with achievable energy barriers and strong thermodynamic driving forces. Adding in explicit solvent molecules around the potassium atom gave more realistic energy profile of the transformation. In the examples in THF dehalogenation is the only possible transformation, however in benzene aryl radicals can be produced and these can undergo alternative pathways. This explains why although the energy profile for both transformations are similar that the experimental yields are lower in the benzene examples. Another explanation is the solubility of KH in benzene which computational calculations don't take into account and this is an alternative explanation of the lower observed experimental yield.

The abstraction of bromine by alkyl radicals **7.32** and **7.35** was shown to be a favourable process and this was surprising as it is not a commonly expected transformation. The explanation however, is that the bromine was forcing the *tert*-butyl groups into a strained position and after abstraction these relax meaning the abstraction is favorable. Moving to isopropyl groups the bromine has less effect and the abstraction of bromine by alkyl radical **7.38** is less favorable as a result.

Moving to aryl radicals abstracting hydrogen atoms from benzene rings, the results are unsurprising. All the abstractions are possible in these cases however the energy barriers decrease as the steric hindrance around the radical centre decreases.

There is still no conclusive explanation of why the dihalodurenes do not form any significant quantities of coupled product as energetically it is favorable compared to *meta*-xylene radical. It is possible that the formation of products **7.41** and **7.42** could also be formed *via* the four-member transition states previously discussed.

7.7 Future Work

As there are still questions over the formation of radicals in this process, future work would be to explain the formation of original aryl radicals, this could be an experimental or computational study looking at potential formation of electron donors or trace metal ions in sources of KH which could produce aryl radicals.

Another piece of future work would be to further explore the reactions of dihalodurenes, modelling the Pierre mechanism on these substrates could explain the formation **7.41** and **7.42**.

It would also be interesting explore chloroarenes in these transformations to observe changes in reactivity, both computationally and experimentally these would be interesting investigations.

8. Overall Conclusions

In chapter 4 six additives that had the potential to form electron donors capable of initiating the BHAS cycle were investigated both computationally and experimentally. To form a species capable of donating an electron to haloarenes the sp^3 carbon required to be deprotonated and this would produce an alkene surrounded by heteroatoms. It would have been predicted that when the heteroatoms had been deprotonated before the sp^3 carbon then these would be even more electron-rich and therefore more efficient electron donors. However, as there would be a build-up of negative charge these would be less likely to form.

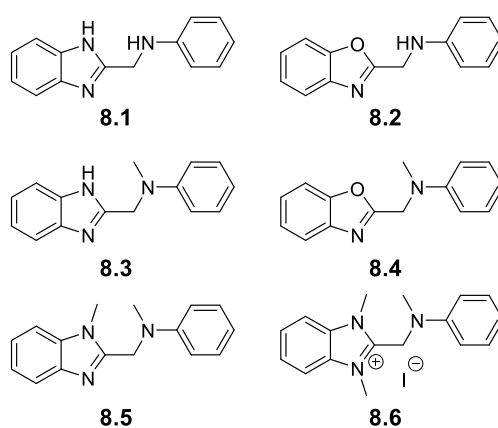


Figure 8.1 – Additives investigated computationally and experimentally in Chapter 4

The computational study suggested that a trianion formed from **8.1** would be the least likely to be formed however, should it form would be the most efficient electron donor. Dianions formed from **8.1** to **8.3** were all predicted to be capable of being formed and were expected to be efficient electron donors all with small barriers and strong thermodynamic driving force. Similarly, monoanions formed from donors **8.1** to **8.5** were shown to be formed favourably, in all cases though, the electron transfer to iodobenzene was found to be endergonic. Although the energy profile were not unreasonable these species were less likely to be efficient electron donors. The neutral electron-rich alkene formed from salt **8.6**, despite being the easiest to form was found to be the most unlikely to donate an electron to iodobenzene. The conclusion from the computational study was that **8.1,8.2** and **8.3** were all capable of forming at least dianionic species that would be efficient electron donors, additives **8.4** and **8.5** would

only be able to form monoanionic species that would be less favourable electron donors but it would not be unreasonable to observe some electron transfer from these species. Additive **8.6** is very unlikely to form an efficient electron donor.

In experiments what was found was that **8.1** and **8.2** were the best additives for achieving successful coupling of iodoarenes to benzene. Additive **8.3** was also relatively successful but not to the same extent as **8.1** and **8.2**. The unhindered iodoarenes produced a high yield of coupled product whereas, when 2-iodo-*m*-xylene was used as the arene the yield was lower in comparison but was a good yield compared to previous published studies. Additives **8.4** to **8.6** were predicted to be unsuccessful in initiating the BHAS cycle and this was found to be the case. Although small amounts of coupled products were formed in reactions with unhindered iodoarenes when the benzyne formation was blocked the reactivity was almost completely removed.

This study highlighted that computational studies are effective in helping to predict which substrates are likely to form efficient electron donors, however, these are not conclusive so do not detract from the importance of physical experiment. It was also noted that when no additive was present that small amounts of coupled product were formed and this lead on to Chapter 5.

The proposed background initiation mechanism for reactions when there is no electron donor is benzyne acting as a biradical. Chapter 5 set out to add in external sources of biradicals to observe whether or not when benzyne formation is blocked from alternative sources. Two different methods of forming biradicals were employed in this study, *o*-benzyne formed from HDDA rearrangements and *p*-benzyne formed from a Bergman cyclisation.

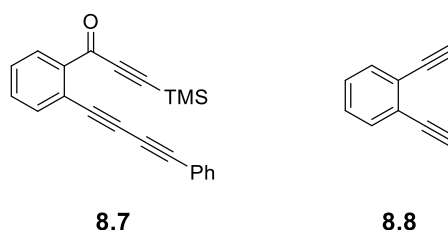
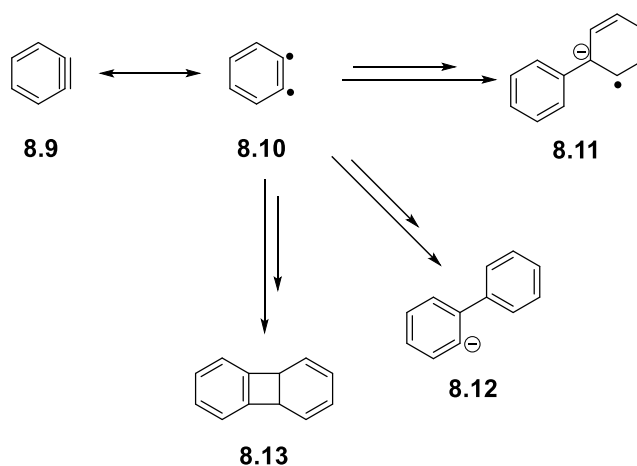


Figure 8.2 – Example substrates employed in Chapter 5, **8.7** underwent HDDA reactions and **8.8** undergoes a Bergman cyclisation

The work in Chapter 5 showed that substrates of the type **8.7** and **8.8** are capable of initiating transition metal-free coupling reactions between 2-iodo-*m*-xylene and benzene. Biradical initiation is often a significantly slower process than the more common electron transfer as there are a number of alternative paths for the biradicals to go down as well as the desired one towards initiating the cycle, this results in the need for higher temperatures or longer reaction times compared to previously reported electron-donor promoted transition-metal free coupling reactions. As a result of the slower reactions the yields are also lower than those with standard electron donors.

In addition to biradical initiation radical initiators such as di-*tert*-butylperoxide and AIBN were used as additives for these coupling reactions. It was found that these were also capable of initiating the BHAS cycle in relatively good yield.

Chapter 6 was a continuation of investigating the initiation of the BHAS cycle by benzyne. This time the study was computational. What was found was that although benzyne is capable of forming radical anion **8.11** that would be capable of initiating the BHAS mechanism it was not the only possible pathway. There were alternative pathways such as forming a 4-member ringed structure **8.13** and alternatively a biradical anion **8.12** neither of which would be capable of initiating the BHAS cycle.

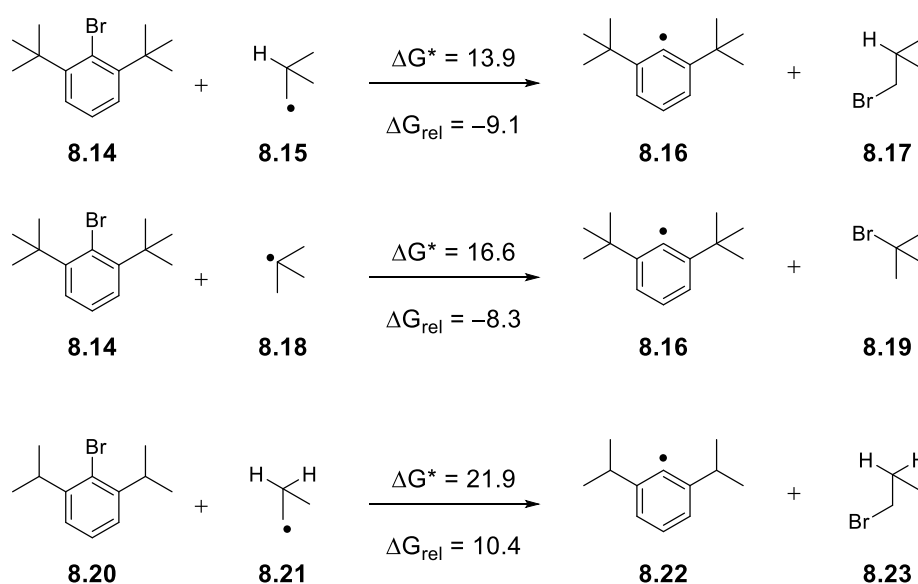


Scheme 8.1 – Possible pathways from benzyne biradical **8.10**

As chapter 7 showed halide abstraction by alkyl radicals it is possible that the biradical benzyne could be abstracting iodine from the aryl iodides and the aryl radical formed could be initiating the BHAS cycle.

While exploring reactions of haloarenes with KH in chapter 7 a number of different observations were made. The investigation into the Pierre iodide displacement by KH has been shown to likely occur *via* a four-membered transition state. These transformations were found to have achievable barriers and the formation of KI was found to be a strong thermodynamic driving force. Adding in explicit solvent molecules had a small effect.

The abstraction of bromine by alkyl radicals **8.15** and **8.18** was shown to be a favourable process and this was surprising as it is not a commonly expected transformation. The explanation however, is that the bromine was forcing the *tert*-butyl groups into a strained position and after abstraction these relax meaning the abstraction is favorable. Moving to isopropyl groups the bromine has less effect and the abstraction of bromine by alkyl radical **8.21** is less favorable as a result.



Scheme 8.2 – Bromine abstraction by alkyl radicals

Moving to aryl radicals abstracting hydrogen atoms from benzene rings, the results are unsurprising. All the abstractions are possible in these cases however the energy barriers decrease as the steric hindrance around the radical centre decreases.

The investigation into reactions with dihalodurenes gave no conclusive explanation of why if radicals are formed they do not form any significant quantities of coupled product as energetically it is favorable compared to *meta*-xylene radical.

This work has investigated the mechanism of the BHAS reaction. It has aimed to show that computational and experimental work can work together to aid one another. This combination is useful in further explaining reaction mechanisms to support proposed routes and observe new reactions.

9. Experimental

9.1 General experimental information

All reagents were bought from commercial suppliers and used without further purification unless stated otherwise. All the reactions not performed using a glovebox were carried out under argon atmosphere. Diethyl ether, tetrahydrofuran, dichloromethane and hexane were dried with a Pure-Solv 400 solvent purification system supplied by Innovative Technology Inc., U.S.A. Organic extracts were, in general, dried over anhydrous sodium sulfate (Na_2SO_4). A Büchi rotary evaporator was used to concentrate the reaction mixtures. Thin layer chromatography (TLC) was performed using aluminium-backed sheets of silica gel and visualised under a UV lamp (254 nm). The plates were developed using phosphomolybdic acid or KMnO_4 solution. Column chromatography was performed by using silica gel 60 (200-400 mesh).

The electron transfer reactions were carried out within a glove box (Innovative Technology Inc., U.S.A.) under nitrogen atmosphere, and performed in oven-dried or flame-dried apparatus using anhydrous solvents, which were degassed under reduced pressure, then purged with argon and dried over activated molecular sieves (3 Å), prior to being sealed and transferred to the glovebox. All solvents or samples placed into the glovebox were transferred in through the port, which was evacuated and purged with nitrogen ten times before entry. When the reaction mixtures were prepared, the reaction vessel was removed from the glove box and the rest of the reaction was performed in the fumehood.

Proton (^1H) NMR spectra were recorded at 400, 400 and 500 MHz, on Bruker AV3, AV400 and AV500 spectrometers, respectively. Carbon ($^{13}\text{C}^{170}$) NMR spectra were recorded using broadband decoupled mode at 101, 101 and 126 MHz, on Bruker AV3, AV400 and AV500 spectrometers, respectively. Spectra were recorded in either deuterated chloroform (CDCl_3) or deuterated dimethyl sulfoxide ($\text{d}^6\text{-DMSO}$), depending on the solubility of the compounds. The chemical shifts are reported in parts per million (ppm) calibrated on the residual non-deuterated solvent signal in ^1H and the ^{13}C based on the

d-solvent, and the coupling constants, J , are reported in Hertz (Hz). The peak multiplicities are denoted using the following abbreviations: s, singlet; d, doublet; t, triplet; q, quartet; m, multiplet; dd, doublet of doublets; dt, doublet of triplets; td, triplet of doublets.

Infra-Red spectra were recorded on an ATR-IR spectrometer.

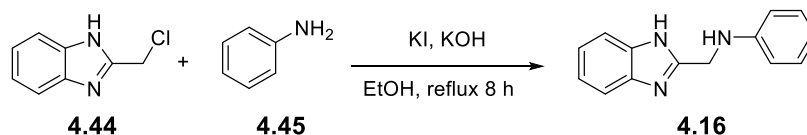
Melting points were determined on a Gallenkamp Melting point apparatus.

The mass spectra were recorded by gas-phase chromatography (GCMS) using ionisation techniques, as stated for each compound: electron ionisation (EI), electrospray ionisation (ESI). GCMS data were recorded using an Agilent Technologies 7890A GC system coupled to a 5975C inert XL EI/CI MSD detector. Separation was performed using the DB5MS-UI column (30 m x 0.25 mm x 0.25 μm) at a temperature of 320 $^{\circ}\text{C}$, using helium as the carrier gas.

High-resolution mass spectrometry (HRMS) was performed at the Swansea University, in the EPSRC National Mass Spectrometry Centre. Accurate mass was obtained using atmospheric pressure chemical ionisation (APCI), chemical ionisation (CI), electron ionisation (EI), or electrospray ionisation (ESI) with a LTQ Orbitrap XL mass spectrometer.

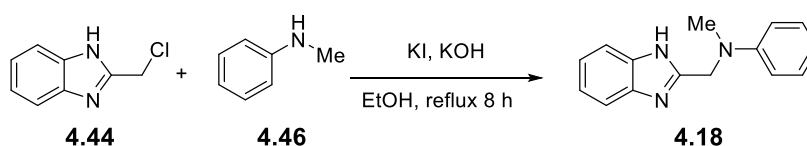
9.2 Experimental Procedures for Chapter 4

Synthesis of *N*-((1*H*-benzo[*d*]imidazole-2-yl)methyl)aniline **4.16**



To a 250 mL round-bottomed flask was added 2-chloromethylbenzimidazole, **4.44** (4.3 g, 25 mmol), potassium iodide (4.3 g, 25 mmol), and aniline, **4.45** (2.3 g, 25 mmol) were added. Ethanol (100 mL) was then added and the reaction heated to reflux with stirring for 6 h. Potassium hydroxide (1.6 g, 25 mmol) was dissolved in H₂O (5 mL) and added and the reaction continued for a further 2 h. After cooling to room temperature ice water (100 mL) was added to the reaction and a green precipitate appeared. The solid was collected by vacuum filtration and purified by recrystallisation from ethanol/petroleum ether to afford **4.16** as a dark green solid (2.79 g, 50%) mp 142-144 °C ¹H NMR (400 MHz, d⁶ DMSO) δ 7.58-7.54 (2H, m) 7.25-7.21 (2H, m) 7.08 (2 H, t, *J* = 8.0 Hz) 6.8 (1H, t, *J* = 7.2 Hz) 6.6 (2H, d, *J* = 8 Hz) 4.56 (2H, s) ppm, ¹³C NMR (101 MHz, d⁶ DMSO) δ 153.8, 148.2, 136.7, 128.9, 122.5, 116.8, 114.5, 112.5, 41.4 ppm, [Found: (HRMS-ESI) 224.1180. C₁₄H₁₄N₃⁺ (M+H)⁺ requires 224.1182].¹⁷¹

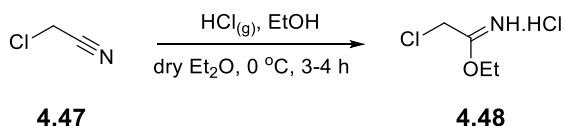
Synthesis of *N*-((1*H*-benzo[*d*]imidazol-2-yl)methyl)-*N*-methylaniline **4.18**



To a 250 mL round-bottomed flask was added 2-chloromethylbenzimidazole, **4.44** (4.3 g, 25 mmol), potassium iodide (4.3 g, 25 mmol), and *N*-methylaniline, **4.46** (2.7 g, 25 mmol). Ethanol (100 mL) was then added and the reaction heated to reflux with stirring for 6 h. Potassium hydroxide (1.6 g, 25 mmol) was dissolved in H₂O (5 mL) and added and the reaction continued for a further 2 h. After cooling to room temperature ice water (100 mL) was added to the reaction and a yellow precipitate appeared. The solid was collected by vacuum filtration and purified by recrystallisation from ethanol to

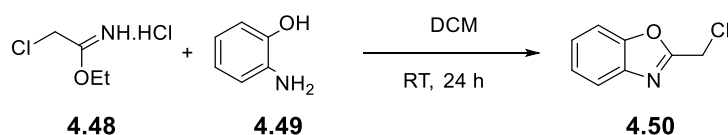
afford **4.18** as a pale yellow solid (3.57 g, 61%) mp 208-209 °C. ¹H NMR (400 MHz, d⁶ DMSO) δ 12.26 (1H, s) 7.50- 7.46 (2H, m) 7.17-7.10 (4H, m) 6.79 (2H, d, *J* = 8 Hz) 6.63 (1H, t, *J* = 8.0 Hz) 4.71 (s, 2H) 3.11 (s, 3H) ppm, ¹³C NMR (101 MHz, d⁶ DMSO) δ 152.7, 149.1, 128.9, 121.4, 116.5, 112.4, 50.7 ppm, (sp³ CH₂ carbon peak DMSO solvent peak) [Found: (HRMS-ESI) 238.1338. C₁₅H₁₇N₃⁺ (M+H)⁺ requires 238.1339].

Synthesis of ethyl 2-chloroacetimidate hydrochloride **4.48**



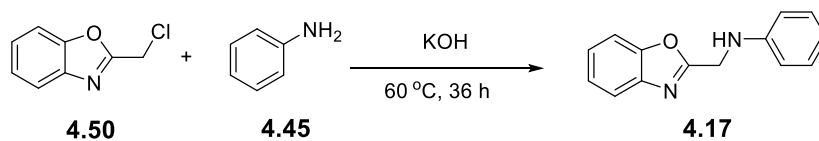
Chloroacetonitrile, **4.47** (5 mL, 79 mmol), absolute ethanol (6 mL, 102.9 mmol) and dry diethyl ether (20 mL) were added to an oven-dried 100 mL 3-necked flask. The flask was then placed in an ice bath and the reaction mixture stirred. Hydrogen chloride gas was generated *in situ* by dropping concentrated HCl into CaCl₂¹⁷² and this was used to saturate the reaction mixture. After 3-4 h a white precipitate formed, this solid was collected and dried by vacuum filtration. The crude product was used without any further purification.¹⁷³

Synthesis of 2-chloromethylbenzoxazole **4.50**



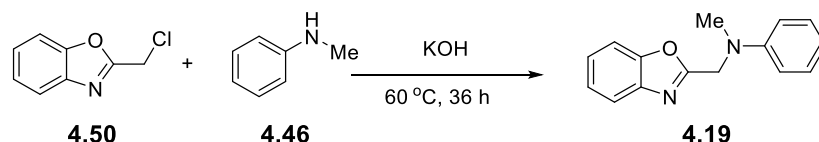
To an oven-dried 50 mL round-bottomed flask was added 2-aminophenol (0.5 g, 4.58 mmol), chloroacetimidic acid ethyl ester hydrochloride (1 g, 6.87 mmol) and dry DCM (10 mL). The resultant slurry was stirred at room temperature overnight. The reaction mixture was filtered through a pad of celite. This was then concentrated to afford **4.50** as a brown oil (0.28 g, 37%). The crude product was used without any further purification. ¹H NMR (400 MHz, CDCl₃) δ 7.7 (1H, m) 7.5 (1H, m) 7.35 (2H, m) 4.76 (2H, s) ppm.¹⁷³

Synthesis of N-(benzo[d]oxazol-2-ylmethyl)aniline **4.18**



To a 25 mL round-bottomed flask was added 2-(chloromethyl)benzo[d]oxazole, **4.50** (334 mg, 0.2 mmol) in aniline, **4.45** (5 mL). This was stirred at 60 °C for 1 hour, 1 equiv KOH was then added and reaction continued for 36 h. After cooling to room temperature the reaction was quenched with 1M HCl_(aq) (25 mL) and organic portion extracted with DCM (3 x 30 mL). The organic extracts were combined washed with 1M HCl_(aq) (25 mL) then dried over Na₂SO₄ before being concentrated. The crude product was purified by column chromatography (DCM) to afford **4.17** as a pale pink powder, (394 mg, 88%). Mp 103-105 °C. ¹H NMR (400 MHz, CDCl₃) δ 7.73-7.69 (1H, m) 7.53-7.49 (1H, m) 7.35-7.31 (2H, m) 7.23 (2H, t, *J* = 6.8 Hz) 6.80-6.75 (3H, m) 4.62 (2H, s) 4.51 (1H, s) ppm, ¹³C NMR (101 MHz, CDCl₃) δ 164.2, 151.1, 147.0, 141.1, 129.5, 125.2, 124.6, 120.1, 118.8, 113.4, 110.8, 42.1 ppm, [Found: (HRMS-ESI) 225.1022. C₁₄H₁₂N₂O⁺ (M+H)⁺ requires 225.1022].

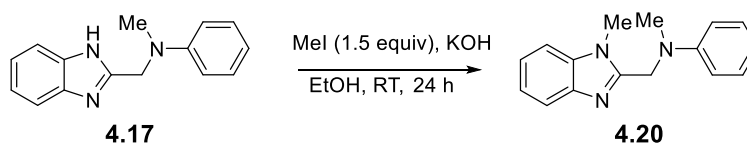
Synthesis of N-(benzo[d]oxazol-2-ylmethyl)-N-methylaniline **4.19**



To a 25 mL round-bottomed flask was added 2-chloromethylbenzoxazole, **4.50** (3.34 g, 20 mmol) and N-methylaniline, **4.46** (4.28 g, 40 mmol). This was stirred at 60 °C for 1 hour, potassium hydroxide (1.3 g, 20 mmol) was then added and reaction continued for 36 h. After cooling to room temperature the reaction was quenched with 1M HCl_(aq) (25 mL) and the organic portion extracted with DCM (3 x 30 mL). The organic extracts were combined, washed with 1M HCl_(aq) (25 mL), then dried over Na₂SO₄ before being concentrated. The crude product was purified by column chromatography (DCM) to afford **4.19** as a yellow oil (1.62 g, 34%). ¹H NMR (400 MHz, CDCl₃) δ = 7.73-7.71 (1H, m) 7.51-7.47 (1H, m) 7.34-7.25 (4H, m) 6.91 (1H, d, *J* = 8 Hz) 6.79 (2H, t, *J* = 8 Hz) 4.78 (2H, s) 3.22 (3H, s) ppm, ¹³C NMR (101 MHz, CDCl₃) δ 163.9, 151.0, 148.9, 141.1, 129.4, 125.1,

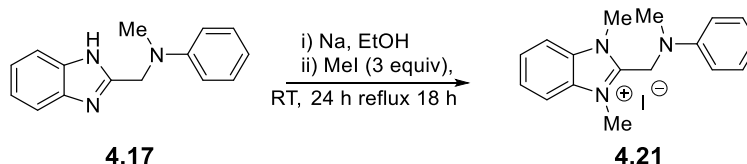
124.4, 120.1, 117.9, 113.1, 110.8, 50.6, 39.4 ppm, [Found: (HRMS-ESI) 239.1178. $C_{15}H_{15}N_2O^+$ (M+H)⁺ requires 239.1179].

Synthesis of N-methyl-N-((1-methyl-1H-benzo[d]imidazol-2-yl)methyl)aniline **4.20**



To a 50 mL three-neck flask N-((1H-benzo[d]imidazol-2-yl)methyl)-N-methylaniline, **4.17** (1.18 g, 5 mmol) crushed potassium hydroxide (0.56 g, 10 mmol) and ethanol (25 mL) were added. Under an argon flow, with stirring, methyl iodide (1.07 g, 7.5 mmol) was added dropwise over a period of 30 min. The reaction was left to continue at room temperature for 24 h. Water (30 mL) was added to quench the reaction and organic products extracted with DCM (3 x 30 mL). The extracts were combined, washed with brine, dried over Na_2SO_4 and then concentrated. The crude reaction mixture was purified by column chromatography (DCM:MeOH 1:0-9:1) to afford **4.20** as an off-white powder (817 mg, 65%). 1H NMR (400 MHz, d_6 DMSO) δ = 7.56 (1H, d, J = 7.6 Hz) 7.51 (1H, d, J = 8 Hz) 7.23-7.13 (4H, m) 6.89 (2H, d, J = 8 Hz) 6.66 (1H, t, J = 8 Hz) 4.81 (2H, s) 3.78 (3H, s) 3.01 (3H, s) ppm, ^{13}C NMR (101 MHz, d_6 DMSO) δ 151.7, 150.0, 142.4, 136.5, 129.5, 122.8, 122.2, 119.8, 118.7, 114.4, 109.2, 50.9, 38.5, 30.3 ppm, [Found: (HRMS-ESI) 252.1492. $C_{16}H_{20}N_3^+$ (M+H)⁺ requires 252.1495].¹⁷⁴

Synthesis of 1,3-dimethyl-2-((methyl(phenyl)amino)methyl)-1H-benzo[d]imidazol-3-ium iodide **4.21**

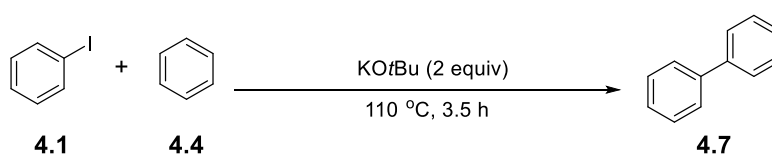


Clean sodium metal (0.18 g, 8 mmol) was dissolved in ethanol (10 mL). To this was added **4.17** (1.04 g, 8 mmol), methyl iodide (1.5 mL, 24 mmol) and additional ethanol (10 mL). The reaction mixture was then left to stir at room temperature for 24 h. After 24 h, the reaction was heated to reflux for a further 18 h. After cooling to room temperature, a

pale orange precipitate appeared. The crude solid was purified by column chromatography (DCM) and **4.21** was collected as a pale orange powder (723 mg, 23%). MP 159-161 °C ^1H NMR (400 MHz, d^6 DMSO) 7.99 (2H, d, $J = 8$ Hz) 7.72 (1H, d, $J = 8$ Hz) 7.63-7.54 (2H, m) 7.25 (2H, t, $J = 7.6$ Hz) 6.89 (2H, d, $J = 8$ Hz) 6.78 (1H, t, $J = 8$ Hz) 5.13 (2H, s) 3.99 (3H, s) 3.36 (3H, s) 3.11 (3H, s) ppm, [Found: (HRMS-ESI) 266.1652. $\text{C}_{17}\text{H}_{23}\text{N}_3^+$ (M-I) $^+$ requires 266.1652].

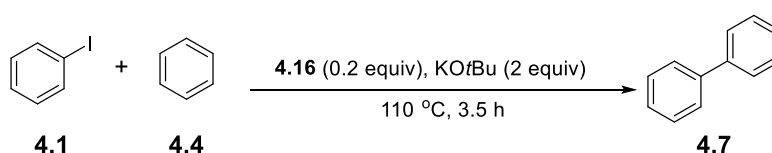
Formation of biphenyl **4.7** in table 4.5

Table 4.5 entry 1,a



Iodobenzene **4.1** (102 mg, 0.5 mmol) was added to an oven-dried 15 mL pressure tube charged with a magnetic stirrer bar. This was then transferred to a glovebox and KOtBu (112 mg, 1 mmol) and benzene (5 mL) were added and the pressure tube sealed. The sealed tube was placed in a preheated oil bath at 110 °C for 3.5 h. After cooling to room temperature, the reaction mixture was quenched with 1M HCl_(aq) (20 mL) and organic product extracted with EtOAc (3 x 20 mL). The organic extracts were combined and dried over Na₂SO₄, this was then concentrated and the crude product purified by column chromatography (hexanes) to afford biphenyl **4.7** (5 mg, 7%) of white crystals. ^1H NMR (400 MHz, CDCl₃) $\delta = 7.62$ - 7.59 , (4H, m), 7.47 - 7.42 (4H, m) 7.35 (2 H, t, $J = 8$ Hz) ppm, ^{13}C NMR (101 MHz, CDCl₃) δ 141.4, 128.9, 127.4, 127.3 ppm, m/z (EI $^+$) 154.1 [M] $^+$.

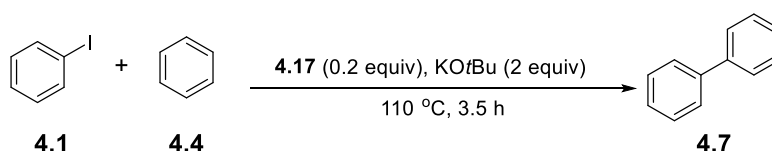
Table 4.5 entry 2,a



Iodobenzene **4.1** (102 mg, 0.5 mmol) and **4.16** (22 mg, 0.1 mmol) were added to an oven-dried 15 mL pressure tube charged with a magnetic stirrer bar. This was then transferred to a glovebox and KOtBu (112 mg, 1 mmol) and benzene (5 mL) were added

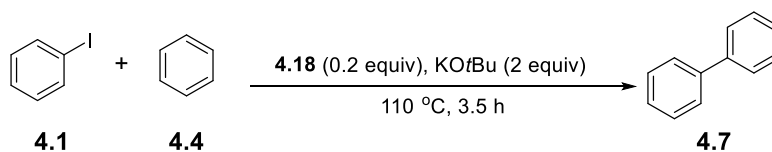
and the pressure tube sealed. The sealed tube was placed in a preheated oil bath at 110 °C for 3.5 h. After cooling to room temperature, the reaction mixture was quenched with 1M HCl_(aq) (20 mL) and organic product extracted with EtOAc (3 x 20 mL). The organic extracts were combined and dried over Na₂SO₄, this was then concentrated and the crude product purified by column chromatography (hexanes) to afford biphenyl **4.7** (68 mg, 88%) of white crystals. ¹H NMR (400 MHz, CDCl₃) δ = 7.62-7.59, (4H, m), 7.47-7.42 (4H, m) 7.35 (2 H, t, *J* = 8 Hz) ppm, ¹³C NMR (101 MHz, CDCl₃) δ 141.4, 128.9, 127.4, 127.3 ppm, *m/z* (EI⁺) 154.1 [M]⁺.

Table 4.5 entry 3,a



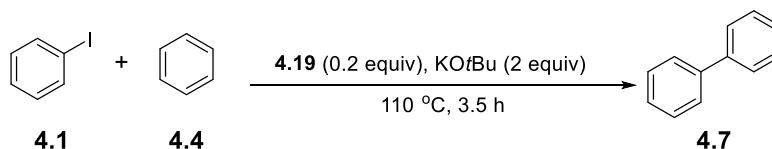
Iodobenzene **4.1** (102 mg, 0.5 mmol) and **4.17** (23 mg, 0.1 mmol) were added to an oven-dried 15 mL pressure tube charged with a magnetic stirrer bar. This was then transferred to a glovebox and KOtBu (112 mg, 1 mmol) and benzene (5 mL) were added and the pressure tube sealed. The sealed tube was placed in a preheated oil bath at 110 °C for 3.5 h. After cooling to room temperature, the reaction mixture was quenched with 1M HCl_(aq) (20 mL) and organic product extracted with EtOAc (3 x 20 mL). The organic extracts were combined and dried over Na₂SO₄, this was then concentrated and the crude product purified by column chromatography (hexanes) to afford biphenyl **4.7** (57 mg, 74 %) of white crystals. ¹H NMR (400 MHz, CDCl₃) δ = 7.62-7.59, (4H, m), 7.47-7.42 (4H, m) 7.35 (2 H, t, *J* = 8 Hz) ppm, ¹³C NMR (101 MHz, CDCl₃) δ 141.4, 128.9, 127.4, 127.3 ppm, *m/z* (EI⁺) 154.1 [M]⁺.

Table 4.5 entry 4,a



Iodobenzene **4.1** (102 mg, 0.5 mmol) and **4.18** (24 mg, 0.1 mmol) were added to an oven-dried 15 mL pressure tube charged with a magnetic stirrer bar. This was then transferred to a glovebox and KOtBu (112 mg, 1 mmol) and benzene (5 mL) were added and the pressure tube sealed. The sealed tube was placed in a preheated oil bath at 110 °C for 3.5 h. After cooling to room temperature, the reaction mixture was quenched with 1M HCl_(aq) (20 mL) and organic product extracted with EtOAc (3 x 20 mL). The organic extracts were combined and dried over Na₂SO₄, this was then concentrated and the crude product purified by column chromatography (hexanes) to afford biphenyl **4.7** (36 mg, 47%) of white crystals. ¹H NMR (400 MHz, CDCl₃) δ = 7.62-7.59, (4H, m), 7.47-7.42 (4H, m) 7.35 (2 H, t, *J* = 8 Hz) ppm, ¹³C NMR (101 MHz, CDCl₃) δ 141.4, 128.9, 127.4, 127.3 ppm, *m/z* (EI⁺) 154.1 [M]⁺.

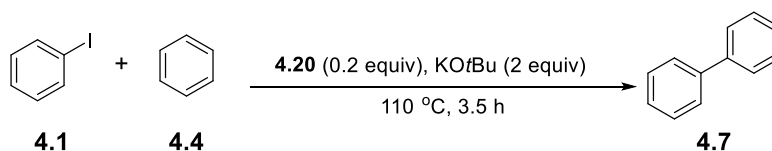
Table 4.5 entry 5,a



Iodobenzene **4.1** (102 mg, 0.5 mmol) and **4.19** (24 mg, 0.1 mmol) were added to an oven-dried 15 mL pressure tube charged with a magnetic stirrer bar. This was then transferred to a glovebox and KOtBu (112 mg, 1 mmol) and benzene (5 mL) were added and the pressure tube sealed. The sealed tube was placed in a preheated oil bath at 110 °C for 3.5 h. After cooling to room temperature, the reaction mixture was quenched with 1M HCl_(aq) (20 mL) and organic product extracted with EtOAc (3 x 20 mL). The organic extracts were combined and dried over Na₂SO₄, this was then concentrated and the crude product purified by column chromatography (hexanes) to afford biphenyl **4.7** (32 mg, 42%) of white crystals. ¹H NMR (400 MHz, CDCl₃) δ = 7.62-7.59, (4H, m), 7.47-7.42

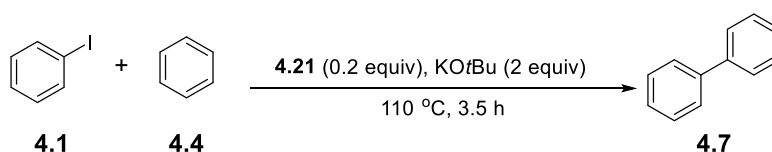
(4H, m) 7.35 (2 H, t, $J = 8$ Hz) ppm, ^{13}C NMR (101 MHz, CDCl_3) δ 141.4, 128.9, 127.4, 127.3 ppm, m/z (EI^+) 154.1 [M] $^+$.

Table 4.5 entry 6,a



Iodobenzene **4.1** (102 mg, 0.5 mmol) and **4.20** (24 mg, 0.1 mmol) were added to an oven-dried 15 mL pressure tube charged with a magnetic stirrer bar. This was then transferred to a glovebox and KOtBu (112 mg, 1 mmol) and benzene (5 mL) were added and the pressure tube sealed. The sealed tube was placed in a preheated oil bath at 110 °C for 3.5 h. After cooling to room temperature, the reaction mixture was quenched with 1M $\text{HCl}_{(\text{aq})}$ (20 mL) and organic product extracted with EtOAc (3 x 20 mL). The organic extracts were combined and dried over Na_2SO_4 , this was then concentrated and the crude product purified by column chromatography (hexanes) to afford biphenyl **4.7** (15 mg, 19%) of white crystals. ^1H NMR (400 MHz, CDCl_3) $\delta = 7.62$ - 7.59 , (4H, m), 7.47 - 7.42 (4H, m) 7.35 (2 H, t, $J = 8$ Hz) ppm, ^{13}C NMR (101 MHz, CDCl_3) δ 141.4, 128.9, 127.4, 127.3 ppm, m/z (EI^+) 154.1 [M] $^+$.

Table 4.5 entry 7,a

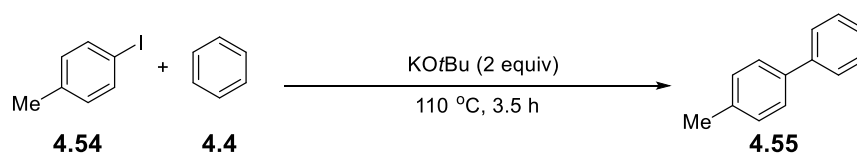


Iodobenzene **4.1** (102 mg, 0.5 mmol) and **4.21** (26 mg, 0.1 mmol) were added to an oven-dried 15 mL pressure tube charged with a magnetic stirrer bar. This was then transferred to a glovebox and KOtBu (112 mg, 1 mmol) and benzene (5 mL) were added and the pressure tube sealed. The sealed tube was placed in a preheated oil bath at 110 °C for 3.5 h. After cooling to room temperature, the reaction mixture was quenched with 1M $\text{HCl}_{(\text{aq})}$ (20 mL) and organic product extracted with EtOAc (3 x 20 mL). The organic extracts were combined and dried over Na_2SO_4 , this was then concentrated and the

crude product purified by column chromatography (hexanes) to afford biphenyl **4.7** (11 mg, 14%) of white crystals. ^1H NMR (400 MHz, CDCl_3) δ = 7.62-7.59, (4H, m), 7.47-7.42 (4H, m) 7.35 (2 H, t, J = 8 Hz) ppm, ^{13}C NMR (101 MHz, CDCl_3) δ 141.4, 128.9, 127.4, 127.3 ppm, m/z (EI^+) 154.1 [M] $^+$.

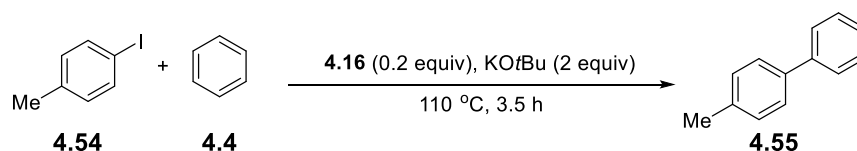
Formation of 4-methylbiphenyl **4.55** in table 4.5

Table 4.5 entry 1,b



4-Iodotoluene **4.54** (109 mg, 0.5 mmol) was added to an oven-dried 15 mL pressure tube charged with a magnetic stirrer bar. This was then transferred to a glovebox and KOtBu (112 mg, 1 mmol) and benzene (5 mL) were added and the pressure tube sealed. The sealed tube was placed in a preheated oil bath at 110 °C for 3.5 h. After cooling to room temperature, the reaction mixture was quenched with 1M $\text{HCl}_{(\text{aq})}$ (20 mL) and organic product extracted with EtOAc (3 x 20 mL). The organic extracts were combined and dried over Na_2SO_4 , this was then concentrated and the crude product purified by column chromatography (hexanes) to afford 4-methylbiphenyl **4.55** (4 mg, 5%) of a colourless oil. ^1H NMR (400 MHz, CDCl_3) δ 7.59 (2H, d, J = 8 Hz) 7.50 (2H, d, J = 8 Hz) 7.43 (2H, t, J = 8 Hz) 7.33 (1H, t, J = 8 Hz) 7.26 (2H, d, J = 8 Hz) 2.44 (3H, s) ppm, ^{13}C -NMR (101 MHz, CDCl_3) δ 141.3, 138.5, 137.1, 129.6, 128.8, 127.1, 21.2 ppm, m/z (EI^+) 168.1 [M] $^+$.

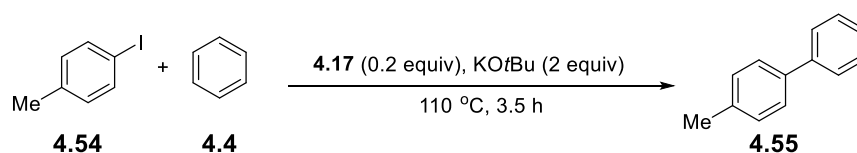
Table 4.5 entry 2,b



4-Iodotoluene **4.54** (109 mg, 0.5 mmol) and **4.16** (22 mg, 0.1 mmol) were added to an oven-dried 15 mL pressure tube charged with a magnetic stirrer bar. This was then transferred to a glovebox and KOtBu (112 mg, 1 mmol) and benzene (5 mL) were added and the pressure tube sealed. The sealed tube was placed in a preheated oil bath at 110

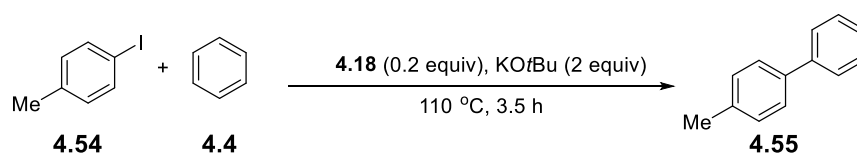
°C for 3.5 h. After cooling to room temperature, the reaction mixture was quenched with 1M HCl_(aq) (20 mL) and organic product extracted with EtOAc (3 x 20 mL). The organic extracts were combined and dried over Na₂SO₄, this was then concentrated and the crude product purified by column chromatography (hexanes) to afford 4-methylbiphenyl **4.55** (60 mg, 71%) of a colourless oil. ¹H NMR (400 MHz, CDCl₃) δ 7.59 (2H, d, *J* = 8 Hz) 7.50 (2H, d, *J* = 8 Hz) 7.43 (2H, t, *J* = 8 Hz) 7.33 (1H, t, *J* = 8 Hz) 7.26 (2H, d, *J* = 8 Hz) 2.44 (3H, s) ppm, ¹³C-NMR (101 MHz, CDCl₃) δ 141.3, 138.5, 137.1, 129.6, 128.8, 127.1, 21.2 ppm, *m/z* (EI⁺) 168.1 [M]⁺.

Table 4.5 entry 3,b



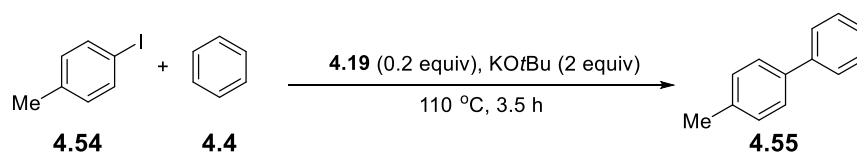
4-Iodotoluene **4.54** (109 mg, 0.5 mmol) and **4.17** (23 mg, 0.1 mmol) were added to an oven-dried 15 mL pressure tube charged with a magnetic stirrer bar. This was then transferred to a glovebox and KOtBu (112 mg, 1 mmol) and benzene (5 mL) were added and the pressure tube sealed. The sealed tube was placed in a preheated oil bath at 110 °C for 3.5 h. After cooling to room temperature, the reaction mixture was quenched with 1M HCl_(aq) (20 mL) and organic product extracted with EtOAc (3 x 20 mL). The organic extracts were combined and dried over Na₂SO₄, this was then concentrated and the crude product purified by column chromatography (hexanes) to afford 4-methylbiphenyl **4.55** (58 mg, 69%) of a colourless oil. ¹H NMR (400 MHz, CDCl₃) δ 7.59 (2H, d, *J* = 8 Hz) 7.50 (2H, d, *J* = 8 Hz) 7.43 (2H, t, *J* = 8 Hz) 7.33 (1H, t, *J* = 8 Hz) 7.26 (2H, d, *J* = 8 Hz) 2.44 (3H, s) ppm, ¹³C-NMR (101 MHz, CDCl₃) δ 141.3, 138.5, 137.1, 129.6, 128.8, 127.1, 21.2 ppm, *m/z* (EI⁺) 168.1 [M]⁺.

Table 4.5 entry 4,b



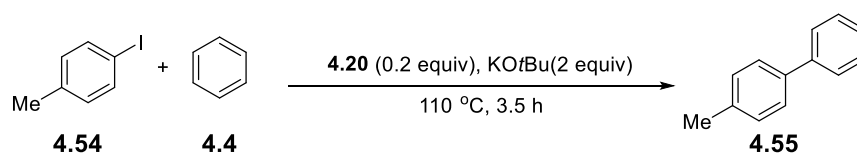
4-Iodotoluene **4.54** (109 mg, 0.5 mmol) and **4.18** (23 mg, 0.1 mmol) were added to an oven-dried 15 mL pressure tube charged with a magnetic stirrer bar. This was then transferred to a glovebox and KOtBu (112 mg, 1 mmol) and benzene (5 mL) were added and the pressure tube sealed. The sealed tube was placed in a preheated oil bath at 110 °C for 3.5 h. After cooling to room temperature, the reaction mixture was quenched with 1M HCl_(aq) (20 mL) and organic product extracted with EtOAc (3 x 20 mL). The organic extracts were combined and dried over Na₂SO₄, this was then concentrated and the crude product purified by column chromatography (hexanes) to afford 4-methylbiphenyl **4.55** (18 mg, 22%) of a colourless oil. ¹H NMR (400 MHz, CDCl₃) δ 7.59 (2H, d, *J* = 8 Hz) 7.50 (2H, d, *J* = 8 Hz) 7.43 (2H, t, *J* = 8 Hz) 7.33 (1H, t, *J* = 8 Hz) 7.26 (2H, d, *J* = 8 Hz) 2.44 (3H, s) ppm, ¹³C-NMR (101 MHz, CDCl₃) δ 141.3, 138.5, 137.1, 129.6, 128.8, 127.1, 21.2 ppm, *m/z* (EI⁺) 168.1 [M]⁺.

Table 4.5 entry 5,b



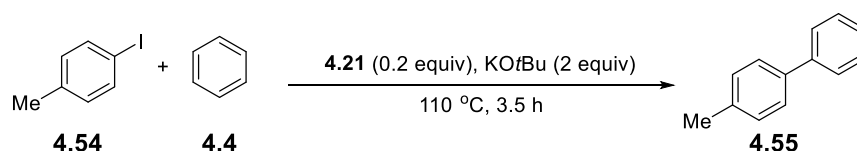
4-Iodotoluene **4.54** (109 mg, 0.5 mmol) and **4.19** (24 mg, 0.1 mmol) were added to an oven-dried 15 mL pressure tube charged with a magnetic stirrer bar. This was then transferred to a glovebox and KOtBu (112 mg, 1 mmol) and benzene (5 mL) were added and the pressure tube sealed. The sealed tube was placed in a preheated oil bath at 110 °C for 3.5 h. After cooling to room temperature, the reaction mixture was quenched with 1M HCl_(aq) (20 mL) and organic product extracted with EtOAc (3 x 20 mL). The organic extracts were combined and dried over Na₂SO₄, this was then concentrated and the crude product purified by column chromatography (hexanes) to afford 4-methylbiphenyl **4.55** (3 mg, 4%) of a colourless oil. ¹H NMR (400 MHz, CDCl₃) δ 7.59 (2H, d, *J* = 8 Hz) 7.50 (2H, d, *J* = 8 Hz) 7.43 (2H, t, *J* = 8 Hz) 7.33 (1H, t, *J* = 8 Hz) 7.26 (2H, d, *J* = 8 Hz) 2.44 (3H, s) ppm, ¹³C-NMR (101 MHz, CDCl₃) δ 141.3, 138.5, 137.1, 129.6, 128.8, 127.1, 21.2 ppm, *m/z* (EI⁺) 168.1 [M]⁺.

Table 4.5 entry 6,b



4-Iodotoluene **4.54** (109 mg, 0.5 mmol) and **4.20** (24 mg, 0.1 mmol) were added to an oven-dried 15 mL pressure tube charged with a magnetic stirrer bar. This was then transferred to a glovebox and KOtBu (112 mg, 1 mmol) and benzene (5 mL) were added and the pressure tube sealed. The sealed tube is placed in a preheated oil bath at 110 °C for 3.5 h. After cooling to room temperature the reaction mixture is quenched with 1M HCl_(aq) (20 mL) and organic product extracted with EtOAc (3 x 20 mL). The organic extracts were combined and dried over Na₂SO₄, this was then concentrated and crude product purified by column chromatography (hexanes) to afford 4-methylbiphenyl **4.55** 10 mg (12%) of a colourless oil. ¹H NMR (400 MHz, CDCl₃) δ 7.59 (2H, d, *J* = 8 Hz) 7.50 (2H, d, *J* = 8 Hz) 7.43 (2H, t, *J* = 8 Hz) 7.33 (1H, t, *J* = 8 Hz) 7.26 (2H, d, *J* = 8 Hz) 2.44 (3H, s) ppm, ¹³C-NMR (101 MHz, CDCl₃) δ 141.3, 138.5, 137.1, 129.6, 128.8, 127.1, 21.2 ppm, *m/z* (EI⁺) 168.1 [M]⁺.

Table 4.5 entry 7,b

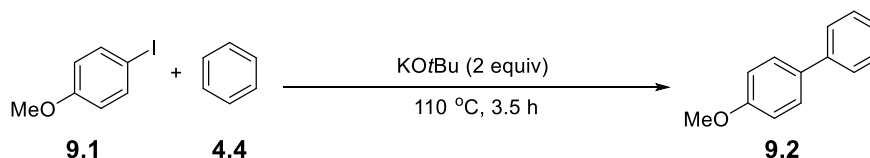


4-Iodotoluene **4.54** (109 mg, 0.5 mmol) and **4.21** (26 mg, 0.1 mmol) were added to an oven-dried 15 mL pressure tube charged with a magnetic stirrer bar. This was then transferred to a glovebox and KOtBu (112 mg, 1 mmol) and benzene (5 mL) were added and the pressure tube sealed. The sealed tube was placed in a preheated oil bath at 110 °C for 3.5 h. After cooling to room temperature, the reaction mixture was quenched with 1M HCl_(aq) (20 mL) and organic product extracted with EtOAc (3 x 20 mL). The organic extracts were combined and dried over Na₂SO₄, this was then concentrated and the crude product purified by column chromatography (hexanes) to afford 4-methylbiphenyl **4.55** (4 mg, 5%) of a colourless oil. ¹H NMR (400 MHz, CDCl₃) δ 7.59 (2H,

d, $J = 8$ Hz) 7.50 (2H, d, $J = 8$ Hz) 7.43 (2H, t, $J = 8$ Hz) 7.33 (1H, t, $J = 8$ Hz) 7.26 (2H, d, $J = 8$ Hz) 2.44 (3H, s) ppm, ^{13}C -NMR (101 MHz, CDCl_3) δ 141.3, 138.5, 137.1, 129.6, 128.8, 127.1, 21.2 ppm, m/z (EI^+) 168.1 $[\text{M}]^+$.

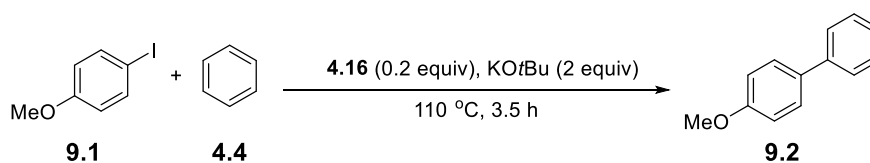
Formation of 4-methoxybiphenyl **9.2** in table 4.5

Table 4.5 entry 1,c



4-Iodoanisole **9.1** (117 mg, 0.5 mmol) was added to an oven-dried 15 mL pressure tube charged with a magnetic stirrer bar. This was then transferred to a glovebox and KOtBu (112 mg, 1 mmol) and benzene (5 mL) were added and the pressure tube sealed. The sealed tube was placed in a preheated oil bath at 110 °C for 3.5 h. After cooling to room temperature, the reaction mixture was quenched with 1M $\text{HCl}_{(\text{aq})}$ (20 mL) and organic product extracted with EtOAc (3 x 20 mL). The organic extracts were combined and dried over Na_2SO_4 , this was then concentrated and the crude product purified by column chromatography (10% EtOAc in hexanes), no coupled product was isolated.

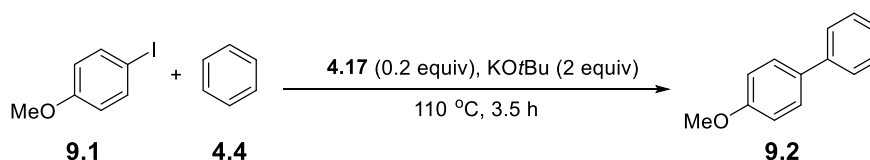
Table 4.5 entry 2,c



4-Iodoanisole **9.1** (117 mg, 0.5 mmol) and **4.16** (22 mg, 0.1 mmol) were added to an oven-dried 15 mL pressure tube charged with a magnetic stirrer bar. This was then transferred to a glovebox and KOtBu (112 mg, 1 mmol) and benzene (5 mL) were added and the pressure tube sealed. The sealed tube was placed in a preheated oil bath at 110 °C for 3.5 h. After cooling to room temperature, the reaction mixture was quenched with 1M $\text{HCl}_{(\text{aq})}$ (20 mL) and organic product extracted with EtOAc (3 x 20 mL). The organic extracts were combined and dried over Na_2SO_4 , this was then concentrated and the crude product purified by column chromatography (10% EtOAc in hexanes) to afford 4-

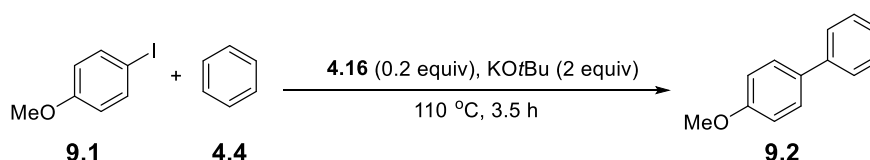
methoxybiphenyl **9.2** (73 mg, 79%) of a white solid. ^1H NMR (400 MHz, CDCl_3) 7.57-7.51 (4H, m) 7.43 (2H, t, $J = 8$ Hz) 7.31 (1H, t, $J = 8$ Hz) 6.98 (2H, d, $J = 8$ Hz) 3.86 (3H, s) ppm, ^{13}C -NMR (101 MHz, CDCl_3) δ 141.0, 128.9, 128.3, 126.9, 126.8, 114.3 ppm, m/z (EI^+) 184.2 $[\text{M}]^+$.

Table 4.5 entry 3,c



4-Iodoanisole **9.1** (117 mg, 0.5 mmol) and **4.17** (23 mg, 0.1 mmol) were added to an oven-dried 15 mL pressure tube charged with a magnetic stirrer bar. This was then transferred to a glovebox and KOtBu (112 mg, 1 mmol) and benzene (5 mL) were added and the pressure tube sealed. The sealed tube was placed in a preheated oil bath at 110 °C for 3.5 h. After cooling to room temperature, the reaction mixture was quenched with 1M $\text{HCl}_{(\text{aq})}$ (20 mL) and organic product extracted with EtOAc (3 x 20 mL). The organic extracts were combined and dried over Na_2SO_4 , this was then concentrated and the crude product purified by column chromatography (10% EtOAc in hexanes) to afford 4-methoxybiphenyl **9.2** (62 mg, 67%) of a white solid. ^1H NMR (400 MHz, CDCl_3) 7.57-7.51 (4H, m) 7.43 (2H, t, $J = 8$ Hz) 7.31 (1H, t, $J = 8$ Hz) 6.98 (2H, d, $J = 8$ Hz) 3.86 (3H, s) ppm, ^{13}C -NMR (101 MHz, CDCl_3) δ 141.0, 128.9, 128.3, 126.9, 126.8, 114.3 ppm, m/z (EI^+) 184.2 $[\text{M}]^+$.

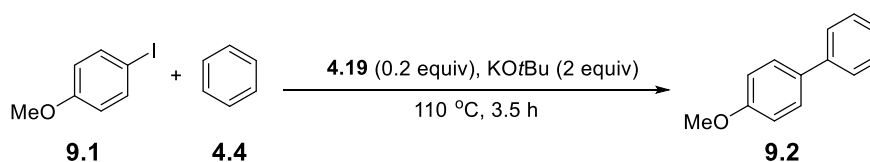
Table 4.5 entry 4,c



4-Iodoanisole **9.1** (117 mg, 0.5 mmol) and **4.18** (23 mg, 0.1 mmol) were added to an oven-dried 15 mL pressure tube charged with a magnetic stirrer bar. This was then transferred to a glovebox and KOtBu (112 mg, 1 mmol) and benzene (5 mL) were added and the pressure tube sealed. The sealed tube was placed in a preheated oil bath at 110

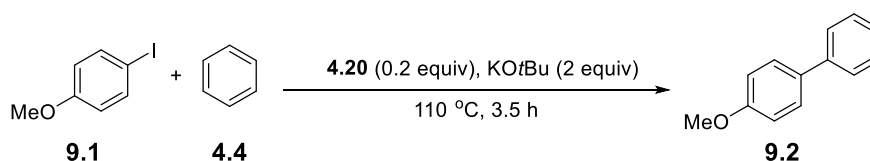
°C for 3.5 h. After cooling to room temperature, the reaction mixture was quenched with 1M HCl_(aq) (20 mL) and organic product extracted with EtOAc (3 x 20 mL). The organic extracts were combined and dried over Na₂SO₄, this was then concentrated and the crude product purified by column chromatography (10% EtOAc in hexanes) to afford 4-methoxybiphenyl **9.2** (35 mg, 38%) of a white solid. ¹H NMR (400 MHz, CDCl₃) 7.57-7.51 (4H, m) 7.43 (2H, t, *J* = 8 Hz) 7.31 (1H, t, *J* = 8 Hz) 6.98 (2H, d, *J* = 8 Hz) 3.86 (3H, s) ppm, ¹³C-NMR (101 MHz, CDCl₃) δ 141.0, 128.9, 128.3, 126.9, 126.8, 114.3 ppm, *m/z* (EI⁺) 184.2 [M]⁺.

Table 4.5 entry 5,c



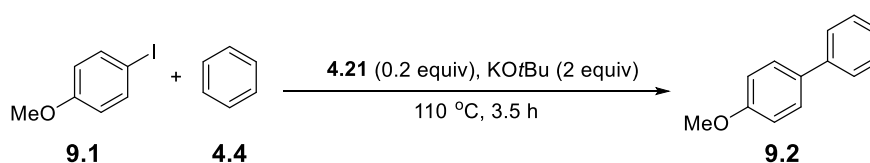
4-Iodoanisole **9.1** (117 mg, 0.5 mmol) and **4.19** (24 mg, 0.1 mmol) were added to an oven-dried 15 mL pressure tube charged with a magnetic stirrer bar. This was then transferred to a glovebox and KOtBu (112 mg, 1 mmol) and benzene (5 mL) were added and the pressure tube sealed. The sealed tube was placed in a preheated oil bath at 110 °C for 3.5 h. After cooling to room temperature, the reaction mixture was quenched with 1M HCl_(aq) (20 mL) and organic product extracted with EtOAc (3 x 20 mL). The organic extracts were combined and dried over Na₂SO₄, this was then concentrated and the crude product purified by column chromatography (10% EtOAc in hexanes) to afford 4-methoxybiphenyl **9.2** (13 mg, 14%) of a white solid. ¹H NMR (400 MHz, CDCl₃) 7.57-7.51 (4H, m) 7.43 (2H, t, *J* = 8 Hz) 7.31 (1H, t, *J* = 8 Hz) 6.98 (2H, d, *J* = 8 Hz) 3.86 (3H, s) ppm, ¹³C-NMR (101 MHz, CDCl₃) δ 141.0, 128.9, 128.3, 126.9, 126.8, 114.3 ppm, *m/z* (EI⁺) 184.2 [M]⁺.

Table 4.5 entry 6,c



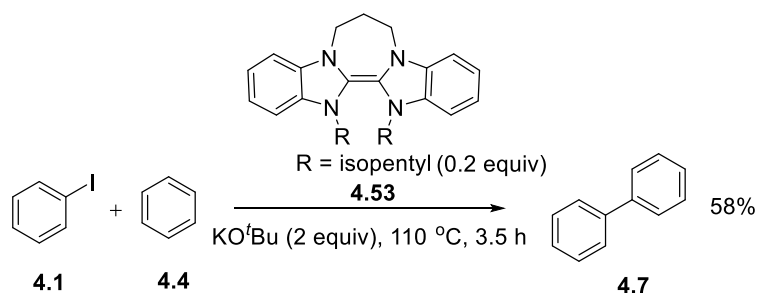
4-Iodoanisole **9.1** (117 mg, 0.5 mmol) and **4.20** (24 mg, 0.1 mmol) were added to an oven-dried 15 mL pressure tube charged with a magnetic stirrer bar. This was then transferred to a glovebox and KOtBu (112 mg, 1 mmol) and benzene (5 mL) were added and the pressure tube sealed. The sealed tube was placed in a preheated oil bath at 110 °C for 3.5 h. After cooling to room temperature, the reaction mixture was quenched with 1M HCl_(aq) (20 mL) and organic product extracted with EtOAc (3 x 20 mL). The organic extracts were combined and dried over Na₂SO₄, this was then concentrated and the crude product purified by column chromatography (10% EtOAc in hexanes) to afford 4-methoxybiphenyl **9.2** (35 mg, 38%) of a white solid. ¹H NMR (400 MHz, CDCl₃) 7.57-7.51 (4H, m) 7.43 (2H, t, *J* = 8 Hz) 7.31 (1H, t, *J* = 8 Hz) 6.98 (2H, d, *J* = 8 Hz) 3.86 (3H, s) ppm, ¹³C-NMR (101 MHz, CDCl₃) δ 141.0, 128.9, 128.3, 126.9, 126.8, 114.3 ppm, m/z (EI⁺) 184.2 [M]⁺.

Table 4.5 entry 7,c



4-Iodoanisole **9.1** (117 mg, 0.5 mmol) and **4.21** (26 mg, 0.1 mmol) were added to an oven-dried 15 mL pressure tube charged with a magnetic stirrer bar. This was then transferred to a glovebox and KOtBu (112 mg, 1 mmol) and benzene (5 mL) were added and the pressure tube sealed. The sealed tube was placed in a preheated oil bath at 110 °C for 3.5 h. After cooling to room temperature, the reaction mixture was quenched with 1M HCl_(aq) (20 mL) and organic product extracted with EtOAc (3 x 20 mL). The organic extracts were combined and dried over Na₂SO₄, this was then concentrated and the crude product purified by column chromatography (10% EtOAc in hexanes) to afford 4-methoxybiphenyl **9.2** (6 mg, 6%) of a white solid. ¹H NMR (400 MHz, CDCl₃) 7.57-7.51 (4H, m) 7.43 (2H, t, *J* = 8 Hz) 7.31 (1H, t, *J* = 8 Hz) 6.98 (2H, d, *J* = 8 Hz) 3.86 (3H, s) ppm, ¹³C-NMR (101 MHz, CDCl₃) δ 141.0, 128.9, 128.3, 126.9, 126.8, 114.3 ppm, m/z (EI⁺) 184.2 [M]⁺.

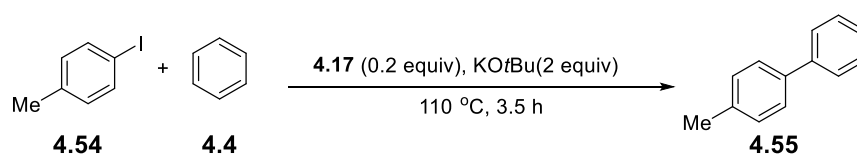
Reaction with known benzimidazole additive **4.53**



Iodobenzene **4.1** (102 mg, 0.5 mmol) and **4.53** (42 mg, 0.1 mmol) were added to an oven-dried 15 mL pressure tube charged with a magnetic stirrer bar. This was then transferred to a glovebox and KO^tBu (112 mg, 1 mmol) and benzene (5 mL) were added and the pressure tube sealed. The sealed tube was placed in a preheated oil bath at 110 °C for 3.5 h. After cooling to room temperature, the reaction mixture was quenched with 1M HCl_(aq) (20 mL) and organic product extracted with EtOAc (3 x 20 mL). The organic extracts were combined and dried over Na₂SO₄, this was then concentrated and the crude product purified by column chromatography (hexanes) to afford biphenyl **4.7** (45 mg, 58%) of white crystals. ¹H NMR (400 MHz, CDCl₃) δ = 7.62-7.59, (4H, m), 7.47-7.42 (4H, m) 7.35 (2 H, t, *J* = 8 Hz) ppm, ¹³C NMR (101 MHz, CDCl₃) δ 141.4, 128.9, 127.4, 127.3 ppm, *m/z* (EI⁺) 154.1 [M]⁺

Repeatability Study using additive **4.17** to couple with 4-iodotoluene **4.54**

Three identical experiments were performed according to the following procedure:



4-Iodotoluene **4.54** (109 mg, 0.5 mmol) and **4.17** (23 mg, 0.1 mmol) were added to an oven-dried 15 mL pressure tube charged with a magnetic stirrer bar. This was then transferred to a glovebox and KO^tBu (112 mg, 1 mmol) and benzene (5 mL) were added and the pressure tube sealed. The sealed tube was placed in a preheated oil bath at 110 °C for 3.5 h. After cooling to room temperature, the reaction mixture was quenched with 1M HCl_(aq) (20 mL) and organic product extracted with EtOAc (3 x 20 mL). The organic

extracts were combined and dried over Na₂SO₄, this was then concentrated and the crude product purified by column chromatography (hexanes) to afford 4-methylbiphenyl as a colourless oil. Spectra were consistent with reactions in table 4.5 entry 2b.

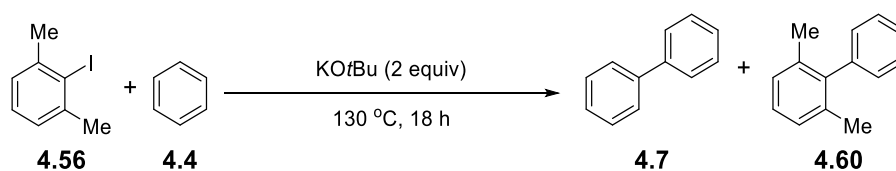
Reaction 1 afforded 60 mg (71%)

Reaction 2 afforded 58 mg (69%)

Reaction 3 afforded 62 mg (74%)

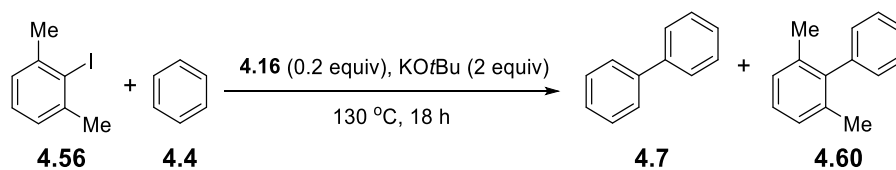
2-iodo-m-xylene **4.56** coupling with benzene **4.4**

Table 4.6 entry 1



2-iodo-m-xylene **4.56** (116 mg, 0.5 mmol) was added to an oven-dried 15 mL pressure tube charged with a magnetic stirrer bar. This is then transferred to a glovebox and KOtBu (112 mg, 1 mmol) and benzene (5 mL) were added and the pressure tube sealed. The sealed tube was placed in a preheated oil bath at 130 °C for 18 h. After cooling to room temperature the reaction mixture was quenched with 1M HCl_(aq) (20 mL) and organic product extracted with EtOAc (3 x 20 mL). The organic extracts were combined and dried over Na₂SO₄, this was then concentrated and crude product purified by column chromatography (hexane) no coupled product was isolated

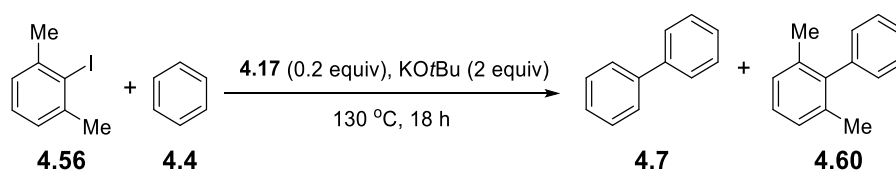
Table 4.6 entry 2



2-iodo-m-xylene **4.56** (116 mg, 0.5 mmol) and **4.16** (22 mg, 0.1 mmol) were added to an oven-dried 15 mL pressure tube charged with a magnetic stirrer bar. This is then

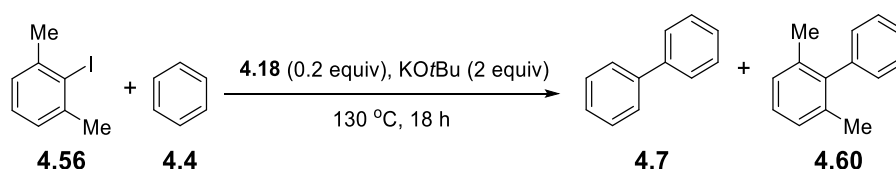
transferred to a glovebox and KOtBu (112 mg, 1 mmol) and benzene (5 mL) were added and the pressure tube sealed. The sealed tube was placed in a preheated oil bath at 130 °C for 18 h. After cooling to room temperature the reaction mixture was quenched with 1M HCl_(aq) (20 mL) and organic product extracted with EtOAc (3 x 20 mL). The organic extracts were combined and dried over Na₂SO₄, this was then concentrated and crude product purified by column chromatography (hexane) to afford biphenyl **4.7** and 2,6-dimethylbiphenyl **4.60** as an inseparable mixture. Combined yield of **4.7** and **4.60** 40 mg.

Table 4.6 entry 3



2-iodo-*m*-xylene **4.56** (116 mg, 0.5 mmol) and **4.17** (23 mg, 0.1 mmol) were added to an oven-dried 15 mL pressure tube charged with a magnetic stirrer bar. This is then transferred to a glovebox and KOtBu (112 mg, 1 mmol) and benzene (5 mL) were added and the pressure tube sealed. The sealed tube was placed in a preheated oil bath at 130 °C for 18 h. After cooling to room temperature the reaction mixture was quenched with 1M HCl_(aq) (20 mL) and organic product extracted with EtOAc (3 x 20 mL). The organic extracts were combined and dried over Na₂SO₄, this was then concentrated and crude product purified by column chromatography (hexane) to afford biphenyl **4.7** and 2,6-dimethylbiphenyl **4.60** as an inseparable mixture. Combined yield of **4.7** and **4.60** 34 mg in a ratio of 3.8:1.

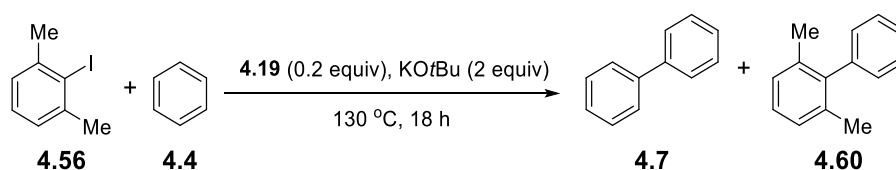
Table 4.6 entry 4



2-iodo-*m*-xylene **4.56** (116 mg, 0.5 mmol) and **4.18** (23 mg, 0.1 mmol) were added to an oven-dried 15 mL pressure tube charged with a magnetic stirrer bar. This is then transferred to a glovebox and KOtBu (112 mg, 1 mmol) and benzene (5 mL) were added

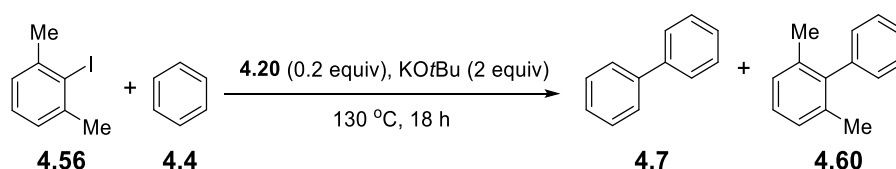
and the pressure tube sealed. The sealed tube was placed in a preheated oil bath at 130 °C for 18 h. After cooling to room temperature the reaction mixture was quenched with 1M HCl_(aq) (20 mL) and organic product extracted with EtOAc (3 x 20 mL). The organic extracts were combined and dried over Na₂SO₄, this was then concentrated and crude product purified by column chromatography (hexane) to afford biphenyl **4.7** and 2,6-dimethylbiphenyl **4.60** as an inseparable mixture. Combined yield of **4.7** and **4.60** 20 mg in a ratio of 3.8:1.

Table 4.6 entry 5



2-iodo-*m*-xylene **4.56** (116 mg, 0.5 mmol) and **4.19** (24 mg, 0.1 mmol) were added to an oven-dried 15 mL pressure tube charged with a magnetic stirrer bar. This is then transferred to a glovebox and KOtBu (112 mg, 1 mmol) and benzene (5 mL) were added and the pressure tube sealed. The sealed tube was placed in a preheated oil bath at 130 °C for 18 h. After cooling to room temperature the reaction mixture was quenched with 1M HCl_(aq) (20 mL) and organic product extracted with EtOAc (3 x 20 mL). The organic extracts were combined and dried over Na₂SO₄, this was then concentrated and crude product purified by column chromatography (hexane) to afford biphenyl **4.7** and 2,6-dimethylbiphenyl **4.60** as an inseparable mixture. Combined yield of **4.7** and **4.60** 16 mg in a ratio of 3.8:1.

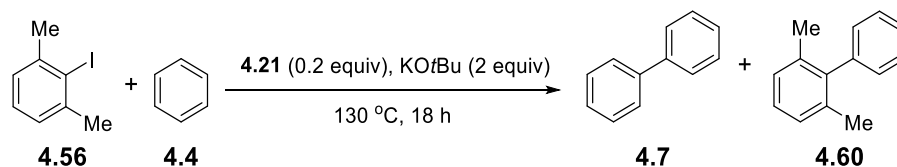
Table 4.6 entry 6



2-iodo-*m*-xylene **4.56** (116 mg, 0.5 mmol) and **4.24** (22 mg, 0.1 mmol) were added to an oven-dried 15 mL pressure tube charged with a magnetic stirrer bar. This is then transferred to a glovebox and KOtBu (112 mg, 1 mmol) and benzene (5 mL) were added

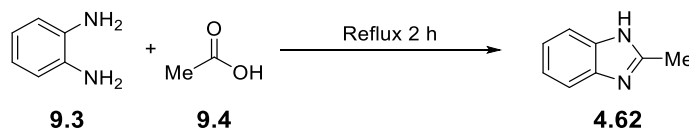
and the pressure tube sealed. The sealed tube was placed in a preheated oil bath at 130 °C for 18 h. After cooling to room temperature the reaction mixture was quenched with 1M HCl_(aq) (20 mL) and organic product extracted with EtOAc (3 x 20 mL). The organic extracts were combined and dried over Na₂SO₄, this was then concentrated and crude product purified by column chromatography (hexane) no coupled product was isolated.

Table 4.6 entry 7



2-iodo-*m*-xylene **4.56** (116 mg, 0.5 mmol) and **4.21** (26 mg, 0.1 mmol) were added to an oven-dried 15 mL pressure tube charged with a magnetic stirrer bar. This is then transferred to a glovebox and KOtBu (112 mg, 1 mmol) and benzene (5 mL) were added and the pressure tube sealed. The sealed tube was placed in a preheated oil bath at 130 °C for 18 h. After cooling to room temperature the reaction mixture was quenched with 1M HCl_(aq) (20 mL) and organic product extracted with EtOAc (3 x 20 mL). The organic extracts were combined and dried over Na₂SO₄, this was then concentrated and crude product purified by column chromatography (hexane) to afford biphenyl **4.7** and 2,6-dimethylbiphenyl **4.60** as an inseparable mixture. Combined yield of **4.7** and **4.60** 2.4 mg in a ratio of 3.8:1.

Synthesis of 2-methyl-1H-benzo[d]imidazole **4.62**

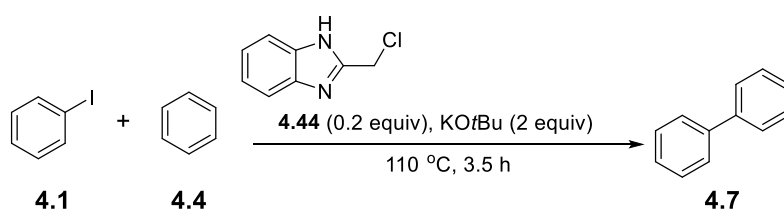


To an oven-dried 50 mL round-bottomed flask *o*-phenylenediamine, **9.3** (5.4 g, 50 mmol) and acetic acid, **9.4** (10 mL) were added. The reaction mixture was heated to reflux for 2 h. Once cooled to room temperature the reaction mixture was poured over ice and basified with aqueous potassium hydroxide. The organic product was extracted with DCM (3 x 50 mL) and the crude material was purified by recrystallisation (water) to afford **4.62** as brown crystals (37%). ¹H NMR (400 MHz, CDCl₃) δ 7.55-7.52 (2H, m) 7.23-

7.19 (2H, m) 2.62 (3H, s) ppm, ^{13}C -NMR (101 MHz, d^6 DMSO) δ 151.2, 121.2, 120.8, 117.8, 110.5, 14.6 ppm,.

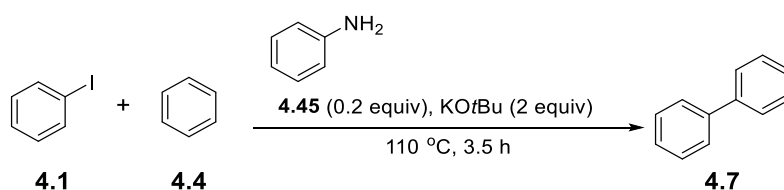
Coupling reactions with partial additives

Table 4.7 entry 1



Iodobenzene **4.1** (102 mg, 0.5 mmol) and **4.44** (15 mg, 0.1 mmol) were added to an oven-dried 15 mL pressure tube charged with a magnetic stirrer bar. This was then transferred to a glovebox and KOtBu (112 mg, 1 mmol) and benzene (5 mL) were added and the pressure tube sealed. The sealed tube was placed in a preheated oil bath at 110 °C for 3.5 h. After cooling to room temperature the reaction mixture was quenched with 1M HCl_(aq) (20 mL) and organic product extracted with EtOAc (3 x 20 mL). The organic extracts were combined and dried over Na₂SO₄, this was then concentrated and crude product purified by column chromatography (hexanes) to afford biphenyl **4.7** (38 mg, 50%) of white crystals. ^1H NMR (400 MHz, CDCl₃) δ = 7.62-7.59, (4H, m), 7.47-7.42 (4H, m) 7.35 (2 H, t, J = 8 Hz) ppm, ^{13}C NMR (101 MHz, CDCl₃) δ 141.4, 128.9, 127.4, 127.3 ppm, m/z (EI⁺) 154.1 [M]⁺.

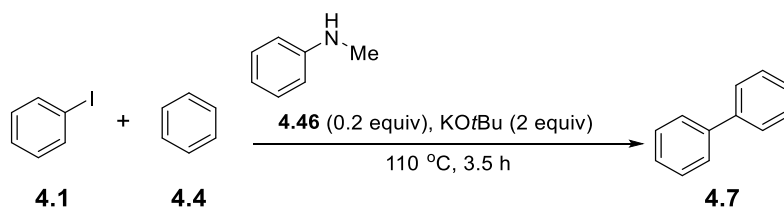
Table 4.7 entry 2



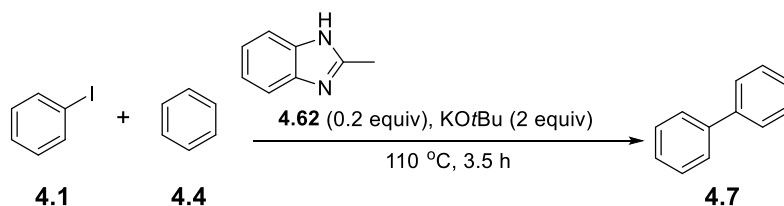
Iodobenzene **4.1** (102 mg, 0.5 mmol) and **4.45** (9 mg, 0.1 mmol) were added to an oven-dried 15 mL pressure tube charged with a magnetic stirrer bar. This was then transferred to a glovebox and KOtBu (112 mg, 1 mmol) and benzene (5 mL) were added and the pressure tube sealed. The sealed tube was placed in a preheated oil bath at 110 °C for

3.5 h. After cooling to room temperature the reaction mixture was quenched with 1M HCl_(aq) (20 mL) and organic product extracted with EtOAc (3 x 20 mL). The organic extracts were combined and dried over Na₂SO₄, this was then concentrated and crude product purified by column chromatography (hexanes) no coupled product was isolated.

Table 4.7 entry 3



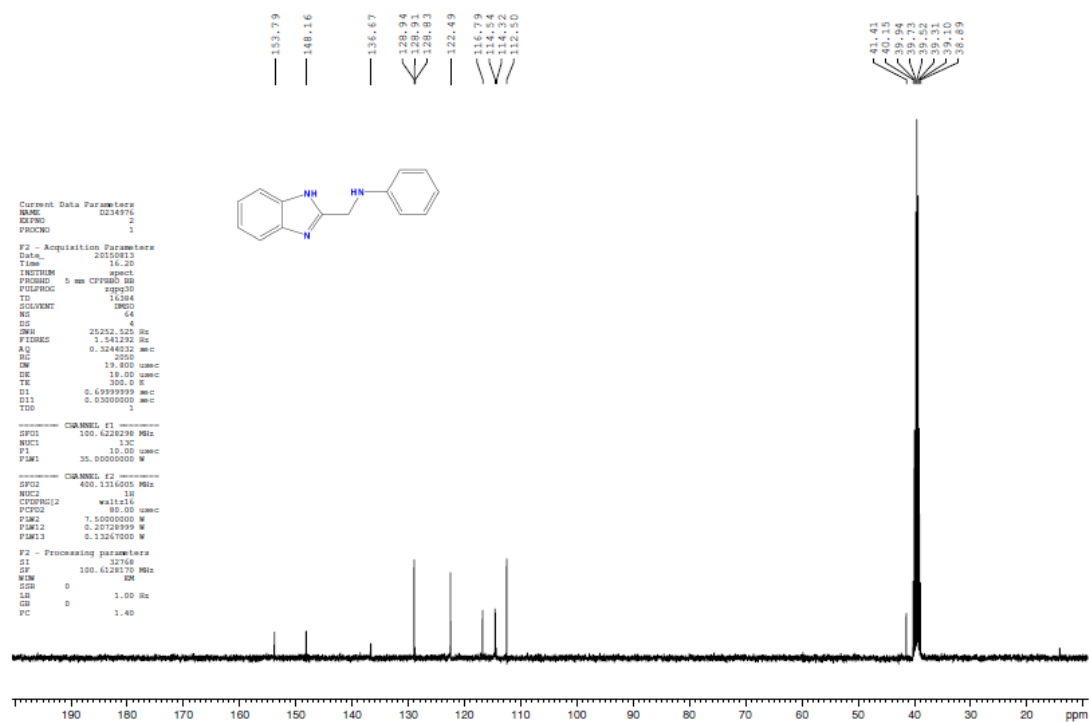
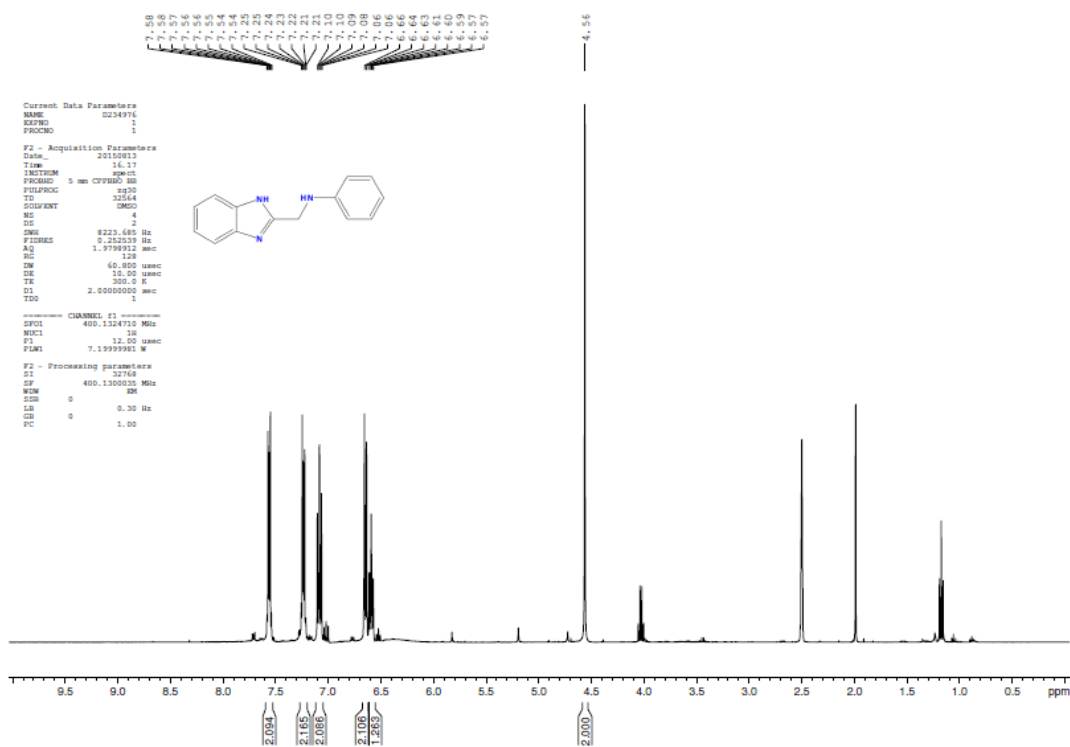
Iodobenzene **4.1** (102 mg, 0.5 mmol) and **4.46** (11 mg, 0.1 mmol) were added to an oven-dried 15 mL pressure tube charged with a magnetic stirrer bar. This was then transferred to a glovebox and KOtBu (112 mg, 1 mmol) and benzene (5 mL) were added and the pressure tube sealed. The sealed tube was placed in a preheated oil bath at 110 °C for 3.5 h. After cooling to room temperature the reaction mixture was quenched with 1M HCl_(aq) (20 mL) and organic product extracted with EtOAc (3 x 20 mL). The organic extracts were combined and dried over Na₂SO₄, this was then concentrated and crude product purified by column chromatography (hexanes) no coupled product was isolated.

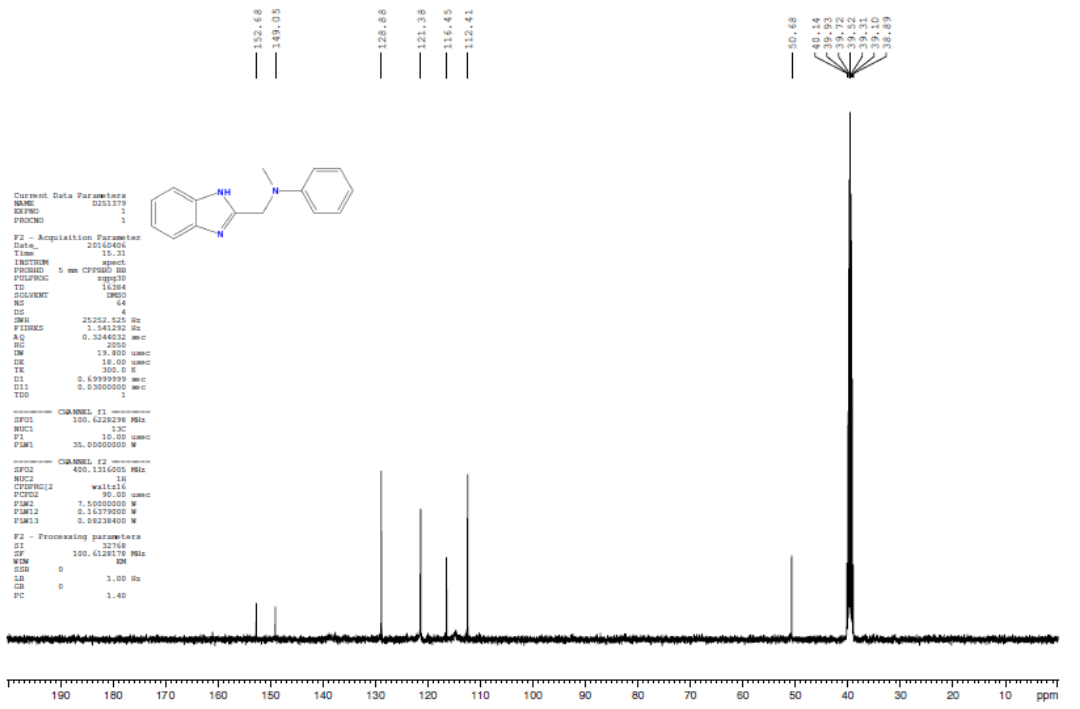
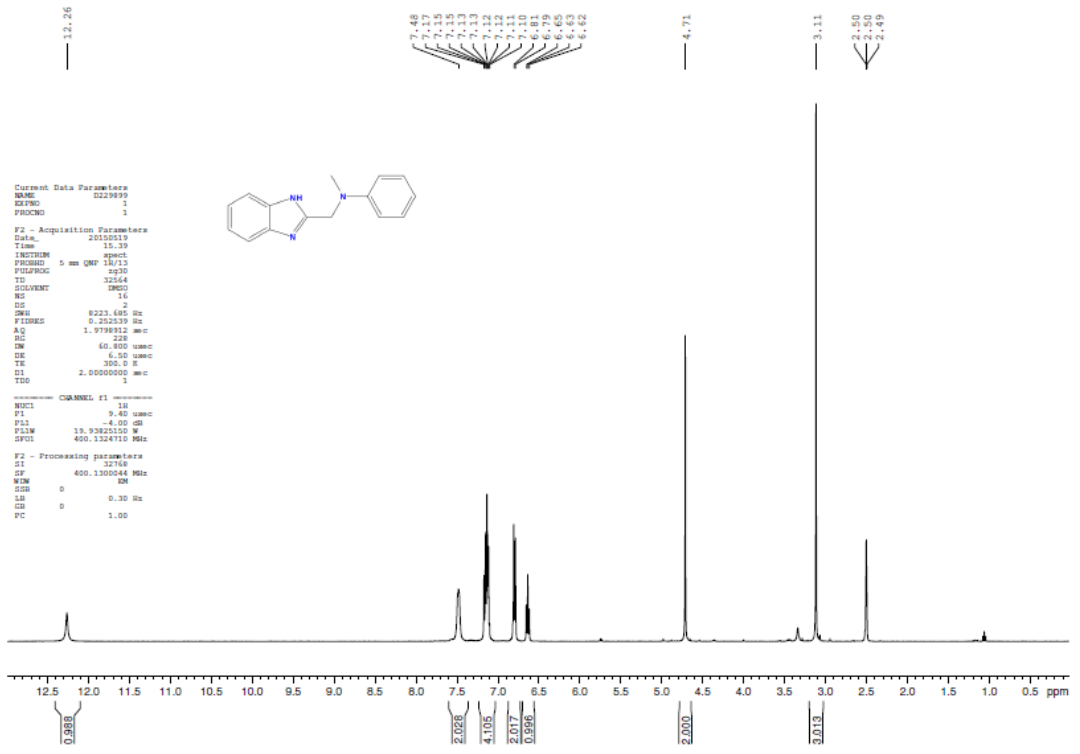


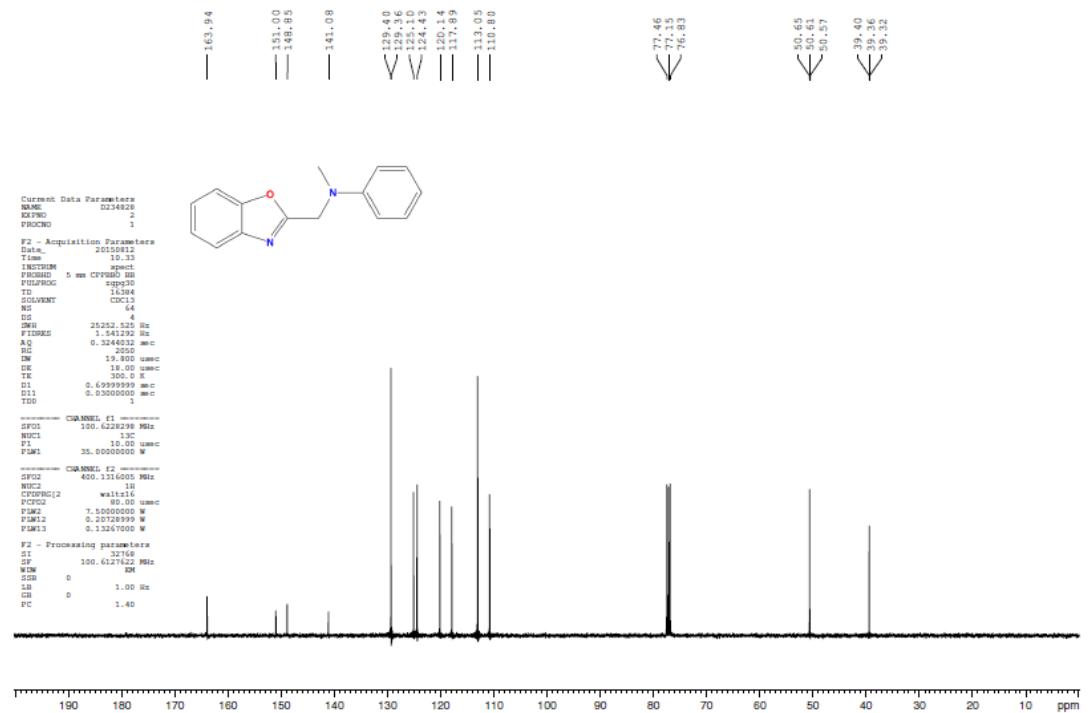
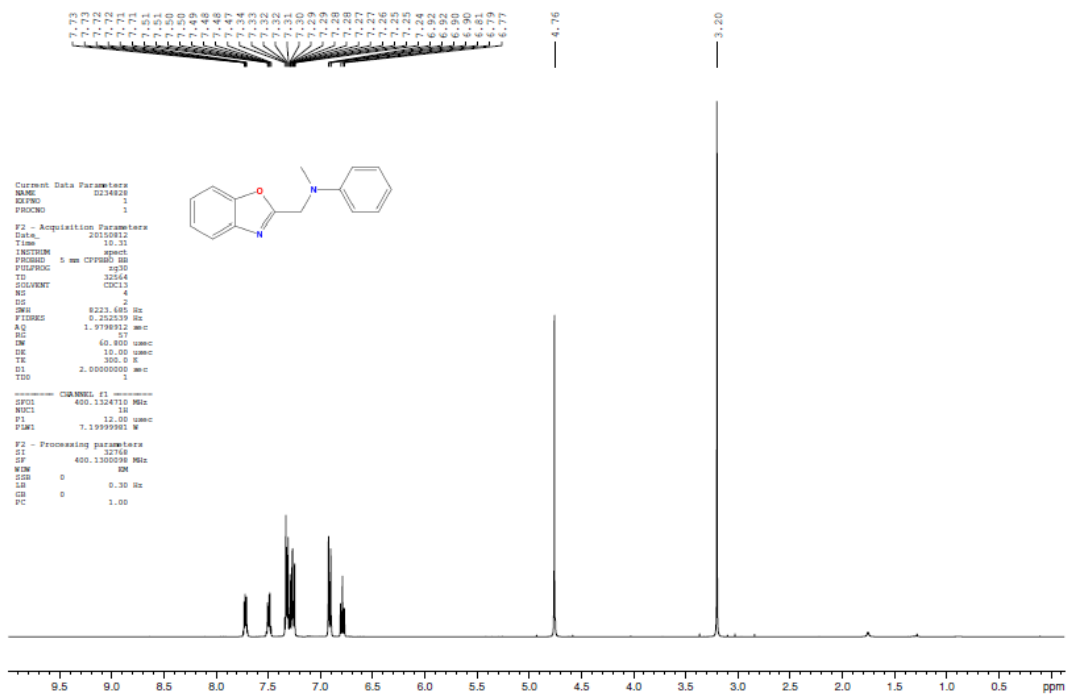
Iodobenzene **4.1** (102 mg, 0.5 mmol) and **4.62** (15 mg, 0.1 mmol) were added to an oven-dried 15 mL pressure tube charged with a magnetic stirrer bar. This was then transferred to a glovebox and KOtBu (112 mg, 1 mmol) and benzene (5 mL) were added and the pressure tube sealed. The sealed tube was placed in a preheated oil bath at 110 °C for 3.5 h. After cooling to room temperature the reaction mixture was quenched with 1M HCl_(aq) (20 mL) and organic product extracted with EtOAc (3 x 20 mL). The organic extracts were combined and dried over Na₂SO₄, this was then concentrated and crude product purified by column chromatography (hexanes) to afford biphenyl **4.7** (2 mg, 1%)

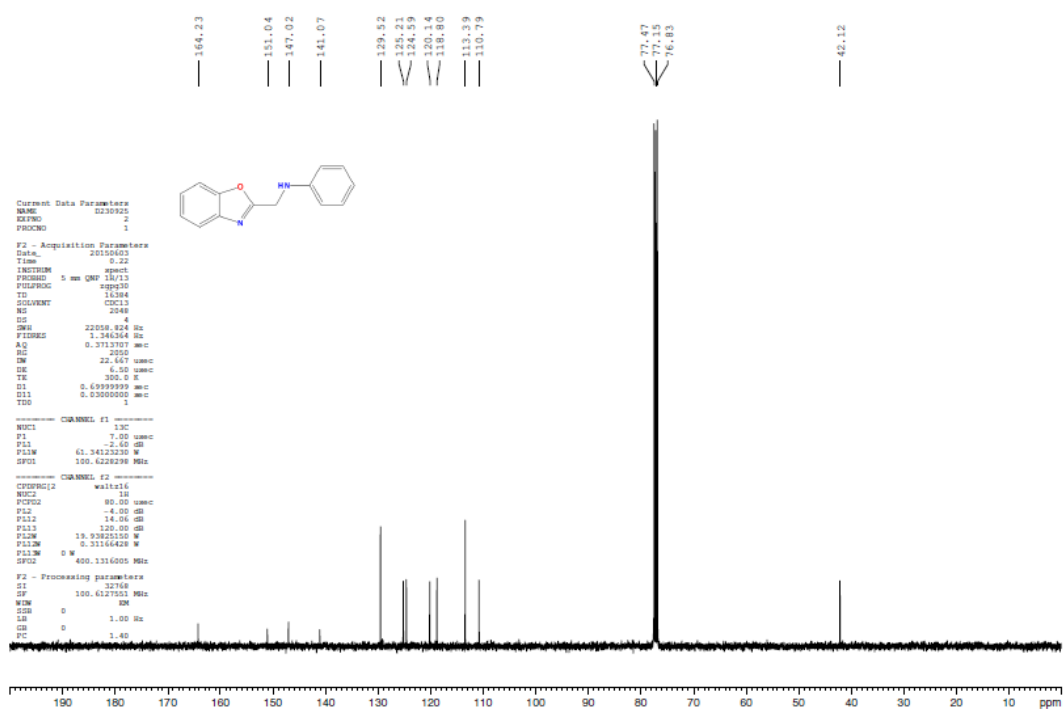
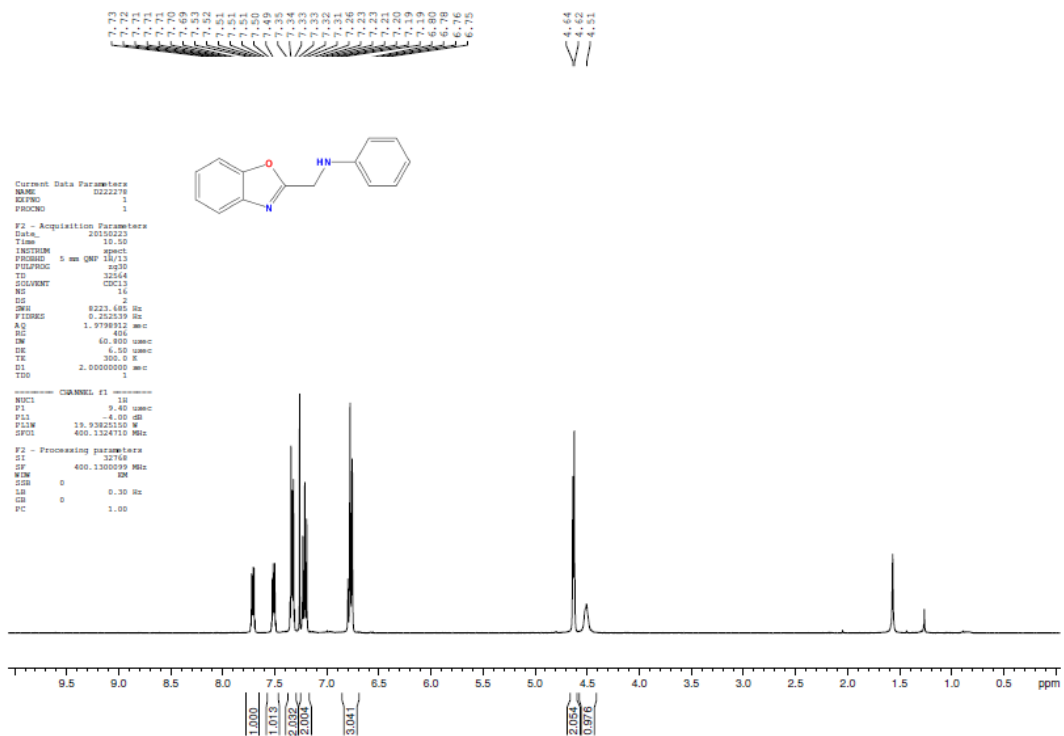
of white crystals. ^1H NMR (400 MHz, CDCl_3) δ = 7.62-7.59, (4H, m), 7.47-7.42 (4H, m) 7.35 (2 H, t, J = 8 Hz) ppm, ^{13}C NMR (101 MHz, CDCl_3) δ 141.4, 128.9, 127.4, 127.3 ppm, m/z (EI^+) 154.1 $[\text{M}]^+$.

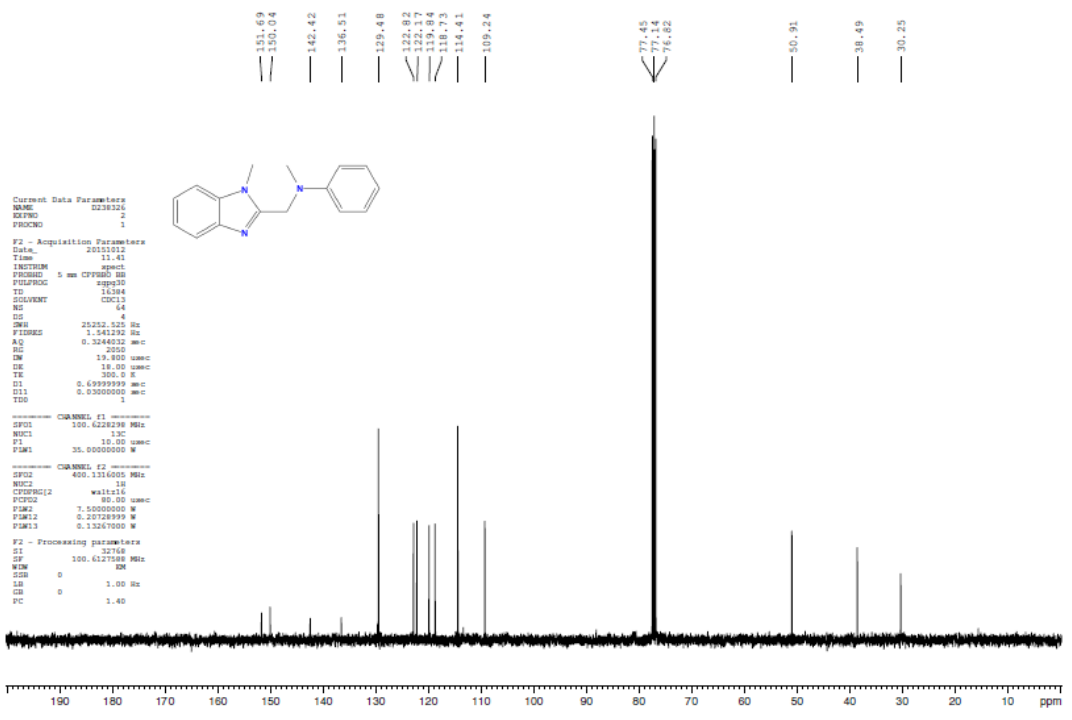
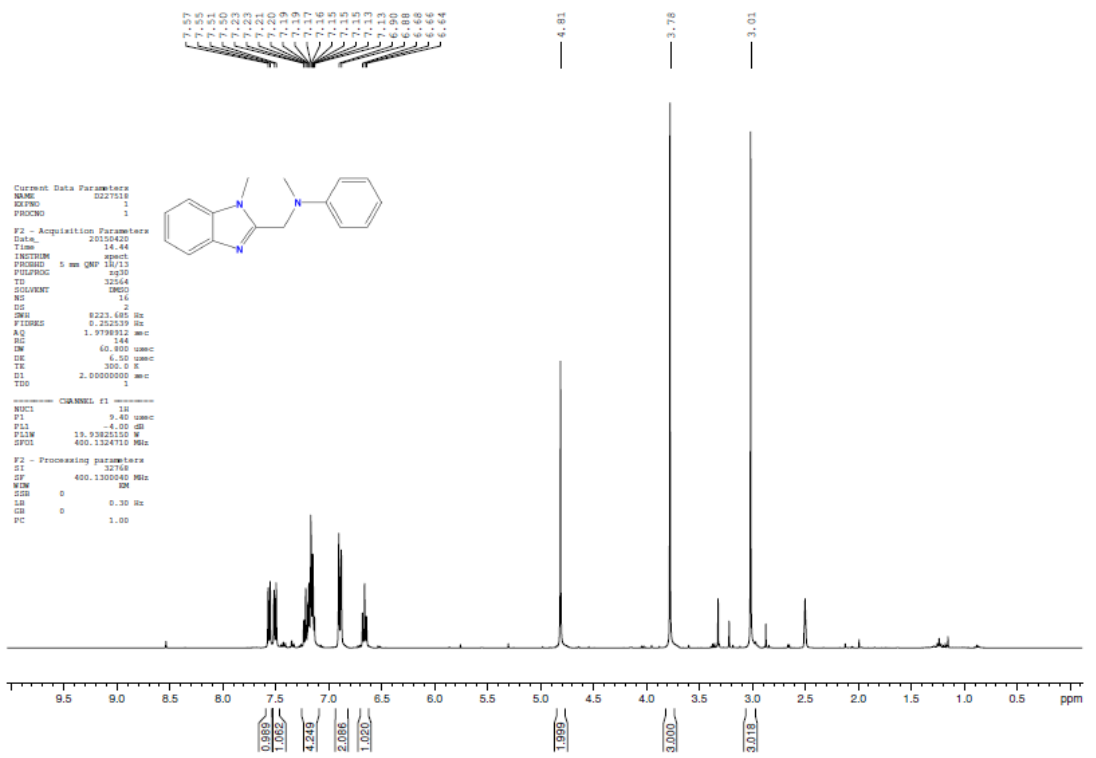
9.3 NMR spectra for compounds synthesised in Chapter 4

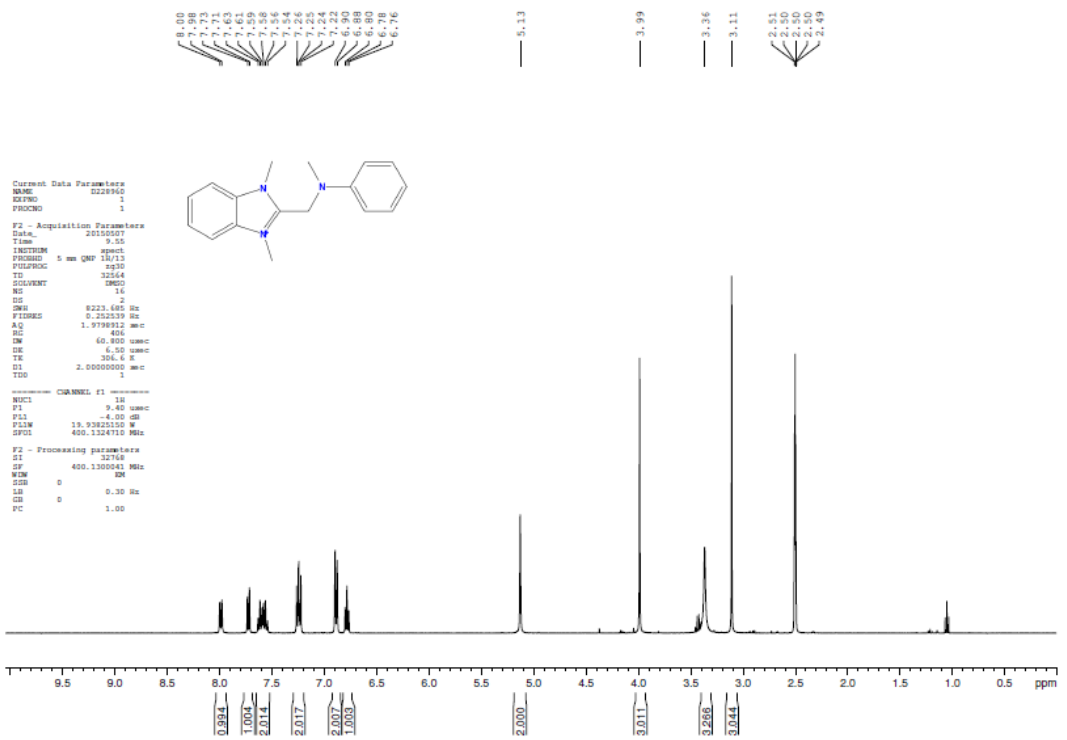


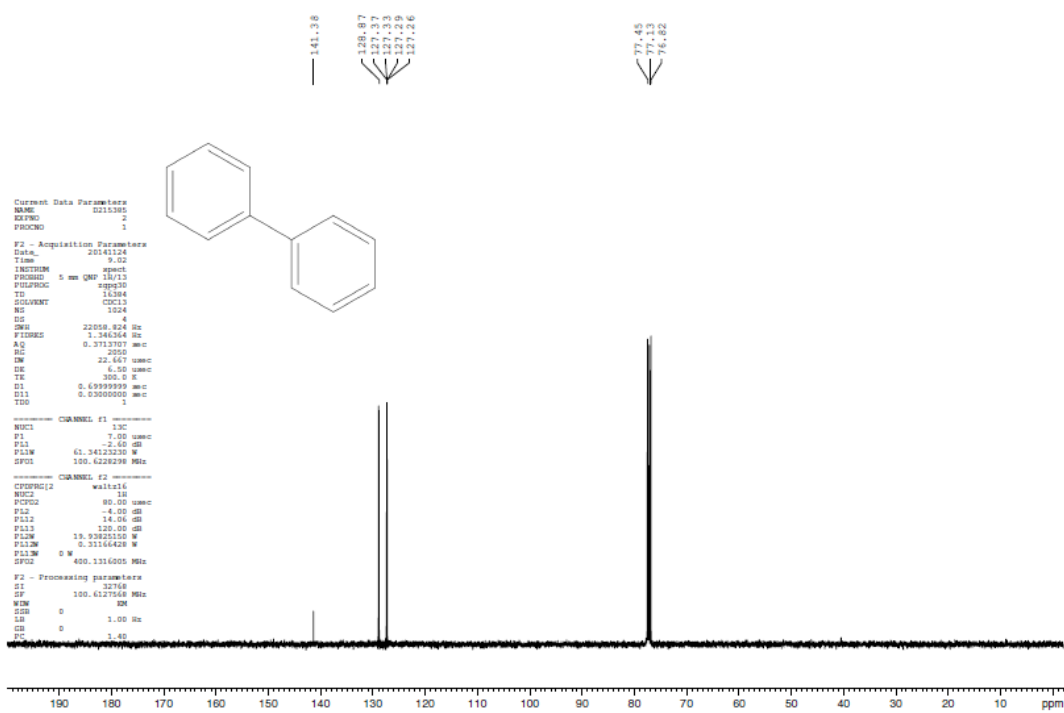
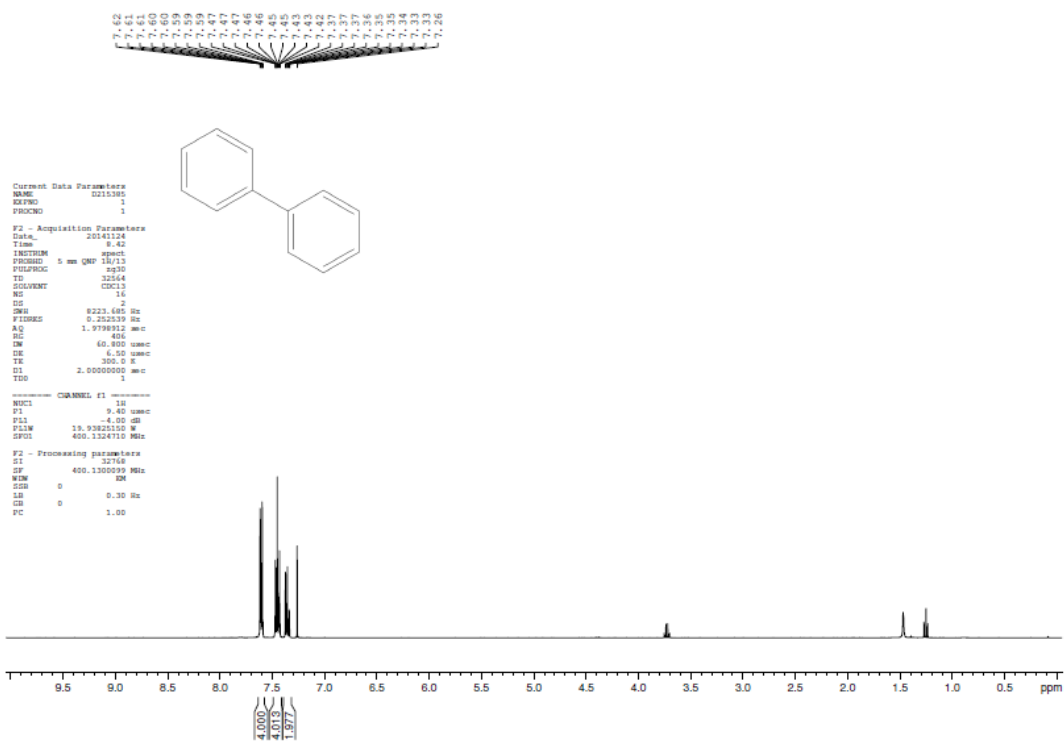


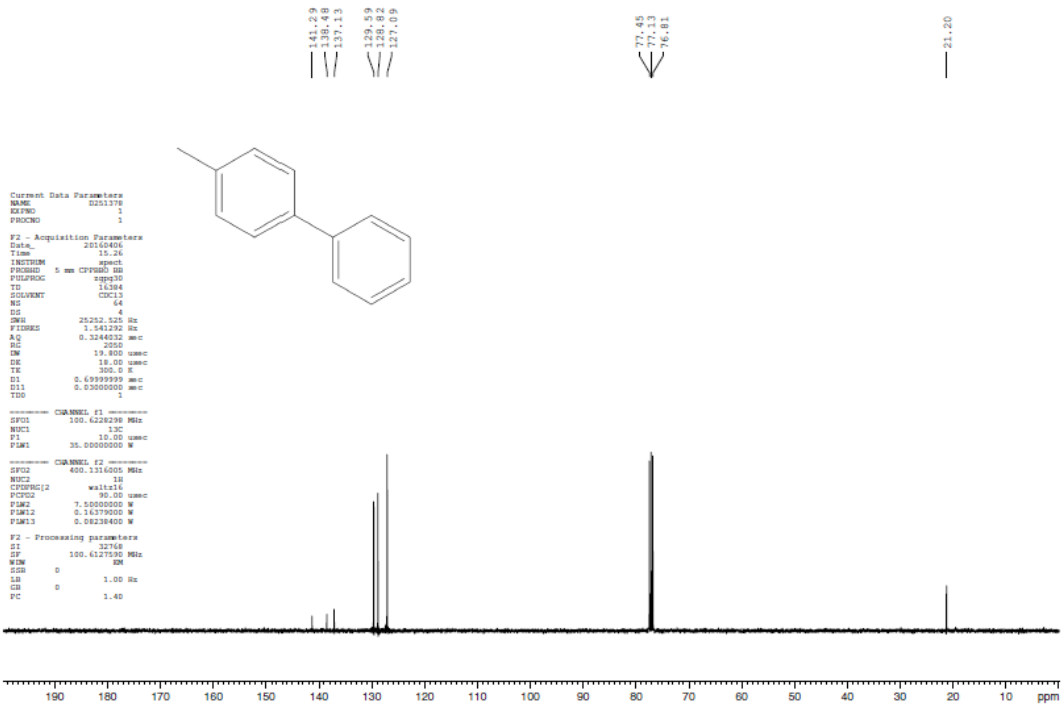
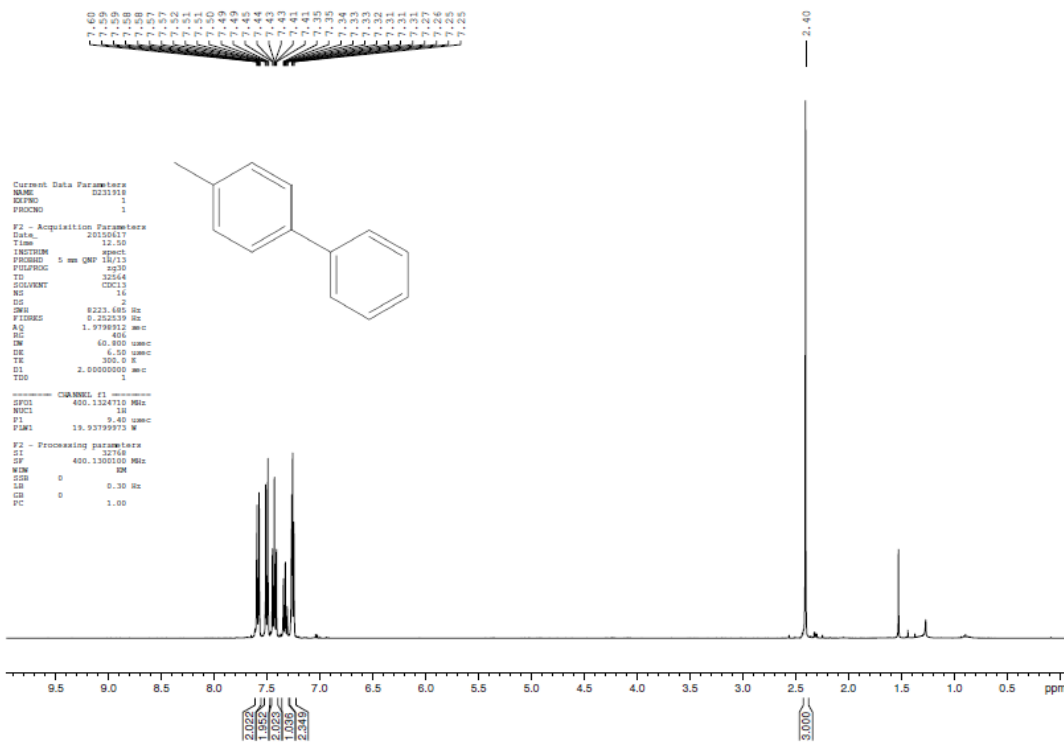


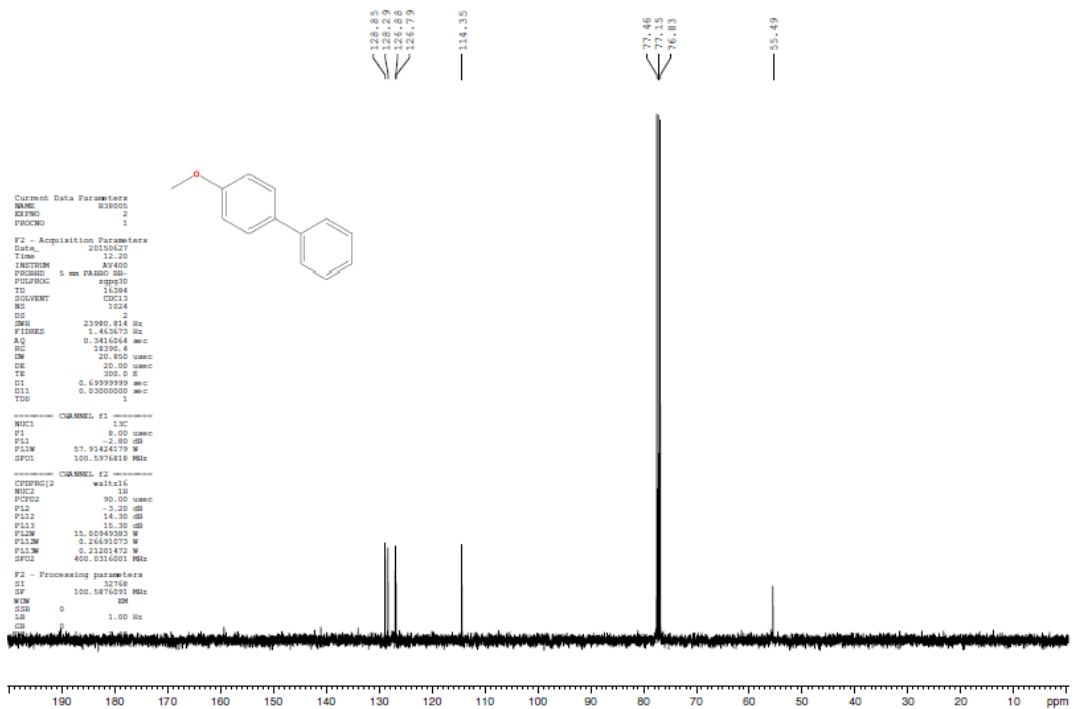
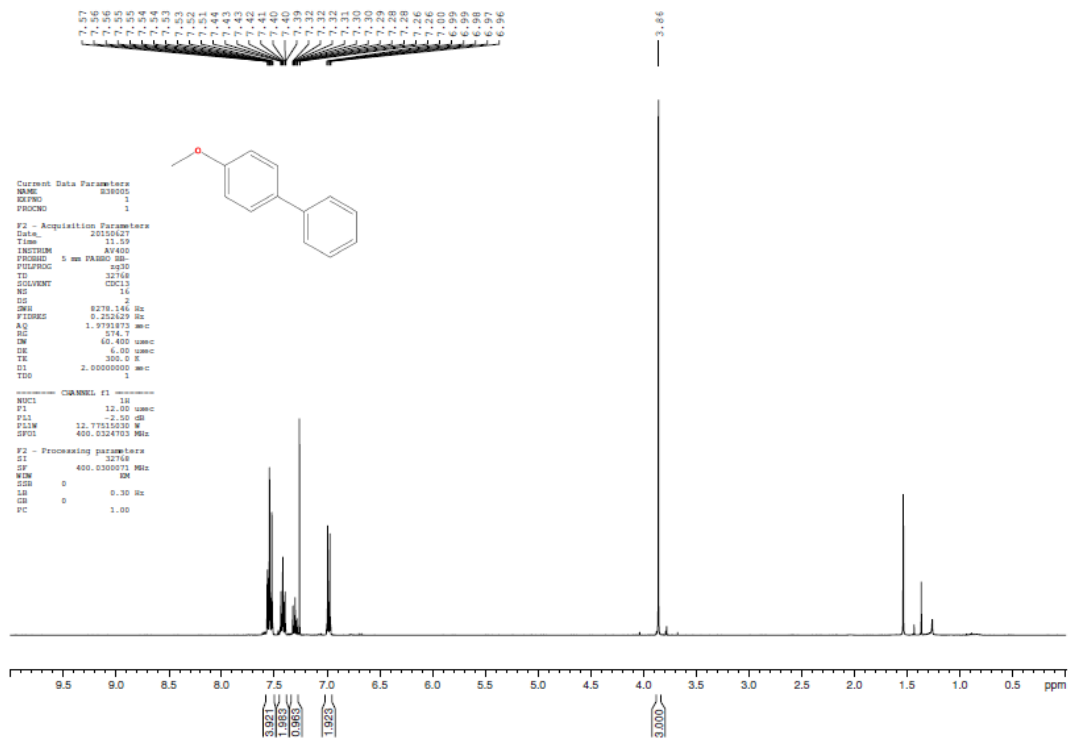


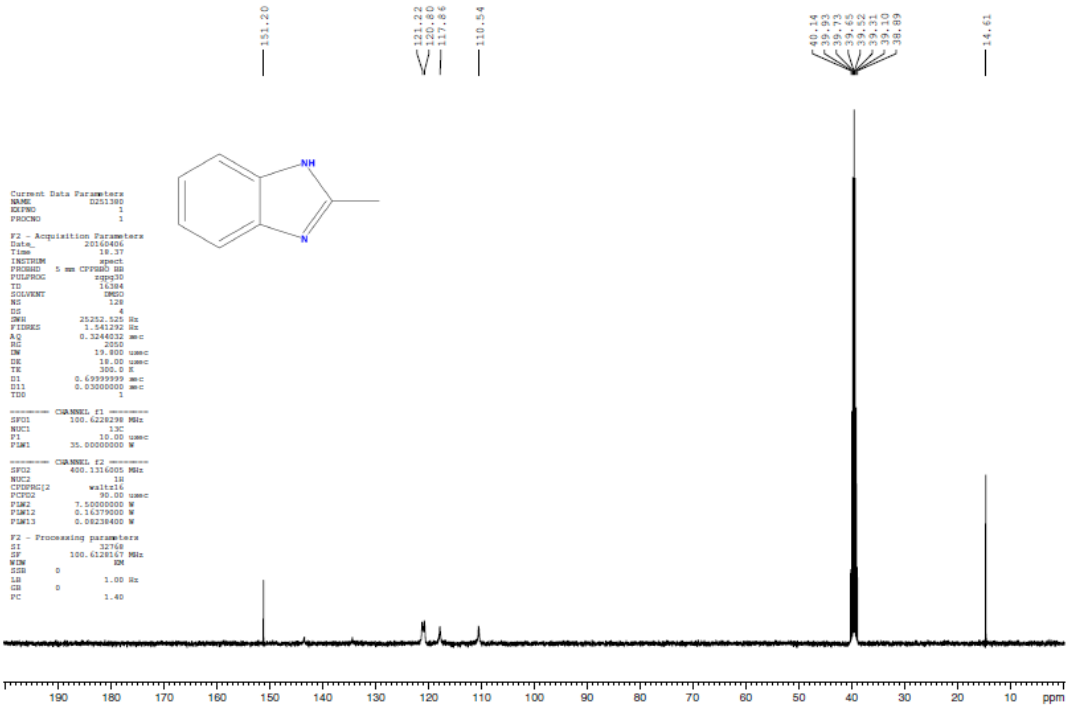
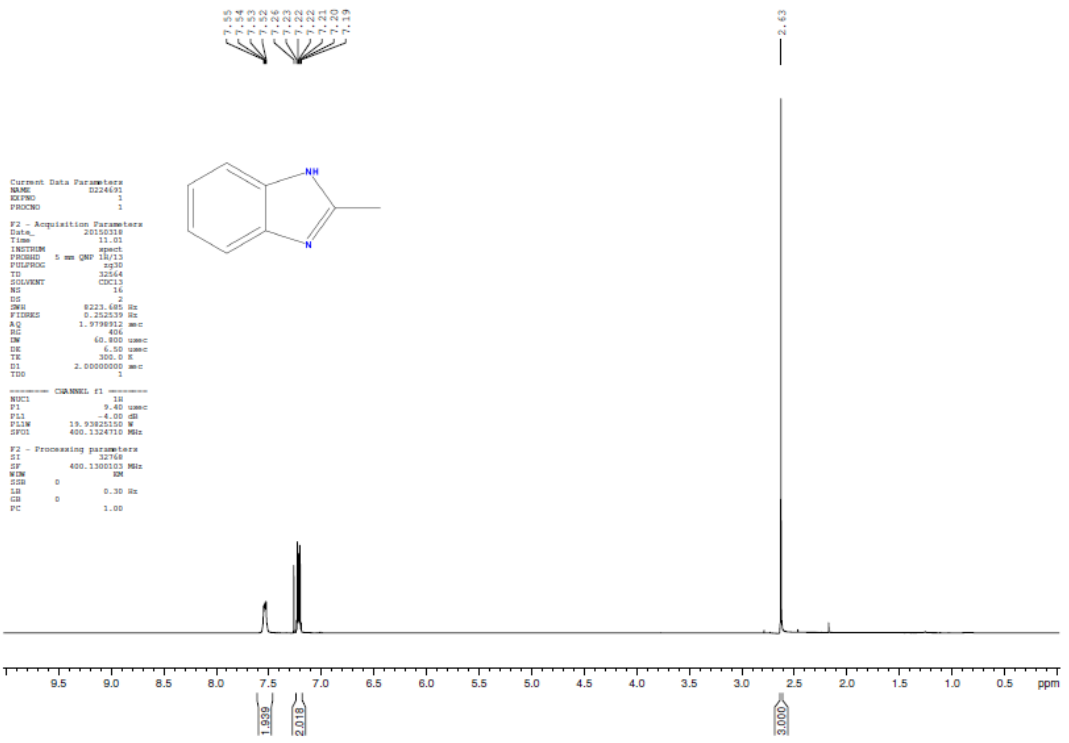






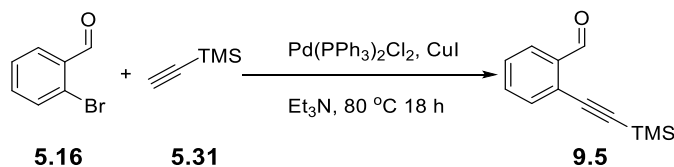






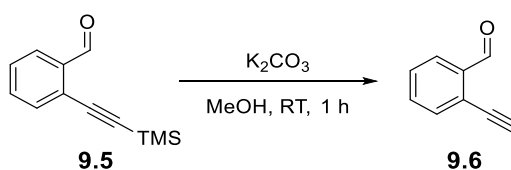
9.4 Experimental procedures for Chapter 5

Preparation of 2-((trimethylsilyl)ethynyl)benzaldehyde, **9.5**



To a 100 mL round-bottomed flask was added bis(triphenylphosphine)palladium chloride (70 mg, 0.1 mmol), copper iodide (25 mg, 0.05 mmol), 2-bromobenzaldehyde, **5.16** (0.925g, 5 mmol), and triethylamine (20 mL). This was then purged with argon for 20 min. Ethynyltrimethylsilane, **5.31** (0.539 g, 5.1 mmol), was then added to the reaction mixture and this was heated to $80\text{ }^\circ\text{C}$ for 18 h. After cooling to room temperature, the ammonium salts were removed by filtration and the resulting solution was concentrated. This crude product was purified by column chromatography (hexane/EtOAc 10/1) to afford 2-((trimethylsilyl)ethynyl)benzaldehyde, **9.5**, as a brown oil (747 mg, 74%).¹⁷⁵ FTIR ν_{max} (neat) 2957 (C-H), 2838 (C-H), 2155 (C \equiv C), 1698 cm^{-1} (C=O); ^1H NMR (400 MHz CDCl_3) δ 10.53 (1H, s), 7.87 (1H, d, $J = 8$ Hz), 7.55-7.48 (2H, m), 7.40 (1H, t, $J = 8$ Hz), 0.26 (9H, s) ppm, ^{13}C NMR (101 MHz, CDCl_3) δ 191.8, 136.3, 133.7, 133.6, 128.9, 126.9, 126.8, 100.5, 100.2, -0.2 ppm, m/z (EI $^+$) 201.0 [M] $^+$.

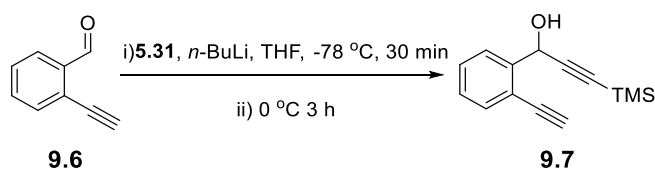
Preparation of 2-ethynylbenzaldehyde, **9.6**



2-((Trimethylsilyl)ethynyl)benzaldehyde, **9.5** (1.01 g, 5 mmol), potassium carbonate (1.38 g, 10 mmol) and methanol (50 mL) were placed in a 100 mL round-bottomed flask. This was stirred at room temperature for 1 h. The reaction was diluted with water (50 mL) and extracted with DCM (3 x 40 mL). The combined extracts were washed with brine and dried over Na_2SO_4 then concentrated. The crude product was purified by column chromatography (hexane/EtOAc 10/1) to afford 2-ethynylbenzaldehyde, **9.6** as a brown crystalline solid (490 mg, 76%).¹⁷⁵ MP $61\text{--}62\text{ }^\circ\text{C}$ (lit. $62\text{--}65\text{ }^\circ\text{C}$)¹⁷⁵ FTIR ν_{max} (neat) 3230 (C-

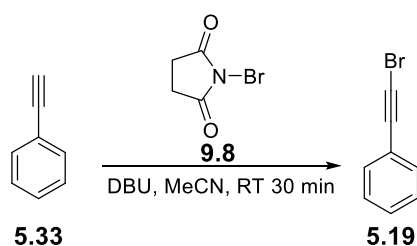
H) 3069 (C-H), 2098 (C≡C), 1687 cm^{-1} (C=O); ^1H NMR (400 MHz CDCl_3) δ 10.54 (1H, s), 7.93 (1H, dd, $J = 8$ Hz, 2Hz), 7.63-7.46 (3H, m), 3.46 (1H, s) ppm, (no OH peak was observed) ^{13}C NMR (101 MHz, CDCl_3) δ 191.5, 136.7, 134.0, 133.8, 129.4, 127.4, 125.6, 84.4, 79.3 ppm, m/z (EI^+) 130.0 $[\text{M}]^+$.¹⁷⁵

Preparation of 1-(2-ethynylphenyl)-3-(trimethylsilyl)prop-2-yn-1-ol, **9.7**



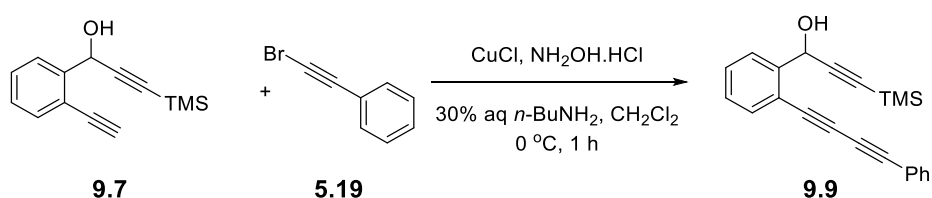
To a flame-dried 3-neck 100 mL flask, ethynyltrimethylsilane, **5.31**, (0.4 g, 4.5 mmol) and THF were added. The solution was then cooled to $-78\text{ }^\circ\text{C}$ and 2.5M $n\text{-BuLi}$ in hexanes (8 mL) was added and the mixture stirred for 30 min. 2-Ethynylbenzaldehyde, **9.6**, (0.4 g, 3 mmol) was dissolved in THF and this was added dropwise to the mixture. The temperature was allowed to increase to $0\text{ }^\circ\text{C}$ over 3 h. At $0\text{ }^\circ\text{C}$, acetic acid (1 mL) and THF (1 mL) were added. *sat* NaHCO_3 (10 mL) was added and the temperature of the solution was allowed to increase to room temperature. The organic layer was separated and the aqueous layer was extracted with Et_2O (3 x 15 mL). The organic extracts were combined, washed with brine and dried over Na_2SO_4 . The solution was then concentrated. The crude mixture was purified by column chromatography (hexane/ EtOAc , 15/1) to give 1-(2-ethynylphenyl)-3-(trimethylsilyl)prop-2-yn-1-ol, **9.7** as an orange oil (684 mg, 99%).¹⁷⁵ FTIR ν_{max} (neat) 3314 (C-H) 2969 (C-H) 2176 cm^{-1} (C≡C); ^1H NMR (400 MHz CDCl_3) δ 7.73 (1H, d, $J = 8$ Hz), 7.52 (1H, d, $J = 8$ Hz), 7.41 (1H, t, $J = 8$ Hz), 7.30 (1H, t, $J = 8$ Hz), 5.88 (1H, s), 3.36 (1H, s), 0.20 (9H, s) ppm, ^{13}C NMR (101 MHz, CDCl_3) δ 142.7, 133.3, 129.5, 128.4, 127.0, 120.7, 104.2, 91.8, 82.7, 81.1, 63.4, -0.1 ppm, m/z (ESI^+) 227.1 $[\text{M}-\text{H}]^+$.¹⁷⁵

Preparation of (bromoethynyl)benzene, **5.19**



N-Bromosuccinimide, **9.8** (4.9 g, 28 mmol), was dissolved in MeCN (45 mL). To this phenylacetylene, **5.33** (2.2 mL, 20 mmol), was added and the reaction stirred for 5 min. DBU (3.2 mL, 25 mmol) was then added and the reaction turned black. The reaction was stirred for a further 30 min. The mixture was then poured into water (250 mL) and extracted with DCM (3 x 100 mL). The combined extracts were washed with brine, dried over Na₂SO₄ and concentrated (in a fume hood). The crude product was purified by column chromatography (petroleum ether) to afford (bromoethynyl)benzene, **5.19** (2.8 g, 77%) as a pale yellow oil.¹⁷⁶ FTIR ν_{max} (neat) 3239 (C-H), 2281 (C≡C); ¹H NMR (400 MHz CDCl₃) δ 7.49-7.46 (2H, m), 7.38-7.30 (3 H, m) ppm, ¹³C NMR (101 MHz, CDCl₃) δ 132.1, 128.8, 128.4, 122.8, 80.2, 49.9 ppm, m/z (EI⁺) 181.0 [M]⁺.¹⁷⁶

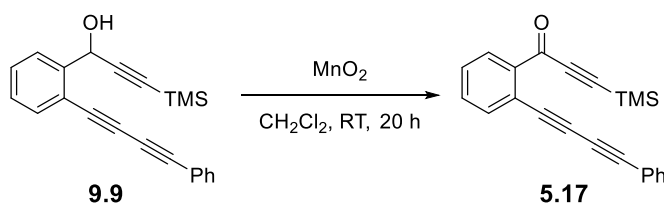
Preparation of 1-(2-(phenylbuta-1,3-diyne-1-yl)phenyl)-3-(trimethylsilyl)prop-2-yn-1-ol **9.9**



A 30% *n*-BuNH₂ solution in water (30 mL) was purged with argon for 20 min. CuCl (25 mg, 0.25 mmol) and NH₂OH.HCl (300 mg, 4 mmol) were added. The flask was evacuated and back filled with argon. A mixture of **9.7** (1.14g, 5 mmol) and **5.19** (1.35 g, 7.5 mmol) was dissolved in DCM (20 mL). This solution was then added dropwise. After addition, the reaction was left to stir at 0 °C for 1 h. Then *sat. aq.* NH₄Cl (30 mL) was added to the mixture. The organic layer was separated and aqueous layer extracted with DCM (3 x 20 mL). The extracts were combined, washed with brine, dried over Na₂SO₄ and concentrated. The crude product was purified by column chromatography to yield **9.9** as a black viscous oil (828 mg, 50%).¹⁴⁶ FTIR ν_{max} (neat) 3530 (O-H), 3148 (C-H ar), 2971

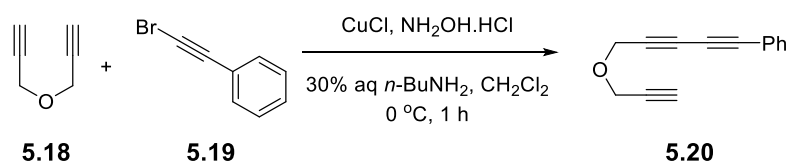
(C-H α), 2221 (C \equiv C), 2192 cm⁻¹ (C \equiv C); ¹H NMR (400 MHz CDCl₃) δ 7.73 (1H, d, J = 8Hz), 7.57-7.53 (3H, m), 7.44-7.29 (5H, m), 5.88 (1H, s), 0.22 (9H, s) ppm, ¹³C NMR (101 MHz, CDCl₃) δ 143.5, 133.7, 132.7, 132.6, 129.8, 129.4, 128.6, 128.6, 128.5, 127.1, 121.7, 120.5, 104.2, 91.9, 83.1, 79.2, 78.7, 73.8, 63.5, -0.1 ppm, m/z (EI⁺) 329.0 [M+2H]⁺ (When heated substrated **9.9** will undergo HDDA rearrangement through a radical pathway and it is expected that two hydrogen atoms are picked up from residual organics in the column).

Preparation of additive 1-(2-(phenylbuta-1,3-diyne-1-yl)phenyl)-3-(trimethylsilyl)prop-2-yn-1-one **5.17**



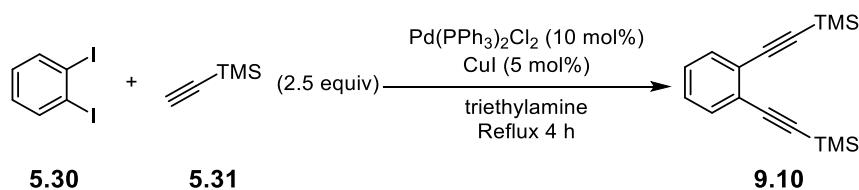
Compound **9.9** (750 mg, 2.2 mmol) was dissolved in DCM (15 mL). MnO₂ was then added and the reaction allowed to stir at room temperature for 20 h. The mixture was then filtered through a pad of celite and washed with DCM. The crude product was purified by column chromatography (hexane/EtOAc 20/1) to give **5.17** as a viscous brown oil (503 mg, 70%).¹⁴⁶ FTIR ν_{max} (neat) 3156 (C-H), 2970 (C-H), 2314 (C \equiv C), 2206 (C \equiv C), 1692 cm⁻¹ (C=O); ¹H NMR (400 MHz CDCl₃) δ 8.11 (1H, dd, J = 8 Hz, 1.2 Hz), 7.66 (1H, dd, J = 8Hz, 1.2 Hz), 7.67-7.51 (3H, m), 7.47 (1H, td, J = 8 Hz, 1.2 Hz), 7.38-7.34 (3H, m), 0.32 (9H,s) ppm, ¹³C NMR (101 MHz, CDCl₃) δ 176.6, 139.0, 135.7, 132.7, 132.7, 132.6, 131.9, 129.5, 128.8, 128.6, 121.9, 101.8, 101.5, 83.8, 80.1, 79.7, 74.5, -0.6 ppm, m/z (EI⁺) 328.0 [M+2H]⁺ (When heated substrated **5.17** will undergo HDDA rearrangement through a radical pathway and it is expected that two hydrogen atoms are picked up from residual organics in the column).

Preparation of (5-(prop-2-yn-1-yloxy)penta-1,3-diyne-1-yl)benzene **5.20**



A 30% *n*-BuNH₂ solution in water (30 mL) was purged with argon for 20 min. CuCl (25 mg, mmol) and NH₂OH.HCl (300 mg, 4 mmol) were added. The flask was evacuated and back filled with argon. A mixture of propargyl ether, **5.18** (0.2 g, 2 mmol) and 1-bromophenylacetylene, **5.20** (1.00 g, 5.5 mmol), was dissolved in DCM (20 mL). This solution was then added dropwise. After addition, the reaction was left to stir at 0 °C for 1 h. *Sat. aq.* NH₄Cl (30 mL) was then added to the mixture. The organic layer was separated and aqueous layer extracted with DCM (3 x 20 mL). The combined extracts were washed with brine and dried over Na₂SO₄, then concentrated. The crude product was purified by column chromatography (hexanes) to yield **5.20** as an orange oil (331 mg, 43%).¹⁴⁶ FTIR ν_{max} (neat) 3238 (C-H) 2974 (C-H), 2329 cm⁻¹ (C≡C); ¹H NMR (400 MHz CDCl₃) δ 7.54-7.41 (2H, m), 7.39-7.30 (3H, m), 4.42 (2H, s), 4.30 (2H, d, *J* = 2.4 Hz), 2.49 (1H, t, *J* = 2.4 Hz) ppm, ¹³C NMR (101 MHz, CDCl₃) δ 132.7, 129.5, 128.5, 121.4, 78.7, 78.4, 77.8, 75.4, 73.3, 71.6, 57.2, 56.7 ppm.¹⁴⁶

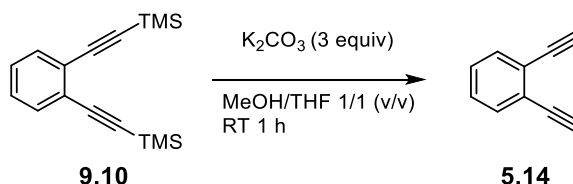
Preparation of 1,2-bis((trimethylsilyl)ethynyl) benzene, **9.10**



To a 100 mL round-bottomed flask 1,2-diodobenzene, **5.30** (2.5 g, 7.5 mmol), copper iodide (0.25 g, 1 mmol), bis(triphenylphosphine)palladium chloride (0.25 g, 3.8 mmol) and triethylamine (50 mL) was added. This solution was purged with argon for 20 min. Ethynyltrimethylsilane, **5.31**, (1.7 g, 18 mmol) was then added to the reaction mixture and this was heated to reflux for 4 h. After cooling to room temperature, the ammonium salts were removed by filtration and washed with Et₂O. The resulting solution was concentrated then purified by column chromatography (hexane/EtOAc 9/1) to produce 1,2-bis((trimethylsilyl)ethynyl) benzene, **9.10** as a yellow oil (2.02 g, 94%).¹⁷⁷ FTIR ν_{max}

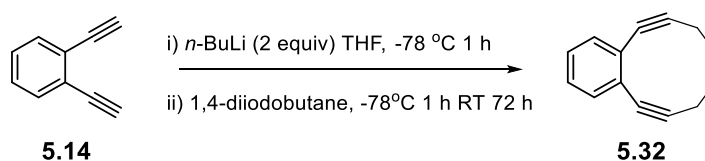
(neat) 3026 (C-H) 2964 (C-H) 2253 cm^{-1} ($\text{C}\equiv\text{C}$); ^1H NMR (400 MHz CDCl_3) δ 7.48-7.44 (2H, m), 7.25-7.21 (2H, m), 0.28 (18H, s) ppm, ^{13}C NMR (101 MHz, CDCl_3) δ 132.4, 128.2, 125.9, 103.4, 98.6, 0.2 ppm, m/z (EI^+) 293.1 $[\text{M}+\text{Na}]^+$.¹⁷⁷

Preparation of 1,2-diethynylbenzene, **5.14**.



1,2-Bis((trimethylsilyl)ethynyl) benzene, **9.10**, (1.5 g, 5.5 mmol) and potassium carbonate (2.3 g, 16.5 mmol) was added to 250 mL three-neck flask. A 1/1 mixture of methanol and DCM (80 mL) was added to the flask and the mixture stirred for 4 h. The reaction was quenched with sat. aq. NH_4Cl and extracted with DCM (3 x 30 mL). The combined extracts were washed with brine, dried over Na_2SO_4 and concentrated. The crude product was purified by column chromatography (hexane/ EtOAc 9/1) to afford 1,2-diethynylbenzene **5.14** as a dark orange oil (447 mg, 71%).¹⁷⁷ FTIR ν_{max} (neat) 3282 (C-H) 3059 (C-H) 2107 cm^{-1} ($\text{C}\equiv\text{C}$); ^1H NMR (400 MHz CDCl_3) δ 7.54-7.49 (2H, m), 7.32-7.27 (2H, m), 3.35 (2H, s) ppm, ^{13}C NMR (101 MHz, CDCl_3) δ 132.7, 128.6, 125.1, 81.9, 81.3 ppm, m/z (EI^+) 149.0 $[\text{M}+\text{Na}]^+$.¹⁷⁷

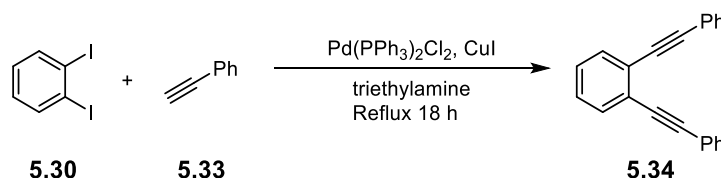
Preparation of benzo[3,4]-cyclodec-3-ene-1,5-diyne, **5.32**



1,2-Diethynylbenzene, **5.14** (228 mg, 1.8 mmol) was dissolved in THF (43 mL) and cooled to -78°C . $n\text{-BuLi}$ (1.5 mL, 2.5 M in hexanes) was then added and the mixture stirred for 1 h. 1,4-Diiodobutane (560 mg, 1.8 mmol) was then added and the reaction continued at -78°C for 1 h then 72 h at room temperature. The reaction mixture was quenched with sat. aq. NH_4Cl and extracted with DCM (3 x 30 mL). The combined extracts were washed with brine and dried over Na_2SO_4 then concentrated. The crude product was purified by column chromatography (hexane/DCM 5/1) to afford benzo[3,4]-cyclodec-3-ene-1,5-diyne, **5.32** as a pale yellow oil (122 mg, 38%).¹⁴⁷ FTIR ν_{max} (neat) 3057 (C-H),

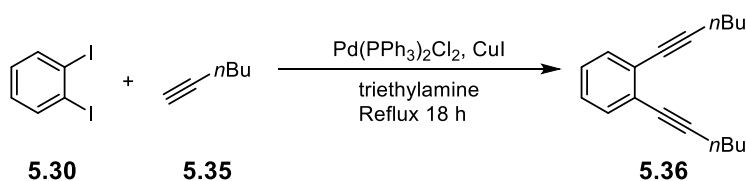
2929 (C-H), 2858 (C-H), 2226 cm^{-1} ($\text{C}\equiv\text{C}$); ^1H NMR (400 MHz CDCl_3) δ 7.32-7.28 (m, 2H), 7.21-7.18 (m, 2H), 2.47-2.44 (m, 4H), 1.98-1.95 (m, 4H) ppm, ^{13}C NMR (101 MHz, CDCl_3) δ 129.7, 128.3, 127.4, 100.1, 82.4, 28.8, 21.6 ppm, m/z (EI^+) 181.1 $[\text{M}+\text{H}]^+$.¹⁴⁷

Preparation of 1,2-bis(phenylethynyl)benzene, **5.34**



To a 100 mL round-bottomed flask, 1,2-diiodobenzene, **5.30** (1.5 g, 4.5 mmol), copper iodide (193 mg, 1 mmol) and bistrisphenylphosphinepalladium (II) chloride (352 mg, 0.5 mmol) was added with triethylamine (40 mL). The reaction mixture was purged with argon for 20 min. Phenylacetylene, **5.33** (1.02 g, 10 mmol), was added and the reaction heated to reflux for 18 h. After cooling to room temperature, the reaction mixture was filtered through celite and washed with NH_4Cl *sat aq*. The organic phase was extracted with DCM (3 x 50 mL). The combined extracts were washed with brine and dried over Na_2SO_4 and then concentrated. The crude product was purified by column chromatography (hexanes) to give 1,2-bis(phenylethynyl)benzene, **5.34** as an orange oil (0.798 g, 64%).¹⁴⁸ ^1H NMR (400 MHz CDCl_3) δ 7.60-7.57 (6H, m), 7.37-7.31 (8H, m) ppm, ^{13}C NMR (101 MHz, CDCl_3) δ 131.9, 131.8, 128.6, 128.5, 128.1, 126.0, 123.5, 93.8, 88.5 ppm, m/z (EI^+) 278.1 $[\text{M}]^+$.¹⁴⁸

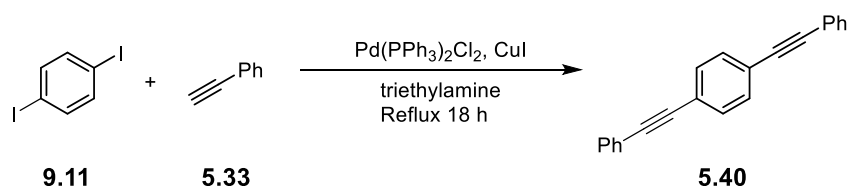
Preparation of 1,2-di(hex-1-yn-1-yl)benzene, **5.36**



To a 100 mL round-bottomed flask, 1,2-diiodobenzene, **5.30** (1.5 g, 4.5 mmol), copper iodide (193 mg, 1 mmol) and bistrisphenylphosphinepalladium (II) chloride (352 mg, 0.5 mmol) was added with triethylamine (40 mL). The reaction mixture was purged with argon for 20 min. Hex-1-yne, **5.35** (0.82 g, 10 mmol), was added and the reaction heated to reflux for 18 h. After cooling to room temperature, the reaction mixture was filtered through celite and washed with NH_4Cl *sat aq*. The organic phase was extracted with DCM

(3 x 50 mL). The combined extracts were washed with brine and dried over Na₂SO₄ and then concentrated. The crude product was purified by column chromatography (hexanes) to give 1,2-di(hex-1-yn-1-yl)benzene, **5.36** as an orange oil (136 mg, 13%). ¹H NMR (400 MHz CDCl₃) δ 7.39-7.36 (2H, m), 7.19-7.16 (2H, m), 2.50 (4H, t, *J* = 6.8 Hz), 1.67-1.49 (8H, m), 0.98 (6H, t, *J* = 7.2 Hz) ppm, ¹³C NMR (101 MHz, CDCl₃) δ 131.9, 127.2, 126.5, 94.2, 79.7, 31.0, 22.1, 19.5, 13.8 ppm, *m/z* (EI⁺) 238.2 [M]⁺.

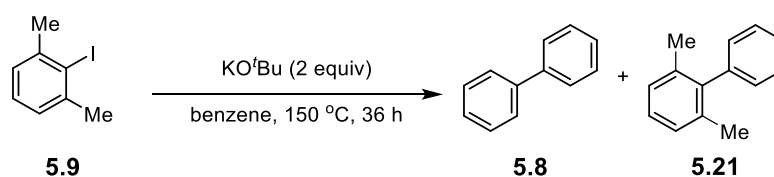
Preparation of 1,4-bis(phenylethynyl)benzene, **5.40**



To a 100 mL round-bottomed flask 1,4-diiodobenzene, **9.11** (0.5 g, 1.5 mmol), copper iodide (65 mg, 0.3 mmol) and bistriphenylphosphinepalladium (II) chloride (120 mg, 0.17 mmol) were added to triethylamine (20 mL). The reaction mixture was purged with argon for 20 min. Phenylacetylene, **5.33** (0.34 g, 3.3 mmol), was added and the reaction heated to reflux for 18 h. After cooling to room temperature the reaction mixture was filtered through celite and washed with NH₄Cl *sat aq*. The organic phase was extracted with DCM (3 x 25 mL). The combined extracts were washed with brine, dried over Na₂SO₄ and then concentrated. The crude product was purified by column chromatography (hexanes) to give 1,4-bis(phenylethynyl)benzene, **5.40** as an orange oil (0.1 g, 8%). ¹H NMR (400 MHz CDCl₃) δ 7.55-7.53 (4H, m), 7.51 (4H, s), 7.37-7.32 (6H, m) ppm, ¹³C NMR (101 MHz, CDCl₃) δ 133.8, 131.7, 128.8, 128.6, 128.5, 123.3, 91.4, 89.3 ppm, *m/z* (EI⁺) 278.1[M]⁺.¹⁷⁸

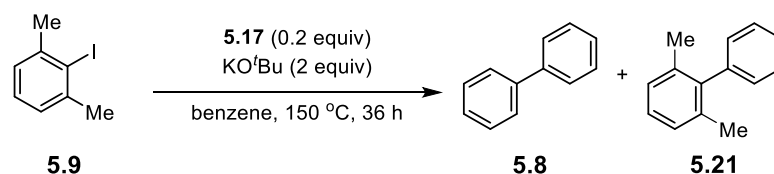
Coupling reaction between 2-iodo-*m*-xylene and benzene with *o*-benzyne precursors

Table 5.1 entry 1



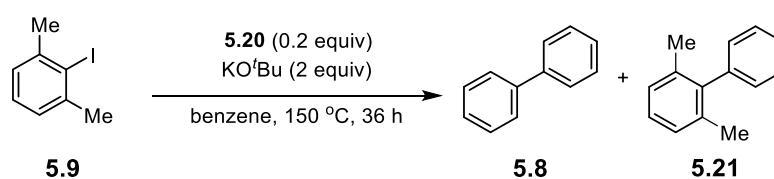
To an oven-dried pressure tube, 2-iodo-*m*-xylene, **5.9** (116 mg, 0.5 mmol) was added. Under an inert atmosphere, KO^tBu (112 mg, 1 mmol) and benzene (5 mL) were added and the tube sealed. The sealed tube was placed in a pre-heated oil bath at 150 °C for 36 h. After cooling to room temperature, the reaction was quenched with 1M HCl_(aq) (20 mL) and extracted with Et₂O (3 x 20 mL). The combined extracts were washed with brine, dried over Na₂SO₄ and concentrated. To determine the yield, 1,3,5-trimethoxybenzene (8.4 mg, 0.05 mmol) was added to the crude product as an internal standard. The yields were calculated as biphenyl **5.8** (1%) and 2,6-dimethylbiphenyl **5.21** (<1%) identifying the products by their characteristic peaks at δ 7.6 (biphenyl 4H) and δ 2.1 (methyl 6H) respectively.

Table 5.1 entry 2



To an oven-dried pressure tube, 2-iodo-*m*-xylene, **5.9** (116 mg, 0.5 mmol), and **5.17** (33 mg, 0.1 mmol) were added. Under an inert atmosphere, KO^tBu (112 mg, 1 mmol) and benzene (5 mL) were added and the tube sealed. The sealed tube was placed in a pre-heated oil bath at 150 °C for 36 h. After cooling to room temperature, the reaction was quenched with 1M HCl_(aq) (20 mL) and extracted with Et₂O (3 x 20 mL). The combined extracts were washed with brine, dried over Na₂SO₄ and concentrated. To determine the yield, 1,3,5-trimethoxybenzene (8.4 mg, 0.05 mmol) was added to the crude product as an internal standard. The yields were calculated as biphenyl **5.8** (9%) and 2,6-dimethylbiphenyl **5.21** (3%) identifying the products by their characteristic peaks at δ 7.6 (biphenyl 4H) and δ 2.1 (methyl 6H) respectively.

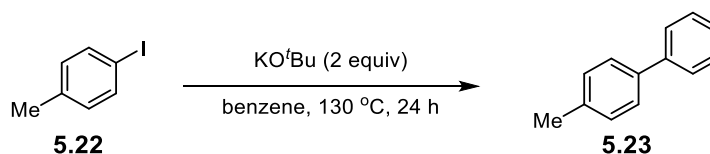
Table 5.1 entry 3



To an oven-dried pressure tube, 2-iodo-*m*-xylene, **5.9** (116 mg, 0.5 mmol), and **5.20** (19 mg, 0.1 mmol) were added. Under an inert atmosphere, KO^tBu (112 mg, 1 mmol) and benzene (5 mL) were added and the tube sealed. The sealed tube was placed in a pre-heated oil bath at 150 °C for 36 h. After cooling to room temperature, the reaction was quenched with 1M HCl_(aq) (20 mL) and extracted with Et₂O (3 x 20 mL). The combined extracts were washed with brine, dried over Na₂SO₄ and concentrated. To determine the yield, 1,3,5-trimethoxybenzene (8.4 mg, 0.05 mmol) was added to the crude product as an internal standard. The yields were calculated as biphenyl **5.8** (29%) and 2,6-dimethylbiphenyl **5.21** (7%) identifying the products by their characteristic peaks at δ 7.6 (biphenyl 4H) and δ 2.1 (methyl 6H) respectively.

Coupling reaction between 4-iodotoluene and benzene with *o*-benzyne precursors

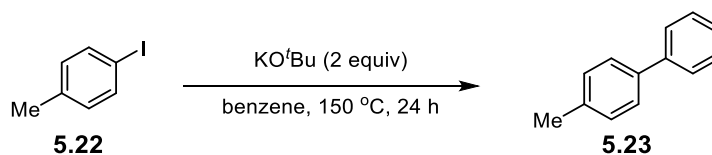
Table 5.2 entry 1a



To an oven-dried pressure tube, 4-iodotoluene, **5.22** (114 mg, 0.5 mmol) was added. Under an inert atmosphere, KO^tBu (112 mg, 1 mmol) and benzene (5 mL) were added and the tube sealed. The sealed tube was placed in a pre-heated oil bath at 130 °C for 24 h. After cooling to room temperature, the reaction was quenched with 1M HCl_(aq) (20 mL) and extracted with Et₂O (3 x 20 mL). The combined extracts were washed with brine, dried over Na₂SO₄ and concentrated. The crude product was purified by column chromatography (hexane) to afford 4-methylbiphenyl **5.23** as a colourless oil (17 mg, 20%).¹⁰⁵ ¹H NMR (400 MHz, CDCl₃) δ 7.63 (2H, d, *J* = 8 Hz), (2H, d, *J* = 8 Hz), (2H, t, *J* = 8 Hz), (1H, t, *J* = 8 Hz), (2H, d, *J* = 8 Hz), 2.44 (3H, s) ppm, ¹³C NMR (101 MHz, CDCl₃)* δ 141.3, 138.5, 137.1, 129.6, 128.8, 127.1, 127.07, 21.2 ppm, *m/z* (EI⁺) 168.1 [M]⁺.

*Remaining sp² carbon is not observed consistent with literature.¹⁰⁵

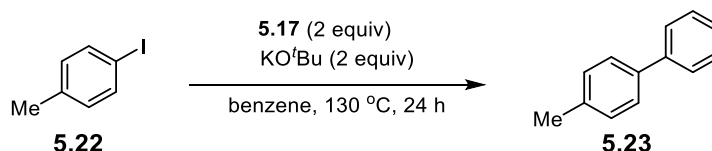
Table 5.2 entry 1b



To an oven-dried pressure tube, 4-iodotoluene, **5.22** (114 mg, 0.5 mmol) was added. Under an inert atmosphere, KO^tBu (112 mg, 1 mmol) and benzene (5 mL) were added and the tube sealed. The sealed tube was placed in a pre-heated oil bath at 150 °C for 24 h. After cooling to room temperature, the reaction was quenched with 1M HCl_(aq) (20 mL) and extracted with Et₂O (3 x 20 mL). The combined extracts were washed with brine, dried over Na₂SO₄ and concentrated. The crude product was purified by column chromatography (hexane) to afford 4-methylbiphenyl **5.23** as a colourless oil (31 mg, 37%).¹⁰⁵ ¹H NMR (400 MHz, CDCl₃) δ 7.63 (2H, d, *J* = 8 Hz), (2H, d, *J* = 8 Hz), (2H, t, *J* = 8 Hz), (1H, t, *J* = 8 Hz), (2H, d, *J* = 8 Hz), 2.44 (3H,s) ppm,, ¹³C NMR (101 MHz, CDCl₃)* δ 141.3, 138.5, 137.1, 129.6, 128.8, 127.1, 127.07, 21.2 ppm, *m/z* (EI⁺) 168.1 [M]⁺.

*Remaining sp² carbon is not observed consistent with literature.¹⁰⁵

Table 5.2 entry 2

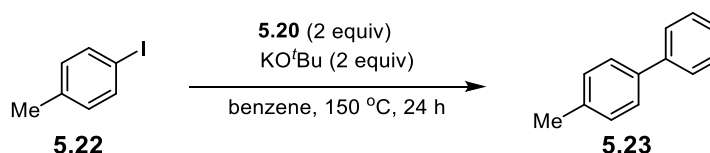


To an oven-dried pressure tube, 4-iodotoluene, **5.22** (114 mg, 0.5 mmol), and **5.17** (33 mg, 0.1 mmol) were added. Under an inert atmosphere, KO^tBu (112 mg, 1 mmol) and benzene (5 mL) were added and the tube sealed. The sealed tube was placed in a pre-heated oil bath at 150 °C for 24 h. After cooling to room temperature, the reaction was quenched with 1M HCl_(aq) (20 mL) and extracted with Et₂O (3 x 20 mL). The combined extracts were washed with brine, dried over Na₂SO₄ and concentrated. The crude product was purified by column chromatography (hexane) to afford 4-methylbiphenyl **5.23** as a colourless oil (35 mg, 42%).¹⁰⁵ ¹H NMR (400 MHz, CDCl₃) δ 7.63 (2H, d, *J* = 8 Hz), (2H, d, *J* = 8 Hz), (2H, t, *J* = 8 Hz), (1H, t, *J* = 8 Hz), (2H, d, *J* = 8 Hz), 2.44 (3H,s) ppm, ¹³C

NMR (101 MHz, CDCl₃)* δ 141.3, 138.5, 137.1, 129.6, 128.8, 127.1, 127.07, 21.2 ppm, *m/z* (EI⁺) 168.1 [M]⁺.

*Remaining sp² carbon is not observed consistent with literature.¹⁰⁵

Table 5.2 entry 3

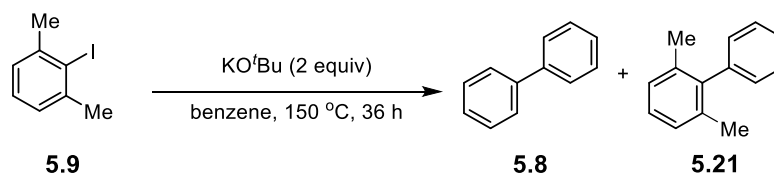


To an oven-dried pressure tube, 4-iodotoluene, **5.22** (114 mg, 0.5 mmol), and **5.20** (19 mg, 0.1 mmol) were added. Under an inert atmosphere, KO^tBu (112 mg, 1 mmol) and benzene (5 mL) were added and the tube sealed. The sealed tube was placed in a pre-heated oil bath at 150 °C for 24 h. After cooling to room temperature, the reaction was quenched with 1M HCl_(aq) (20 mL) and extracted with Et₂O (3 x 20 mL). The combined extracts were washed with brine, dried over Na₂SO₄ and concentrated. The crude product was purified by column chromatography (hexane) to afford 4-methylbiphenyl **5.23** as a colourless oil (51 mg, 61%).¹⁰⁵ ¹H NMR (400 MHz, CDCl₃) δ 7.63 (2H, d, *J* = 8 Hz), (2H, d, *J* = 8 Hz), (2H, t, *J* = 8 Hz), (1H, t, *J* = 8 Hz), (2H, d, *J* = 8 Hz), 2.44 (3H, s) ppm, ¹³C NMR (101 MHz, CDCl₃)* δ 141.3, 138.5, 137.1, 129.6, 128.8, 127.1, 127.07, 21.2 ppm, *m/z* (EI⁺) 168.1 [M]⁺.

*Remaining sp² carbon is not observed consistent with literature.¹⁰⁵

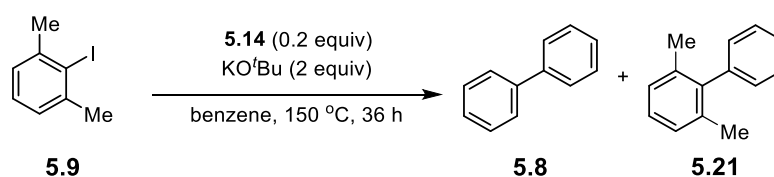
Coupling reaction between 2-iodo-*m*-xylene and benzene with *p*-benzyne precursors

Table 5.3 entry 1



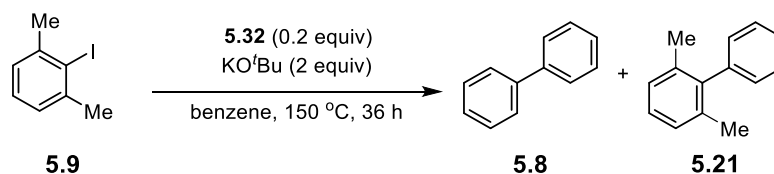
To an oven-dried pressure tube, 2-iodo-*m*-xylene, **5.9** (116 mg, 0.5 mmol) was added. Under an inert atmosphere, KO^tBu (112 mg, 1 mmol) and benzene (5 mL) were added and the tube sealed. The sealed tube was placed in a pre-heated oil bath at 150 °C for 36 h. After cooling to room temperature, the reaction was quenched with 1M HCl_(aq) (20 mL) and extracted with Et₂O (3 x 20 mL). The combined extracts were washed with brine, dried over Na₂SO₄ and concentrated. To determine the yield 1,3,5-trimethoxybenzene (8.4 mg, 0.05 mmol) was added to the crude product as an internal standard. The yields were calculated as biphenyl **5.8** (1%) and 2,6-dimethylbiphenyl **5.21** (<1%) identifying the products by their characteristic peaks at δ 7.6 (biphenyl 4H) and δ 2.1 (methyl 6H) respectively.

Table 5.3 entry 2



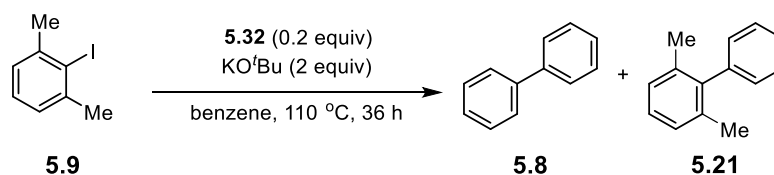
To an oven-dried pressure tube, 2-iodo-*m*-xylene, **5.9** (116 mg, 0.5 mmol), and **5.14** (13 mg, 0.1 mmol) were added. Under an inert atmosphere, KO^tBu (112 mg, 1 mmol) and benzene (5 mL) were added and the tube sealed. The sealed tube was placed in a pre-heated oil bath at 150 °C for 36 h. After cooling to room temperature, the reaction was quenched with 1M HCl_(aq) (20 mL) and extracted with Et₂O (3 x 20 mL). The combined extracts were washed with brine, dried over Na₂SO₄ and concentrated. To determine the yield 1,3,5-trimethoxybenzene (8.4 mg, 0.05 mmol) was added to the crude product as an internal standard. The yields were calculated as biphenyl **5.8** (13%) and 2,6-dimethylbiphenyl **5.21** (4%) identifying the products by their characteristic peaks at δ 7.6 (biphenyl 4H) and δ 2.1 (methyl 6H) respectively.

Table 5.3 entry 3



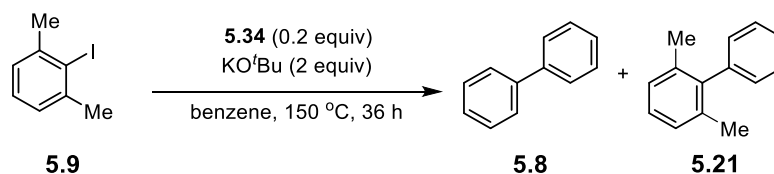
To an oven-dried pressure, tube 2-iodo-*m*-xylene, **5.9** (116 mg, 0.5 mmol), and **5.32** (18 mg, 0.1 mmol) were added. Under an inert atmosphere, KO^tBu (112 mg, 1 mmol) and benzene (5 mL) were added and the tube sealed. The sealed tube was placed in a pre-heated oil bath at 150 °C for 36 h. After cooling to room temperature, the reaction was quenched with 1M HCl_(aq) (20 mL) and extracted with Et₂O (3 x 20 mL). The combined extracts were washed with brine, dried over Na₂SO₄ and concentrated. To determine the yield 1,3,5-trimethoxybenzene (8.4 mg, 0.05 mmol) was added to the crude product as an internal standard. The yields were calculated as biphenyl **5.8** (26%) and 2,6-dimethylbiphenyl **5.21** (6%) identifying the products by their characteristic peaks at δ 7.6 (biphenyl 4H) and δ 2.1 (methyl 6H) respectively.

Table 5.3 entry 4



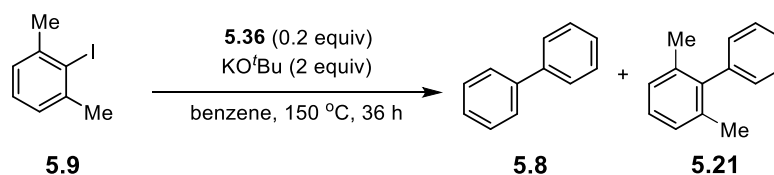
To an oven-dried pressure tube, 2-iodo-*m*-xylene, **5.9** (116 mg, 0.5 mmol), and **5.32** (18 mg, 0.1 mmol) were added. Under an inert atmosphere, KO^tBu (112 mg, 1 mmol) and benzene (5 mL) were added and the tube sealed. The sealed tube was placed in a pre-heated oil bath at 110 °C for 36 h. After cooling to room temperature, the reaction was quenched with 1M HCl_(aq) (20 mL) and extracted with Et₂O (3 x 20 mL). The combined extracts were washed with brine, dried over Na₂SO₄ and concentrated. To determine the yield 1,3,5-trimethoxybenzene (8.4 mg, 0.05 mmol) was added to the crude product as an internal standard. The yields were calculated as biphenyl **5.8** (12%) and 2,6-dimethylbiphenyl **5.21** (2%) identifying the products by their characteristic peaks at δ 7.6 (biphenyl 4H) and δ 2.1 (methyl 6H) respectively.

Table 5.3 entry 5



To an oven-dried pressure tube, 2-iodo-*m*-xylene, **5.9** (116 mg, 0.5 mmol), and **5.20** (29 mg, 0.1 mmol) were added. Under an inert atmosphere, KO^tBu (112 mg, 1 mmol) and benzene (5 mL) were added and the tube sealed. The sealed tube was placed in a pre-heated oil bath at 150 °C for 36 h. After cooling to room temperature, the reaction was quenched with 1M HCl_(aq) (20 mL) and extracted with Et₂O (3 x 20 mL). The combined extracts were washed with brine, dried over Na₂SO₄ and concentrated. To determine the yield 1,3,5-trimethoxybenzene (8.4 mg, 0.05 mmol) was added to the crude product as an internal standard. The yields were calculated as biphenyl **5.8** (11%) and 2,6-dimethylbiphenyl **5.21** (3%) identifying the products by their characteristic peaks at δ 7.6 (biphenyl 4H) and δ 2.1 (methyl 6H) respectively.

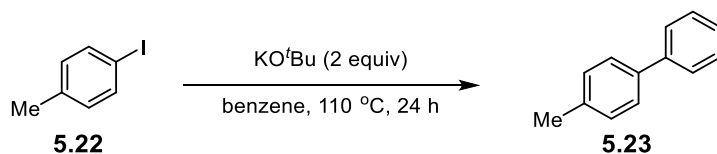
Table 5.3 entry 6



To an oven-dried pressure tube, 2-iodo-*m*-xylene, **5.9** (116 mg, 0.5 mmol), and **5.36** (24 mg, 0.1 mmol) were added. Under an inert atmosphere, KO^tBu (112 mg, 1 mmol) and benzene (5 mL) were added and the tube sealed. The sealed tube was placed in a pre-heated oil bath at 150 °C for 36 h. After cooling to room temperature, the reaction was quenched with 1M HCl_(aq) (20 mL) and extracted with Et₂O (3 x 20 mL). The combined extracts were washed with brine, dried over Na₂SO₄ and concentrated. To determine the yield 1,3,5-trimethoxybenzene (8.4 mg, 0.05 mmol) was added to the crude product as an internal standard. The yields were calculated as biphenyl **5.8** (30%) and 2,6-dimethylbiphenyl **5.21** (8%) identifying the products by their characteristic peaks at δ 7.6 (biphenyl 4H) and δ 2.1 (methyl 6H) respectively.

Coupling reaction between 4-iodotoluene and benzene with *o*-benzyne precursors

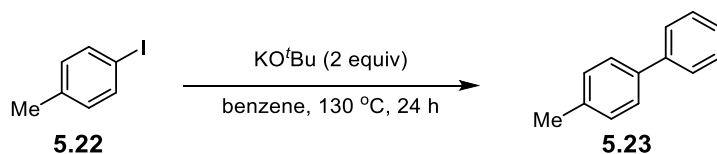
Table 5.4 entry 1a



To an oven-dried pressure tube, 4-iodotoluene, **5.22** (114 mg, 0.5 mmol) was added. Under an inert atmosphere, KO^tBu (112 mg, 1 mmol) and benzene (5 mL) were added and the tube sealed. The sealed tube was placed in a pre-heated oil bath at 150 °C for 24 h. After cooling to room temperature, the reaction was quenched with 1M HCl_(aq) (20 mL) and extracted with Et₂O (3 x 20 mL). The combined extracts were washed with brine, dried over Na₂SO₄ and concentrated. The crude product was purified by column chromatography (hexane) to afford 4-methylbiphenyl **5.23** as a colourless oil (4 mg, 5%).¹⁰⁵ ¹H NMR (400 MHz, CDCl₃) δ 7.63 (2H, d, *J* = 8 Hz), (2H, d, *J* = 8 Hz), (2H, t, *J* = 8 Hz), (1H, t, *J* = 8 Hz), (2H, d, *J* = 8 Hz), 2.44 (3H,s) ppm, ¹³C NMR (101 MHz, CDCl₃)* δ 141.3, 138.5, 137.1, 129.6, 128.8, 127.1, 127.07, 21.2 ppm, *m/z* (EI⁺) 168.1 [M]⁺.

*Remaining sp² carbon is not observed consistent with literature.¹⁰⁵

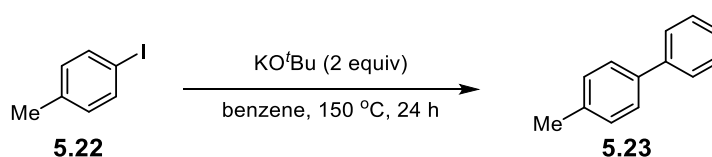
Table 5.4 entry 1b



To an oven-dried pressure tube, 4-iodotoluene, **5.22** (114 mg, 0.5 mmol) was added. Under an inert atmosphere, KO^tBu (112 mg, 1 mmol) and benzene (5 mL) were added and the tube sealed. The sealed tube was placed in a pre-heated oil bath at 150 °C for 24 h. After cooling to room temperature, the reaction was quenched with 1M HCl_(aq) (20 mL) and extracted with Et₂O (3 x 20 mL). The combined extracts were washed with brine, dried over Na₂SO₄ and concentrated. The crude product was purified by column chromatography (hexane) to afford 4-methylbiphenyl **5.23** as a colourless oil (17 mg, 20%).¹⁰⁵ ¹H NMR (400 MHz, CDCl₃) δ 7.63 (2H, d, *J* = 8 Hz), (2H, d, *J* = 8 Hz), (2H, t, *J* = 8 Hz), (1H, t, *J* = 8 Hz), (2H, d, *J* = 8 Hz), 2.44 (3H,s) ppm, ¹³C NMR (101 MHz, CDCl₃)* δ 141.3, 138.5, 137.1, 129.6, 128.8, 127.1, 127.07, 21.2 ppm, *m/z* (EI⁺) 168.1 [M]⁺.

*Remaining sp² carbon is not observed consistent with literature.¹⁰⁵

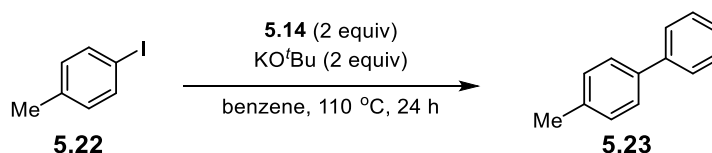
Table 5.4 entry 1c



To an oven-dried pressure tube, 4-iodotoluene, **5.22** (114 mg, 0.5 mmol) was added. Under an inert atmosphere, KO^tBu (112 mg, 1 mmol) and benzene (5 mL) were added and the tube sealed. The sealed tube was placed in a pre-heated oil bath at 150 °C for 24 h. After cooling to room temperature, the reaction was quenched with 1M HCl_(aq) (20 mL) and extracted with Et₂O (3 x 20 mL). The combined extracts were washed with brine, dried over Na₂SO₄ and concentrated. The crude product was purified by column chromatography (hexane) to afford 4-methylbiphenyl **5.23** as a colourless oil (31 mg, 37%).¹⁰⁵ ¹H NMR (400 MHz, CDCl₃) δ 7.63 (2H, d, *J* = 8 Hz), (2H, d, *J* = 8 Hz), (2H, t, *J* = 8 Hz), (1H, t, *J* = 8 Hz), (2H, d, *J* = 8 Hz), 2.44 (3H, s) ppm, ¹³C NMR (101 MHz, CDCl₃)* δ 141.3, 138.5, 137.1, 129.6, 128.8, 127.1, 127.07, 21.2 ppm, *m/z* (EI⁺) 168.1 [M]⁺.

*Remaining sp² carbon is not observed consistent with literature.¹⁰⁵

Table 5.4 entry 2a

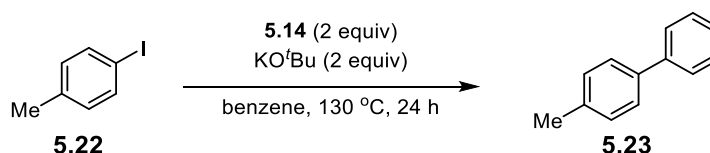


To an oven-dried pressure tube, 4-iodotoluene, **5.22** (114 mg, 0.5 mmol), and **5.14** (13 mg, 0.1 mmol) were added. Under an inert atmosphere, KO^tBu (112 mg, 1 mmol) and benzene (5 mL) were added and the tube sealed. The sealed tube was placed in a pre-heated oil bath at 150 °C for 24 h. After cooling to room temperature, the reaction was quenched with 1M HCl_(aq) (20 mL) and extracted with Et₂O (3 x 20 mL). The combined extracts were washed with brine, dried over Na₂SO₄ and concentrated. The crude product was purified by column chromatography (hexane) to afford 4-methylbiphenyl **5.23** as a colourless oil (29 mg, 34%).¹⁰⁵ ¹H NMR (400 MHz, CDCl₃) δ 7.63 (2H, d, *J* = 8 Hz), (2H, d, *J* = 8 Hz), (2H, t, *J* = 8 Hz), (1H, t, *J* = 8 Hz), (2H, d, *J* = 8 Hz), 2.44 (3H, s) ppm, ¹³C

NMR (101 MHz, CDCl₃)* δ 141.3, 138.5, 137.1, 129.6, 128.8, 127.1, 127.07, 21.2 ppm, m/z (EI⁺) 168.1 [M]⁺.

*Remaining sp² carbon is not observed consistent with literature.¹⁰⁵

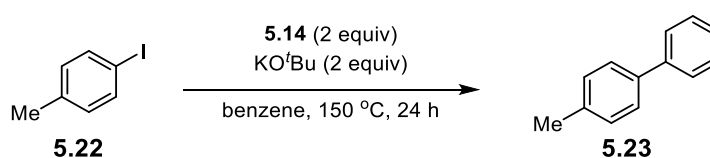
Table 5.4 entry 2b



To an oven-dried pressure tube, 4-iodotoluene, **5.22** (114 mg, 0.5 mmol), and **5.14** (13 mg, 0.1 mmol) were added. Under an inert atmosphere, KO^tBu (112 mg, 1 mmol) and benzene (5 mL) were added and the tube sealed. The sealed tube was placed in a pre-heated oil bath at 150 °C for 24 h. After cooling to room temperature, the reaction was quenched with 1M HCl_(aq) (20 mL) and extracted with Et₂O (3 x 20 mL). The combined extracts were washed with brine, dried over Na₂SO₄ and concentrated. The crude product was purified by column chromatography (hexane) to afford 4-methylbiphenyl **5.23** as a colourless oil (34 mg, 41%).¹⁰⁵ ¹H NMR (400 MHz, CDCl₃) δ 7.63 (2H, d, J = 8 Hz), (2H, d, J = 8 Hz), (2H, t, J = 8 Hz), (1H, t, J = 8 Hz), (2H, d, J = 8 Hz), 2.44 (3H, s) ppm, ¹³C NMR (101 MHz, CDCl₃)* δ 141.3, 138.5, 137.1, 129.6, 128.8, 127.1, 127.07, 21.2 ppm, m/z (EI⁺) 168.1 [M]⁺.

*Remaining sp² carbon is not observed consistent with literature.¹⁰⁵

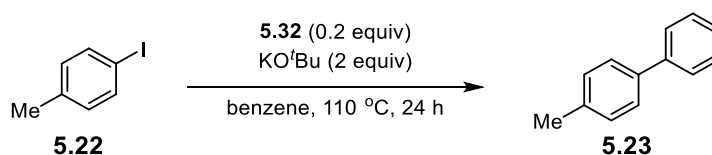
Table 5.4 entry 2c



To an oven-dried pressure tube, 4-iodotoluene, **5.22** (114 mg, 0.5 mmol), and **5.14** (13 mg, 0.1 mmol) were added. Under an inert atmosphere, KO^tBu (112 mg, 1 mmol) and benzene (5 mL) were added and the tube sealed. The sealed tube was placed in a pre-heated oil bath at 150 °C for 24 h. After cooling to room temperature, the reaction was quenched with 1M HCl_(aq) (20 mL) and extracted with Et₂O (3 x 20 mL). The combined extracts were washed with brine, dried over Na₂SO₄ and concentrated. The crude product was purified by column chromatography (hexane) to afford 4-methylbiphenyl **5.23** as a colourless oil (57 mg, 68%).¹⁰⁵ ¹H NMR (400 MHz, CDCl₃) δ 7.63 (2H, d, *J* = 8 Hz), (2H, d, *J* = 8 Hz), (2H, t, *J* = 8 Hz), (1H, t, *J* = 8 Hz), (2H, d, *J* = 8 Hz), 2.44 (3H, s) ppm, ¹³C NMR (101 MHz, CDCl₃)* δ 141.3, 138.5, 137.1, 129.6, 128.8, 127.1, 127.07, 21.2 ppm, *m/z* (EI⁺) 168.1 [M]⁺.

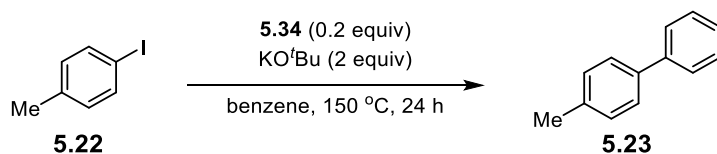
*Remaining sp² carbon is not observed consistent with literature.¹⁰⁵

Table 5.4 entry 3



To an oven-dried pressure tube, 4-iodotoluene, **5.22** (114 mg, 0.5 mmol), and **5.32** (18 mg, 0.1 mmol) were added. Under an inert atmosphere, KO^tBu (112 mg, 1 mmol) and benzene (5 mL) were added and the tube sealed. The sealed tube was placed in a pre-heated oil bath at 150 °C for 24 h. After cooling to room temperature, the reaction was quenched with 1M HCl_(aq) (20 mL) and extracted with Et₂O (3 x 20 mL). The combined extracts were washed with brine, dried over Na₂SO₄ and concentrated. The crude product was purified by column chromatography (hexane) to afford 4-methylbiphenyl **5.23** as a colourless oil (27 mg, 33%).¹⁰⁵ ¹H NMR (400 MHz, CDCl₃) δ 7.63 (2H, d, *J* = 8 Hz), (2H, d, *J* = 8 Hz), (2H, t, *J* = 8 Hz), (1H, t, *J* = 8 Hz), (2H, d, *J* = 8 Hz), 2.44 (3H, s) ppm, ¹³C NMR (101 MHz, CDCl₃) δ 141.3, 138.5, 137.1, 129.6, 128.8, 127.1, 127.07, 21.2 ppm, *m/z* (EI⁺) 168.1 [M]⁺.

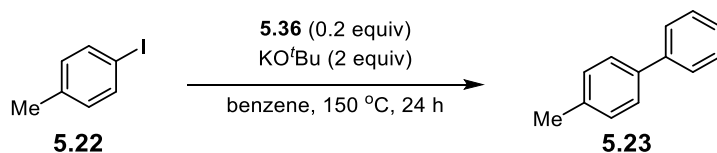
Table 5.4 entry 4



To an oven-dried pressure tube, 4-iodotoluene, **5.22** (114 mg, 0.5 mmol), and **5.34** (28 mg, 0.1 mmol) were added. Under an inert atmosphere, KO^tBu (112 mg, 1 mmol) and benzene (5 mL) were added and the tube sealed. The sealed tube was placed in a pre-heated oil bath at 150 °C for 24 h. After cooling to room temperature, the reaction was quenched with 1M HCl_(aq) (20 mL) and extracted with Et₂O (3 x 20 mL). The combined extracts were washed with brine, dried over Na₂SO₄ and concentrated. The crude product was purified by column chromatography (hexane) to afford 4-methylbiphenyl **5.23** as a colourless oil (14 mg, 17%).¹⁰⁵ ¹H NMR (400 MHz, CDCl₃) δ 7.63 (2H, d, *J* = 8 Hz), (2H, d, *J* = 8 Hz), (2H, t, *J* = 8 Hz), (1H, t, *J* = 8 Hz), (2H, d, *J* = 8 Hz), 2.44 (3H, s) ppm, ¹³C NMR (101 MHz, CDCl₃)* δ 141.3, 138.5, 137.1, 129.6, 128.8, 127.1, 127.07, 21.2 ppm, *m/z* (EI⁺) 168.1 [M]⁺.

*Remaining sp² carbon is not observed consistent with literature.¹⁰⁵

Table 5.4 entry 5

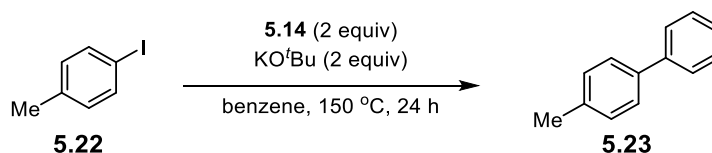


To an oven-dried pressure tube, 4-iodotoluene, **5.22** (114 mg, 0.5 mmol), and **5.36** (25 mg, 0.1 mmol) were added. Under an inert atmosphere, KO^tBu (112 mg, 1 mmol) and benzene (5 mL) were added and the tube sealed. The sealed tube was placed in a pre-heated oil bath at 150 °C for 24 h. After cooling to room temperature, the reaction was quenched with 1M HCl_(aq) (20 mL) and extracted with Et₂O (3 x 20 mL). The combined extracts were washed with brine, dried over Na₂SO₄ and concentrated. The crude product was purified by column chromatography (hexane) to afford 4-methylbiphenyl **5.23** as a colourless oil (55 mg 66%)¹⁰⁵ ¹H NMR (400 MHz, CDCl₃) δ 7.63 (2H, d, *J* = 8 Hz), (2H, d, *J* = 8 Hz), (2H, t, *J* = 8 Hz), (1H, t, *J* = 8 Hz), (2H, d, *J* = 8 Hz), 2.44 (3H, s) ppm, ¹³C NMR (101 MHz, CDCl₃)* δ 141.3, 138.5, 137.1, 129.6, 128.8, 127.1, 127.07, 21.2 ppm, *m/z* (EI⁺) 168.1 [M]⁺.

*Remaining sp² carbon is not observed consistent with literature.¹⁰⁵

Coupling reactions between aryl iodides and benzene with additive **5.14**

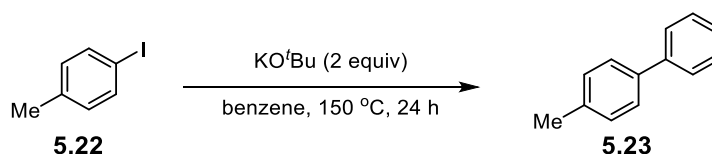
Table 5.5 entry 1a



To an oven-dried pressure tube, 4-iodotoluene, **5.22** (114 mg, 0.5 mmol), and **5.14** (13 mg, 0.1 mmol) were added. Under an inert atmosphere, KO^tBu (112 mg, 1 mmol) and benzene (5 mL) were added and the tube sealed. The sealed tube was placed in a pre-heated oil bath at 150 °C for 24 h. After cooling to room temperature, the reaction was quenched with 1M HCl_(aq) (20 mL) and extracted with Et₂O (3 x 20 mL). The combined extracts were washed with brine, dried over Na₂SO₄ and concentrated. The crude product was purified by column chromatography (hexane) to afford 4-methylbiphenyl **5.23** as a colourless oil (57 mg, 68%).¹⁰⁵ ¹H NMR (400 MHz, CDCl₃) δ 7.63 (2H, d, *J* = 8 Hz), (2H, d, *J* = 8 Hz), (2H, t, *J* = 8 Hz), (1H, t, *J* = 8 Hz), (2H, d, *J* = 8 Hz), 2.44 (3H, s) ppm, ¹³C NMR (101 MHz, CDCl₃)* δ 141.3, 138.5, 137.1, 129.6, 128.8, 127.1, 127.07, 21.2 ppm, *m/z* (EI⁺) 168.1 [M]⁺.

*Remaining sp² carbon is not observed consistent with literature.¹⁰⁵

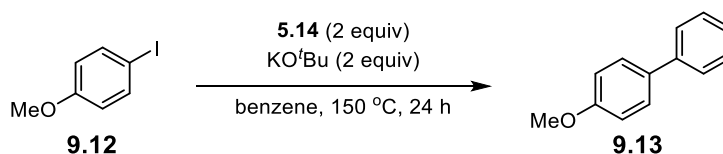
Table 5.5 entry 1b



To an oven-dried pressure tube, 4-iodotoluene, **5.22** (114 mg, 0.5 mmol) was added. Under an inert atmosphere, KO^tBu (112 mg, 1 mmol) and benzene (5 mL) were added and the tube sealed. The sealed tube was placed in a pre-heated oil bath at 150 °C for 24 h. After cooling to room temperature, the reaction was quenched with 1M HCl_(aq) (20 mL) and extracted with Et₂O (3 x 20 mL). The combined extracts were washed with brine, dried over Na₂SO₄ and concentrated. The crude product was purified by column chromatography (hexane) to afford 4-methylbiphenyl **5.23** as a colourless oil (31 mg, 37%).¹⁰⁵ ¹H NMR (400 MHz, CDCl₃) δ 7.63 (2H, d, *J* = 8 Hz), (2H, d, *J* = 8 Hz), (2H, t, *J* = 8 Hz), (1H, t, *J* = 8 Hz), (2H, d, *J* = 8 Hz), 2.44 (3H, s) ppm, ¹³C NMR (101 MHz, CDCl₃)* δ 141.3, 138.5, 137.1, 129.6, 128.8, 127.1, 127.07, 21.2 ppm, *m/z* (EI⁺) 168.1 [M]⁺.

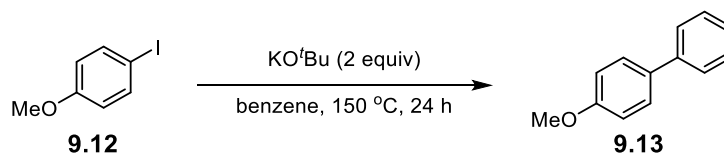
*Remaining sp² carbon is not observed consistent with literature.¹⁰⁵

Table 5.5 entry 2a



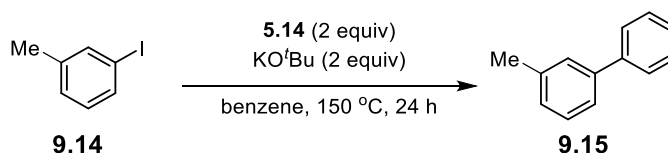
To an oven-dried pressure, tube 4-iodoanisole, **9.12** (117 mg, 0.5 mmol), and **5.14** (13 mg, 0.1 mmol) were added. Under an inert atmosphere, KO^tBu (112 mg, 1 mmol) and benzene (5 mL) were added and the tube sealed. The sealed tube was placed in a pre-heated oil bath at 150 °C for 24 h. After cooling to room temperature, the reaction was quenched with 1M HCl_(aq) (20 mL) and extracted with Et₂O (3 x 20 mL). The combined extracts were washed with brine, dried over Na₂SO₄ and concentrated. The crude product was purified by column chromatography (hexane/EtOAc 19/1) of 4-methoxybiphenyl, **9.13** was obtained as a white solid (78 mg, 85%). ¹H NMR (400 MHz, CDCl₃) δ 7.57-7.51(4H, m), 7.43 (2H, t, *J* = 8 Hz), 7.31 (1H, t, *J* = 7.4 Hz), 6.98 (2H, d, *J* = 8 Hz), 3.86 (3H, s) ppm, ¹³C NMR (101 MHz, CDCl₃) δ 158.8, 141.0, 134.4, 128.9, 128.3, 126.9, 126.8, 114.3, 55.4 ppm, *m/z* (EI⁺) 184.2 [M]⁺.¹⁷⁹

Table 5.5 entry 2b



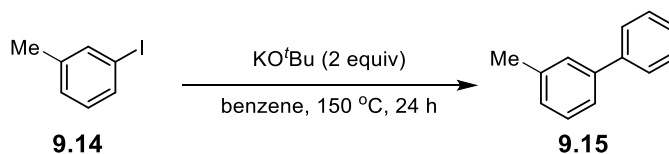
To an oven-dried pressure tube, 4-iodoanisole, **9.12** (117 mg, 0.5 mmol) was added. Under an inert atmosphere, KO^tBu (112 mg, 1 mmol) and benzene (5 mL) were added and the tube sealed. The sealed tube was placed in a pre-heated oil bath at 150 °C for 24 h. After cooling to room temperature, the reaction was quenched with 1M HCl_(aq) (20 mL) and extracted with Et₂O (3 x 20 mL). The combined extracts were washed with brine, dried over Na₂SO₄ and concentrated. The crude product was purified by column chromatography (hexane/EtOAc 19/1) 4-methoxybiphenyl, **9.13** was obtained as a white solid (25 mg, 27%). ¹H NMR (400 MHz, CDCl₃) δ 7.57-7.51(4H, m) , 7.43 (2H, t, *J* = 8 Hz), 7.31 (1H, t, *J* = 7.4 Hz), 6.98 (2H, d, *J* = 8 Hz), 3.86 (3H, s) ppm, ¹³C NMR (101 MHz, CDCl₃) δ 158.8, 141.0, 134.4, 128.9, 128.3, 126.9, 126.8, 114.3, 55.4 ppm, *m/z* (EI⁺) 184.2 [M]⁺.¹⁷⁹

Table 5.5 entry 3a



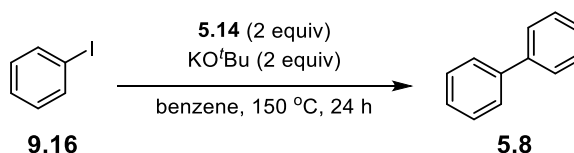
To an oven-dried pressure, tube 3-iodotoluene, **9.14** (114 mg, 0.5 mmol), and **5.14** (13 mg, 0.1 mmol) were added. Under an inert atmosphere, KO^tBu (112 mg, 1 mmol) and benzene (5 mL) were added and the tube sealed. The sealed tube was placed in a pre-heated oil bath at 150 °C for 24 h. After cooling to room temperature, the reaction was quenched with 1M HCl_(aq) (20 mL) and extracted with Et₂O (3 x 20 mL). The combined extracts were washed with brine, dried over Na₂SO₄ and concentrated. The crude product was purified by column chromatography (hexane) to afford 3-methylbiphenyl, **9.15** was obtained as a white solid (55 mg, 65%). ¹H NMR (400 MHz, CDCl₃) δ 7.64 (2H, d, *J* = 7.5 Hz), 7.49-7.43 (4H, m), 7.38 (2H, t, *J* = 7 Hz), 7.20 (1H, d, *J* = 7 Hz), 2.46 (3H, s) ppm, ¹³C NMR (101 MHz, CDCl₃) δ 141.4, 141.2, 138.4, 128.8, 128.7, 128.1, 128.0 127.3, 127.2, 124.4, 21.6 ppm, *m/z* (EI⁺) 168.1 [M]⁺.¹⁸⁰

Table 5.5 entry 3b



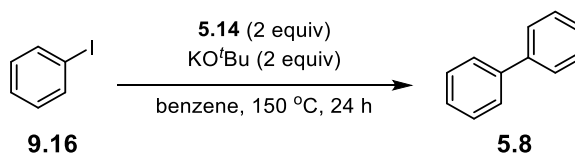
To an oven-dried pressure tube, 3-iodotoluene, **9.14** (114 mg, 0.5 mmol) was added. Under an inert atmosphere, KO^tBu (112 mg, 1 mmol) and benzene (5 mL) were added and the tube sealed. The sealed tube was placed in a pre-heated oil bath at 150 °C for 24 h. After cooling to room temperature, the reaction was quenched with 1M HCl_(aq) (20 mL) and extracted with Et₂O (3 x 20 mL). The combined extracts were washed with brine, dried over Na₂SO₄ and concentrated. The crude product was purified by column chromatography (hexane) to afford 3-methylbiphenyl, **9.15** was obtained as a white solid (27 mg, 32%). ¹H NMR (400 MHz, CDCl₃) δ 7.64 (2H, d, *J* = 7.5 Hz), 7.49-7.43 (4H, m), 7.38 (2H, t, *J* = 7 Hz), 7.20 (1H, d, *J* = 7 Hz), 2.46 (3H, s) ppm, ¹³C NMR (101 MHz, CDCl₃) δ 141.4, 141.2, 138.4, 128.8, 128.7, 128.1, 128.0, 127.3, 127.2, 124.4, 21.6 ppm, *m/z* (EI⁺) 168.1 [M]⁺.¹⁸⁰

Table 5.5 entry 4a



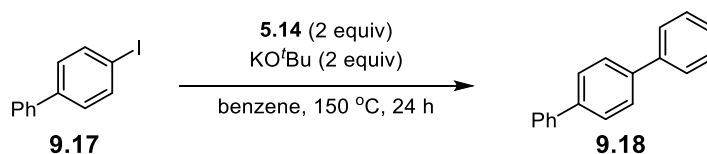
To an oven-dried pressure tube, iodobenzene, **9.16** (102 mg, 0.5 mmol), and **5.14** (13 mg, 0.1 mmol) were added. Under an inert atmosphere, KO^tBu (112 mg, 1 mmol) and benzene (5 mL) were added and the tube sealed. The sealed tube was placed in a pre-heated oil bath at 150 °C for 24 h. After cooling to room temperature, the reaction was quenched with 1M HCl_(aq) (20 mL) and extracted with Et₂O (3 x 20 mL). The combined extracts were washed with brine, dried over Na₂SO₄ and concentrated. The crude product was purified by column chromatography (hexane) to afford biphenyl, **5.8** was obtained as a white solid (47 mg, 61%). ¹H NMR (400 MHz, CDCl₃) δ 7.72 (4H, d, Hz), 7.46 (4H, t, Hz), 7.37 (2H, t, Hz). ¹³C NMR (101 MHz, CDCl₃) δ 141.3, 128.9, 127.4, 127.3. *m/z* (EI⁺) 154.1 [M]⁺.¹⁷⁹

Table 5.5 entry 4b



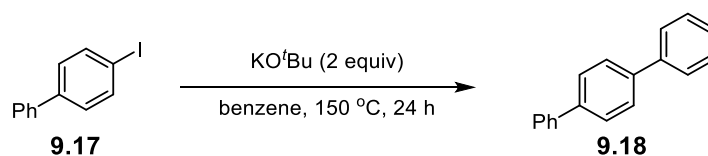
To an oven-dried pressure tube, iodobenzene, **9.16** (102 mg, 0.5 mmol) was added. Under an inert atmosphere, KO^tBu (112 mg, 1 mmol) and benzene (5 mL) were added and the tube sealed. The sealed tube was placed in a pre-heated oil bath at 150 °C for 24 h. After cooling to room temperature, the reaction was quenched with 1M HCl_(aq) (20 mL) and extracted with Et₂O (3 x 20 mL). The combined extracts were washed with brine, dried over Na₂SO₄ and concentrated. The crude product was purified by column chromatography (hexane) to afford biphenyl, **5.8** was obtained as a white solid (33 mg, 43%). ¹H NMR (400 MHz, CDCl₃) δ 7.72 (4H, d, Hz), 7.46 (4H, t, Hz), 7.37 (2H, t, Hz) ppm, ¹³C NMR (101 MHz, CDCl₃) δ 141.3, 128.9, 127.4, 127.3 ppm, *m/z* (EI⁺) 154.1 [M]⁺¹⁷⁹

Table 5.5 entry 5a



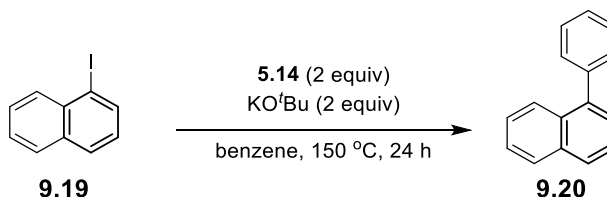
To an oven-dried pressure tube, 4-iodobiphenyl, **9.17** (140 mg, 0.5 mmol), and **5.14** (13 mg, 0.1 mmol) were added. Under an inert atmosphere, KO^tBu (112 mg, 1 mmol) and benzene (5 mL) were added and the tube sealed. The sealed tube was placed in a pre-heated oil bath at 150 °C for 24 h. After cooling to room temperature, the reaction was quenched with 1M HCl_(aq) (20 mL) and extracted with Et₂O (3 x 20 mL). The combined extracts were washed with brine, dried over Na₂SO₄ and concentrated. The crude product was purified by column chromatography (hexane) to afford *p*-terphenyl, **9.18** was obtained as a white solid (75 mg, 65%). ¹H NMR (400 MHz, CDCl₃) δ 7.70-7.61 (8H, m), 7.48 (4H, t, *J* = 7.4 Hz), 7.38 (2H, t, *J* = 7.2 Hz) ppm, ¹³C NMR (101 MHz, CDCl₃) δ 140.9, 140.3, 128.9, 127.7, 127.5, 127.2 ppm, *m/z* (EI⁺) 230.2 [M+H]⁺¹⁷⁹

Table 5.5 entry 5b



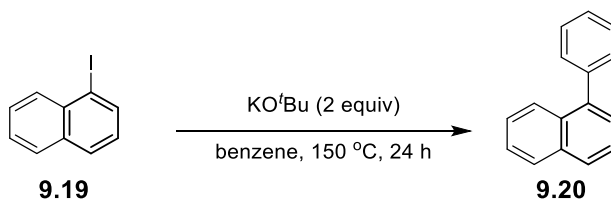
To an oven-dried pressure tube, 4-iodobiphenyl, **9.17** (140 mg, 0.5 mmol) was added. Under an inert atmosphere, KO^tBu (112 mg, 1 mmol) and benzene (5 mL) were added and the tube sealed. The sealed tube was placed in a pre-heated oil bath at 150 °C for 24 h. After cooling to room temperature, the reaction was quenched with 1M HCl_(aq) (20 mL) and extracted with Et₂O (3 x 20 mL). The combined extracts were washed with brine, dried over Na₂SO₄ and concentrated. The crude product was purified by column chromatography (hexane) to afford of *p*-terphenyl, **9.18** was obtained as a white solid (62 mg, 54%). ¹H NMR (400 MHz, CDCl₃) δ 7.70-7.61 (8H, m), 7.48 (4H, t, *J* = 7.4 Hz), 7.38 (2H, t, *J* = 7.2 Hz) ppm, ¹³C NMR (101 MHz, CDCl₃) δ 140.9, 140.3, 128.9, 127.7, 127.5, 127.2 ppm, *m/z* (EI⁺) 230.2 [M+H]⁺¹⁷⁹

Table 5.5 entry 6a



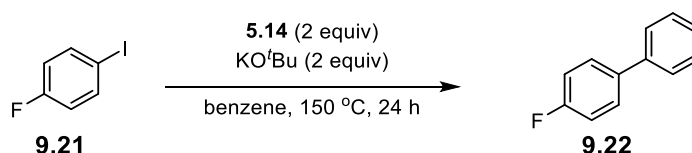
To an oven-dried pressure tube, 1-iodonaphthalene, **9.19** (127 mg, 0.5 mmol), and **5.14** (13 mg, 0.1 mmol) were added. Under an inert atmosphere, KO^tBu (112 mg, 1 mmol) and benzene (5 mL) were added and the tube sealed. The sealed tube was placed in a pre-heated oil bath at 150 °C for 24 h. After cooling to room temperature, the reaction was quenched with 1M HCl_(aq) (20 mL) and extracted with Et₂O (3 x 20 mL). The combined extracts were washed with brine, dried over Na₂SO₄ and concentrated. The crude product was purified by column chromatography (hexane) to afford (hexane) 1-phenylnaphthalene, **9.20** was obtained as a yellow oil (45 mg, 44%). ¹H NMR (400 MHz, CDCl₃) δ 7.96-7.94 (2H, m), 7.88 (1H, d, *J* = 8 Hz), 7.63-7.43 (9H, m) ppm, ¹³C NMR (101 MHz, CDCl₃) δ 140.9, 140.4, 133.9, 131.7, 130.2, 128.9, 128.4, 128.3, 127.8, 127.3, 127.0, 126.1, 125.9, 125.5 ppm, *m/z* (EI⁺) 204.2 [M]⁺¹⁷⁹

Table 5.5 entry 6b



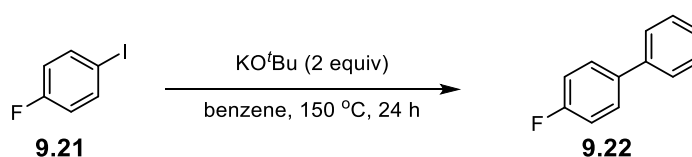
To an oven-dried pressure tube, 1-iodonaphthalene, **9.19** (127 mg, 0.5 mmol) was added. Under an inert atmosphere, KO^tBu (112 mg, 1 mmol) and benzene (5 mL) were added and the tube sealed. The sealed tube was placed in a pre-heated oil bath at 150 °C for 24 h. After cooling to room temperature, the reaction was quenched with 1M HCl_(aq) (20 mL) and extracted with Et₂O (3 x 20 mL). The combined extracts were washed with brine, dried over Na₂SO₄ and concentrated. The crude product was purified by column chromatography (hexane) to afford (hexane) 19 mg (19%) of 1-phenylnaphthalene, **9.20** was obtained as a yellow oil. ¹H NMR (400 MHz, CDCl₃) δ 7.93 (2H, d, *J* = 10 Hz), 7.88 (1H, d, *J* = 8 Hz), 7.63-7.43 (9H, m) ppm, ¹³C NMR (101 MHz, CDCl₃) δ 140.9, 140.4, 133.9, 131.7, 130.2, 128.9, 128.4, 128.3, 127.8, 127.3, 127.0, 126.1, 125.9, 125.5 ppm, *m/z* (EI⁺) 204.2 [M]⁺.¹⁷⁹

Table 5.5 entry 7a



To an oven-dried pressure tube, 4-fluoroiodobenzene, **9.21** (111 mg, 0.5 mmol), and **5.14** (13 mg, 0.1 mmol) were added. Under an inert atmosphere, KO^tBu (112 mg, 1 mmol) and benzene (5 mL) were added and the tube sealed. The sealed tube was placed in a pre-heated oil bath at 150 °C for 24 h. After cooling to room temperature, the reaction was quenched with 1M HCl_(aq) (20 mL) and extracted with Et₂O (3 x 20 mL). The combined extracts were washed with brine, dried over Na₂SO₄ and concentrated. The crude product was purified by column chromatography (hexane) to afford (hexane) 4-fluorobiphenyl, **9.22** was obtained as a white solid (43 mg, 52%). ¹H NMR (400 MHz, CDCl₃) δ 7.60-7.50 (4H, m), 7.40 (2H, t, *J* = 7.3 Hz), 7.35 (1H, t, *J* = 7.4 Hz), 7.16-7.12 (2H, m) ppm, ¹³C NMR (101 MHz, CDCl₃) δ 162.6 (d, *J* = 244.5 Hz), 140.4, 137.5 (d, *J* = 3 Hz), 128.9, 128.3(d, *J* = 7.5 Hz) 127.3, 127.1, 115.6 (d, *J* = 21 Hz) ppm, *m/z* (EI⁺) 172.1 [M]⁺.¹⁷⁹

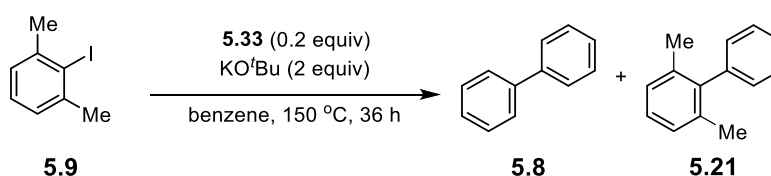
Table 5.5 entry 7b



To an oven-dried pressure tube, 4-fluoro-iodobenzene, **9.21** (111 mg, 0.5 mmol) was added. Under an inert atmosphere, KO^tBu (112 mg, 1 mmol) and benzene (5 mL) were added and the tube sealed. The sealed tube was placed in a pre-heated oil bath at 150 °C for 24 h. After cooling to room temperature, the reaction was quenched with 1M HCl_(aq) (20 mL) and extracted with Et₂O (3 x 20 mL). The combined extracts were washed with brine, dried over Na₂SO₄ and concentrated. The crude product was purified by column chromatography (hexane) to afford (hexane) 4-fluorobiphenyl, **9.22** was obtained as a white solid (7 mg 8%). ¹H NMR (400 MHz, CDCl₃) δ 7.60-7.50 (4H, m), 7.40 (2H, t, *J* = 7.3 Hz), 7.35 (1H, t, *J* = 7.4 Hz), 7.16-7.12 (2H, m) ppm, ¹³C NMR (101 MHz, CDCl₃) δ 162.6 (d, *J* = 244.5 Hz), 140.4, 137.5 (d, *J* = 3 Hz), 128.9, 128.3 (d, *J* = 7.5 Hz) 127.3, 127.1, 115.6 (d, *J* = 21 Hz) ppm, *m/z* (EI⁺) 172.1 [M]⁺.¹⁷⁹

Control coupling reactions of 2-iodo-*m*-xylene and benzene

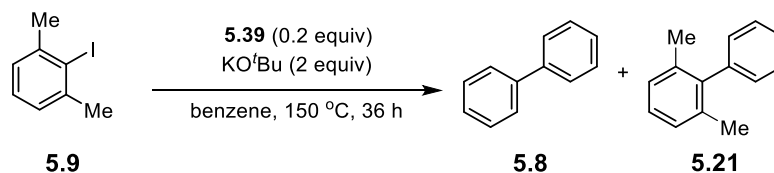
Table 5.6 entry 1



To an oven-dried pressure tube, 2-iodo-*m*-xylene, **5.9** (116 mg, 0.5 mmol), and **5.33** (10 mg, 0.1 mmol). Under an inert atmosphere, KO^tBu (112 mg, 1 mmol) and benzene (5 mL) were added and the tube sealed. The sealed tube was placed in a pre-heated oil bath at 150 °C for 36 h. After cooling to room temperature, the reaction was quenched with 1M HCl_(aq) (20 mL) and extracted with Et₂O (3 x 20 mL). The combined extracts were washed with brine, dried over Na₂SO₄ and concentrated. To determine the yield 1,3,5-trimethoxybenzene (8.4 mg, 0.05 mmol) was added to the crude product as an internal standard. The yields were calculated as biphenyl **5.8** (6%) and 2,6-dimethylbiphenyl **5.21**

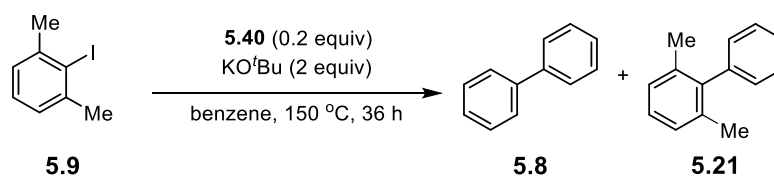
(1%) identifying the products by their characteristic peaks at δ 7.6 (biphenyl 4H) and δ 2.1 (methyl 6H) respectively.

Table 5.6 entry 2



To an oven-dried pressure tube, 2-iodo-*m*-xylene, **5.9** (116 mg, 0.5 mmol), and **5.39** (20 mg, 0.1 mmol). Under an inert atmosphere, KO^tBu (112 mg, 1 mmol) and benzene (5 mL) were added and the tube sealed. The sealed tube was placed in a pre-heated oil bath at 150 °C for 36 h. After cooling to room temperature, the reaction was quenched with 1M HCl_(aq) (20 mL) and extracted with Et₂O (3 x 20 mL). The combined extracts were washed with brine, dried over Na₂SO₄ and concentrated. To determine the yield 1,3,5-trimethoxybenzene (8.4 mg, 0.05 mmol) was added to the crude product as an internal standard. The yields were calculated as biphenyl **5.8** (4%) and 2,6-dimethylbiphenyl **5.21** (1%) identifying the products by their characteristic peaks at δ 7.6 (biphenyl 4H) and δ 2.1 (methyl 6H) respectively.

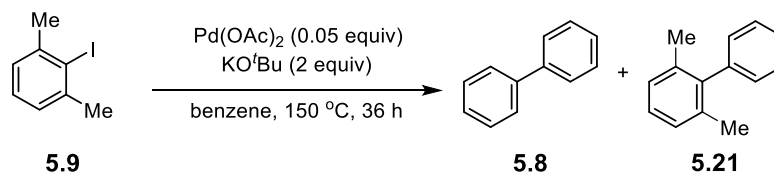
Table 5.6 entry 3



To an oven-dried pressure tube, 2-iodo-*m*-xylene, **5.9** (116 mg, 0.5 mmol), and **5.40** (28 mg, 0.1 mmol). Under an inert atmosphere, KO^tBu (112 mg, 1 mmol) and benzene (5 mL) were added and the tube sealed. The sealed tube was placed in a pre-heated oil bath at 150 °C for 36 h. After cooling to room temperature, the reaction was quenched with 1M HCl_(aq) (20 mL) and extracted with Et₂O (3 x 20 mL). The combined extracts were washed with brine, dried over Na₂SO₄ and concentrated. To determine the yield 1,3,5-trimethoxybenzene (8.4 mg, 0.05 mmol) was added to the crude product as an internal standard. The yields were calculated as biphenyl **5.8** (5%) and 2,6-dimethylbiphenyl **5.21**

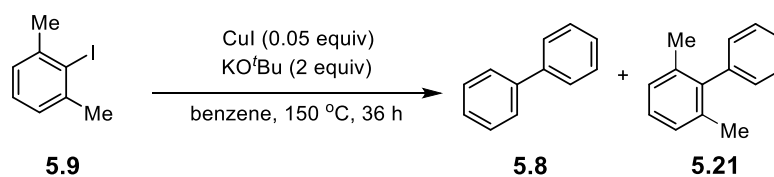
(1%) identifying the products by their characteristic peaks at δ 7.6 (biphenyl 4H) and δ 2.1 (methyl 6H) respectively.

Table 5.6 entry 4



To an oven-dried pressure tube, 2-iodo-*m*-xylene, **5.9** (116 mg, 0.5 mmol), and Pd(OAc)₂ (6 mg, 0.025 mmol). Under an inert atmosphere, KO^tBu (112 mg, 1 mmol) and benzene (5 mL) were added and the tube sealed. The sealed tube was placed in a pre-heated oil bath at 150 °C for 36 h. After cooling to room temperature, the reaction was quenched with 1M HCl_(aq) (20 mL) and extracted with Et₂O (3 x 20 mL). The combined extracts were washed with brine, dried over Na₂SO₄ and concentrated. To determine the yield 1,3,5-trimethoxybenzene (8.4 mg, 0.05 mmol) was added to the crude product as an internal standard. The yields were calculated as biphenyl **5.8** (5%) and 2,6-dimethylbiphenyl **5.21** (11%) identifying the products by their characteristic peaks at δ 7.6 (biphenyl 4H) and δ 2.1 (methyl 6H) respectively.

Table 5.6 entry 5

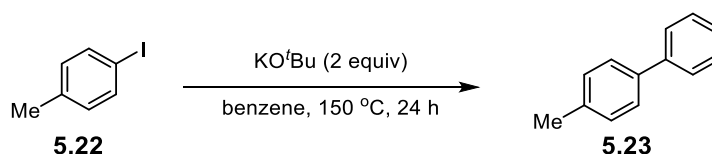


To an oven-dried pressure tube, 2-iodo-*m*-xylene, **5.9** (116 mg, 0.5 mmol), and CuI (5 mg, 0.025 mmol). Under an inert atmosphere, KO^tBu (112 mg, 1 mmol) and benzene (5 mL) were added and the tube sealed. The sealed tube was placed in a pre-heated oil bath at 150 °C for 36 h. After cooling to room temperature, the reaction was quenched with 1M HCl_(aq) (20 mL) and extracted with Et₂O (3 x 20 mL). The combined extracts were washed with brine, dried over Na₂SO₄ and concentrated. To determine the yield 1,3,5-trimethoxybenzene (8.4 mg, 0.05 mmol) was added to the crude product as an internal

standard. The yields were calculated as biphenyl **5.8** (1%) and 2,6-dimethylbiphenyl **5.21** (<1%) identifying the products by their characteristic peaks at δ 7.6 (biphenyl 4H) and δ 2.1 (methyl 6H) respectively.

Coupling reactions between 4-iodotoluene and benzene with radical initiators

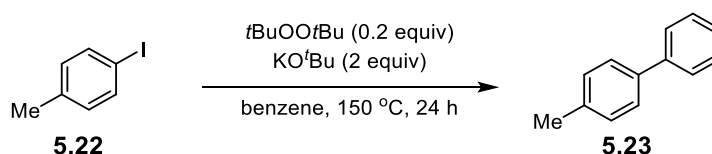
Table 5.7 entry 1



To an oven-dried pressure tube, 4-iodotoluene, **5.22** (114 mg, 0.5 mmol) was added. Under an inert atmosphere, KO^tBu (112 mg, 1 mmol) and benzene (5 mL) were added and the tube sealed. The sealed tube was placed in a pre-heated oil bath at 150 °C for 24 h. After cooling to room temperature, the reaction was quenched with 1M HCl_(aq) (20 mL) and extracted with Et₂O (3 x 20 mL). The combined extracts were washed with brine, dried over Na₂SO₄ and concentrated. The crude product was purified by column chromatography (hexane) to afford 4-methylbiphenyl **5.23** as a colourless oil (31 mg, 37%).¹⁰⁵ ¹H NMR (400 MHz, CDCl₃) δ 7.63 (2H, d, J = 8 Hz), (2H, d, J = 8 Hz), (2H, t, J = 8 Hz), (1H, t, J = 8 Hz), (2H, d, J = 8 Hz), 2.44 (3H, s) ppm, ¹³C NMR (101 MHz, CDCl₃)* δ 141.3, 138.5, 137.1, 129.6, 128.8, 127.1, 127.07, 21.2 ppm, m/z (EI⁺) 168.1 [M]⁺.

*Remaining sp² carbon is not observed consistent with literature.¹⁰⁵

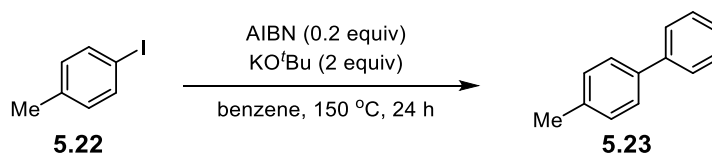
Table 5.7 entry 2



To an oven-dried pressure tube, 4-iodotoluene, **5.22** (114 mg, 0.5 mmol), and di-*tert*-butyl peroxide (13 mg, 0.1 mmol). Under an inert atmosphere, KO^{*t*}Bu (112 mg, 1 mmol) and benzene (5 mL) were added and the tube sealed. The sealed tube was placed in a pre-heated oil bath at 150 °C for 24 h. After cooling to room temperature, the reaction was quenched with 1M HCl_(aq) (20 mL) and extracted with Et₂O (3 x 20 mL). The combined extracts were washed with brine, dried over Na₂SO₄ and concentrated. The crude product was purified by column chromatography (hexane) to afford 4-methylbiphenyl **5.23** as a colourless oil (74 mg, 88%).¹⁰⁵ ¹H NMR (400 MHz, CDCl₃) δ 7.63 (2H, d, *J* = 8 Hz), (2H, d, *J* = 8 Hz), (2H, t, *J* = 8 Hz), (1H, t, *J* = 8 Hz), (2H, d, *J* = 8 Hz), 2.44 (3H, s) ppm, ¹³C NMR (101 MHz, CDCl₃)* δ 141.3, 138.5, 137.1, 129.6, 128.8, 127.1, 127.07, 21.2 ppm, *m/z* (EI⁺) 168.1 [M]⁺.

*Remaining sp² carbon is not observed consistent with literature.¹⁰⁵

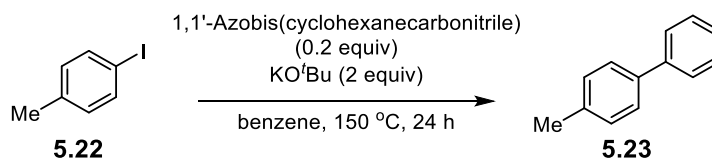
Table 5.7 entry 3



To an oven-dried pressure tube, 4-iodotoluene, **5.22** (114 mg, 0.5 mmol), and AIBN (16 mg, 0.1 mmol). Under an inert atmosphere, KO^{*t*}Bu (112 mg, 1 mmol) and benzene (5 mL) were added and the tube sealed. The sealed tube was placed in a pre-heated oil bath at 150 °C for 24 h. After cooling to room temperature, the reaction was quenched with 1M HCl_(aq) (20 mL) and extracted with Et₂O (3 x 20 mL). The combined extracts were washed with brine, dried over Na₂SO₄ and concentrated. The crude product was purified by column chromatography (hexane) to afford methylbiphenyl **5.23** as a colourless oil (34 mg, 40%).¹⁰⁵ ¹H NMR (400 MHz, CDCl₃) δ 7.63 (2H, d, *J* = 8 Hz), (2H, d, *J* = 8 Hz), (2H, t, *J* = 8 Hz), (1H, t, *J* = 8 Hz), (2H, d, *J* = 8 Hz), 2.44 (3H, s) ppm, ¹³C NMR (101 MHz, CDCl₃)* δ 141.3, 138.5, 137.1, 129.6, 128.8, 127.1, 127.07, 21.2 ppm, *m/z* (EI⁺) 168.1 [M]⁺.

*Remaining sp² carbon is not observed consistent with literature.¹⁰⁵

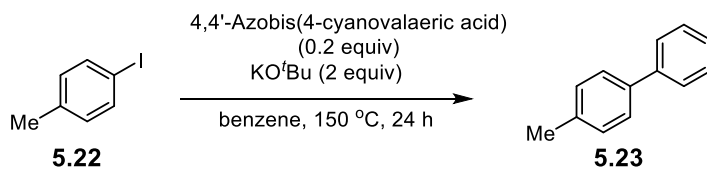
Table 5.7 entry 4



To an oven-dried pressure tube, 4-iodotoluene, **5.22** (114 mg, 0.5 mmol), and 1,1'-Azobis(cyclohexanecarbonitrile) (24 mg, 0.1 mmol). Under an inert atmosphere, KO^tBu (112 mg, 1 mmol) and benzene (5 mL) were added and the tube sealed. The sealed tube was placed in a pre-heated oil bath at 150 °C for 24 h. After cooling to room temperature, the reaction was quenched with 1M HCl_(aq) (20 mL) and extracted with Et₂O (3 x 20 mL). The combined extracts were washed with brine, dried over Na₂SO₄ and concentrated. The crude product was purified by column chromatography (hexane) to afford 4-methylbiphenyl **5.23** as a colourless oil (26 mg, 31%).¹⁰⁵ ¹H NMR (400 MHz, CDCl₃) δ 7.63 (2H, d, *J* = 8 Hz), (2H, d, *J* = 8 Hz), (2H, t, *J* = 8 Hz), (1H, t, *J* = 8 Hz), (2H, d, *J* = 8 Hz), 2.44 (3H, s) ppm, ¹³C NMR (101 MHz, CDCl₃)* δ 141.3, 138.5, 137.1, 129.6, 128.8, 127.1, 127.07, 21.2 ppm, *m/z* (EI⁺) 168.1 [M]⁺.

*Remaining sp² carbon is not observed consistent with literature.¹⁰⁵

Table 5.7 entry 5



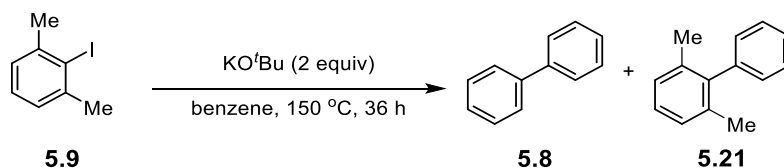
To an oven-dried pressure tube, 4-iodotoluene, **5.22** (114 mg, 0.5 mmol), and 4,4'-Azobis(4-cyanovaleric acid) (28 mg, 0.1 mmol). Under an inert atmosphere, KO^tBu (112 mg, 1 mmol) and benzene (5 mL) were added and the tube sealed. The sealed tube was placed in a pre-heated oil bath at 150 °C for 24 h. After cooling to room temperature, the reaction was quenched with 1M HCl_(aq) (20 mL) and extracted with Et₂O (3 x 20 mL). The combined extracts were washed with brine, dried over Na₂SO₄ and concentrated. The crude product was purified by column chromatography (hexane) to 4-methylbiphenyl **5.23** as a colourless oil (18 mg, 22%).¹⁰⁵ ¹H NMR (400 MHz, CDCl₃) δ 7.63 (2H, d, *J* = 8 Hz), (2H, d, *J* = 8 Hz), (2H, t, *J* = 8 Hz), (1H, t, *J* = 8 Hz), (2H, d, *J* = 8 Hz), 2.44

(3H,s) ppm, ^{13}C NMR (101 MHz, CDCl_3)* δ 141.3, 138.5, 137.1, 129.6, 128.8, 127.1, 127.07, 21.2 ppm, m/z (EI^+) 168.1 $[\text{M}]^+$.

*Remaining sp^2 carbon is not observed consistent with literature.¹⁰⁵

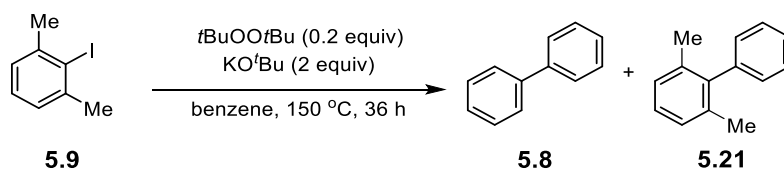
Coupling reactions between 2-iodo-*m*-xylene and benzene with radical initiators

Table 5.8 entry 1



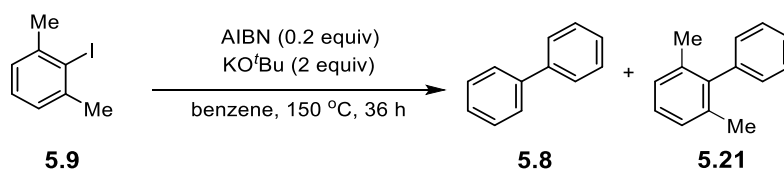
To an oven-dried pressure tube, 2-iodo-*m*-xylene, **5.9** (116 mg, 0.5 mmol) was added. Under an inert atmosphere, KO^tBu (112 mg, 1 mmol) and benzene (5 mL) were added and the tube sealed. The sealed tube was placed in a pre-heated oil bath at $150\text{ }^\circ\text{C}$ for 36 h. After cooling to room temperature, the reaction was quenched with 1M $\text{HCl}_{(\text{aq})}$ (20 mL) and extracted with Et_2O (3 x 20 mL). The combined extracts were washed with brine, dried over Na_2SO_4 and concentrated. To determine the yield 1,3,5-trimethoxybenzene (8.4 mg, 0.05 mmol) was added to the crude product as an internal standard. The yields were calculated as biphenyl **5.8** (1%) and 2,6-dimethylbiphenyl **5.21** (<1%) identifying the products by their characteristic peaks at δ 7.6 (biphenyl 4H) and δ 2.1 (methyl 6H) respectively.

Table 5.8 entry 2



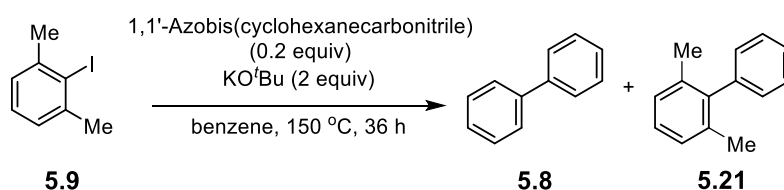
To an oven-dried pressure tube, 2-iodo-*m*-xylene, **5.9** (116 mg, 0.5 mmol), and di-*t*erbutyl peroxide (15 mg, 0.1 mmol). Under an inert atmosphere, KO^{*t*}Bu (112 mg, 1 mmol) and benzene (5 mL) were added and the tube sealed. The sealed tube was placed in a pre-heated oil bath at 150 °C for 36 h. After cooling to room temperature, the reaction was quenched with 1M HCl_(aq) (20 mL) and extracted with Et₂O (3 x 20 mL). The combined extracts were washed with brine, dried over Na₂SO₄ and concentrated. To determine the yield 1,3,5-trimethoxybenzene (8.4 mg, 0.05 mmol) was added to the crude product as an internal standard. The yields were calculated as biphenyl **5.8** (12%) and 2,6-dimethylbiphenyl **5.21** (3%) identifying the products by their characteristic peaks at δ 7.6 (biphenyl 4H) and δ 2.1 (methyl 6H) respectively.

Table 5.8 entry 3



To an oven-dried pressure tube, 2-iodo-*m*-xylene, **5.9** (116 mg, 0.5 mmol), and AIBN (16 mg, 0.1 mmol). Under an inert atmosphere, KO^{*t*}Bu (112 mg, 1 mmol) and benzene (5 mL) were added and the tube sealed. The sealed tube was placed in a pre-heated oil bath at 150 °C for 36 h. After cooling to room temperature, the reaction was quenched with 1M HCl_(aq) (20 mL) and extracted with Et₂O (3 x 20 mL). The combined extracts were washed with brine, dried over Na₂SO₄ and concentrated. To determine the yield 1,3,5-trimethoxybenzene (8.4 mg, 0.05 mmol) was added to the crude product as an internal standard. The yields were calculated as biphenyl **5.8** (11%) and 2,6-dimethylbiphenyl **5.21** (3%) identifying the products by their characteristic peaks at δ 7.6 (biphenyl 4H) and δ 2.1 (methyl 6H) respectively.

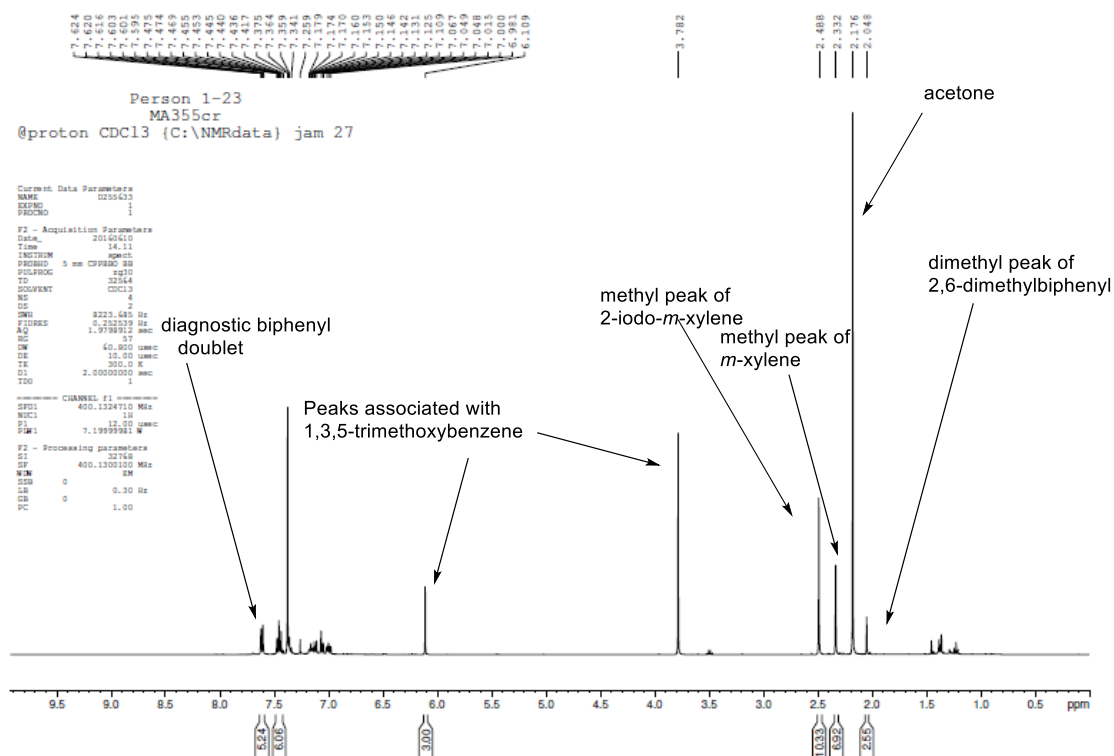
Table 5.8 entry 4



To an oven-dried pressure tube, 2-iodo-*m*-xylene, **5.9** (116 mg, 0.5 mmol), and 1,1'-Azobis(cyclohexanecarbonitrile) (24 mg, 0.1 mmol). Under an inert atmosphere, KO^tBu (112 mg, 1 mmol) and benzene (5 mL) were added and the tube sealed. The sealed tube was placed in a pre-heated oil bath at 150 °C for 36 h. After cooling to room temperature, the reaction was quenched with 1M HCl_(aq) (20 mL) and extracted with Et₂O (3 x 20 mL). The combined extracts were washed with brine, dried over Na₂SO₄ and concentrated. To determine the yield 1,3,5-trimethoxybenzene (8.4 mg, 0.05 mmol) was added to the crude product as an internal standard. The yields were calculated as biphenyl **5.8** (11%) and 2,6-dimethylbiphenyl **5.21** (4%) identifying the products by their characteristic peaks at δ 7.6 (biphenyl 4H) and δ 2.1 (methyl 6H) respectively.

9.5 Example Internal Standard Calculation

9.5.1 Reactions with 2-iodo-*m*-xylene



1,3,5-Trimethoxybenzene (8.4 mg, 0.05 mmol) was added to the crude mixture. The integral for the aromatic protons (δ 6.1) is set to 3 units representing 3 protons.

A characteristic peak for biphenyl is the doublet at 7.6 representing 4 protons and for 2,6-dimethylbiphenyl at 2.1 representing 6 protons. Any residual 2-iodo-*m*-xylene can be identified by the peak at 2.5 also representing 6 protons.

100% yield of biphenyl would mean the signal at δ 7.6 would integrate to 40. Therefore, to calculate the yield is to divide the integral by 40 and multiply by 100.

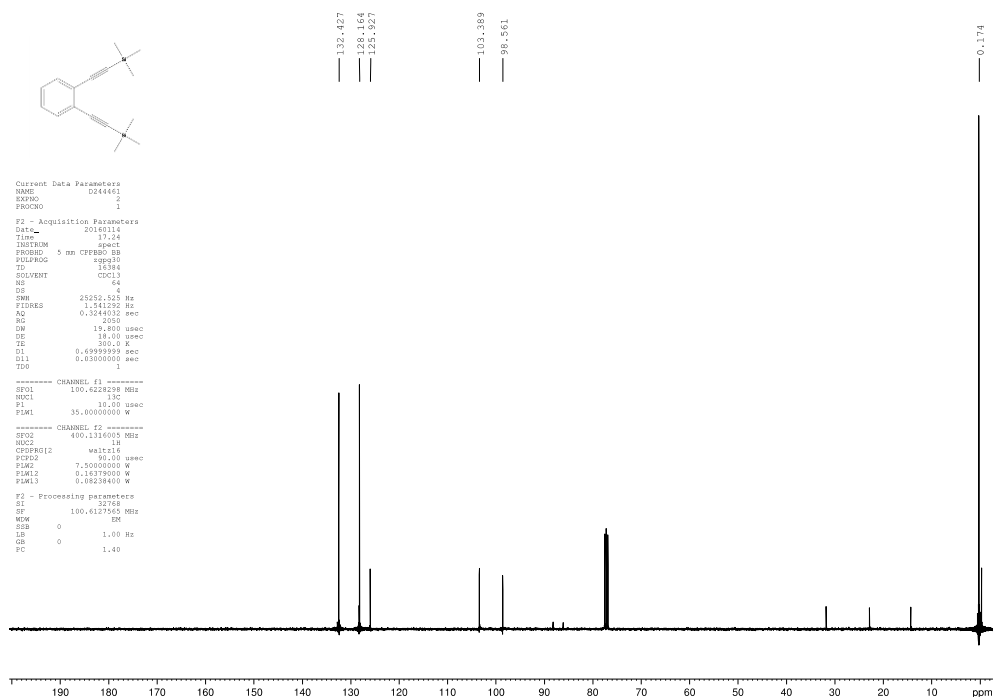
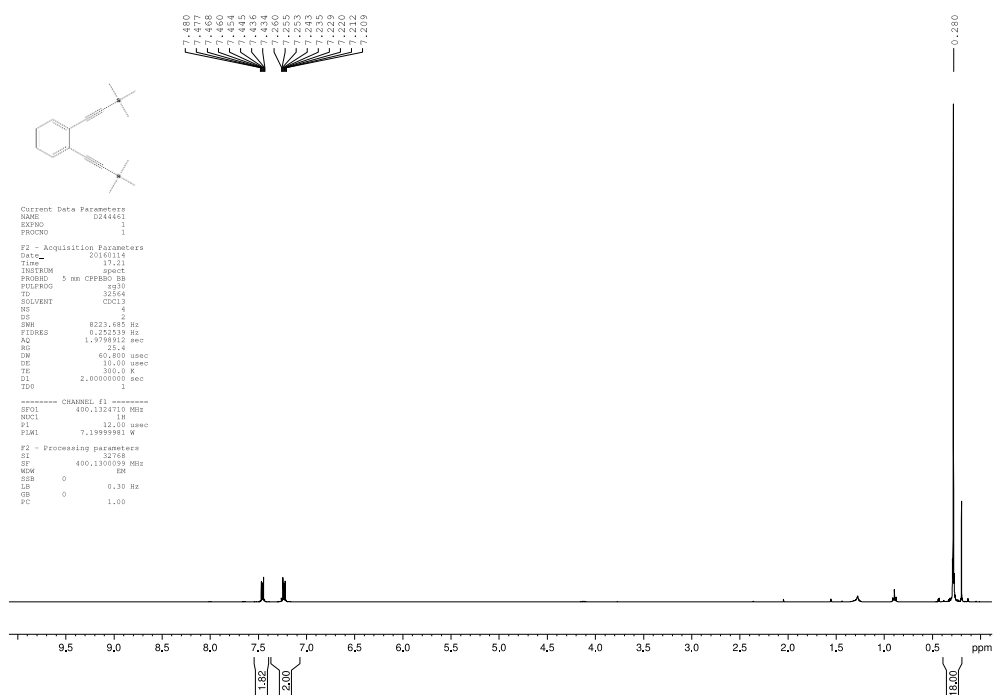
$$\text{Yield biphenyl} = 5.2/40.0 \times 100 = 13\%$$

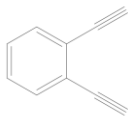
100% yield of 2,6-dimethylbiphenyl would mean the signal at δ 2.1 would integrate to 60. Therefore, to calculate the yield is to divide the integral by 60 and multiply by 100.

$$\text{Yield biphenyl} = 2.6/60.0 \times 100 = 4\%$$

Residual 2-iodo-*m*-xylene = $10.3/60 \times 100 = 17.1\%$

9.6 NMR structures for compounds synthesised in Chapter 5





```

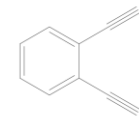
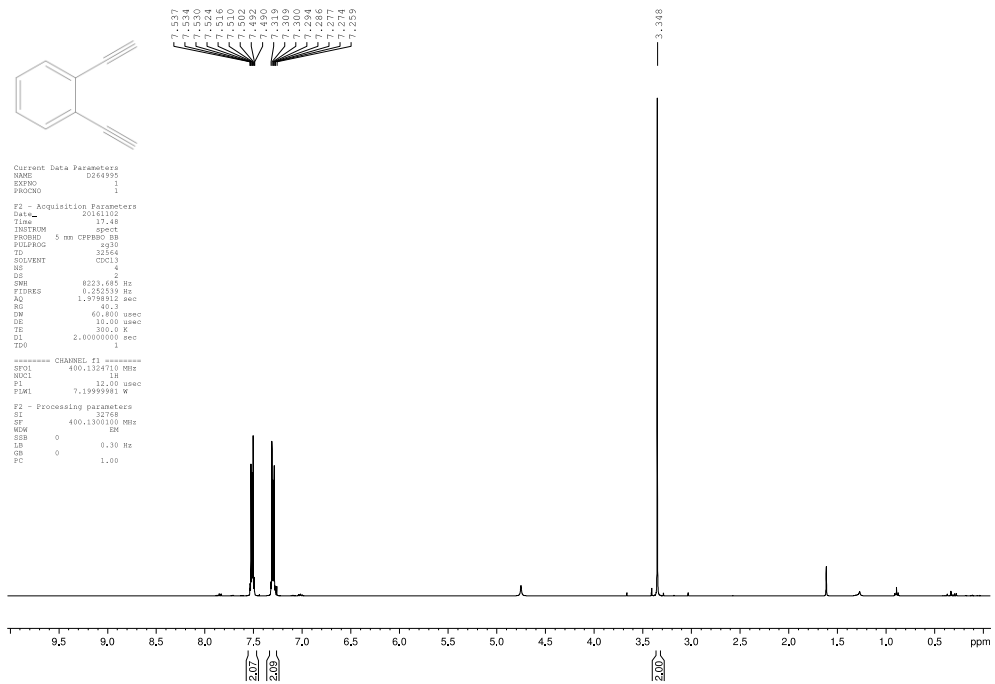
Current Data Parameters
NAME      D044005
EXPNO    1
PROCNO   1

F2 - Acquisition Parameters
Date_    2011102
Time     17.48
INSTRUM  spect
PROBHD   5 mm CPBPR5 BB
PULPROG  zgpg30
TD       32768
SOLVENT  CDCl3
NS       4
DS       2
SWH      823.685 Hz
FIDRES   0.342659 Hz
AQ       1.3798912 sec
RG       40.0
DN       40.800 usec
DE       16.00 usec
TE       300.0 K
DQ       2.0000000 sec
TD0      1

===== CHANNEL f1 =====
NUC1     13C
NUC2     1H
SI       12.00 usec
PL1     7.19499901 W

F2 - Processing parameters
SI       32768
SF       400.130100 MHz
WDW      EM
SSB      0
LB       0.30 Hz
GB       0
PC       1.00
  
```

7.534
7.530
7.524
7.517
7.510
7.496
7.480
7.319
7.300
7.294
7.286
7.274
7.259



```

Current Data Parameters
NAME      D044005
EXPNO    2
PROCNO   1

F2 - Acquisition Parameters
Date_    2011102
Time     17.50
INSTRUM  spect
PROBHD   5 mm CPBPR5 BB
PULPROG  zgpg30
TD       15344
SOLVENT  CDCl3
NS       64
DS       0
SWH      2325.525 Hz
FIDRES   1.141250 Hz
AQ       0.3244032 sec
RG       40.0
DN       19.800 usec
DE       16.00 usec
TE       300.0 K
DQ       0.6999999 sec
DIL      0.0300000 sec
TD0      1

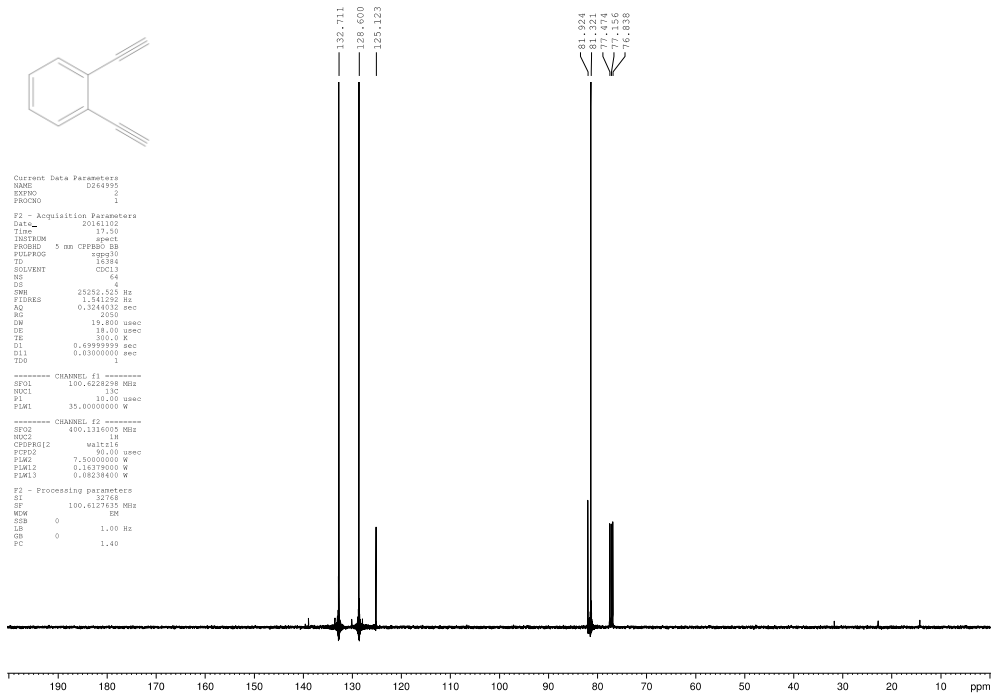
===== CHANNEL f1 =====
NUC1     13C
NUC2     13C
SI       12.00 usec
PL1     35.00000000 W

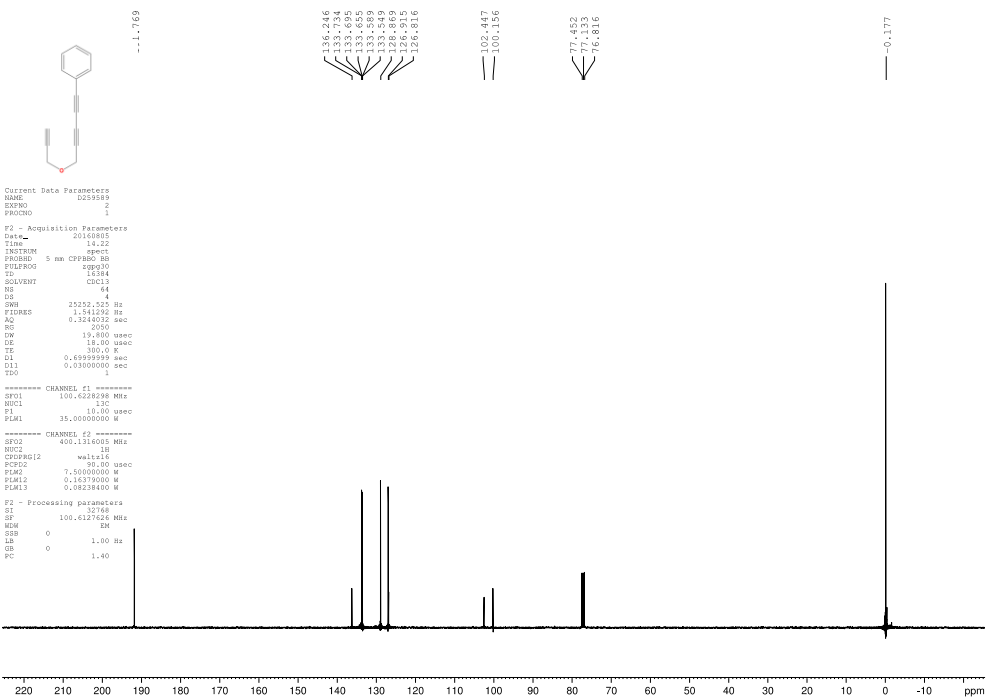
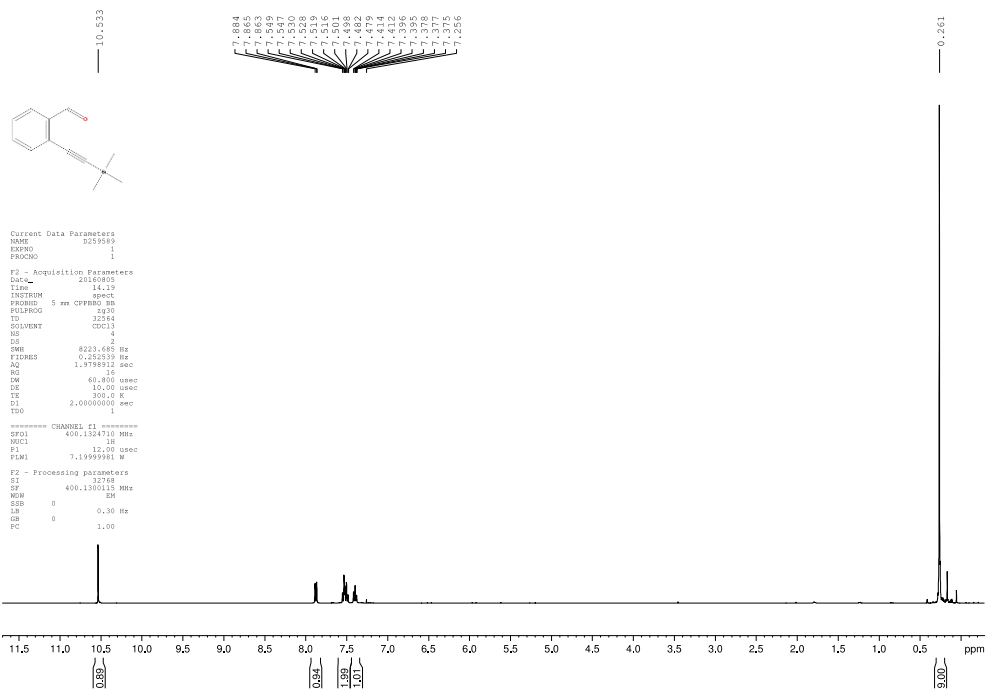
===== CHANNEL f2 =====
NUC1     13C
NUC2     13C
SI       12.00 usec
PL1     35.00000000 W

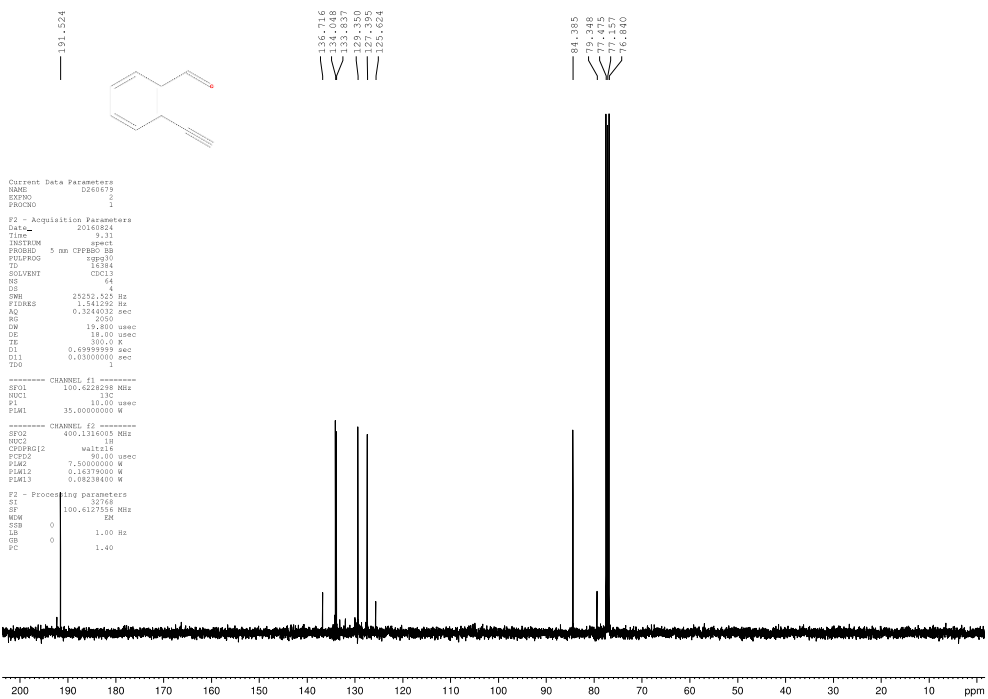
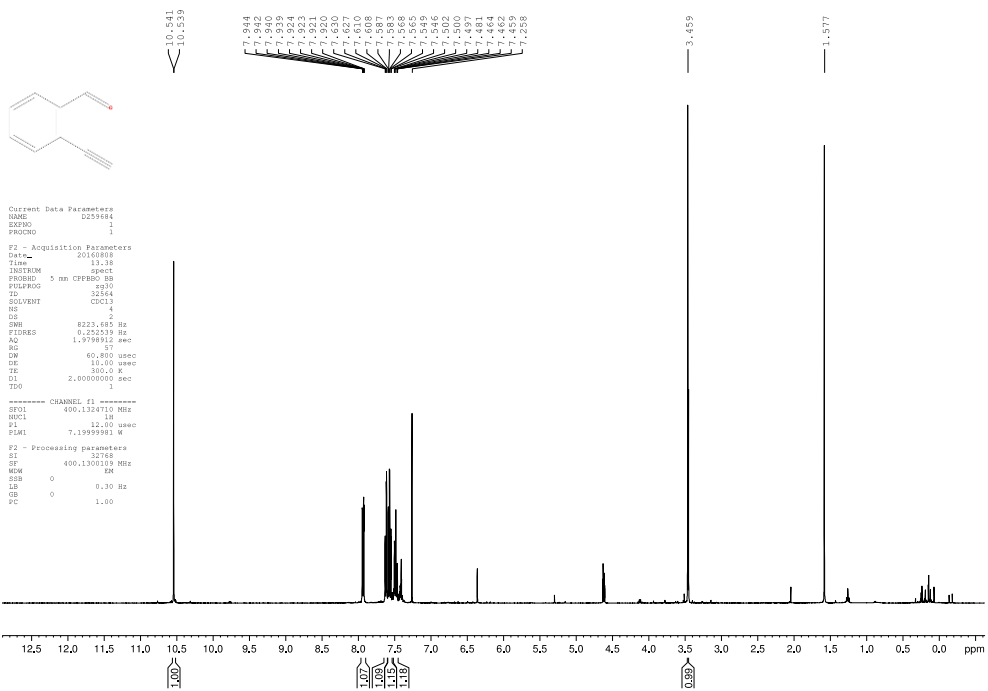
F2 - Processing parameters
SI       32768
SF       100.617833 MHz
WDW      EM
SSB      0
LB       1.00 Hz
GB       0
PC       1.40
  
```

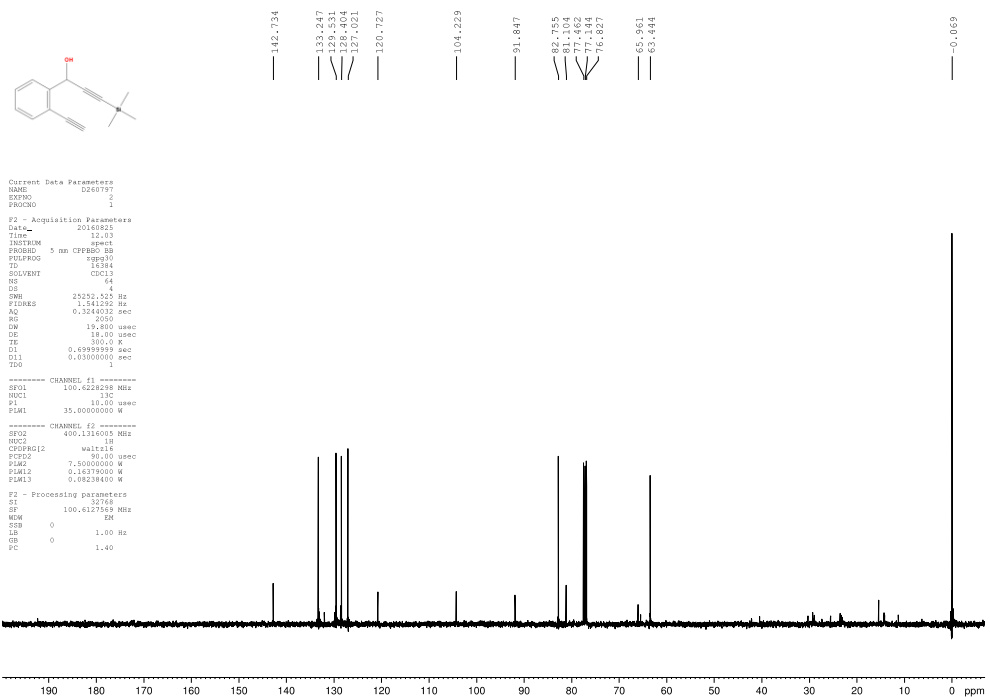
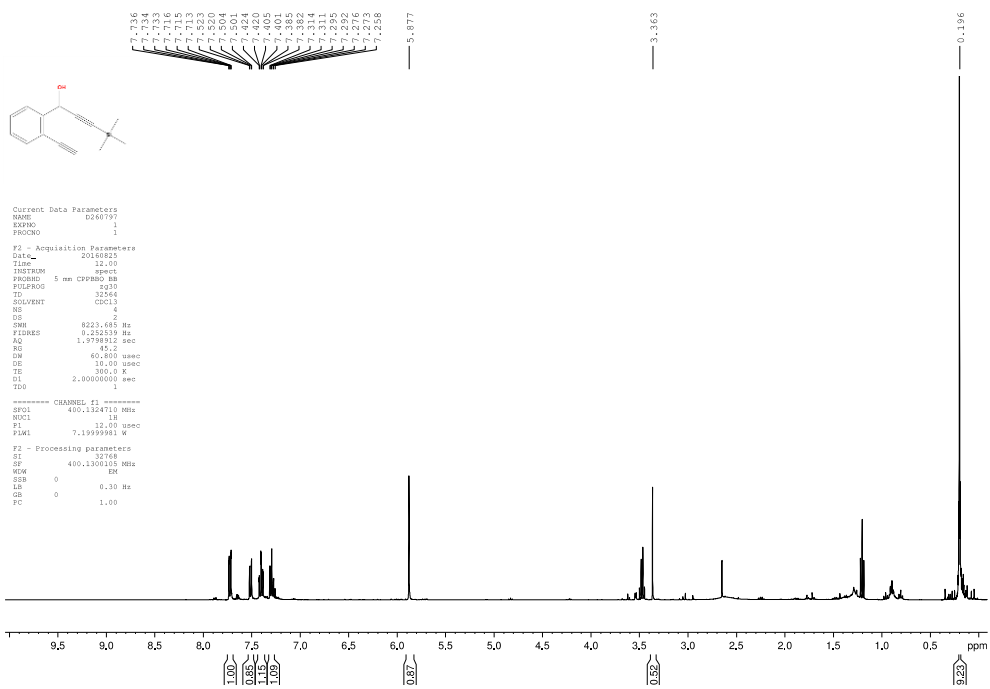
132.711
128.600
125.123

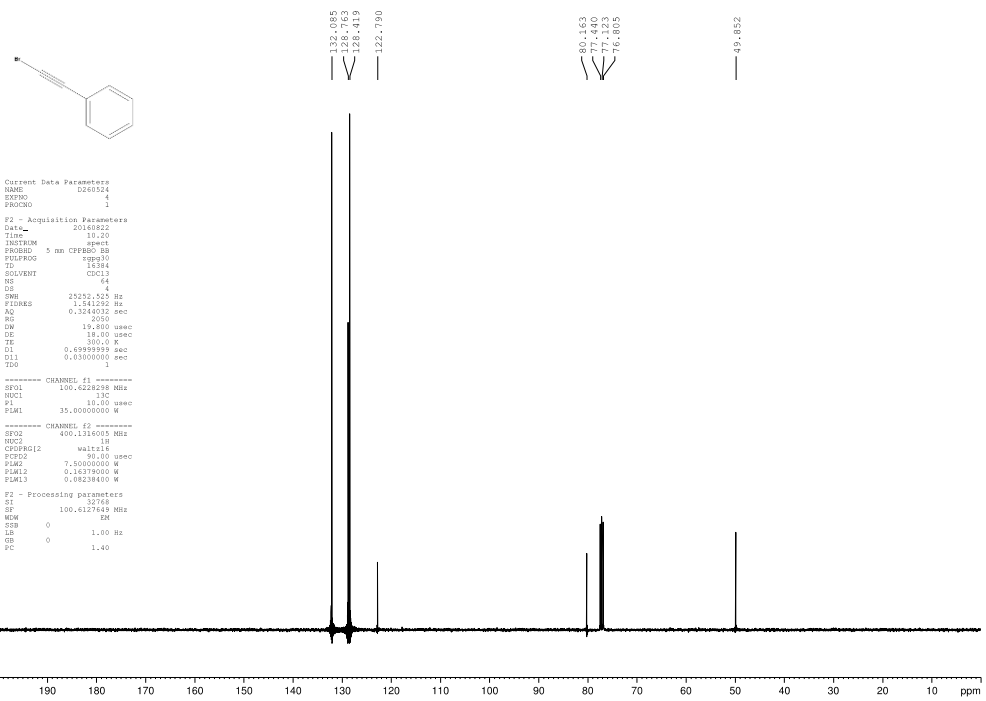
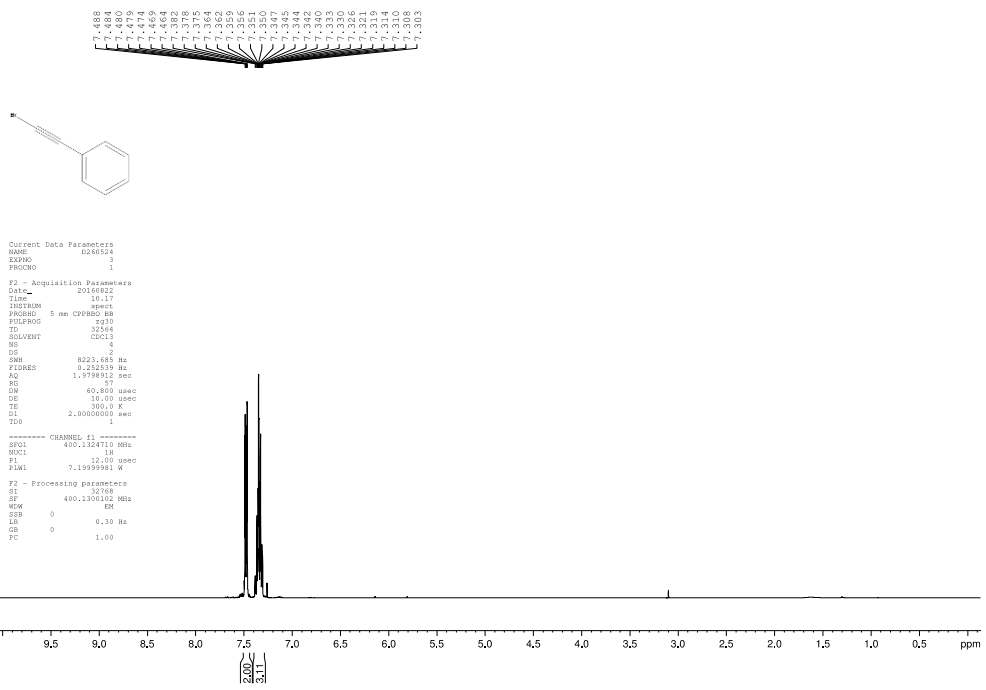
81.924
81.221
77.517
76.838

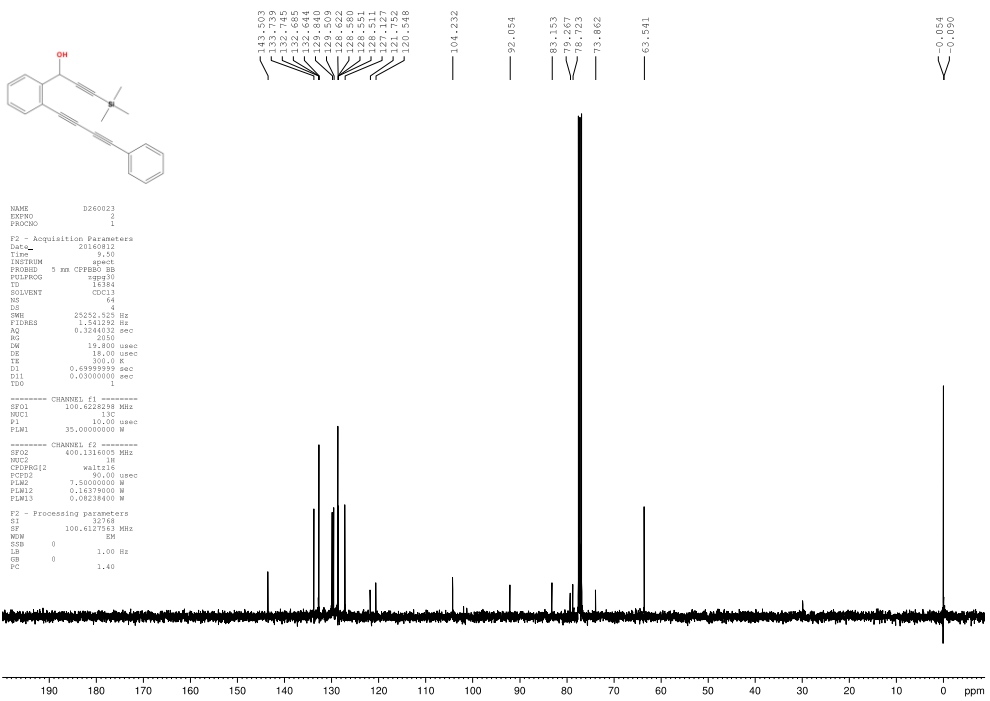
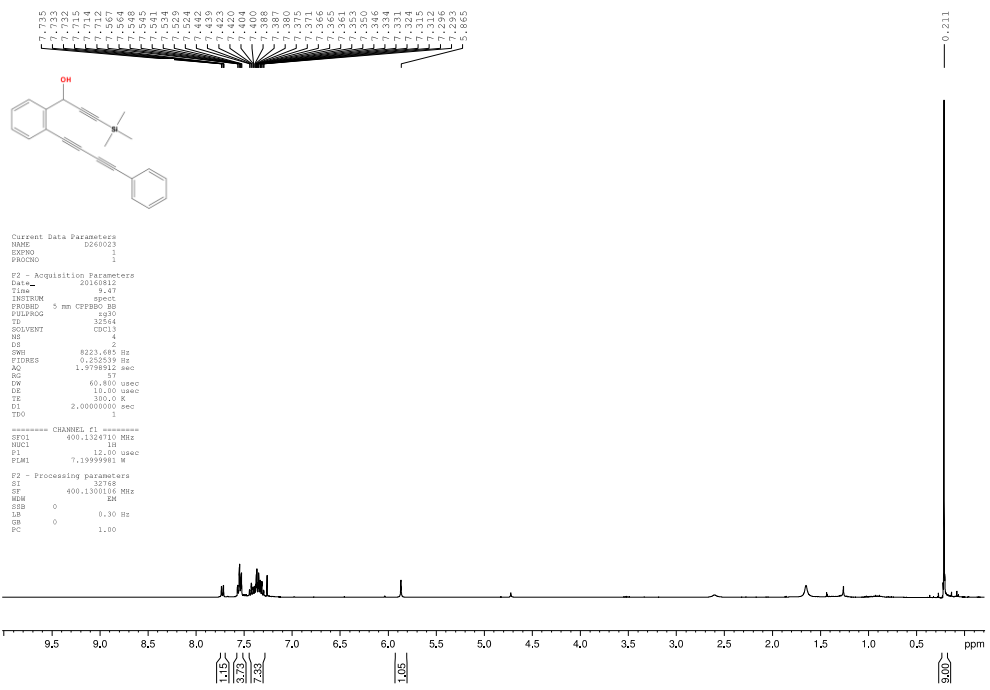


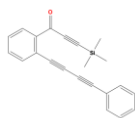












```

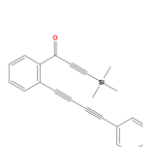
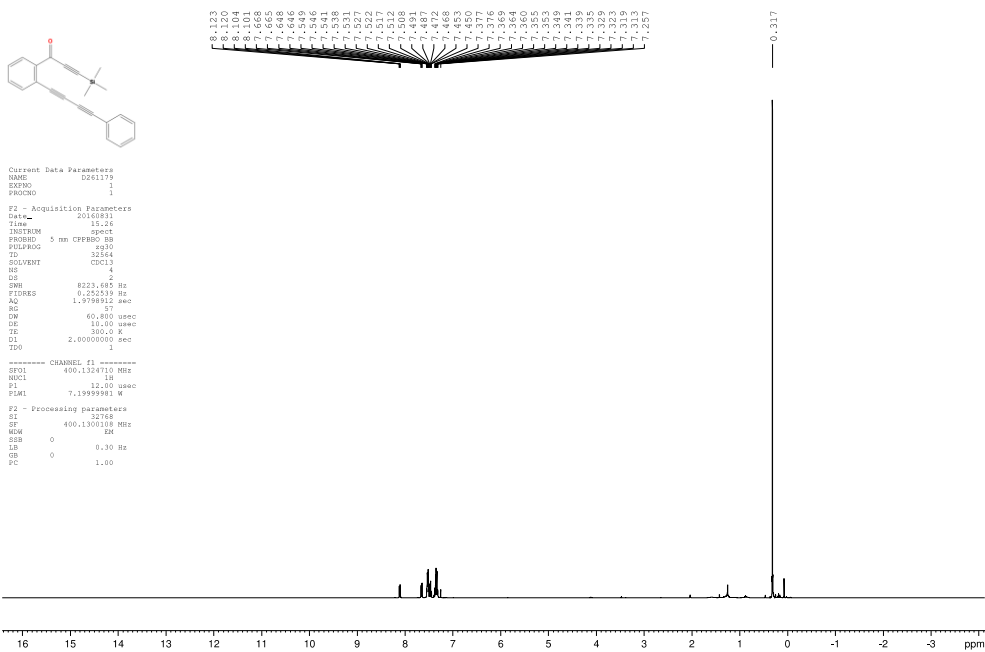
Current Data Parameters
NAME      DS61178
EXPNO    1
PROCNO   1

F2 - Acquisition Parameters
Date_    20160811
Time     15:26
INSTRUM  spect
PROBHD   5 mm CPBPR80 BB
PULPROG  zgpg30
TD       32764
SOLVENT  CDCl3
NS       2
DS       4
SWH      823.685 Hz
FIDRES   0.342919 Hz
AQ       1.3798912 sec
RG       57
DN       40.800 usec
DE       16.00 usec
TE       300.0 K
D1       2.0000000 sec
ZPD      1

===== CHANNEL f1 =====
SFO1    400.130100 MHz
NUC1    1H
P1      12.00 usec
PLM1    7.19999981 W

F2 - Processing parameters
SI      32768
SF      400.130100 MHz
WDW     EM
SSB     0
LB      0.30 Hz
GB      0
PC      1.00
  
```

8.123
8.092
8.050
8.010
7.968
7.926
7.884
7.842
7.800
7.758
7.716
7.674
7.632
7.590
7.548
7.506
7.464
7.422
7.380
7.338
7.296
7.254
7.212
7.170
7.128
7.086
7.044
7.002
6.960
6.918
6.876
6.834
6.792
6.750
6.708
6.666
6.624
6.582
6.540
6.498
6.456
6.414
6.372
6.330
6.288
6.246
6.204
6.162
6.120
6.078
6.036
6.000
5.964
5.928
5.892
5.856
5.820
5.784
5.748
5.712
5.676
5.640
5.604
5.568
5.532
5.496
5.460
5.424
5.388
5.352
5.316
5.280
5.244
5.208
5.172
5.136
5.100
5.064
5.028
4.992
4.956
4.920
4.884
4.848
4.812
4.776
4.740
4.704
4.668
4.632
4.596
4.560
4.524
4.488
4.452
4.416
4.380
4.344
4.308
4.272
4.236
4.200
4.164
4.128
4.092
4.056
4.020
3.984
3.948
3.912
3.876
3.840
3.804
3.768
3.732
3.696
3.660
3.624
3.588
3.552
3.516
3.480
3.444
3.408
3.372
3.336
3.300
3.264
3.228
3.192
3.156
3.120
3.084
3.048
3.012
2.976
2.940
2.904
2.868
2.832
2.796
2.760
2.724
2.688
2.652
2.616
2.580
2.544
2.508
2.472
2.436
2.400
2.364
2.328
2.292
2.256
2.220
2.184
2.148
2.112
2.076
2.040
2.004
1.968
1.932
1.896
1.860
1.824
1.788
1.752
1.716
1.680
1.644
1.608
1.572
1.536
1.500
1.464
1.428
1.392
1.356
1.320
1.284
1.248
1.212
1.176
1.140
1.104
1.068
1.032
0.996
0.960
0.924
0.888
0.852
0.816
0.780
0.744
0.708
0.672
0.636
0.600
0.564
0.528
0.492
0.456
0.420
0.384
0.348
0.312
0.276
0.240
0.204
0.168
0.132
0.096
0.060
0.024
0.000



```

Current Data Parameters
NAME      DS61178
EXPNO    2
PROCNO   1

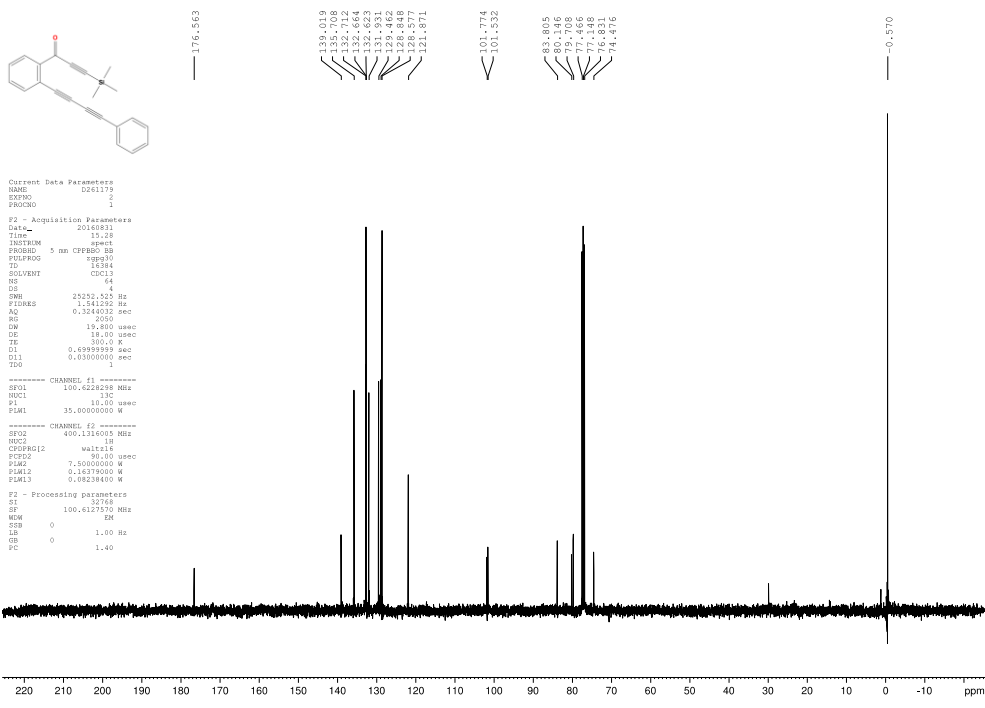
F2 - Acquisition Parameters
Date_    20160811
Time     15:28
INSTRUM  spect
PROBHD   5 mm CPBPR80 BB
PULPROG  zgpg30
TD       15384
SOLVENT  CDCl3
NS       4
DS       4
SWH      23232.523 Hz
FIDRES   1.141250 Hz
AQ       0.3244032 sec
RG       2050
DN       19.800 usec
DE       16.00 usec
TE       300.0 K
D1       0.6999999 sec
D11      0.0300000 sec
ZPD      1

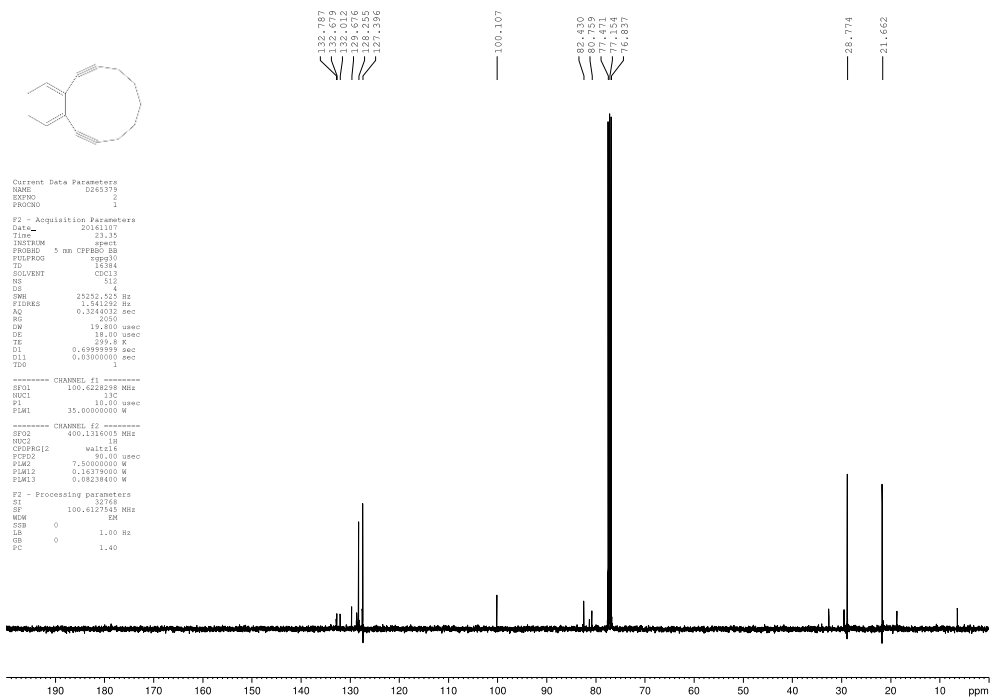
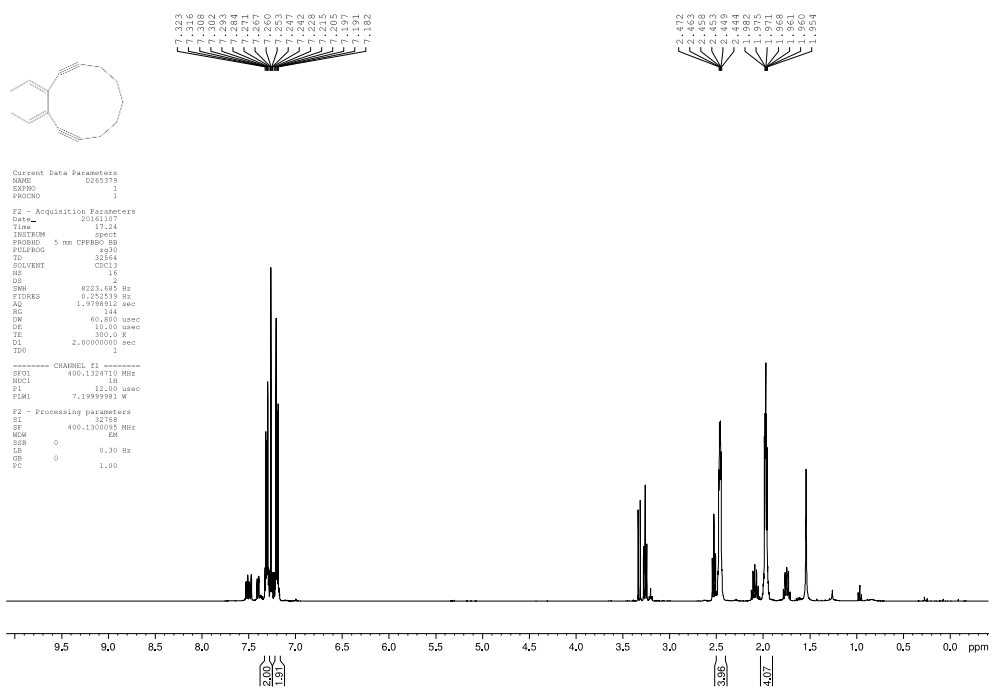
===== CHANNEL f1 =====
SFO1    100.628210 MHz
NUC1    13C
P1      12.00 usec
PLM1    35.0000000 W

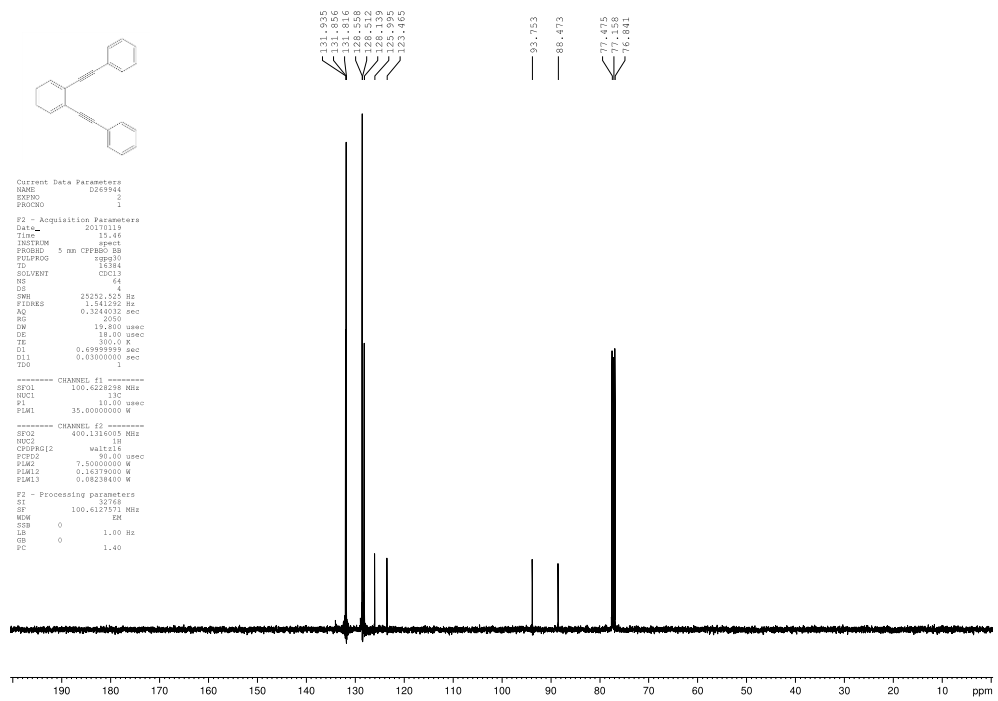
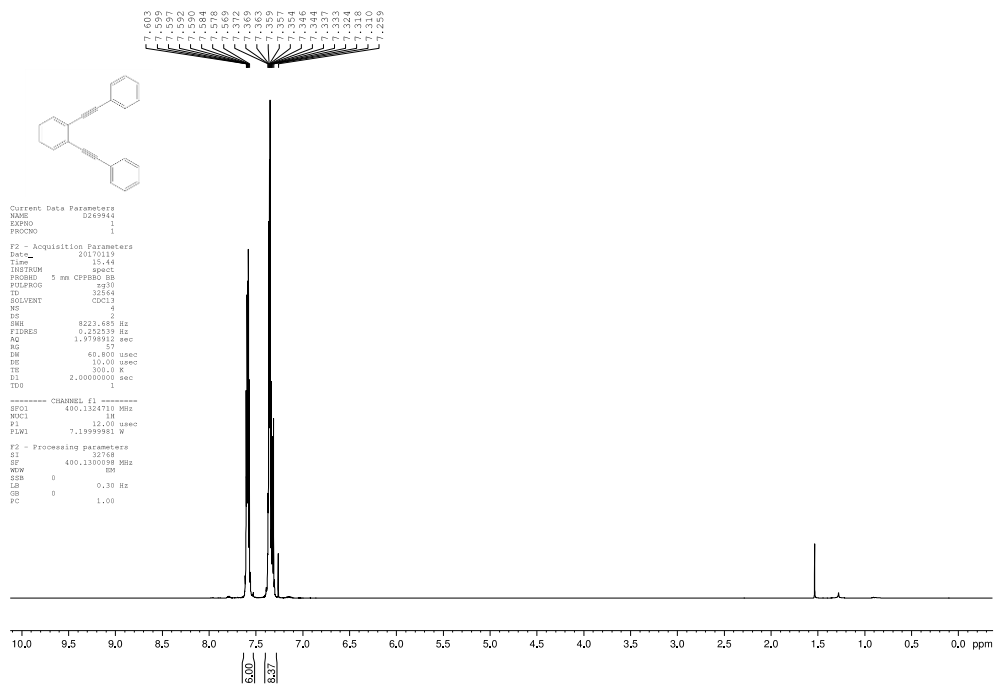
===== CHANNEL f2 =====
SFO2    400.130100 MHz
NUC2    1H
PCPDPRG2 waltraic
P1PD2   96.00 usec
PLM2    7.5000000 W
PLM12   0.14279000 W
PLM13   0.00238000 W

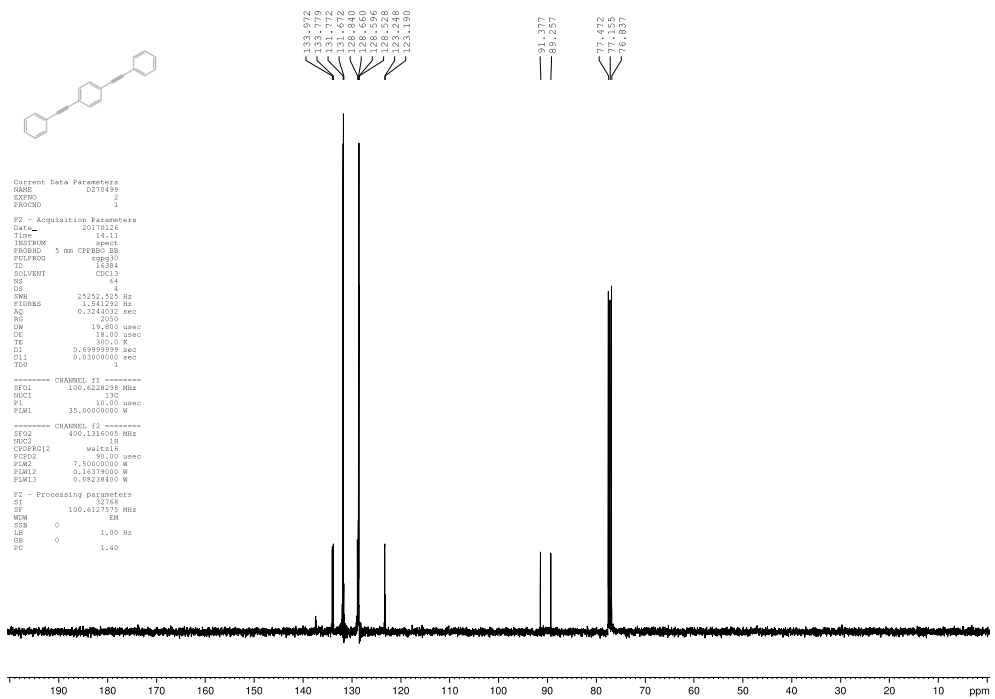
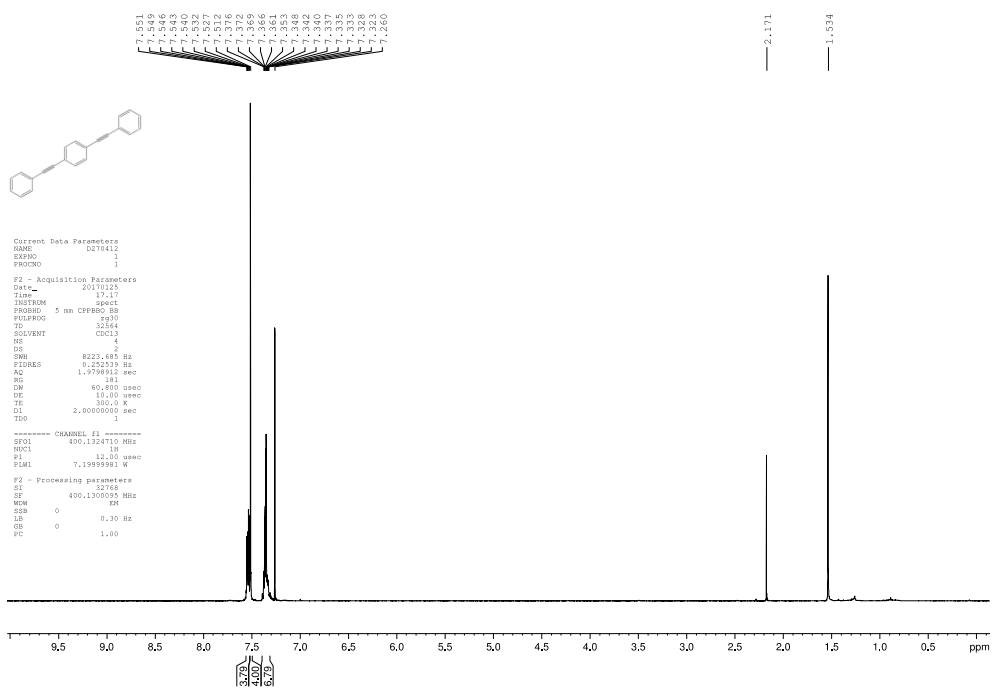
F2 - Processing parameters
SI      32768
SF      100.617970 MHz
WDW     EM
SSB     0
LB      1.00 Hz
GB      0
PC      1.40
  
```

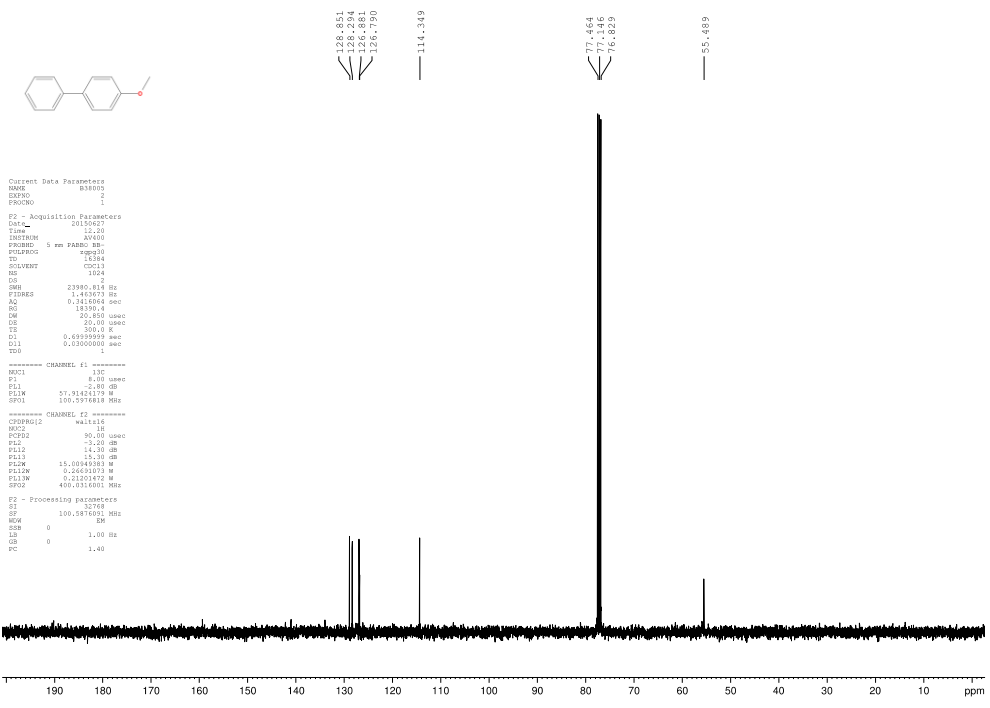
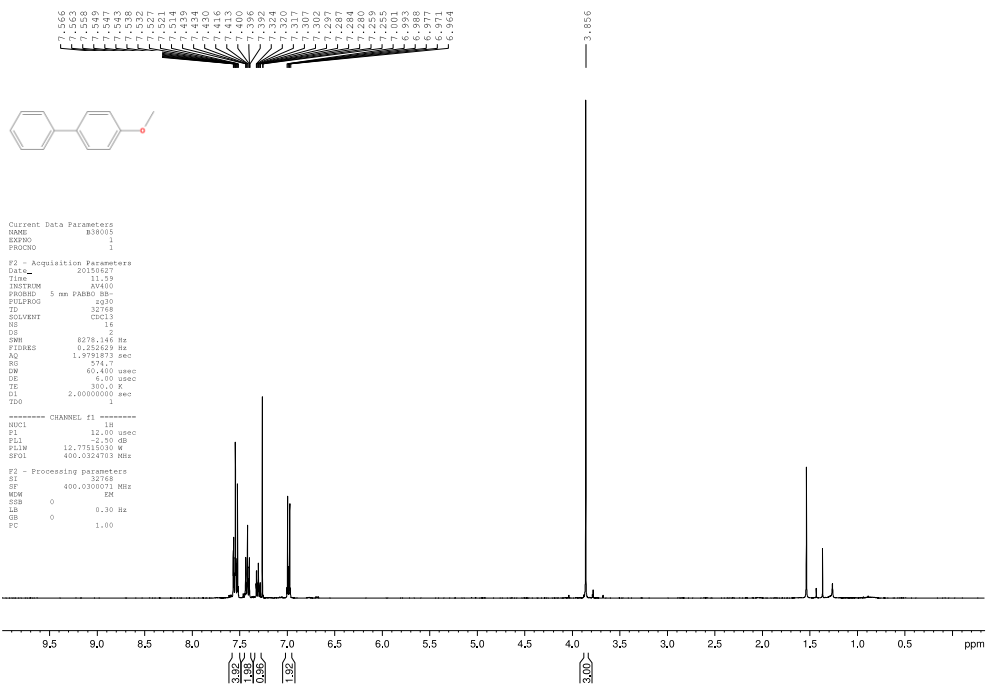
176.563
139.019
135.708
132.442
129.176
125.910
122.644
119.378
116.112
112.846
109.580
106.314
103.048
100.000
101.774
101.532
83.805
80.146
79.708
77.488
76.431
74.876

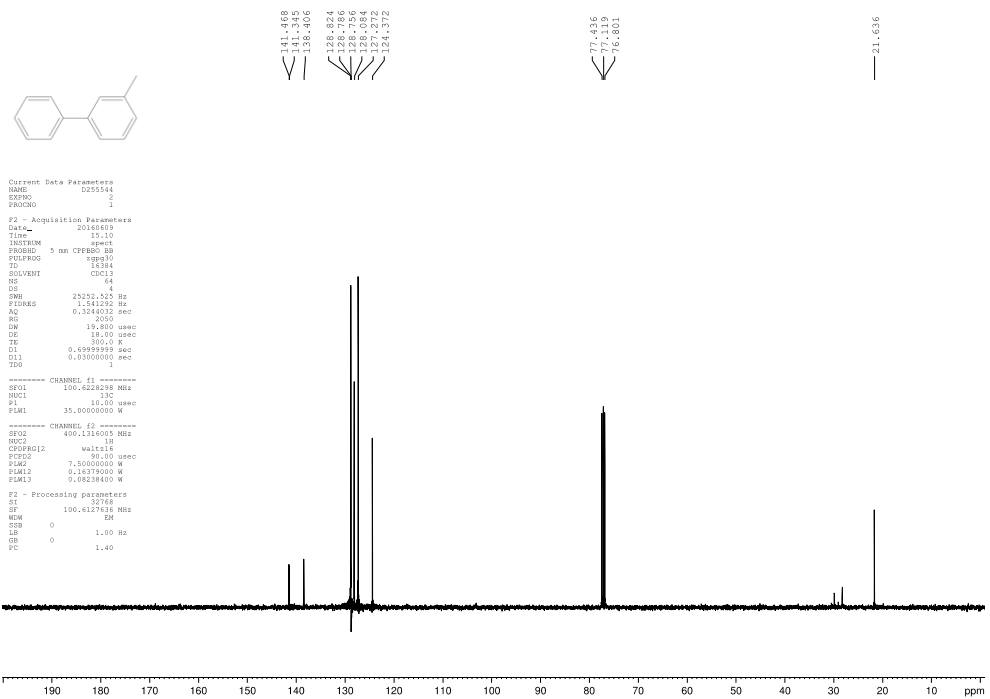
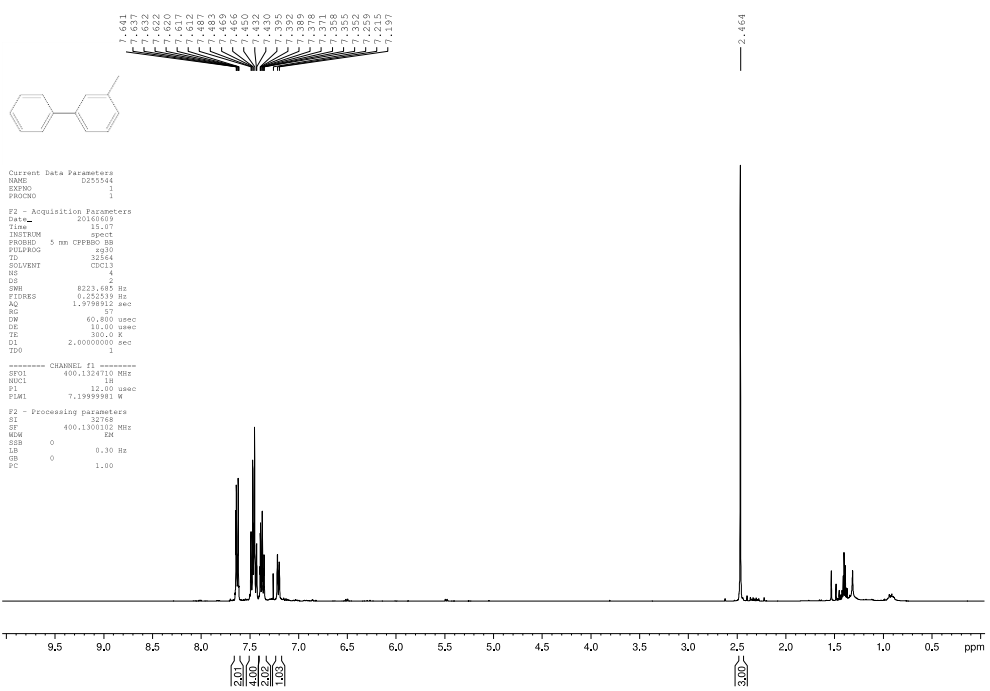


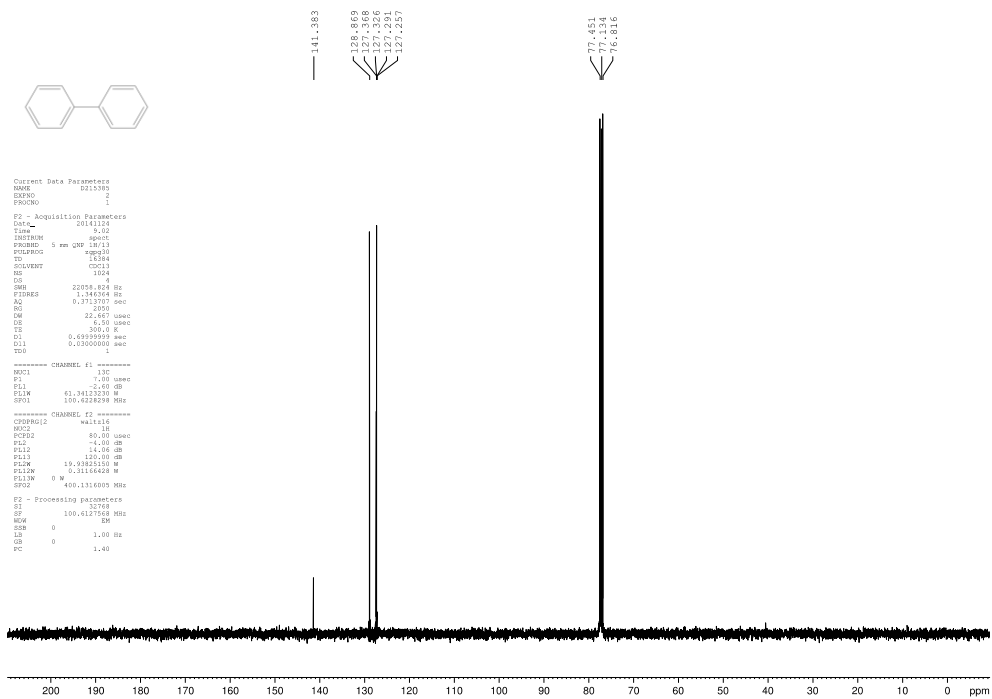
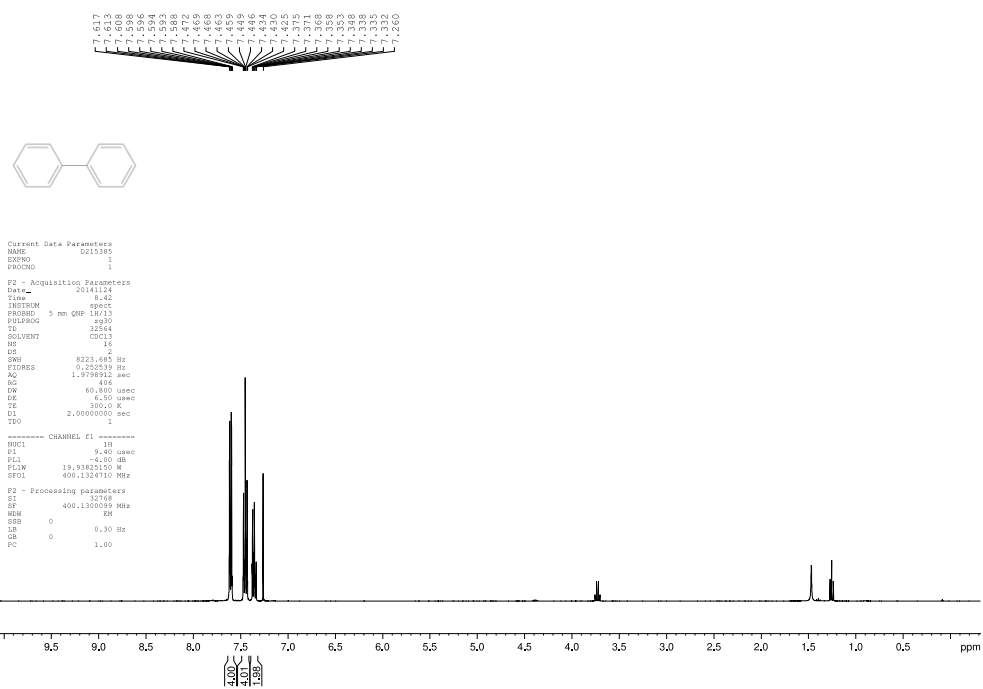


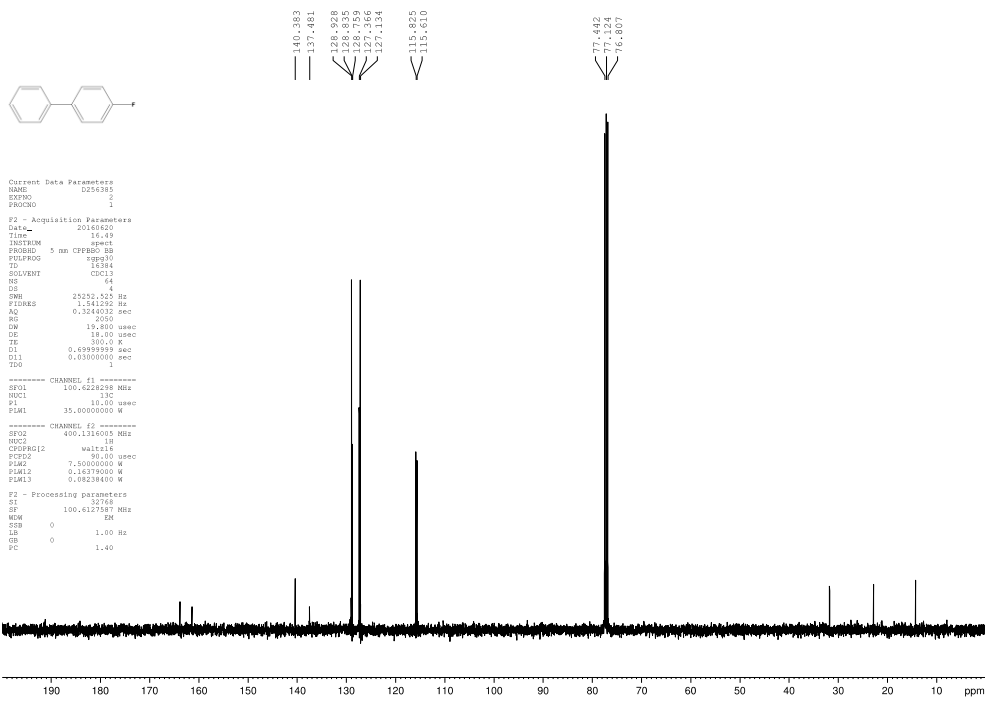
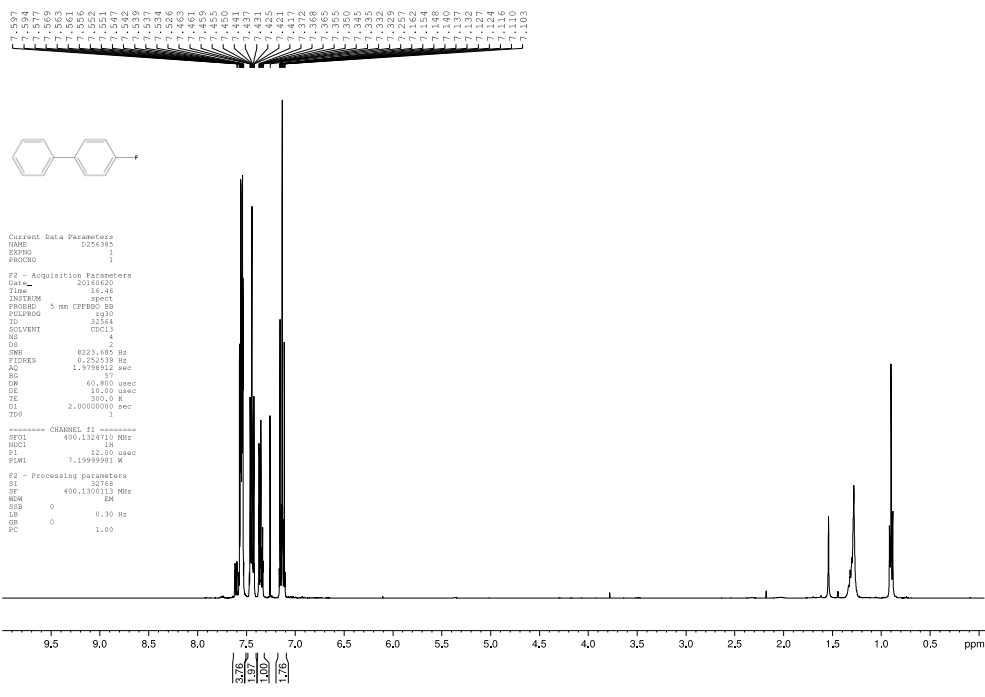


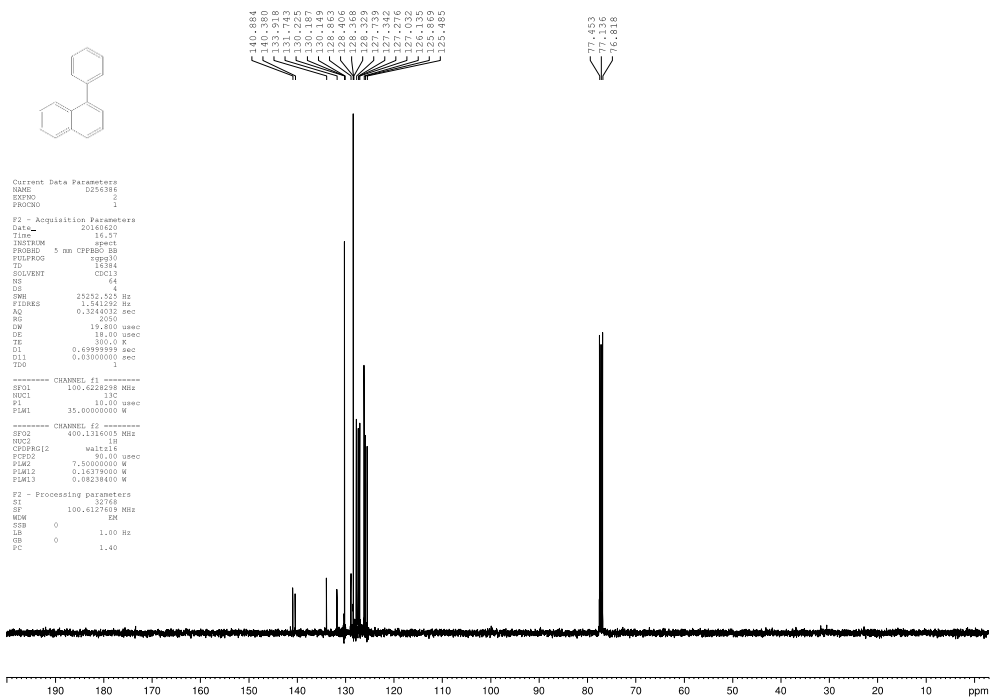
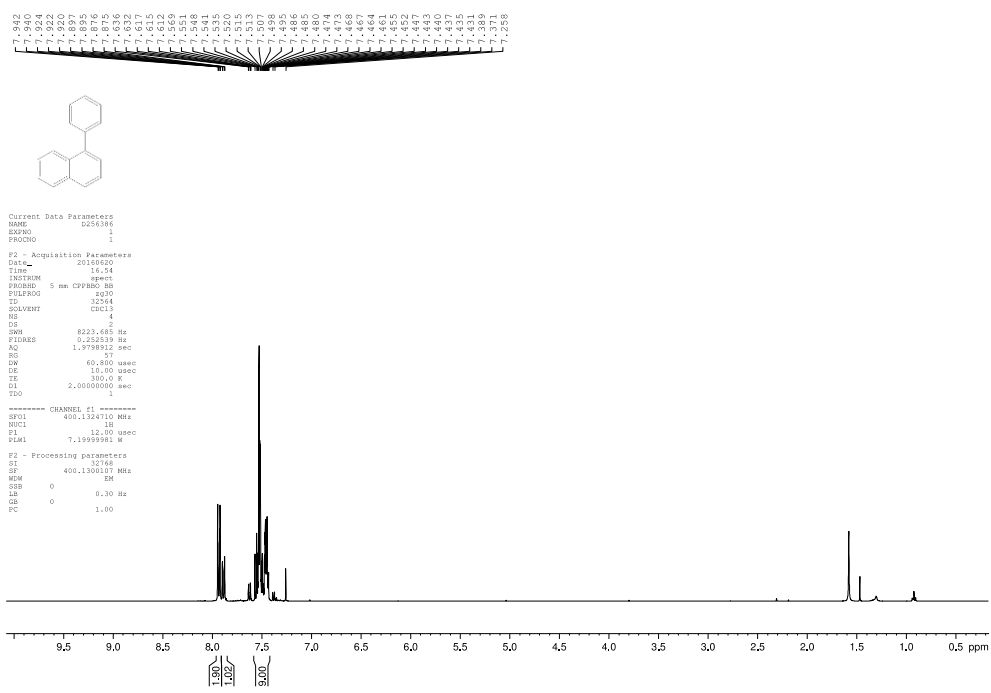












10. References

1. Johansson Seechurn, C. C.; Kitching, M. O.; Colacot, T. J.; Snieckus, V., *Angew Chem Int Ed* **2012**, *51* (21), 5062-85.
2. "The Nobel Prize in Chemistry 2010".
http://www.nobelprize.org/nobel_prizes/chemistry/laureates/2010/ (accessed 30th June 2017).
3. Heck, R. F., *J Am Chem Soc*, **1968**, *90* (20), 5531-&.
4. Heck, R. F.; Nolley, J. P., *J Org Chem* **1972**, *37* (14), 2320-&.
5. Mizoroki, T.; Mori, K.; Ozaki, A., *Bull Chem Soc Jpn* **1971**, *44* (2), 581-+.
6. Miyaura, N.; Suzuki, A., *J Chem Soc Chem Commun* **1979**, (19), 866-867.
7. Milstein, D.; Stille, J. K., *J Am Chem Soc*, **1978**, *100* (11), 3636-3638.
8. Tamao, K.; Sumitani, K.; Kumada, M., *J Am Chem Soc*, **1972**, *94* (12), 4374-&.
9. Negishi, E.; Valente, L. F.; Kobayashi, M., *J Am Chem Soc*, **1980**, *102* (9), 3298-3299.
10. Hatanaka, Y.; Hiyama, T., *J Org Chem* **1988**, *53* (4), 918-920.
11. Tohda, Y.; Sonogashira, K.; Hagihara, N., *J Chem Soc Chem Commun* **1975**, (2), 54-55.
12. Lennox, A. J. J.; Lloyd-Jones, G. C., *Isr J Chem* **2010**, *50* (5-6), 664-674.
13. Carrow, B. P.; Hartwig, J. F., *J Am Chem Soc*, **2011**, *133* (7), 2116-2119.
14. Kitamura, Y.; Sakurai, A.; Udzu, T.; Maegawa, T.; Monguchi, Y.; Sajiki, H., *Tetrahedron* **2007**, *63* (43), 10596-10602.
15. Asano, S.; Kamioka, S.; Isobe, Y., *Tetrahedron* **2012**, *68* (1), 272-279.
16. Matos, K.; Soderquist, J. A., *J Org Chem* **1998**, *63* (3), 461-470.
17. Maluenda, I.; Navarro, O., *Molecules* **2015**, *20* (5), 7528-7557.
18. Koyama, Y.; Lear, M. J.; Yoshimura, F.; Ohashi, I.; Mashimo, T.; Hiram, M., *Org Lett* **2005**, *7* (2), 267-270.
19. Cooke, J. W. B.; Bright, R.; Coleman, M. J.; Jenkins, K. P., *Org Process Res Dev* **2001**, *5* (4), 383-386.
20. Tobe, Y.; Umeda, R.; Sonoda, M.; Wakabayashi, T., *Chem Eur J* **2005**, *11* (5), 1603-1609.
21. Chinchilla, R.; Najera, C., *Chem Rev* **2007**, *107* (3), 874-922.
22. Leadbeater, N. E.; Marco, M., *Org Lett* **2002**, *4* (17), 2973-2976.
23. Leadbeater, N. E.; Marco, M., *Angew Chem Int Ed* **2003**, *42* (12), 1407-1409.
24. Leadbeater, N. E.; Marco, M., *J Org Chem* **2003**, *68* (14), 5660-7.
25. Thathagar, M. B.; Beckers, J.; Rothenberg, G., *J Am Chem Soc*, **2002**, *124* (40), 11858-11859.
26. Arvela, R. K.; Leadbeater, N. E.; Sangi, M. S.; Williams, V. A.; Granados, P.; Singer, R. D., *J Org Chem* **2005**, *70* (1), 161-8.
27. Wittig, G., *Naturwissenschaften* **1942**, *30*, 696-703.
28. Bunnett, J. F., *J Chem Educ* **1961**, *38* (6), 278-285.
29. Gann, A. W.; Amoroso, J. W.; Einck, V. J.; Rice, W. P.; Chambers, J. J.; Schnarr, N. A., *Org Lett* **2014**, *16* (7), 2003-2005.
30. Himeshima, Y.; Sonoda, T.; Kobayashi, H., *Chem Lett* **1983**, (8), 1211-1214.
31. Wentrup, C., *Aust J Chem* **2010**, *63* (7), 979-986.
32. Hoye, T. R.; Baire, B.; Niu, D. W.; Willoughby, P. H.; Woods, B. P., *Nature* **2012**, *490* (7419), 208-212.
33. Kitamura, T., *Aust J Chem* **2010**, *63* (7), 987-1001.
34. Medina, J. M.; Jackl, M. K.; Susick, R. B.; Garg, N. K., *Tetrahedron* **2016**, *72* (26), 3629-3634.
35. Medina, J. M.; Mackey, J. L.; Garg, N. K.; Houk, K. N., *J Am Chem Soc*, **2014**, *136* (44), 15798-15805.
36. Picazo, E.; Houk, K. N.; Garg, N. K., *Tetrahedron Lett* **2015**, *56* (23), 3511-3514.

37. Marell, D. J.; Furan, L. R.; Woods, B. P.; Lei, X. Y.; Bendel-Smith, A. J.; Cramer, C. J.; Hoye, T. R.; Kuwata, K. T., *J Org Chem* **2015**, *80* (23), 11744-11754.
38. Wang, T.; Niu, D. W.; Hoye, T. R., *J Am Chem Soc*, **2016**, *138* (25), 7832-7835.
39. Xu, F.; Xiao, X.; Hoye, T. R., *Org Lett* **2016**, *18* (21), 5636-5639.
40. Zhang, J. T.; Niu, D. W.; Brinker, V. A.; Hoye, T. R., *Org Lett* **2016**, *18* (21), 5596-5599.
41. Ross, S. P.; Hoye, T. R., *Nat Chem* **2017**, *9* (6), 523-530.
42. Xu, F.; Xiao, X.; Hoye, T. R., *J Am Chem Soc*, **2017**, *139* (25), 8400-8403.
43. Karmakar, R.; Lee, D., *Org Lett* **2016**, *18* (23), 6105-6107.
44. Sowden, M. J.; Sherburn, M. S., *Org Lett* **2017**, *19* (3), 636-637.
45. Demirer, H.; Kartal, I.; Cakir, M., *Acta Phys Pol A* **2017**, *131* (3), 555-558.
46. Guler, B.; Onen, H. A.; Karahasanoglu, M.; Serhatli, E.; Canak, T. C., *Prog Org Coat* **2017**, *109*, 152-159.
47. Bukhari, S. A. M.; Khan, M. F.; Goswami, A.; McGee, R.; Thundat, T., *Rsc Adv* **2017**, *7* (14), 8415-8420.
48. Guven, M. N.; Altuncu, M. S.; Duman, F. D.; Eren, T. N.; Acar, H. Y.; Avci, D., *J Biomed Mater Res A* **2017**, *105* (5), 1412-1421.
49. Djakovitch, L. W.; Michael, K.; Kohler, K., *J Organomet Chem* **1999**, *592* (2), 225-234.
50. Liu, Z.; Larock, R. C., *Org Lett* **2003**, *5* (24), 4673-5.
51. Liu, Z.; Larock, R. C., *Org Lett* **2004**, *6* (1), 99-102.
52. Liu, Z.; Larock, R. C., *J Org Chem* **2006**, *71* (8), 3198-209.
53. Raminelli, C.; Liu, Z.; Larock, R. C., *J Org Chem* **2006**, *71* (12), 4689-91.
54. Shaibu, B. S.; Kawade, R. K.; Liu, R. S., *Org Biomol Chem* **2012**, *10* (34), 6834-9.
55. Bajracharya, G. B.; Daugulis, O., *Org Lett* **2008**, *10* (20), 4625-8.
56. Doni, E.; Murphy, J. A., *Chem Commun* **2014**, *50* (46), 6073-6087.
57. Pruetz, R. L.; Barr, J. T.; Rapp, K. E.; Bahner, C. T.; Gibson, J. D.; Lafferty, R. H., *J Am Chem Soc* **1950**, *72* (8), 3646-3650.
58. Wudl, F.; Smith, G. M.; Hufnagel, E. J., *J Chem Soc D-Chem Commun* **1970**, (21), 1453-&.
59. Lampard, C.; Murphy, J. A.; Lewis, N., *J Chem Soc Chem Commun* **1993**, (3), 295-297.
60. Murphy, J. A., *J Org Chem* **2014**, *79* (9), 3731-46.
61. Takechi, N.; Ait-Mohand, S.; Medebielle, M.; Dolbier, W. R., *Tetrahedron Lett* **2002**, *43* (24), 4317-4319.
62. Giuglio-Tonolo, G.; Terme, T.; Medebielle, M.; Vanelle, P., *Tetrahedron Lett* **2003**, *44* (34), 6433-6435.
63. Giuglio-Tonolo, G.; Terme, T.; Medebielle, M.; Vanelle, P., *Tetrahedron Lett* **2004**, *45* (26), 5121-5124.
64. Murphy, J. A.; Khan, T. A.; Zhou, S. Z.; Thomson, D. W.; Mahesh, M., *Angew Chem Int Ed* **2005**, *44* (9), 1356-60.
65. Taton, T. A.; Chen, P., *Angew Chem Int Ed* **1996**, *35* (9), 1011-1013.
66. Schoenebeck, F.; Murphy, J. A.; Zhou, S.-z.; Uenoyama, Y.; Miclo, Y.; Tuttle, T., *J Am Chem Soc* **2007**, *129* (44), 13368-+.
67. Garnier, J.; Murphy, J. A.; Zhou, S.-Z.; Turner, A. T., *Synlett* **2008**, (14), 2127-2131.
68. Murphy, J. A.; Garnier, J.; Park, S. R.; Schoenebeck, F.; Zhou, S. Z.; Turner, A. T., *Org Lett* **2008**, *10* (6), 1227-1230.
69. Garnier, J.; Kennedy, A. R.; Berlouis, L. E. A.; Turner, A. T.; Murphy, J. A., *Beilstein J Org Chem* **2010**, *6*.
70. Cutulic, S. P. Y.; Murphy, J. A.; Farwaha, H.; Zhou, S.-Z.; Chrystal, E., *Synlett* **2008**, (14), 2132-2136.
71. Cutulic, S. P. Y.; Findlay, N. J.; Zhou, S.-Z.; Chrystal, E. J. T.; Murphy, J. A., *J Org Chem* **2009**, *74* (22), 8713-8718.
72. Jolly, P. I.; Fleary-Roberts, N.; O'Sullivan, S.; Doni, E.; Zhou, S.; Murphy, J. A., *Org Biomol Chem* **2012**, *10* (30), 5807-5810.

73. Doni, E.; O'Sullivan, S.; Murphy, J. A., *Angew Chem Int Ed* **2013**, *52* (8), 2239-2242.
74. Chua, J., Intramolecular Communication between π -Systems in the Cleavage of C–O and C–C σ -Bonds by Organic Super Electron Donors. Phd Thesis **2017**.
75. O'Sullivan, S.; Doni, E.; Tuttle, T.; Murphy, J. A., *Angew Chem Int Ed* **2014**, *53* (2), 474-478.
76. Doni, E.; Mondal, B.; O'Sullivan, S.; Tuttle, T.; Murphy, J. A., *J Am Chem Soc* **2013**, *135* (30), 10934-10937.
77. Yanagisawa, S.; Ueda, K.; Taniguchi, T.; Itami, K., *Org Lett* **2008**, *10* (20), 4673-6.
78. Liu, W.; Cao, H.; Zhang, H.; Chung, K. H.; He, C. A.; Wang, H. B.; Kwong, F. Y.; Lei, A. W., *J Am Chem Soc* **2010**, *132* (47), 16737-16740.
79. Wotiz, J. H.; Kleopfer, R. D.; Barelski, P. M.; Hinckley, C. C.; Koster, D. F., *J Org Chem* **1972**, *37* (11), 1758-1763.
80. Sun, C. L.; Li, H.; Yu, D. G.; Yu, M.; Zhou, X.; Lu, X. Y.; Huang, K.; Zheng, S. F.; Li, B. J.; Shi, Z. J., *Nat Chem* **2010**, *2* (12), 1044-9.
81. Shirakawa, E.; Itoh, K.; Higashino, T.; Hayashi, T., *J Am Chem Soc* **2010**, *132* (44), 15537-15539.
82. Shirakawa, E.; Hayashi, T., *Chem Lett* **2012**, *41* (2), 130-134.
83. Rueping, M.; Leiendecker, M.; Das, A.; Poisson, T.; Bui, L., *Chem Commun* **2011**, *47* (38), 10629-31.
84. Shirakawa, E.; Zhang, X. J.; Hayashi, T., *Angew Chem Int Ed* **2011**, *50* (20), 4671-4674.
85. Sun, C. L.; Gu, Y. F.; Wang, B.; Shi, Z. J., *Chem Eur J* **2011**, *17* (39), 10844-10847.
86. Guastavino, J. F.; Buden, M. E.; Rossi, R. A., *J Org Chem* **2014**, *79* (19), 9104-9111.
87. Rossi, R. A.; Pierini, A. B.; Penenory, A. B., *Chem Rev* **2003**, *103* (1), 71-167.
88. Schmidt, L. C.; Arguello, J. E.; Penenory, A. B., *J Org Chem* **2007**, *72* (8), 2936-2944.
89. Studer, A.; Curran, D. P., *Angew Chem Int Ed* **2011**, *50* (22), 5018-22.
90. Studer, A.; Curran, D. P., *Nat Chem* **2014**, *6* (9), 765-73.
91. Wu, Y.; Wong, S. M.; Mao, F.; Chan, T. L.; Kwong, F. Y., *Org Lett* **2012**, *14* (20), 5306-9.
92. Qiu, Y.; Liu, Y.; Yang, K.; Hong, W.; Li, Z.; Wang, Z.; Yao, Z.; Jiang, S., *Org Lett* **2011**, *13* (14), 3556-9.
93. Tintori, G.; Nabokoff, P.; Buhaibeh, R.; Berge-Lefranc, D.; Redon, S.; Broggi, J.; Vanelle, P., *Angew Chem Int Ed* **2018**, *57* (12), 3148-3153.
94. Liu, H. L.; Yin, B. L.; Gao, Z. Q.; Li, Y. W.; Jiang, H. F., *Chem Commun* **2012**, *48* (14), 2033-2035.
95. Yong, G. P.; She, W. L.; Zhang, Y. M.; Li, Y. Z., *Chem Commun* **2011**, *47* (42), 11766-11768.
96. Tanimoro, K.; Ueno, M.; Takeda, K.; Kirihata, M.; Tanimori, S., *J Org Chem* **2012**, *77* (18), 7844-9.
97. Zhao, H. Q.; Shen, J.; Guo, J. J.; Ye, R. J.; Zeng, H. Q., *Chem Commun* **2013**, *49* (23), 2323-2325.
98. Sharma, S.; Kumar, M.; Kumar, V.; Kumar, N., *Tetrahedron Lett* **2013**, *54* (36), 4868-4871.
99. Buden, M. E.; Guastavino, J. F.; Rossi, R. A., *Org Lett* **2013**, *15* (6), 1174-1177.
100. Liu, W.; Xu, L. G., *Tetrahedron* **2015**, *71* (30), 4974-4981.
101. Roman, D. S.; Takahashi, Y.; Charette, A. B., *Org Lett* **2011**, *13* (12), 3242-5.
102. Bhakuni, B. S.; Kumar, A.; Balkrishna, S. J.; Sheikh, J. A.; Konar, S.; Kumar, S., *Org Lett* **2012**, *14* (11), 2838-2841.
103. Bhakuni, B. S.; Yadav, A.; Kumar, S.; Patel, S.; Sharma, S., *J Org Chem* **2014**, *79* (7), 2944-2954.
104. Zhou, S.; Anderson, G. M.; Mondal, B.; Doni, E.; Ironmonger, V.; Kranz, M.; Tuttle, T.; Murphy, J. A., *Chem Sci* **2014**, *5* (2), 476-482.

105. Zhou, S.; Doni, E.; Anderson, G. M.; Kane, R. G.; MacDougall, S. W.; Ironmonger, V. M.; Tuttle, T.; Murphy, J. A., *J Am Chem Soc* **2014**, *136* (51), 17818-17826.
106. Ashby, E. C.; Goel, A. B.; Depriest, R. N., *J Org Chem* **1981**, *46* (11), 2429-2431.
107. Cuthbertson, J.; Gray, V. J.; Wilden, J. D., *Chem Commun* **2014**, *50* (20), 2575-2578.
108. Yi, H.; Jutand, A.; Lei, A., *Chem Commun* **2015**, *51* (3), 545-8.
109. De, S.; Ghosh, S.; Bhunia, S.; Sheikh, J. A.; Bisai, A., *Org Lett* **2012**, *14* (17), 4466-4469.
110. De, S.; Mishra, S.; Kakde, B. N.; Dey, D.; Bisai, A., *J Org Chem* **2013**, *78* (16), 7823-7844.
111. Drapeau, M. P.; Fabre, I.; Grimaud, L.; Ciofini, I.; Ollevier, T.; Taillefer, M., *Angew Chem Int Ed* **2015**, *54* (36), 10587-10591.
112. Barham, J.; Coulthard, G.; Emery, K.; Doni, E.; Cumine, F.; Nocera, G.; John, M.; Berlouis, L.; McGuire, T.; Tuttle, T.; Murphy, J., *J Am Chem Soc* **2016**, *138* (23), 7402-7410.
113. Patil, M., *J Org Chem* **2016**, *81* (2), 632-639.
114. Chen, W. C.; Hsu, Y. C.; Shih, W. C.; Lee, C. Y.; Chuang, W. H.; Tsai, Y. F.; Chen, P. P. Y.; Ong, T. G., *Chem Commun* **2012**, *48* (53), 6702-6704.
115. Khan, T. A.; Murphy, J. A., *Abst Am Chem Soc* **2006**, 231.
116. Pieber, B.; Cantillo, D.; Kappe, C. O., *Chem Eur J* **2012**, *18* (16), 5047-5055.
117. Jensen, F., *Introduction to Computational Chemistry*. 2nd ed.; Wiley: London, 2006; p 620.
118. Hohenberg, P.; Kohn, W., *Phys Rev B* **1964**, *136* (3B), B864-+.
119. Kohn, W.; Sham, L. J., *Phys Rev* **1965**, *140* (4A), 1133-&.
120. Zhao, Y.; Truhlar, D. G., *Theor Chem Acc* **2007**, *120* (1-3), 215-241.
121. Hehre, W. J.; Stewart, R. F.; Pople, J. A., *J Chem Phys* **1969**, *51* (6), 2657-+.
122. Marcus, R. A., *J Chem Phys* **1956**, *24* (5), 979-989.
123. Marcus, R. A., *J Chem Phys* **1956**, *24* (5), 966-978.
124. Marcus, R. A., *J Chem Phys* **1957**, *26* (4), 867-871.
125. Marcus, R. A., *J Chem Phys* **1957**, *26* (4), 872-877.
126. Anderson, G. M.; Cameron, I.; Murphy, J. A.; Tuttle, T., *Rsc Adv* **2016**, *6* (14), 11335-11343.
127. Sun, C. L.; Shi, Z. J., *Chem Rev* **2014**, *114* (18), 9219-80.
128. Frisch, M. J.; Trucks, G. W.; Schlegel, H. B.; Scuseria, G. E.; Robb, M. A.; Cheeseman, J. R.; Scalmani, G.; Barone, V.; Mennucci, B.; Petersson, G. A.; Nakatsuji, H.; Caricato, M.; Li, X.; Hratchian, H. P.; Izmaylov, A. F.; Bloino, J.; Zheng, G.; Sonnenberg, J. L.; Hada, M.; Ehara, M.; Toyota, K.; Fukuda, R.; Hasegawa, J.; Ishida, M.; Nakajima, T.; Honda, Y.; Kitao, O.; Nakai, H.; Vreven, T.; Montgomery Jr, J. A.; Peralta, J. E.; Ogliaro, F.; Bearpark, M. J.; Heyd, J.; Brothers, E. N.; Kudin, K. N.; Staroverov, V. N.; Kobayashi, R.; Normand, J.; Raghavachari, K.; Rendell, A. P.; Burant, J. C.; Iyengar, S. S.; Tomasi, J.; Cossi, M.; Rega, N.; Millam, N. J.; Klene, M.; Knox, J. E.; Cross, J. B.; Bakken, V.; Adamo, C.; Jaramillo, J.; Gomperts, R.; Stratmann, R. E.; Yazyev, O.; Austin, A. J.; Cammi, R.; Pomelli, C.; Ochterski, J. W.; Martin, R. L.; Morokuma, K.; Zakrzewski, V. G.; Voth, G. A.; Salvador, P.; Dannenberg, J. J.; Dapprich, S.; Daniels, A. D.; Farkas, Ö.; Foresman, J. B.; Ortiz, J. V.; Cioslowski, J.; Fox, D. J. *Gaussian 09*, Gaussian, Inc.: Wallingford, CT, USA, 2009.
129. Ditchfield, R.; Hehre, W. J.; Pople, J. A., *J Chem Phys* **1971**, *54* (2), 724-+.
130. Krishnan, R.; Binkley, J. S.; Seeger, R.; Pople, J. A., *J Chem Phys* **1980**, *72* (1), 650-654.
131. Cossi, M.; Barone, V., *J Chem Phys* **1998**, *109* (15), 6246-6254.
132. Cossi, M.; Rega, N.; Scalmani, G.; Barone, V., *J Comp Chem* **2003**, *24* (6), 669-681.
133. Chisholm, M. H.; Drake, S. R.; Naiini, A. A.; Streib, W. E., *Polyhedron* **1991**, *10* (3), 337-345.
134. Emery, K. J.; Tuttle, T.; Murphy, J. A., *Org Biomol Chem* **2017**, *15* (41), 8810-8819.
135. Barham, J.; Coulthard, G.; Kane, R.; Delgado, N.; John, M.; Murphy, J., *Angew Chem Int Ed* **2016**, *55* (14), 4492-4496.
136. Nelsen, S. F.; Blackstock, S. C.; Kim, Y., *J Am Chem Soc* **1987**, *109* (3), 677-682.
137. Yang, H.; Zhang, L.; Jiao, L., *Chem Eur J* **2017**, *23* (1), 65-69.

138. Gassman, P. G.; Benecke, H. P., *Tetrahedron Lett* **1969**, (14), 1089-&.
139. Bowne, A. T.; Christopher, T. A.; Levin, R. H., *Tetrahedron Lett* **1976**, (46), 4111-4114.
140. Jones, R. R.; Bergman, R. G., *J Am Chem Soc* **1972**, *94* (2), 660-&.
141. Wang, Y. S.; Finn, M. G., *J Am Chem Soc* **1995**, *117* (30), 8045-8046.
142. Nicolaou, K. C.; Dai, W. M., *Angew Chem Int Ed* **1991**, *30* (11), 1387-1416.
143. Nicolaou, K. C.; Dai, W. M.; Tsay, S. C.; Estevez, V. A.; Wrasidlo, W., *Science* **1992**, *256* (5060), 1172-1178.
144. Williams, D. E.; Bottriell, H.; Davies, J.; Tietjen, I.; Brockman, M. A.; Andersen, R. J., *Org Lett* **2015**, *17* (21), 5304-5307.
145. Lindahl, S. E.; Park, H.; Pink, M.; Zaleski, J. M., *J Am Chem Soc* **2013**, *135* (10), 3826-3833.
146. Chen, J. H.; Palani, V.; Hoye, T. R., *J Am Chem Soc* **2016**, *138* (13), 4318-4321.
147. Poloukhine, A.; Popik, V. V., *Chem Commun* **2005**, (5), 617-619.
148. Peterson, P. W.; Shevchenko, N.; Alabugin, I. V., *Org Lett* **2013**, *15* (9), 2238-2241.
149. Lewis, K. D.; Matzger, A. J., *J Am Chem Soc* **2005**, *127* (28), 9968-9969.
150. Mukhopadhyay, S.; Rothenberg, G.; Gitis, D.; Sasson, Y., *J Org Chem* **2000**, *65* (10), 3107-3110.
151. Kalvet, I.; Magnin, G.; Schoenebeck, F., *Angew Chem Int Ed* **2017**, *56* (6), 1581-1585.
152. Seechurn, C.; Sperger, T.; Scrase, T. G.; Schoenebeck, F.; Colacot, T. J., *J Am Chem Soc* **2017**, *139* (14), 5194-5200.
153. Canty, A. J.; Ariaifard, A.; Camasso, N. M.; Higgs, A. T.; Yates, B. F.; Sanford, M. S., *Dalton Trans* **2017**, *46* (11), 3742-3748.
154. Topczewski, J. J.; Sanford, M. S., *Chem Sci* **2015**, *6* (1), 70-76.
155. Venning, A. R.; Bohan, P. T.; Alexanian, E. J., *J Am Chem Soc* **2015**, *137* (11), 3731-4.
156. Marsella, M. J.; Yoon, K.; Estassi, S.; Tham, F. S.; Borchardt, D. B.; Bui, B. H.; Schreiner, P. R., *J Org Chem* **2005**, *70* (5), 1881-1884.
157. Garcia-Cruz, I.; Martinez-Magadan, J. M., *Pet Sci Technol* **2007**, *25* (1-2), 67-80.
158. Cramer, C. J.; Truhlar, D. G., *Chem Rev* **1999**, *99* (8), 2161-2200.
159. Cramer, C. J.; Truhlar, D. G., *Phys Chem Chem Phys* **2009**, *11* (46), 10757-10816.
160. Frisch, M. J.; Pople, J. A.; Binkley, J. S., *J Chem Phys* **1984**, *80* (7), 3265-3269.
161. McLean, A. D.; Chandler, G. S., *J Chem Phys* **1980**, *72* (10), 5639-5648.
162. Wenthold, P. G.; Squires, R. R.; Lineberger, W. C., *J Am Chem Soc* **1998**, *120* (21), 5279-5290.
163. Tanimoro, K.; Ueno, M.; Takeda, K.; Kirihata, M.; Tanimori, S., *J Org Chem* **2012**, *77* (18), 7844-7849.
164. Handel, H.; Pasquini, M. A.; Pierre, J. L., *Tetrahedron* **1980**, *36* (22), 3205-3208.
165. Hunter, A.; Renfrew, M.; Rettura, D.; Taylor, J. A.; Whitmore, J. M. J.; Williams, A., *J Am Chem Soc* **1995**, *117* (20), 5484-5491.
166. Nawaz, F.; Mohanan, K.; Charles, L.; Rajzmann, M.; Bonne, D.; Chuzel, O.; Rodriguez, J.; Coquerel, Y., *Chem Eur J* **2013**, *19* (51), 17578-17583.
167. Eumann, C. N. N.; Hooker, J. M.; Ritter, T., *Nature* **2016**, *534* (7607), 369-373.
168. Lloyd-Jones, G. C.; Moseley, J. D.; Renny, J. S., *Synthesis-Stuttgart* **2008**, (5), 661-689.
169. Kaga, A.; Hayashi, H.; Hakamata, H.; Oi, M.; Uchiyama, M.; Takita, R.; Chiba, S., *Angew Chem Int Ed* **2017**, *56* (39), 11807-11811.
170. Abdel Ghani, N. T.; Mansour, A. M., *Spectrochim Acta A Mol Biomol Spectrosc* **2011**, *81* (1), 529-43.
171. Zhang, H. Z.; Damu, G. L.; Cai, G. X.; Zhou, C. H., *Eur J Med Chem* **2013**, *64*, 329-44.
172. Arnaiz, F. J., *J Chem Educ* **1995**, *72* (12), 1139-1139.
173. Sheng, C.; Che, X.; Wang, W.; Wang, S.; Cao, Y.; Yao, J.; Miao, Z.; Zhang, W., *Eur J Med Chem* **2011**, *46* (5), 1706-12.
174. Infante-Castillo, R.; Rivera-Montalvo, L. A.; Hernandez-Rivera, S. P., *J Mol Struct* **2008**, *877* (1-3), 10-19.

175. Suffert, J.; Abraham, E.; Raepfel, S.; Bruckner, R., *Liebigs Ann* **1996**, (4), 447-456.
176. Li, M. R.; Li, Y. J.; Zhao, B. Z.; Liang, F. S.; Jin, L. Y., *Rsc Adv* **2014**, 4 (57), 30046-30049.
177. Hirai, Y.; Nakanishi, T.; Kitagawa, Y.; Fushimi, K.; Seki, T.; Ito, H.; Fueno, H.; Tanaka, K.; Satoh, T.; Hasegawa, Y., *Inorg Chem* **2015**, 54 (9), 4364-4370.
178. Gallop, C. W. D.; Chen, M. T.; Navarro, O., *Org Lett* **2014**, 16 (14), 3724-3727.
179. Cheng, Y. N.; Gu, X. Y.; Li, P. X., *Org Lett* **2013**, 15 (11), 2664-2667.
180. Iglesias, M. J.; Prieto, A.; Nicasio, M. C., *Org Lett* **2012**, 14 (17), 4318-4321.